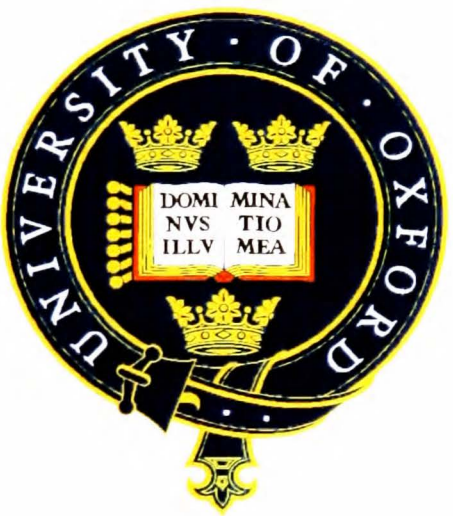
REGULATION OF *DE NOVO* LIPOGENESIS AND FATTY ACID DESATURATION IN HUMAN ADIPOCYTES



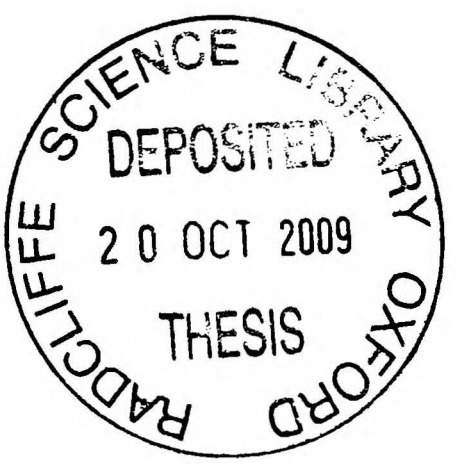
DPhil Thesis

Jennifer Mary Collins

Green Templeton College

University of Oxford

Hilary Term 2009



ABSTRACT

REGULATION OF *DE NOVO* LIPOGENESIS AND FATTY ACID DESATURATION IN HUMAN ADIPOCYTES

A thesis submitted for the degree of Doctor of Philosophy
Jennifer M Collins, Green Templeton College, University of Oxford
Hilary Term 2009

De novo lipogenesis (DNL) in the human adipocyte is not fully understood. While some believe this to be an insignificant pathway, others have argued that adipose tissue may even be the main site of DNL. The enzyme stearoyl-CoA desaturase (SCD) plays a key role in the synthesis of monounsaturated fatty acids and its activity may be co-ordinately regulated with DNL. The recently-described *Scd1* knockout mouse model fuelled interest in this enzyme as a possible target for the treatment of obesity.

Human preadipocytes were isolated from adipose tissue biopsy samples and differentiated *in vitro* for 14 days to produce adipocytes. Using stable isotopes, the main precursors for DNL in human adipocytes were determined, as was the regulation of DNL by an exogenous source of palmitate, the end product of DNL. Finally, SCD loss-of-function studies were employed to assess the importance of this enzyme to adipocyte function.

Human preadipocytes were capable of differentiating to form adipocytes and expressed mRNA for the necessary enzymes for DNL. Glucose proved to be the main carbon contributor to *de novo* fatty acid synthesis, and glutamine was indentified as another source. Palmitate up-regulated DNL, with maximal up-regulation achieved with 50 μM, with a concomitant up-regulation of SCD. Interestingly, some subjects' adipocytes were unable to withstand a high (400 μM) concentration of palmitate showing signs of cell death. Palmitate-intolerant adipocytes had lower expression of SCD mRNA, less intracellular triacylglycerol and greater incorporation of [U-^{13}C]palmitate in phospholipid fatty acids and consequently had a higher saturated-to-monounsaturated fatty acid ratio. Loss of SCD in adipocytes resulted in reduced cell membrane fluidity and reduced insulin sensitivity.

In conclusion, DNL may not function to increase fat stores within adipocytes but may serve as a key regulator, acting in tandem with SCD to maintain cell membrane fluidity and insulin sensitivity within the human adipocyte.

ACKNOWLEDGEMENTS

There are many people I would like to thank, for all their help and support throughout my time spent as a student in the Oxlip group. I have truly loved being a student again and have enjoyed the challenges this project has brought.

I'd like to thank Keith Frayn for believing in my ability to complete a DPhil. I would never have otherwise had this opportunity. In 2005, Bente Ruyter, an academic visitor from Norway, came to visit our group for six months to transfer her skills in salmon preadipocyte culture to human preadipocytes. If she hadn't visited, this project would not have come about. She taught me the preadipocyte isolation technique and introduced tissue culture to the Oxlip group. The Humane Research Trust funded this project and I thank them for their financial support.

My supervisors, Keith Frayn and Matt Neville, have supported me throughout and I couldn't have hoped for better supervisors. I am privileged to have been one of Keith's last students and Matt's first.

The Oxlip group is very close-knit and like a second family to all who are a part of it. I'd like to thank the following people who have made life in the lab a great experience and who have provided assistance: Sandy Humphreys, Barbara Fielding, Matt Neville, Katherine Pinnick, Marje Gilbert, Pauline Sutton, Leanne Hodson, Rachel Roberts, Diva Jain and Mary Chong. Katherine and I have spent a lot of time in tissue culture together and I'd like to thank her for baby-sitting my cells when I've been away. Other group members, in the clinical research unit, helped with the collection of the biopsies and I would like to thank them too for all the help they provided. They are Louise Dennis, Jane Cheeseman, Sara Suliman, Konstantinos Manolopoulos and Siobhán McQuaid. I am also extremely grateful to all those who donated their fat!

Various people outside the Oxlip group have also helped me along the way. Anne Clark is always passionate about all things cellular and has been supportive and enthusiastic with her tissue culture advice and introduced me to the world of histology. I am grateful to Mike Hoppa who taught me how to "FRAP" using the confocal microscope. I would also like to thank Dr Dirk-Jan Reingoud, Dr Theo van Dijk and Professor Folkert Kuipers at the University Medical Centre Groningen of the University of Groningen, the Netherlands, for their input to the MIDA of the isotopomer data in Chapter 3. This is an area our group has not had previous experience in and their input was greatly appreciated.

I have also been lucky to have had support at home, and would like to thank my husband, Mark, for always having faith in me and for providing emotional (and financial) support.

MEMORANDUM

I declare that the work presented in this thesis is my own except for the following:

1. The adipose tissue biopsies were performed by trained medical staff;
2. Analysis of the data presented in Chapter 3 was assisted by Dr Dirk-Jan Reingoud, Dr Theo van Dijk and Professor Folkert Kuipers at the University Medical Centre Groningen of the University of Groningen, the Netherlands;
3. The FRAP analysis technique to test for cell membrane fluidity was initially taught and supervised by Mike Hoppa (OCDEM) though I carried out all of the analyses.

All work was carried out at the Oxford Centre for Diabetes, Endocrinology and Metabolism, Oxford, and none of this work has been submitted for degree at this, or any other, university.

ABBREVIATIONS

14:0	Myristic acid
16:0	Palmitic acid
16:1 *n-7*	Palmitoleic acid
18:0	Stearic acid
18:1 *n-9*	Oleic acid
18:1 *n-7*	Vaccenic acid
18:2 *n-6*	Linoleic acid
2-DOG	2-deoxyglucose
ACC1/*ACACA*	Acetyl-CoA carboxylase
ACLY	ATP-citrate lyase
ADD-1	Adipocyte determination and differentiation factor-1
ADIPOQ	Adiponectin
ADRP	Adipose differentiation-related protein
AGPAT	Acylglycerol-sn-3-phosphate acyltransferase
ANOVA	Analysis of variance
ATGL	Adipose triglyceride lipase
ATP	Adenosine triphosphate
cAMP	Cyclic adenosine monophosphate
C/EBP	CCAAT-enhancer binding protein
CGI-58	Comparative gene identification-58
ChREBP	Carbohydrate response element-binding protein
CLA	Conjugated linoleic acid
CoA	Coenzyme A
CPT-1	Carnitine palmitoyl transferase-1
DAG	Diacylglycerol
DMEM	Dulbecco's Eagle's Medium Nutrient Mixture
DNL	*De novo* lipogenesis
dsRNA	Double stranded RNA
ELOVL6	Elongation of very long chain fatty acids-like 6
ER	Endoplasmic reticulum
FABP4	Fatty acid binding protein 4
FABPpm	Fatty acid binding protein (plasma membrane-associated)

FAME	Fatty acid methyl ester
FAS/*FASN*	Fatty acid synthase
FAT	Fatty acid translocase
FATP	Fatty acid transport protein
FCS	Foetal calf serum
FGF	Fibroblast growth factor
FRAP	Fluorescence recovery after photobleaching
GC	Gas chromatography
GC-MS	Gas chromatography-mass spectrometry
GLUT	Glucose transporter
GOI	Gene of interest
GPAT	Glycerol 3-phosphate acyltransferase
G3-PDH	Glycerol 3-phosphate dehydrogenase
HBSS	Hank's buffered salt solution
HKG	Housekeeping gene
HSL	Hormone-sensitive lipase
IBMX	3-Isobutyl-1-methylxanthine
IGF	Insulin-like growth factor
IL6	Interleukin 6
KRH	Krebs Ringer HEPES
LPA	Lysophosphatidic acid
LPL	Lipoprotein lipase
IRS	Insulin receptor substrate
MIDA	Mass isotopomer distribution analysis
MUFA	Monounsaturated fatty acid
NAD(P)H	Nicotinamide adenine dinucleotide (phosphate) (reduced form)
ORO	Oil red O
PA	Phosphatidic acid
PAP	Phosphatidic acid phosphatase
PBS	Phosphate buffered saline
PCR	Polymerase chain reaction
PEP	Phosphoenolpyruvate
PEPCK	Phophoenolpyruvate carboxykinase
PKA	Protein kinase A

PL	Phospholipid
PPARγ	Peroxisome proliferator-activated receptor γ
PPIA	Peptidylprolyl isomerase A (cyclophilin)
PPRE	Peroxisome proliferator response element
Pref-1	Preadipocyte factor 1
PUFA	Polyunsaturated fatty acid
qPCR	Quantitative polymerase chain reaction
RISC	RNA-induced silencing complexes
RNAi	RNA interference
SAFA	Saturated fatty acid
SCAP	SREBP cleavage activating protein
SCD	Stearoyl-CoA desaturase
shRNA	Short hairpin RNA
siRNA	Small interfering RNA
SRE	Sterol response element
SREBP1c/*SREBF*	Sterol regulatory element binding protein 1c
T_3	Triiodo-$_L$-thyronine
T2DM	Type 2 diabetes mellitus
TG	Triacylglycerol
TIP 47	Tail interacting protein 47
TNFα	Tumour necrosis factor α
TZD	Thiazolidinedione
UBC	Ubiquitin C

TABLE OF CONTENTS

Chapter 1. Introduction 1
1.1. ADIPOSE TISSUE 2
1.2. THE ADIPOCYTE 5
1.3. PREADIPOCYTE DIFFERENTIATION 13
1.4. TRIGLYCERIDE SYNTHESIS 21
1.5. STEAROYL-COA DESATURASE (SCD) 34
1.6. THE ROLE OF FATTY ACIDS IN THE ADIPOCYTE MEMBRANE 41
1.7. ADIPOSE TISSUE MODIFICATIONS IN OBESITY 44
1.8. AIMS OF THE THESIS 45

Chapter 2. Method Development 47
2.1. PREADIPOCYTE ISOLATION 48
2.2. TROGLITAZONE OPTIMISATION 52
2.3. THE USE OF STABLE ISOTOPES TO TRACE FATTY ACID METABOLISM 58
2.4. siRNA-MEDIATED GENE SILENCING 59
2.5. MEASUREMENT OF ADIPOCYTE INSULIN SENSITIVITY VIA LABELLED 2-DEOXYGLUCOSE UPTAKE 67
2.6. MEASUREMENTS OF CELL MEMBRANE FLUIDITY 69
2.7. MICROARRAY DATA ANALYSIS 73

Chapter 3 Characteristics of DNL in the human adipocyte 76
3.1. INTRODUCTION 77
3.2. AIMS 80
3.3. METHODS 80
3.4. RESULTS 85
3.5. DISCUSSION 105

Chapter 4 The effects of exogenous palmitate on *de novo* lipogenesis, fatty acid metabolism and insulin sensitivity of human adipocytes 110
4.1. INTRODUCTION 111
4.2. AIMS 113
4.3. METHODS 114
4.4. RESULTS 116
4.5. DISCUSSION 137

Chapter 5 The effects of a high concentration of palmitate on DNL and SCD and global changes seen in gene expression 143
5.1. INTRODUCTION 144
5.2. AIMS 145
5.3. METHODS 145
5.4. RESULTS 147
5.5. DISCUSSION 180

Chapter 6 The effects of SCD silencing in human adipocytes 187
6.1. INTRODUCTION 188
6.2. AIMS 191
6.3. METHODS 191

6.4. RESULTS 193
6.5. DISCUSSION 211

Chapter 7 Final Discussion 219

References 225

Appendix 1 Experimental Protocols 249
A1.1 PREPARATION OF [U-^{13}C]PALMITATE STOCK SOLUTIONS 250
A1.2 LIPID EXTRACTION FROM ADIPOCYTES 251
A1.3 GAS CHROMATOGRAPHY ANALYSIS OF TG AND PL FATTY ACIDS 252
A1.4 GAS CHROMATOGRAPHY-MASS SPECTROMETRTY ANALYSIS OF ISOTOPICALLY ENRICHED FATTY ACIDS 254
A1.5 GLYCEROL ANALYSIS 257
A1.6 GENE EXPRESSION ANALYSES 259
A1.7 MICROARRAY ANALYSIS 262
A1.8 STAINING OF CELLULAR PROTEINS AND LIPIDS 268
A1.9 MEASUREMENT OF GLYCEROL 3-PHOSPHATE DEHYDROGENASE ACTIVITY 271

Appendix 2 Microarray Data 274
A2.1 GENES CHANGING IN RESPONSE TO PALMITATE, TOLERANCE AND INTERACTION AS DETERMINED BY 2-WAY ANOVA 275
A2.2 PAIRED *T* TEST ANALYSES OF GENES CHANGING IN RESPONSE TO PALMITATE 287

TABLE OF FIGURES

Figure 1-1 Diagram of (a) white and (b) brown adipocyte..... 3

Figure 1-2 Transcriptional events during adipogenesis.....20

Figure 1-3 Overview of DNL and fatty acid modification in the adipocyte 23

Figure 1-4 Schematic diagram of glyceroneogenesis.....32

Figure 1-5 Formation of TG from fatty acids and glycerol 3-phosphate 34

Figure 2-I Adipocytes stained for Pref-1 expression.....51

Figure 2-2 ORO-stained adipocytes.....53

Figure 2-3 Total TG in cells treated with Troglitazone.....54

Figure 2-4 SCD indices for TG fatty acids in Troglitazone-treated adipocytes.....55

Figure 2-5 G-3PDH activity in Troglitazone-treated adipocytes.....56

Figure 2-6 mRNA expression of *PPARG*, *CEBPA*, *LPL*, *FABP4* and *SCD* in Troglitazone-treated adipocytes.....57

Figure 2-7 Pathway of RNAi.....60

Figure 2-8 Preadipocytes fluorescing due to Block-iT siRNA uptake.....63

Figure 2-9 *PPARG* mRNA expresssion in human preadipocytes using siRNA targeted to *PPARG*.....65

Figure 2-10 mRNA expression of genes expressed during adipocyte differentiation.67

Figure 2-11 Fluorescence recovery after photobleaching (FRAP).....71

Figure 3-1 Human adipocytes differentiated in the absence of fatty acids.....79

Figure 3-2 Mass spectrum of palmitate.....82

Figure 3-3 Oil red O stained adipocytes.....86

Figure 3-4 Fatty acid profile of adipocyte TG.....86

Figure 3-5 Relative mRNA expression of DNL-associated genes in differentiated preadipocytes.....87

Figure 3-6 Correlation between SCD indices and mRNA expression.....89

Figure 3-7 Correlation between total TG accumulation in differentiated preadipocytes and age of donor.....91

Figure 3-8 Acetate incorporation into TG fatty acids.....94

Figure 3-9 Total TG accumulation with high and low glucose.....96

Figure 3-10 Isotopomer masses of TG fatty acids showing carbon composition and incorporation of ^{13}C from low and high glucose.....97

Figure 3-11 The percentage contribution of low and high glucose to adipocyte TG fatty acids.....98

Figure 3-12 Isotopomer masses of TG fatty acids showing carbon composition and incorporation of ^{13}C from glutamine.....100

Figure 3-13 The percentage contribution of glutamine carbon to fatty acid synthesis in human adipocytes.....101

Figure 3-14 TG-glycerol derived from [U-^{13}C]glucose and [U-^{13}C]glutamine.....103

Figure 3-15 mRNA expression of *PCK1* and *G6PD* in adipocytes.....104

Figure 3-16 Fatty acid production from glutamine.....108

Figure 4-1 Light micrographs of preadipocytes differentiated with 0 to 200 μM exogenous palmitate.....116

Figure 4-2 Total TG in adipocytes differentiated with 0 to 200 μM palmitate.....117

Figure 4-3 *DGAT2* mRNA expression in response to palmitate.....118

Figure 4-4 Effects of exogenous palmitate on DNL-derived palmitate and myristate.....120

Figure 4-5 mRNA expression of DNL-associated genes in response to palmitate...121

Figure 4-6 Effects of exogenous palmitate on SCD indices.....122

Figure 4-7 Flux through SCD.....123

Figure 4-8 Changes in *SCD* mRNA expression with exogenous palmitate.....124

Figure 4-9 Changes in elongation indices with exogenous palmitate.....125

Figure 4-10 Changes in *ELOVL6* mRNA expression with exogenous palmitate...125

Figure 4-11 Flux through ELOVL6.....126

Figure 4-12 SCD indices of DNL-derived and exogenous TG-fatty acids.....127

Figure 4-13 Elongation indices of DNL-derived and exogenous TG-fatty acids....129

Figure 4-14 DNL and exogenous fatty acid flux though SCD and ELOVL6.....131

Figure 4-15 Myristate, formed by palmitate chain shortening.....132

Figure 4-16 PL fatty acid SAFA:MUFA ratios.....133

Figure 4-17 Changes in cell membrane fluidity determined by FRAP.....135

Figure 4-18 [^{3}H]2-DOG uptake in response to 0,50 and 200 μM palmitate.....137

Figure 4-19 Fatty acid pathways showing how fatty acids acted upon by SCD and ELOVL6 may overlap and disort enzyme product -to-precursor ratios.....139

Figure 5-1 Cell morphology of palmitate-tolerant and palmitate intolerant cells....148

Figure 5-2 Total TG accumulation in palmitate-tolerant and intolerant adipocytes.148

Figure 5-3 *DGAT2* mRNA expression in palmitate-tolerant and intolerant adipocytes.....149

Figure 5-4 Fatty acid composition of TG in palmitate-tolerant and intolerant adipocytes.....150

Figure 5-5 Differences in DNL-derived myristate and palmitate in palmitate-tolerant and intolerant adipocytes.....151

Figure 5-6 Expression of DNL-associated genes in palmitate-tolerant and intolerant adipocytes.....152

Figure 5-7 SCD indices for palmitate-tolerant and intolerant TG-fatty acids.....153

Figure 5-8 ELOVL6 indices in palmitate-tolerant and intolerant groups.....154

Figure 5-9 *SCD* and *ELOVL6* mRNA expression in palmitate-tolerant and intolerant adipocytes.....155

Figure 5-10 Flux through SCD and ELOVL6 in palmitate-tolerant and intolerant adipocytes.....155

Figure 5-11 Source of TG myristate in palmitate-tolerant and intolerant adipocytes.....156

Figure 5-12 Channelling of DNL-derived and exogenous fatty acids towards desaturation by SCD.....157

Figure 5-13 Channelling of DNL-derived and exogenous fatty acids towards elongation.....158

Figure 5-14 PL SAFA:MUFA in the palmitate-tolerant and intolerant groups.....159

Figure 5-15 Incorporation of exogenous palmitate into PL in palmitate-tolerant and intolerant adipocytes.....160

Figure 5-16 Hierarchical cluster analyses of genes changing inresponse to palmitate, tolerance and interaction 163

Figure 5-17 Heatmap showing changes in regulation of genes with interaction of palmitate and tolerance.....165

Figure 5-18 Sample hierarchical clusster analyses of genes changing in response to palmitate, tolerance and interaction.....167

Figure 5-19 Comparison of qPCR and microarray results.....176

Figure 5-20 Genes changing significantly between palmitate-tolerant and intolerant groups of adipocytes.....178

Figure 5-21 Changes in mRNA expression of ER stress-related genes.....180

Figure 6-1 Micrographs of adipocytes after treatment with SCD siRNA.....193

Figure 6-2 *SCD* mRNA knockdown.....194

Figure 6-3 Total TG in adipocytes in response to siRNA-mediated SCD silencing.195

Figure 6-4 Effects of SCD silencing on SCD protein and SCD indices.....197

Figure 6-5 Changes in TG SAFA composition with SCD knockdown.....199

Figure 6-6 SCD indices of DNL-derived and exogenous TG-fatty acids.....200

Figure 6-7 TG-fatty acid product-to-precursor ratios as a measure of ELOVL6 activity in response to SCD knockdown.....202

Figure 6-8 TG-fatty acid product-to-precursor ratios for DNL-derived and exogenous fatty acid elongation.....203

Figure 6-9 PL SAFA:MUFA ratios.....204

Figure 6-10 PL SCD ratios in 0 and 200 μM palmitate-treated adipocytes.....205

Figure 6-11 PL 18:0/16:0 ratios in 0 and 200 μM palmitate-treated cells.....206

Figure 6-12 Changes in cell membrane fluidity with SCD knockdown.....207

Figure 6-13 Changes in insulin sensitivity of adipocytes in response to SCD knockdown.....208

Figure 6-14 Changes in the DNL-associated genes *FASN* and *ACACA* with SCD silencing.....209

Figure 6-15 Changes in DNL with SCD knockdown.....211

Figure A1-1 Typical gas chromatogram from adipocytes differentiated without exogenous fatty acid.....253

Figure A1-2 Quality assessment of RNA.....263

Figure A1-3 Quality assessment of labelled cRNA.....267

TABLE OF TABLES

Table 1-1 Endogenous promoters of preadipocytes differentiation 18

Table 1-2 Exogenous promoters of preadipocyte differentiation 19

Table 1-3 Fatty acid composition of healthy adult adipose tissue.....25

Table 1-4 Summary of studies into the contribution of adipose tissue to whole-body DNL.....29

Table 1-5 Mouse SCD isoforms and their tissue expression.....36

Table 2-1 Recommended reagent volumes and concentrations for RNAi from Invitrogen.....62

Table 3-1 Masses of fatty acid methyl esters in their native and uniformly-13C labelled forms.....95

Table 3-2 Contribution of glucose and glutamine to TG-glycerol.....104

Table 4-1 Fatty acid composition of adipocyte TG.....118

Table 4-2 Correlations between TG and *FABP4* mRNA.....119

Table 5-1 Anthropometric measurements of the subjects whose cells were in the palmitate-tolerant and intolerant groups.....161

Table 5-2 Changes in KEGG pathways from 0 to 50 μM palmitate.....169

Table 5-3 Summary of genes changing significantly with palmitate, tolerance or interaction.....174

Table 6-1 SCD indices in adipocytes.....198

Table 6-2 Knockdown of *SCD*, *FASN* and *ACACA* mRNA with SCD silencing.....210

Table A1-1 Mass-to-charge ratios of FAMEs measured using SIM.....255

Table A1-2 Natural enrichment of fatty acid isotopomers.....256

Table A1-3 Natural enrichment of glycerol.....259

Table A1-4 Applied Biosystems Assays-on-Demand Taqman gene expression assays.....261

Table A2-1 Genes changing signigicantly in reponse to palmitate.....281

Table A2-2 Genes changing signigicantly in reponse to tolerance.....283

Table A2-3 Genes changing signigicantly in reponse to interaction.....286

Table A2-4 List of genes changing signigicantly from 0 to 50 μM palmitate.....291

Table A2-5 List of genes changing signigicantly from 0 to 200 μM palmitate.....291

Table A2-6 List of genes changing signigicantly from 50 to 200 palmitate.....293

Chapter 1

Introduction

1.1. ADIPOSE TISSUE

1.1.1. Cellular composition

Adipose tissue is located throughout the human body in subcutaneous and visceral regions. Cellular composition is varied and comprises predominantly mature adipocytes (approximately 66%) as well as preadipocytes (at least 15%) and endothelial cells (Guo *et al.*, 2007). The cells of the adipose tissue are supported by a scaffolding of extracellular matrix components and are served by both a nerve and blood supply. In mammals there are two types of adipocyte: brown and white (**Figure I-1**), with different cellular origins (Park *et al.*, 2008). Brown adipocytes contain many small lipid droplets and are mitochondria-rich, making them capable of thermogenesis. Brown adipose tissue is present in many animals and newborn humans. Human adults were once believed to possess exclusively white adipose tissue (Heaton, 1972), although recently Nedergaard *et al.* (2007) reported the presence of brown adipose tissue in a number of locations including around the kidneys and neck area.

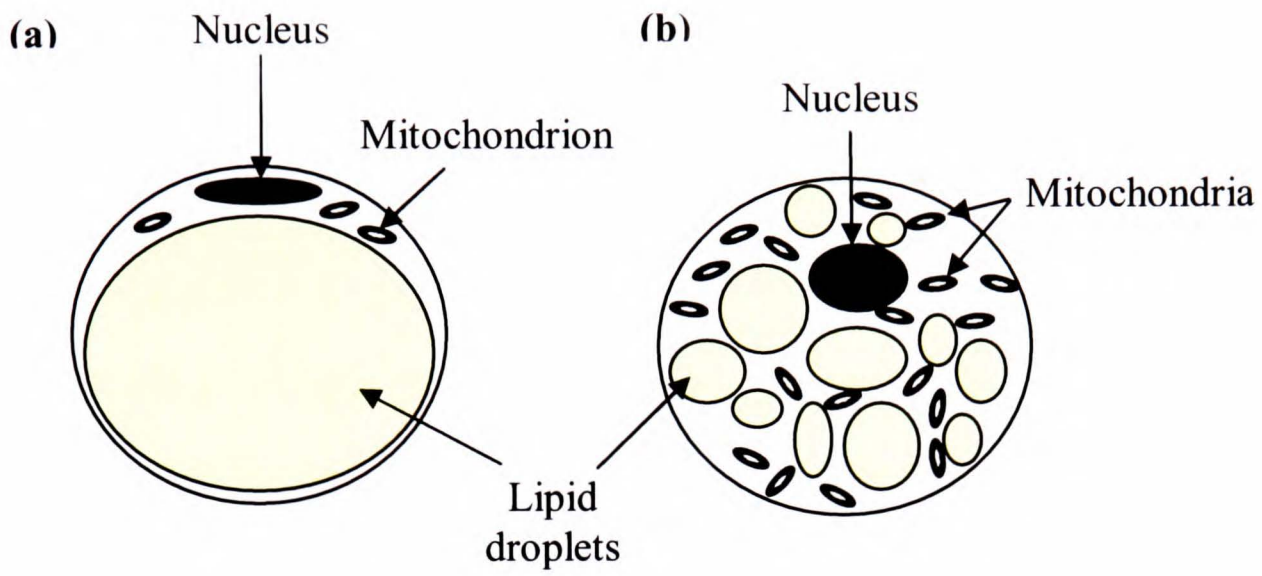


Figure 1-1 Diagram of (a) white and (b) brown adipocyte

1.1.2. Function

1.1.2.1. Storage

The primary role of adipose tissue is to efficiently store excess energy in the form of triglycerides (TG). There are a number of routes by which adipocytes accumulate TG, including from exogenous (or dietary) fat via chylomicrons, endogenous fat exported from the liver (in very low density lipoprotein (VLDL) and intermediate density lipoprotein (IDL)), circulating non-esterified fatty acids (NEFAs) and *de novo* lipogenesis (DNL). As lipids are hydrophobic they require a vehicle to transport them in the bloodstream; TGs are transported in lipoproteins and NEFAs are present bound to albumin.

Uptake of circulating TG present in lipoprotein particles, such as chylomicrons and VLDL, is facilitated by the enzyme lipoprotein lipase (LPL) (Eckel, 1989). LPL is synthesised within the adipocyte and is transported to the capillary. LPL is activated by apolipoprotein C2, present in the passing lipoproteins, and hydrolyses the TG to

release fatty acids. The fatty acids are then taken up by the adipocyte where they are re-esterified and stored as TG.

Plasma NEFAs originate either from adipose tissue TG that has undergone lipolysis by lipases, such as hormone-sensitive lipase (HSL) and adipose triglyceride lipase (ATGL), or from 'spillover' of NEFA released from LPL-hydrolysed TG. NEFAs circulate bound to albumin and can be taken back up by the adipocytes and re-esterified to form TG (Bickerton *et al.*, 2007; Shadid *et al.*, 2007). After an overnight fast, NEFA concentrations range from around 375 to 500 μmol/L in healthy individuals, and around 425 to 700 μmol/L in well-controlled diabetic patients (Tan *et al.*, 2008). Of the individual fatty acids that make up plasma NEFA, palmitate constitutes up to 25 % of circulating NEFA, translating to fasting concentrations of around 95 to 125 μmol/L in healthy individuals, and 105 to 175 μmol/L in diabetics.

Adipocyte fatty acids may also be synthesised *de novo* from non-lipid precursors, mainly carbohydrates. Known as *de novo* lipogenesis (DNL), the significance of this process in humans has been widely debated and will be discussed later.

Therefore, by taking up and removing excess circulating fat, the adipocyte acts as a buffer to maintain and control TG levels, thus protecting other organs from the potentially lipotoxic effects of ectopic fat deposition (Frayn, 2002).

1.1.3. Adipose tissue as an endocrine organ

Although adipose tissue was originally seen as an inert storage tissue, the discovery of leptin in the 1990s unveiled a new role for adipose tissue as an endocrine organ, signalling to the hypothalamus to regulate energy intake (Zhang *et al.*, 1994; Friedman & Halaas, 1998). In addition to leptin, several other hormones and cytokines, collectively termed 'adipokines', have also been found to be secreted by the adipocyte, such as adiponectin (also known as Acrp30), tumour necrosis factor-α (TNF- α) and interleukin-6 (IL-6) (Kern *et al.*, 1995; Scherer *et al.*, 1995; Fried *et al.*, 1998); acting in autocrine, endocrine and paracrine fashions. These findings have revolutionised the way in which adipose tissue is regarded, and have led to much investigation into its role in the regulation of metabolism (Trayhurn & Wood, 2004).

1.2. THE ADIPOCYTE

1.2.1. Characteristics

The majority of the mature white adipocyte is made up of a large, TG-rich, unilocular lipid droplet. This makes the adipocyte atypical in appearance compared with other cells, as the cytoplasm and organelles are displaced to the periphery of the cell. Adipocyte size varies and can exceed 100 μm depending on a number of factors including anatomical site and body weight (Hauner, 2004; Avram *et al.*, 2005).

1.2.2. Lipid droplet formation

The lipid droplet is the major feature of the adipocyte and acts to store neutral lipids, mainly TG and cholesteryl esters, within the cytosol, in a structure coated with a

single phospholipid layer and specialised proteins. Formation of the lipid droplet was thought to occur within the endoplasmic reticulum (ER) membrane leaflets, where disc-like lipid droplets formed then budded off, enveloped in an ER-derived phospholipid (PL) monolayer (Brown, 2001; Wolins *et al.*, 2006; Ducharme & Bickel, 2008). However, this model has recently been challenged. Robenek *et al.* (Robenek *et al.*, 2006) proposed the existence of specialised adipophilin-rich sites in the cytoplasmic ER membrane leaflet that facilitate lipid droplet biogenesis. They stated that the lipid droplet forms alongside the ER, where the ER nurtures the nascent lipid droplet during growth, forming a structure likened to an "egg cup", where the lipid droplet is the "egg". Furthermore, analysis of the PL monolayer surrounding the lipid droplet concluded it could not have originated from the ER membrane (Tauchi-Sato *et al.*, 2002). Whatever the exact mechanism, it is clear that the ER plays a fundamental role in lipid droplet formation.

1.2.3. Lipid droplet-associated proteins

The hydrophobic lipid droplet is coated by proteins, some of which serve to protect the fat store from enzymes such as lipases (Londos *et al.*, 2005). Various proteins have been identified as specific lipid droplet proteins, and include the PAT proteins; perilipin, adipose differentiation-related protein (ADRP/adipophilin), tail-interacting protein of 47 kilodaltons (TIP-47) and S3-12 (Jiang & Serrero, 1992; Londos *et al.*, 1995; Wolins *et al.*, 2001; Wolins *et al.*, 2005). Expression of lipid droplet-associated proteins is tissue-specific (Wolins *et al.*, 2006). In the adipocyte, perilipin A is the most abundant lipid droplet protein and accounts for 0.25 to 0.5 % of total cellular protein (Londos *et al.*, 1999; Brown, 2001). Adipocytes are also known to express mRNA for ADRP, expressed in the very early stages of preadipocyte differentiation,

and S3-12, which is associated with nascent lipid droplets. These three lipid droplet proteins share some sequence homology, although the roles played by each protein may be specific to the stage of maturation of the lipid droplet. The location of lipid droplet protein synthesis is thought not to be the ER, but to be on free, unbound ribosomes (Brasaemle *et al.*, 1997). Association of the proteins with the newly synthesised lipid droplet is not understood.

Perilipin, in its unphosphorylated form, shields the lipid droplet from lipolysis by HSL (Clifford *et al.*, 2000). It is believed that HSL-mediated lipolysis is dependent upon phosphorylation of perilipin by protein kinase A (PKA). Catecholamine stimulation of PKA results in the phosphorylation of both perilipin and HSL. Phosphorylated HSL translocates from the cytoplasm to the lipid droplet surface, where it is thought to tightly associate with phosphorylated perilipin, allowing HSL to access the lipids and hydrolyse them (Granneman *et al.*, 2008). Interestingly, the perilipin knockout mouse showed a compensatory up-regulation of ADRP, although ADRP was a weak protector of the lipid droplet from lipolysis (Martinez-Botas *et al.*, 2000; Tansey *et al.*, 2001).

Although perilipin may protect the lipid droplet from hydrolysis by HSL, this is not the only lipase capable of initiating lipolysis of the stored TG. The recent discovery of adipose triglyceride lipase (ATGL), reshaped the previously-established model of lipolysis in the adipocyte (Zimmermann *et al.*, 2004). Interestingly, the ATGL knockout mouse accumulates excess TG, whereas the HSL knockout mouse does not accumulate TG, but instead accumulates diacylglycerol. It has been proposed that ATGL catalyses the removal of the first fatty acyl chain from TG and that HSL is a

diacylglycerol (DAG) lipase (Haemmerle *et al.*, 2002; Zechner *et al.*, 2005; Haemmerle *et al.*, 2006). Unlike HSL, ATGL is not thought to require phosphorylation for activation (Zimmermann *et al.*, 2004). It is located on the surface of the lipid droplet and is activated by the protein comparative gene identification-58 (CGI-58) (Lass *et al.*, 2006). CGI-58 belongs to an esterase-lipase subfamily of proteins, although it has no intrinsic lipase activity. It is also present at the lipid droplet suface and is bound to perilipin. It is thought that activation of ATGL is brought about by interaction with CGI-58. In the basal state, perilipin binds to CGI-58, preventing its interaction with ATGL; however, upon lipoytic stimulation, it is released and can activate lipolysis. Phosphorylation of perilipin by PKA rapidly dissociates CGI-58 from perilipin, allowing ATGL to access the lipid droplet (Granneman & Moore, 2008).

1.2.4. Fatty acid uptake

Fatty acids may be delivered to the adipocyte for uptake by several means: via hydrolysis of TG in lipoprotein particles, as circulating fatty acids bound to albumin or circulating unbound (although unbound plasma fatty acid concentrations are very low at around 5 to 50 nM (Abumrad *et al.*, 1999)). As only unbound fatty acids can be taken up by the cells, they must either be released from TG in lipoprotein particles by hydrolysis (section **1.1.2.1**) or dissociate from albumin. Long chain fatty acid uptake can occur via different means, that is, by passive diffusion or by protein-mediated transportation. However, the process of fatty acid uptake is not well defined and there have been conflicting reports as to the mechanisms involved (Hamilton & Kamp, 1999; Kampf & Kleinfeld, 2007).

1.2.4.1. Passive diffusion

Passive diffusion describes the movement of unionised fatty acids across the plasma membrane as they become internalised within the cell. This model can be broken down to three steps: association of the fatty acid with the outer leaflet of the plasma membrane, 'flip flop' of the fatty acid between the outer and inner leaflets of the membrane as it rotates 180°, and dissociation from the inner leaflet (Kamp *et al.*, 2003).

Some uncertainties remain concerning the efficacy of this mode of transport. Flip-flop of the fatty acid may represent a rate-limiting step, the composition of the plasma membrane may act as a barrier to hinder fatty acid transport, and different fatty acid carbon chain lengths may determine the rate of transport (Kleinfeld, 2000; Kamp *et al.*, 2003; Kamp & Hamilton, 2006). Furthermore, evidence that fatty acid transport displays saturability gave rise to the theory that the passive diffusion model may not be sufficient to account for all fatty acid uptake, and that there must be involvement of protein transporters (Abumrad *et al.*, 1981; Abumrad *et al.*, 1999; Ehehalt *et al.*, 2006; Kampf & Kleinfeld, 2007). In the case of the adipocyte, passive diffusion is reported to be minimal, with 90 % of fatty acid uptake occurring via a saturable pathway (Stump *et al.*, 2001). Other studies have reported adipocyte fatty acid influx to be highly regulated, protein-mediated and maybe even dependent upon an adenosine triphosphate (ATP)-pump (Abumrad *et al.*, 1981; Kampf & Kleinfeld, 2004).

1.2.4.2. Protein-mediated transportation

Protein-mediated fatty acid transportation across membranes is thought to be facilitated by more than one protein. Proteins involved in this process include the plasma membrane-associated fatty acid binding protein (FABPpm), fatty acid transport protein-1 (FATP-1), fatty acid translocase (FAT/CD36) and caveolin-1 (Zhou *et al.*, 1992; Schaffer & Lodish, 1994; Abumrad *et al.*, 1999; Trigatti *et al.*, 1999).

There are several isoforms of FATP, each with tissue-specific expression. FATP-1 is highly expressed in insulin-sensitive tissues and is expressed mainly in adipose tissue and muscle. Like GLUT-4 (section **1.2.5**), FATP-1 is activated in response to insulin. In the basal state, FATP-1 is located in perinuclear compartments within the adipocyte cytoplasm. Insulin stimulation causes FATP-1 to translocate to the cell membrane where it facilitates fatty acid uptake (Stahl *et al.*, 2002).

FABPpm resides in the outer leaflet of the plasma membrane (Stump *et al.*, 1993). Its expression is up-regulated during differentiation of preadipocytes and increases fatty acid uptake (Zhou *et al.*, 1992).

CD36 belongs to the class B scavenger receptor family and is expressed in various cells and tissues, including the heart, skeletal muscle, platelets and macrophages. In the adipocyte, it is localised to the cell membrane (Stahl *et al.*, 2002) and is up-regulated during preadipocyte differentiation concurrent with cellular fatty acid uptake (Sfeir *et al.*, 1997).

Lipid rafts are lipid microdomains located within the plasma membrane, comprising an outer leaflet of cholesterol and sphingolipids linked to an inner leaflet of phospholipids and cholesterol (Ehehalt *et al.*, 2006). Lipid rafts may exist associated with proteins such as caveolin. Caveolin-positive lipid rafts, known as caveolae, form small (1 nm to I μm) lipid membrane invaginations implicated in signal transduction. Caveolin-1 has been identified as being a fatty acid binding protein, thus linking lipid rafts with fatty acid uptake. One other possible link between lipid rafts and fatty acid uptake, however, may involve FAT/CD36. Plasma membrane FAT/CD36 has also been shown to be closely associated with lipid rafts in the plasma membrane. Caveolin-1 may recruit FAT/CD36 to the plasma membrane for presentation to fatty acids, but this has not yet been fully established (Pohl *et al.*, 2005).

1.2.4.3. Fatty acid activation

Once fatty acids have been taken into the cell they are rapidly converted to their active fatty acyl-CoA form by the enzyme acyl-CoA synthetase (ACS), situated at the plasma membrane or the endoplasmic reticulum (Gargiulo *et al.*, 1999). ACSs comprise a family of enzymes specific to fatty acid chain length: short chain (2 to 3 carbons), medium chain (4 to12 carbons), long chain (13 to 22 carbons) and very long chain (> 22 carbons). Fatty acyl-CoAs are then channelled towards either oxidation in the mitochondria or esterification and storage in the lipid droplet or phospholipid membrane. FATP-1 has been linked with very long chain acyl-CoA synthetase activity. Whereas some believe that the two proteins are co-localised at the adipocyte plasma membrane, where they form a complex to promote fatty acid uptake and activation (Hall *et al.*, 2003; Richards *et al.*, 2006) others have argued that they may be the same protein (Watkins, 2008).

1.2.5. Glucose uptake

Glucose uptake into cells is vital to cell function and is facilitated by various tissue-specific isoforms of the GLUT glucose transporter family, also known as the solute carrier family 2 (facilitated glucose transporter). The adipocyte expresses two glucose transporters, glucose transporter 1 and 4 (GLUT1 and 4). GLUT1 is expressed only at low levels and is present on both the cell membrane and the in the cytoplasm, whereas GLUT4 is the predominant glucose transporter (Watson & Pessin, 2001).

Unlike GLUT1, GLUT4's action is entirely dependent upon insulin. In the basal state it is present in the cytoplasm, contained within intracellular vesicles. Insulin binds to, and activates, the insulin receptor, a tyrosine kinase receptor, on the adipocyte cell membrane. The active insulin receptor phosphorylates insulin receptor substrates (IRS) which, in turn, provides a docking site for proteins triggering a cascade of phosphorylations and protein activation. Activation of these signalling proteins leads to the stimulation of vesicle-contained GLUT4 and translocation of GLUT4 to the cell membrane where it brings about glucose uptake by facilitated diffusion. In the absence of insulin, the membrane-bound GLUT4 returns to the cytoplasmic storage vesicles where it awaits insulin activation once again (Rea & James, 1997; Bryant *et al.*, 2002). The adipocyte, therefore, is a highly insulin-sensitive cell and loss of responsiveness to insulin results in decreased glucose uptake which may affect cell function.

1.3. PREADIPOCYTE DIFFERENTIATION

1.3.1. The preadipocyte

Preadipocytes are mesenchyme-derived fibroblast-like adipocyte precursor cells. They reside in the adipose tissue alongside mature adipocytes and can be recruited to become differentiated adipocytes (a process termed adipogenesis).

The preadipocyte expresses many proteins that inhibit adipogenesis and maintain the preadipocyte phenotype. Preadipocyte factor-1 (Pref-1) is one such protein and is considered to be essential to the preadipocyte in that it prevents differentiation (Smas & Sul, 1996; Smas *et al.*, 1999; Sul *et al.*, 2000; Lee *et al.*, 2003; Wang *et al.*, 2006). In addition to Pref-1, the Wnt family of proteins, specifically Wnt 10b, are known inhibitors of preadipocyte differentiation (Ross *et al.*, 2000; Bennett *et al.*, 2002). Activation of the Wnt signalling pathway leads to the accumulation of cytosolic β-catenin, which translocates to the nucleus and activates transcription of Wnt-regulated target genes that maintain the preadipocyte phenotype. Other proteins expressed by the preadipocytes, such as Krüppel-like factor 2 and GATA-2 and 3, also play important roles in deterring adipocyte development (Ross *et al.*, 2000; Banerjee *et al.*, 2003).

Preadipocyte differentiation is associated with morphological changes, including the formation of lipid droplets, cytoskeleton remodelling, as well as changes in gene expression (Napolitano, 1963; Spiegelman & Farmer, 1982; Kanzaki & Pessin, 2001; Ros-Baro *et al.*, 2001).

1.3.2. Transcriptional control of differentiation

1.3.2.1. CCAAT-enhancer binding proteins (C/EBPs)

The CCAAT-enhancer binding proteins (C/EBPs) are transcription factors, of which several subtypes exist: C/EBPα, β and δ. They can act as both homo- and heterodimers of two different C/EBP subtypes and are involved in regulating various metabolic pathways such as adipocyte differentiation, leptin signalling and cell proliferation (Miller & Ntambi, 1996; Darlington *et al.*, 1998; Wang *et al.*, 2001). C/EBPβ and δ are expressed very early during preadipocyte differentiation and their expression triggers a cascade of signalling events to bring about differentiation. The importance of these transcription factors in preadipocyte differentiation can be seen with loss-of-function studies. The majority of mice lacking the genes for both C/ EBPβ and δ do not live beyond early neonatal development. Those that do survive, however, have reduced adipogenesis and fail to accumulate adipose tissue lipids, despite having normal expression levels of C/EBPα.

1.3.2.2. Peroxisome proliferator-activator receptor gamma (PPARγ)

The peroxisome proliferator-activator receptors (PPARs) are ligand-activated transcription factors belonging to a family of nuclear hormone receptors functioning to control fatty acid metabolism. There are three main subtypes, PPARα, γ and δ. PPARδ is the least well understood of the three subtypes but may be implicated in skeletal muscle fatty acid oxidation (Risérus *et al.*, 2008). PPARα and γ have quite contrasting roles in fatty acid metabolism. PPARα is mainly expressed in the liver and its action promotes fatty acid oxidation, whereas PPARγ is mainly expressed in adipose tissue, where it up-regulates adipocyte differentiation and fatty acid and TG synthesis (Schoonjans *et al.*, 1996).

PPARγ exists as two isoforms, PPARγ1 and 2. Both PPARγ1 and 2 are transcribed from the *PPARG* gene but are alternate splice forms; PPARγ2 has an extra 30 amino acids at its N-terminus. In humans, expression of the two isoforms varies. PPARγ1 is ubiquitously expressed at low levels, whereas PPARγ2 is chiefly expressed in adipose tissue at high levels (Rosen & Spiegelman, 2001).

Activation of PPARs requires heterodimerisation with retinoid-X receptor (RXR) and is ligand-dependent. Ligand binding to either PPAR or RXR leads either to co-repressor displacement or co-activator recruitment. These heterodimers then bind to peroxisome proliferator response elements (PPREs) in target genes and initiate their transcription. PPARγ agonists include polyunsaturated fatty acids (PUFAs), some prostaglandins and the insulin-sensitizing drugs, thiazolidinediones (TZDs) (Forman *et al.*, 1995; Yu *et al.*, 1995; Kliewer *et al.*, 1997) .

PPARγ is deemed to be the master regulator of adipogenesis, and studies have shown its absolute requirement for preadipocyte differentiation. Loss of PPARγ also leads to an inability to express C/EBPα (Rosen *et al.*, 1999; Xu *et al.*, 2006). The *Pparg* null mouse is not viable, and PPARγ is thought to be necessary for placental development (Barak *et al.*, 1999; Kubota *et al.*, 1999); however, chimeric mice generated using wild type embryonic stem cells and *Pparg* null cells showed that PPARγ was crucial for adipogenesis *in vivo* (Rosen *et al.*, 1999). In humans, patients with some, but not all, *PPARG* mutations have been shown to suffer from partial lipodystrophy and other metabolic distubances (Tan *et al.*, 2008).

1.3.2.3. Sterol regulatory element binding protein 1c (SREBP1c/ADD-1)

Sterol regulatory element binding proteins (SREBPs) are ER- and nucleus-associated membrane-bound transcription factors involved in the regulation of cholesterol and fatty acid synthesis. There are three main isoforms of SREBP: SREBP1a, 1c and 2, derived from two different genes. SREBP2 is highly expressed in the liver and is mainly involved in cholesterol homeostasis. SREBP1a and c arise from alternate splicing of the product of the *SREBP1* gene, and regulate fatty acid synthesis in both the liver and adipose tissue (Hua *et al.*, 1995). In adipose tissue, SREBP1c is also known as adipocyte determination and differentiation factor-1 (ADD-1) and is one of a few key regulators of fatty acid biosynthesis (Kim & Spiegelman, 1996).

Membrane-bound SREBP is inactive and activation requires proteolytic cleavage of the protein. The precursor protein of 125 kDa is first transported from the ER to the Golgi by SREBP cleavage activating protein (SCAP), where it is then cleaved by two proteases, site 1 protease and site 2 protease (S1P and S2P), to a smaller 68 kDa active form of SREBP. The active SREBP can then migrate to the nucleus and bind to the sterol response element (SRE) of its target genes, activating their transcription. SREBP is regulated by oxysterols as well as glucose and fatty acids (Edwards *et al.*, 2000; Shimano, 2001).

1.3.2.4. Transcriptional events

The initiation of differentiation triggers a cascade of transcriptional events. Expression of inhibitors of differentiation, such as Pref-1, is switched off and many pro-adipogenic genes are up-regulated. The first of the pro-adipogenic transcription factors to be expressed are C/EBP β and δ. These transcription factors induce the

expression of two other transcription factors, C/EBPα and PPARγ. C/EBPα also stimulates PPARγ and a feedback loop is created, maintaining expression of these important inducers of differentiation. PPARγ and C/EBPα then proceed to up-regulate expression of genes encoding proteins essential to preadipocyte differentiation such as stearoyl-CoA desaturase (SCD), fatty acid binding protein 4 (FABP4) and lipoprotein lipase (LPL), thus maintaining the adipocyte phenotype (Rosen & Spiegelman, 2000; Rosen *et al.*, 2000; MacDougald & Mandrup, 2002; Rosen & MacDougald, 2006).

The transcription factor SREBP1c also plays a role in differentiation. It can promote adipogenesis either directly, by promoting expression of the pro-lipogenic genes acetyl-CoA carboxylase (*ACACA*) and fatty acid synthase (*FASN*) or indirectly, by up-regulating *PPARG* expression, perhaps via production of a PPARγ ligand (Kim *et al.*, 1998b; Rosen & Spiegelman, 2000; MacDougald & Mandrup, 2002; Farmer, 2006).

1.3.3. Factors influencing differentiation

1.3.3.1. Inhibitors of differentiation

Various factors can act to inhibit the progression of adipogenesis. Cytokines such as TNFα and IL-6 have been linked to reduced adipogenesis. They may act to inhibit differentiation by up-regulation of suppressors of differentiation such a Wnt-10b or Pref-1, or by suppression of PPARγ or C/EBPα. Additionally, TNFα can act to delipidate mature adipocytes (Petruschke & Hauner, 1993; Warne, 2003; Gustafson & Smith, 2006).

A number of growth factors also inhibit differentiation, including fibroblast growth factor, epidermal growth factor and platelet-derived growth factor (Serrero & Mills, 1991; Hauner *et al.*, 1995).

Some fatty acids, such as the *trans*-10, *cis*-12 isomer of conjugated linoleic acid (CLA), have also been shown to reduce adipocyte differentiation, leading some to believe CLA to have benefits for weight loss (Choi *et al.*, 2000; Hargrave *et al.*, 2002; Brown & McIntosh, 2003). Medium chain fatty acids, for example octanoate, may inhibit adipogenesis by inhibiting PPARγ (Han *et al.*, 2002; Xie *et al.*, 2006).

1.3.3.2. Promoters of differentiation

Preadipocyte differentiation can be brought about by several endogenous and exogenous factors. **Table 1-1** summarises some known endogenous promoters of differentiation and **Table 1-2** lists some of those exogenous factors known.

Factor	Target	Reference(s)
Polyunsaturated fatty acids (PUFAs)	PPARγ	(Krey *et al.*, 1997)
Insulin	SREBP1c (also up-regulates PPARγ, possibly via production of endogenous PPARγ ligand) IGF-1 receptor (see below)	(Girard *et al.*, 1994; Claycombe *et al.*, 1998; Kim *et al.*, 1998b; Griffin & Sul, 2004)
IGF-1	IGF-1 receptor	(Smith *et al.*, 1988; Schmidt *et al.*, 1990)

Table 1-1 Endogenous promoters of preadipocytes differentiation

Factor	Target	Reference(s)
Thiazolidinediones (TZD)	PPARγ	(Kletzien *et al.*, 1992; Chou *et al.*, 2007; Ruddock *et al.*, 2008)
Glucocorticoids	Glucocorticoid receptor (down-regulate Pref-1 and up-regulate C/EBPδ)	(Hauner *et al.*, 1989; Smas *et al.*, 1999)
Phosphodiesterase inhibitors (isobutylmethylxanthine (IBMX))	C/EBPβ (increase intracellular cyclic AMP (cAMP) levels)	(Cao *et al.*, 1991)

Table 1-2 Exogenous promoters of preadipocyte differentiation

Figure 1-2 summarises the transcriptional cascade initiated during adipogenesis and highlights the various promoters and inhibitors that act to regulate this pathway.

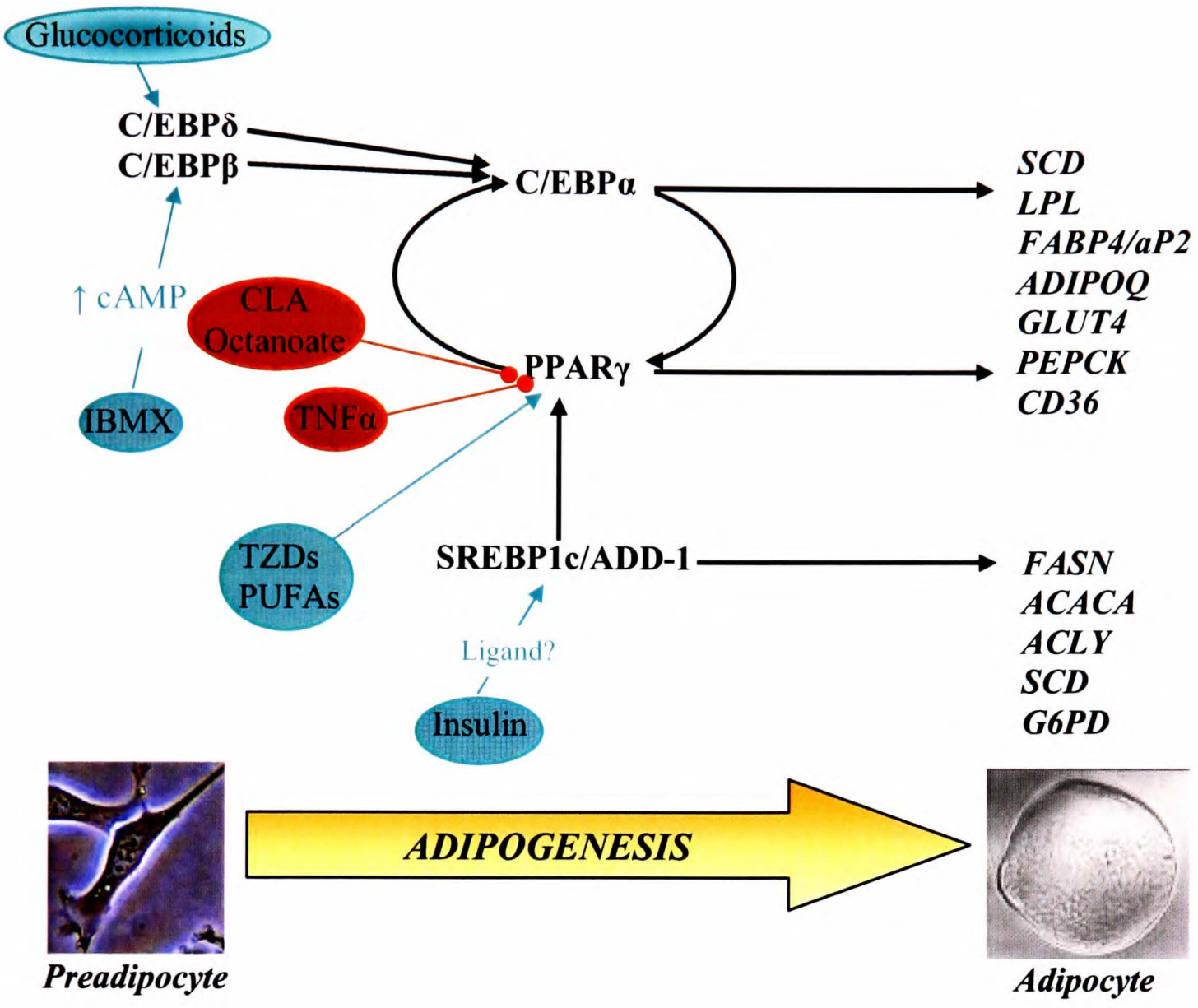


Figure 1-2 Transcriptional events during adipogenesis. Promoters of adipogenesis are in green and inhibitors are in red. The target genes of the pro-adipogenic transcription factors C/EBPα, PPARγ and SREBP1c/ADD-1 are shown in blue.

Key to gene names: stearoyl-CoA desaturase (*SCD*), lipoprotein lipase (*LPL*), fatty acid binding protein 4 (*FABP4/aP2*), adiponectin (*ADIPOQ*), glucose transporter 4 (*GLUT4*), phosphoenolpyruvate carboxykinase (*PEPCK*), CD36 (*CD36*), fatty acid synthase (*FASN*), acetyl-CoA carboxylase (*ACACA*), ATP-citrate lyase (*ACLY*), glucose 6-phosphate dehydrogenase (*G6PD*).

1.4. TRIGLYCERIDE SYNTHESIS

Triglycerides comprise three fatty acids attached to a glycerol backbone by ester bonds. Their synthesis *de novo* therefore requires the creation of both fatty acid and glycerol components and is described below.

1.4.1. *De novo* lipogenesis

De novo lipogenesis (DNL) is the formation of lipids from non-fat precursors such as glucose. In the cell, glycolysis produces pyruvate in the cytosol, which is transported to the mitochondria, where it is converted to acetyl-CoA, then to citrate. Citrate is then transported back into the cytosol, where it is cleaved by the enzyme ATP-citrate lyase to produce oxaloacetate and acetyl-CoA, the initial building block for fatty acid synthesis.

Two-carbon acetyl-CoA is converted to three-carbon malonyl-CoA in a reaction catalysed by the enzyme acetyl-CoA carboxylase (ACC). In the first round of synthesis, malonyl-CoA provides two carbons to the acetyl-CoA precursor, resulting in a four-carbon base. A series of reactions ensues whereby a further two carbons are added to the growing fatty acid chain, catalysed by fatty acid synthase (FAS). The final products of DNL are the saturated fatty acids palmitic acid (16:0) and, to a lesser extent, myristic acid (14:0).

The fatty acid end products of DNL can be acted upon by elongase and desaturase enzymes, which serve to lengthen the carbon chain and to introduce double bonds, respectively. Palmitic acid can be further elongated, by the enzyme elongation of very long chain fatty acids-like 6 (Elovl6), to form stearic acid (18:0). These two

saturated fatty acids can be further converted to the monounsaturated fatty acids palmitoleic acid (16:1 *n-7*) and oleic acid (18:1 *n-9*), respectively, by the enzyme SCD. Elovl6 acts to elongate C16 saturated and monounsaturated fatty acids to C18, and can also convert palmitoleic acid (16:1 *n-7*) to the C18 fatty acid vaccenic acid (18:1 *n-7*) (**Figure 1-3**) (Ntambi, 1995; Jakobsson *et al.*, 2006).

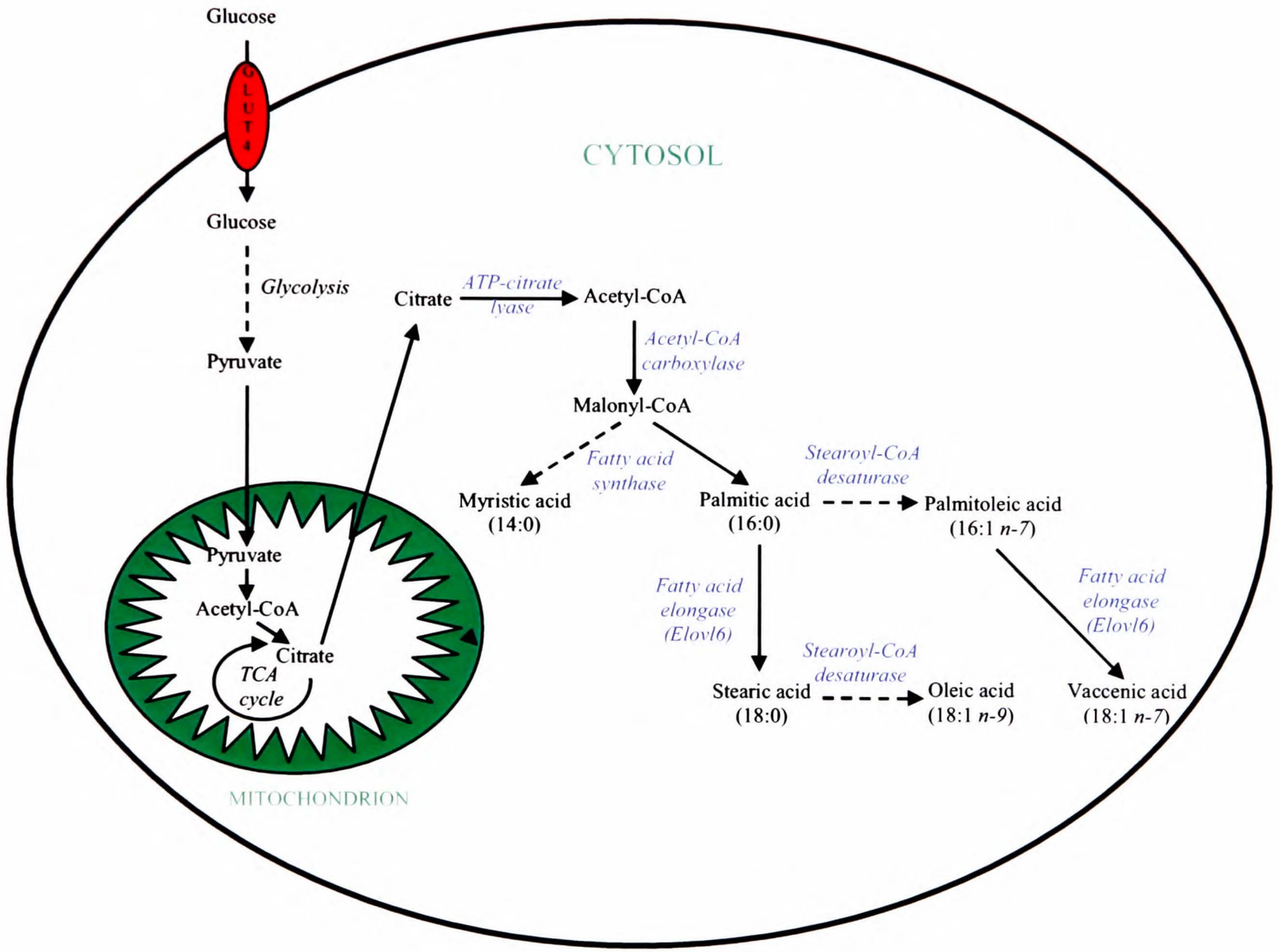


Figure 1-3 Overview of DNL and fatty acid modification in the adipocyte

DNL is an energy-demanding process and is costly to the cell (Acheson & Flatt, 2002). Fatty acid synthesis has a strict requirement for reduced nicotinamide adenine dinucleotide phosphate (NADPH) as a reducing agent. NADPH has two major sources within the cell: the pentose phosphate pathway and malic enzyme (Hillgartner *et al.*, 1995).

The pentose phosphate pathway, also known as the hexose monophosphate shunt, acts to bypass glycolysis and generate NADPH. Glucose 6-phosphate is diverted away from glycolysis and through the pentose phosphate pathway, generating two molecules of NADPH, before forming glyceraldehyde 3-phosphate and rejoining the glycolytic pathway.

Citrate cleavage forms acetyl-CoA for fatty acid synthesis, and oxaloacetate. The latter is then converted to malate which is further metabolised to pyruvate by malic enzyme. This enzyme's action produces one molecule of NADPH from $NADP^+$.

Due to the widespread distribution and vast quantity of adipose tissue, direct *in vivo* measurement of DNL in humans is not straightforward. The following methods have been previously described: comparisons of diet and adipose tissue fatty acid composition, indirect calorimetry, linoleate dilution and the use of stable isotopes as tracers.

The typical fatty acid composition of human adipose tissue is summarised in **Table 1-3**. Adipose tissue fatty acids are thought to mainly reflect dietary fat although changes in adipose tissue fatty acid composition occur very slowly (Hirsch *et al.*,

1960; Beynen *et al.*, 1980). Adipose tissue turnover is very slow and has an estimated half-life ranging from 6 to 24 months (Hirsch *et al.*, 1960; Beynen *et al.*, 1980; Strawford *et al.*, 2004). Age and ethnicity are not thought to influence adipose tissue composition (Insull & Bartsch, 1967) but gender may. While Insull *et al.* did not report gender differences, Heffernan *et al.* (1964) noted higher proportions of saturated fatty acids in males, proposing that they could be due to differences in endogenously produced fat.

Fatty acid	**Abundance (mol %)**
Myristic acid (14:0)	2.8
Palmitic acid (16:0)	21.5
Palmitoleic acid (16:1 *n-7*)	7.2
Stearic acid (18:0)	3.4
Oleic acid (18:1 *n-9*)	43.5
Linoleic acid (18:2 *n-6*)	13.9

Table 1-3 Fatty acid composition of healthy adult human adipose tissue (Hodson *et al.*, 2008).

Indirect calorimetry measures O_2 consumption and CO_2 production. The ratio of CO_2 production to O_2 consumption (VCO_2/VO_2) is used to calculate a respiratory quotient, which, if greater than or equal to 1, indicates that carbohydrate oxidation is occurring and implies net DNL. The disadvantage of this technique is that fatty acid oxidation in one tissue may cancel out fatty acid biosynthesis in another, thus only calculating net DNL (Hellerstein, 1999).

The linoleate dilution method is based on the principle that linoleate (18:2 *n-6*) is an essential fatty acid and can only be obtained from the diet. By measuring the ratio of linoleate to palmitate in sites of DNL, it is possible to determine whether fatty acids have been solely derived from the diet or if there has been a contribution from DNL by calculating the "dilution" of linoleate (Hudgins *et al.*, 1996).

Using stable isotopes (^{13}C or ^{2}H) to trace precursor incorporation into newly synthesised fatty acids is another method used to measure DNL. For example, intravenous infusion of ^{13}C-acetate can be used to measure the rate of palmitate production in VLDL-TG (liver only). Mass isotopomer distribution analysis (MIDA) can be used to calculate incorporation of the tracer and rate of DNL. (This is explained in **Appendix 1**, section **A1.4.1** (Hellerstein *et al.*, 1991)). Another approach is to use deuterated water ($^{2}H_2O$) as a tracer. Consumption of $^{2}H_2O$ to near-plateau body enrichment (1.5 to 2 %) allows direct measurements of adipose tissue DNL to be made. Labelled hydrogen can enrich newly synthesised fatty acids either by direct exchange with cellular water or by labelling hydrogen within NADPH, necessary for fatty acid synthesis. The amount of ^{2}H in newly synthesised fatty acids can be quantitated using gas chromatography-mass spectrometry. Incorporation of ^{2}H into adipose tissue TG fatty acids can then be calculated using MIDA (Parks & Hellerstein, 2006).

Limitations in the direct measurement of DNL in adipose tissue have hindered progress in finding a definitive answer as to its contribution towards whole-body DNL. The main site of DNL (liver or adipose tissue), and the significance of this process in the human adipocyte, have remained controversial matters for years. Many

believe the primary site of DNL in humans to be the liver (Guo *et al.*, 2000; Diraison *et al.*, 2003); however, there is some evidence to suggest this is neither the sole nor the chief site (Chascione *et al.*, 1987; Strawford *et al.*, 2004).

Comparisons of lipogenic enzymes in human and rodent adipose tissue have shown much lower enzyme activity in humans than in rodents (Shrago *et al.*, 1971). It is logical to think that these differences may be influenced by diet; the typical western diet of the human is high in fat, whereas the chow diet of laboratory-fed mice and rats is low in fat. A comparison of human lipogenic enzyme activity with that of both high fat-fed and control rats found that though high-fat feeding in rats reduced overall DNL, the capacity for lipogenesis was still far lower in humans, yet was not an insignificant pathway (Swierczynski *et al.*, 2000). Letexier *et al.* (2003) also compared high fat-fed rats with humans and, while agreeing that human adipose tissue had a lower capacity for DNL than rats, speculated that diet played no part in explaining these differences.

Human studies, on the other hand, have (in some cases) shown diet to play a role in the regulation of DNL, particularly in situations of carbohydrate overfeeding (Acheson *et al.*, 1988; Aarsland *et al.*, 1997). In humans, measurement of adipose tissue DNL has limitations, partly due to the size and distribution of this tissue throughout the body, and because endogenously synthesised fatty acids may be diluted within the vast pool of pre-existing fatty acids. *In vivo* adipose tissue measurements may also be affected by DNL in the liver, as VLDL-TG fatty acids are transported from the liver to the adipose tissue via LPL action (Hellerstein, 1999). Using various measurements and dietary approaches, estimates of adipose tissue DNL

have ranged from being insignificant, to accounting for up to 20 to 40% of whole body DNL. A summary of these findings is listed in **Table 1-4**.

Author	Subjects	Diet and duration	Measurement technique	Findings
Diraison *et al* (2003)	15 healthy males and females	Normal vs high calorie, high CHO diet for 2 days	Isotopes: Ingestion of [U-^{13}C]acetate and $^{2}H_2O$ over 12 hours, adipose tissue biopsies	Hepatic DNL up-regulated but not adipose tissue DNL. Adipose tissue is a minor contributor to whole-body DNL.
Strawford *et al* (2004)	19 healthy males and females	Normal diet plus $^{2}H_2O$ every day for 5-9 weeks.	Isotopes: $^{2}H_2O$ traced to fatty acids	Adipose tissue DNL may account for up to 20% of total DNL
Aarsland *et al* (1997)	5 males	Parenteral feeding of a high CHO, hypercaloric diet for 4 days	Indirect calorimetry and isotopic enrichment ([1,2-^{13}C]acetate) of VLDL-TG	Hepatic DNL increased 35-fold but was thought to only account for a small proportion (2 %) of whole body DNL. Adipose tissue may play a major role in whole body DNL.
Guo *et al* (2000)	6 lean & 6 obese women, 3 Pima Indians	Normal isocaloric diet (50% CHO) supplemented with $^{2}H_2O$ for 14 days.	Isotopes: $^{2}H_2O$ traced to fatty acids in adipose tissue - biopsies taken from gluteal, femoral and abdominal subcutaneous regions on days 0 and 14.	DNL is highly variable amongst individuals. Neither liver nor adipose tissue contribute to DNL greatly with normal feeding. Adipose tissue does not account for the large discrepancy between whole body and hepatic lipogenesis.
Acheson *et al* (1988)	3 healthy males	Glycogen depeletion and 7 days CHO overfeeding then 2 days low CHO	Indirect calorimetry, blood measurements	Net DNL was detected, increased plasma insulin, TG and VLDL after glycogen stores had become saturated (4 days CHO overfeeding).
Chascione *et al* (1987)	Malnourished	High CHO, hypercaloric	Adipose tissue biopsies, indirect calorimetry	Adipose tissue may account for as much as 40 % of whole body DNL.
Minehira *et al* (2003)	9 healthy males/females	Isocaloric diet/CHO overfeeding for 4 days	Indirect calorimetry and isotopes: microinfusion of labelled glucose into gluteal adipose tissue (biopsied)	CHO overfeeding increased net DNL 3-fold. Adipose tissue *SREBF*, *ACACA* and *FASN* mRNA increased post-glucose. Evidence of glucose entry to pentose phosphate pathway in adipose tissue.
Pasquet *et al* (1992)	Male adolescents (tribe in Cameroon)	Guru Walla CHO overfeeding (>7000 kcal per day) for 10 weeks	$^{2}H_2O$, skinfolds	Gained 12 kg (8 kg from CHO). Up-regulation of DNL. Skinfolds increased, showing increased fat deposition, but site of DNL undetermined.

Table 1-4 Summary of studies into the contribution of adipose tissue to whole-body DNL
CHO = carbohydrate, VLDL = very low density lipoprotein, *SREBF* = sterol regulatory element binding protein 1c, *ACACA* = acetyl-CoA carboxylase, *FASN* = fatty acid synthase

Whether or not obesity affects DNL in humans is unclear. Guo *et al.* (2000) reported no significant differences between lean and obese groups under normal feeding conditions, whereas McDevitt *et al.* reported obese subjects to display greater DNL under normal feeding conditions but not CHO overfeeding (McDevitt *et al.*, 2001). Other studies have shown further contrasting results, describing less DNL in obese subjects, either irrespective of diet (Hudgins *et al.*, 2008) or with carbohydrate overfeeding (Minehira *et al.*, 2004). A study by our group associated increased adipocyte size with reduced DNL, suggesting that obesity may play a part in down-regulating adipose tissue lipogenesis (Roberts *et al.*, 2009).

It is important to consider other factors that may impact on DNL in an *in vivo* situation. Insulin is known to be a lipogenic hormone and up-regulates DNL via its actions on SREBP1c (Claycombe *et al.*, 1998; Kim *et al.*, 1998a; Azzout-Marniche *et al.*, 2000; Schwarz *et al.*, 2003; Griffin & Sul, 2004; Mounier & Posner, 2006). As glucose stimulates insulin release from the pancreas, it is possible that insulin up-regulation, as a result of carbohydrate overfeeding, stimulates DNL. In the studies listed in **Table 1-4**, the effect of carbohydrate overfeeding on insulin is inconsistent, with either no effects on insulin (Minehira *et al.*, 2003) or an increase in plasma insulin (Acheson *et al.*, 1988; Diraison *et al.*, 2003). Insulin was not measured in all of the studies (Chascione *et al.*, 1987; Aarsland *et al.*, 1997). Whereas the evidence from these studies is inconclusive, it does not rule out the possibility that increases in plasma insulin may have influenced adipose tissue DNL.

In conclusion, opinions as to the occurrence of DNL within the human adipocyte vary. These differences may, in part, be influenced by the methods employed for the

measurement of this pathway. Recently, muscle was identified as another site of DNL in situations of chronic hyperglycaemia (Aas *et al.*, 2004). The disparities in the literature highlight the requirement for further investigation into this process in humans.

1.4.2. Glycerol synthesis

Low levels of glycerol kinase in the human adipocyte (Tan *et al.*, 2003) mean that most of the glycerol 3-phosphate required for TG synthesis cannot be obtained by recycling glycerol produced during lipolysis, and therefore must be synthesised. In the fed state, glucose is the main precursor for glycerol 3-phosphate synthesis in adipocytes (Galton, 1968; Hanson & Reshef, 2003; Reshef *et al.*, 2003). In an entirely cytosolic process, dihydroxyacetone phosphate, produced during glycolysis, is converted to glycerol 3-phosphate by the enzyme glycerol 3-phosphate dehydrogenase (G3-PDH).

However, glucose is not the only precursor for glycerol 3-phosphate synthesis. Glyceroneogenesis is defined as the *de novo* synthesis of glycerol (or glycerol 3-phosphate) from precursors other than glucose, examples of which include lactate, pyruvate and amino acids (Ballard *et al.*, 1967; Gorin *et al.*, 1969; Hanson & Reshef, 2003). Glyceroneogenesis was first described as "an abbreviated form of gluconeogenesis" (Ballard *et al.*, 1967) and operates when glucose (and insulin, an inhibitor of glyceroneogenesis) levels are low, such as in the fasting state (Quinn & Yeagley, 2005). This pathway facilitates the re-esterification of fatty acids released via lipolysis, estimated to be almost 50 % of the total fatty acid released in healthy individuals (Wolfe *et al.*, 1987).

The precursor (pyruvate, lactate or amino acid) is metabolised in the mitochondrion, via the Krebs Cycle, to form malate. Malate is then shuttled out of the mitochondrion into the cytosol where it is converted to oxaloacetate. Oxaloacetate is subsequently converted to phosphoenolpyruvate (PEP) by the cytosolic form of the enzyme phophoenolpyruvate carboxykinase (PEPCK-c), the rate-limiting enzyme in glyceroneogenesis. PEP then joins the gluconeogenic pathway to form glyceraldehyde 3-phosphate, which then forms dihydroxyacetone phosphate and ultimately glycerol 3-phosphate (**Figure 1-4**).

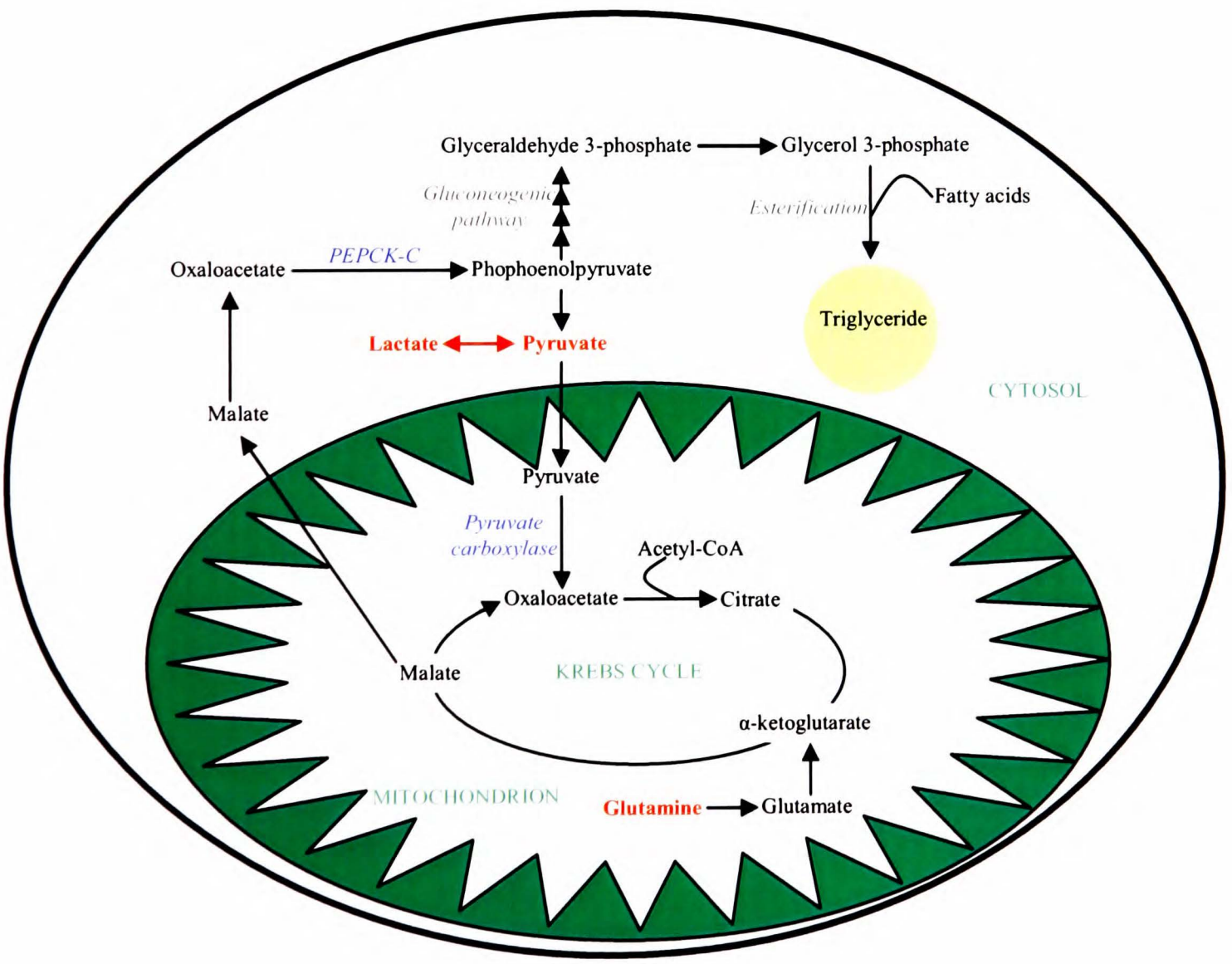


Figure 1-4 Schematic diagram of glyceroneogenesis, showing the involvement of common precursors for this pathway; lactate, pyruvate and glutamine (shown in red).

1.4.3. TG formation

Fatty acids, in their activated form, are esterified to glycerol 3-phosphate within the cytosol to form TG (**Figure 1-5**). Glycerol 3-phosphate acyltransferase (GPAT) catalyses the esterification of the first fatty acid to glycerol 3-phosphate to produce lysophosphatidic acid (LPA), and is believed to be the rate-limiting enzyme of TG formation (Coleman & Lee, 2004). There are two isoforms of GPAT, one mitochondrial and one microsomal. Mitochondrial GPAT isoform that is believed to play a major role in TG synthesis in the liver. Mice lacking mitochondrial GPAT have reduced adipose tissue TG stores (Hammond *et al.*, 2002). Mitochondrial GPAT is located on the outer mitochondrial membrane and its product, LPA, must be transported to the ER where the other enymes for TG formation are located. LPA is converted to phosphatidic acid (PA) by the addition of a second fatty acid, catalysed by acylglycerol-sn-3-phosphate acyltransferase (AGPAT, also called lysophosphatidic acid acyltransferase). Phosphatidic acid is then dephosphorylated by phosphatidic acid phosphatase (PAP) to form DAG.

Diacylglycerol acyltransferase (DGAT) catalyses the final step in TG formation, the addition of the third fatty acid. There are two isoforms of DGAT, DGAT1 and DGAT2, although only DGAT2 is believed to play a major role in TG synthesis (Smith *et al.*, 2000; Choi *et al.*, 2007).

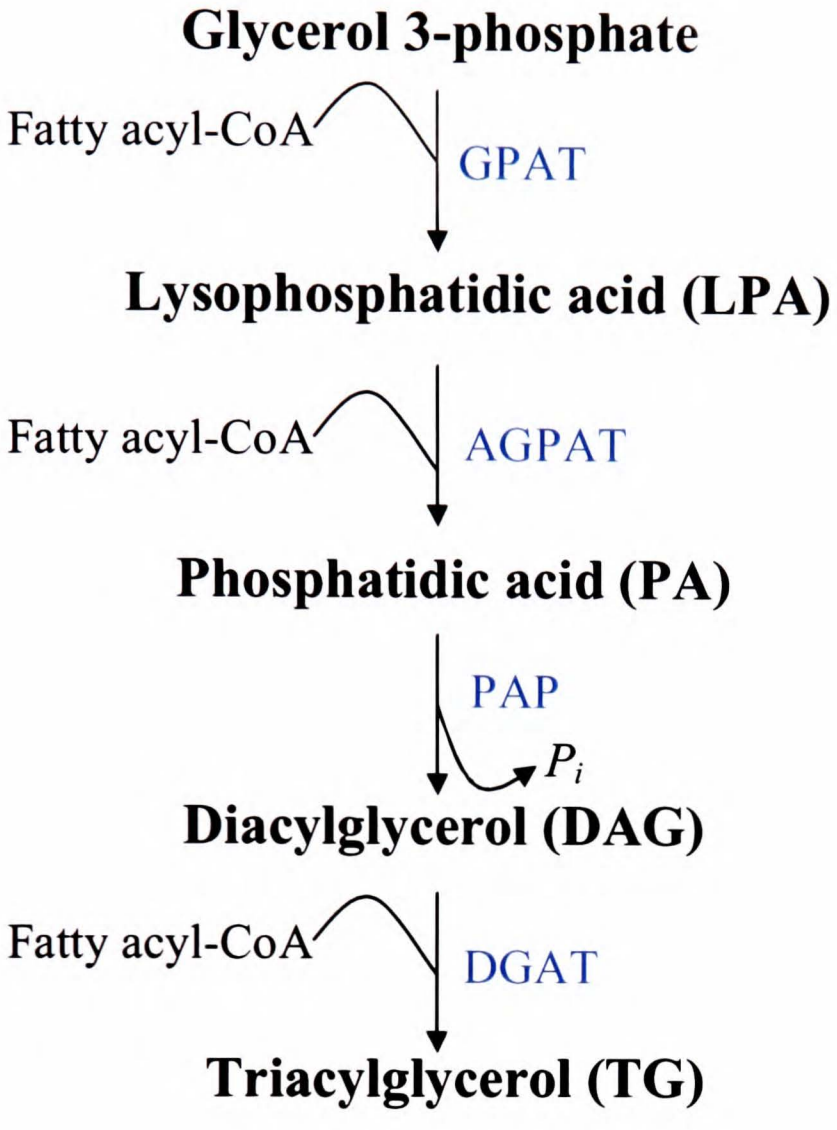


Figure 1-5 Formation of TG from fatty acids and glycerol 3-phosphate

1.5. STEAROYL-COA DESATURASE (SCD)

1.5.1. Characteristics and function

SCD, or delta-9 desaturase, is an iron-containing, ER-associated enzyme. Its function is to catalyse the introduction of a *cis* double bond into the delta-9 position of saturated fatty acyl-CoAs to produce monounsaturated fatty acyl-CoAs. SCD has two preferred substrates, palmitoyl-CoA and stearoyl-CoA, which are converted to palmitoleoyl-CoA and oleoyl-CoA, respectively, although oleoyl-CoA is the main product of SCD action (Miyazaki *et al.*, 2001). SCD action requires NADPH to trigger electron transport through the desaturase complex consisting of three main enzyme components: cytochrome b5 reductase, cytochrome b5 and stearoyl-CoA

desaturase (Ntambi, 1995). Furthermore, regulation of desaturation is dependent upon the terminal desaturase of the complex (Kasturi & Joshi, 1982). The SCD protein has a half-life of 3 hours, compared to 140 and 100 hours for cytochrome b5 reductase and cytochrome b5, respectively (Heinemann & Ozols, 2003), making SCD's existence in the cell transient.

There are many different isoforms of the *Scd* gene in mice, *Scd1-4*, which have tissue-specific expression (Ntambi *et al.*, 1988) (Miyazaki *et al.*, 2003) (Kaestner *et al.*, 1989) (Zheng *et al.*, 2001). The different mouse *Scd* isoforms and where they are expressed are listed in **Table 1-5**. In humans, the predominant isoform found is *SCD1*, which is expressed in many tissues, mainly adipose tissue and liver (Li *et al.*, 1994; Zhang *et al.*, 1999). Another subtype, *SCD5* (also known as *SCD2*) has also been reported to be expressed in brain (Wang *et al.*, 2005). Human *SCD1* shares 85 % sequence homology with the rodent *Scd1* isoform (Zhang *et al.*, 1999). Throughout this thesis, when referring to humans, the *SCD1* isoform will be referred to simply as *SCD*, unless otherwise stated.

Scd isoform	Main tissue expressed in
Scd1	Liver, adipose tissue, lung, skin
Scd2	Brain (adipose tissue, liver, lung, skin)
Scd3 [1]	Skin
Scd4	Heart

Table 1-5 Mouse SCD isoforms and their tissue expression

1.5.2. Regulation of SCD

Palmitoleate and oleate, the products of SCD action, are the most abundant monounsaturated fatty acids (MUFAs) within human adipose tissue (**Table 1-3**). As the melting point of TGs containing stearate is high, stearate is readily converted to oleate (Ntambi, 1999). Composition of the adipocyte lipids is fundamental to function and requires regulation of desaturation. Many factors have been shown to either up- or down-regulate SCD.

1.5.2.1. Transcription factors

SCD is up-regulated by the transcription factors SREBP1c and PPARγ (Shimomura *et al.*, 1998; Tabor *et al.*, 1999; Bene *et al.*, 2001; Risérus *et al.*, 2005; Yao-Borengasser *et al.*, 2008). These transcription factors are also subject to regulation by other factors (sections **1.3.3.1** and **1.3.3.2**).

Liver X receptors (LXRs) are transcription factors associated with cholesterol and lipid metabolism. There are two isoforms, α and β, which are activated by oxysterols,

[1] Murine *Scd3* has only one substrate, palmitate. Biddinger SB, Miyazaki M, Boucher J, Ntambi JM, Kahn CR. Leptin suppresses stearoyl-CoA desaturase 1 by mechanisms independent of insulin and sterol regulatory element-binding protein-1c. *Diabetes* 2006;55:2032-41

resulting in their dimerisation with RXR. LXRβ is ubiquitously expressed, whereas LXRα is expressed only in a few tissues, including adipose tissue and liver. In the liver, LXRα is involved in cholesterol conversion to bile acids, as well as lipogenesis. In adipose tissue, the LXR agonist T0901317 increased DNL by up-regulating expression of *SREBP1c/ADD-1* and its lipogenic target genes *FASN*, *ACACA* and *SCD* (Seo *et al.*, 2004; Darimont *et al.*, 2006). LXR has been shown to activate SREBP1c via interaction with an LXR binding site located on the SREBP1c promoter (Schultz *et al.*, 2000).

1.5.2.2. Hormones

Insulin positively regulates SCD, as well as other genes involved in DNL (Kasturi & Joshi, 1982; Ntambi, 1995; Griffin & Sul, 2004). Insulin-mediated up-regulation of fatty acid synthase (FAS) may be facilitated by the transcription factor SREBP1c, which may act to regulate SCD. Insulin has also been shown to up-regulate LXRs by up-regulating SREBP1c (Tobin *et al.*, 2002; Chen *et al.*, 2004). Therefore, LXRs may act as an intermediate in the pathway of insulin up-regulation of SCD.

Leptin, on the other hand, down-regulates SCD activity (Kakuma *et al.*, 2002). The leptin-deficient ob/ob mouse has elevated levels of SCD, which have been deemed at least partly responsible for the increased TG accumulation and obesity seen in this mouse model (Cohen *et al.*, 2002). The mechanism of action of leptin's regulation of SCD has not been fully established but is thought to be independent of SREBP1c (Biddinger *et al.*, 2006).

The thyroid hormone triiodothyronine (T_3) may influence SCD, although the effects of T_3 on SCD are disputed. T_3 has been reported by one group to potentiate insulin's effects on SCD, yet is said by another to have no effect on insulin-mediated up-regulation of SCD (Joshi & Aranda, 1979; Legrand & Bensadoun, 1991). T_3 increases expression of malic enzyme in brown adipocytes (Garcia-Jimenez *et al.*, 1993). As malic enzyme is a source of NADPH, this may up-regulate lipogenesis and SCD, both processes that are reliant upon NADPH.

1.5.2.3. Lipids

Some fatty acids are known to regulate SCD. For example, sterculic acid, 8-(2-octyl-1-cyclopropenyl)octanoic acid, is a plant fatty acid with the ability to prevent *Scd1*-mediated desaturation in 3T3-L1 adipocytes by inhibiting enzyme activity (Gomez *et al.*, 2003). In the liver, PUFAs down-regulate SCD by decreasing the amount of mature SREBP1c via down-regulation of cleavage of the precursor protein (Yahagi *et al.*, 1999). PUFAs also down-regulate SCD enzyme activity in differentiated 3T3-L1 adipocytes by destabilising *Scd1* mRNA (Sessler *et al.*, 1996). PUFAs are thought to exert their inhibitory action on SCD via interaction with a PUFA response element (PRE), located in the promoter region of the *SCD* gene (Waters *et al.*, 1997). The *trans*-10, *cis*-12 isomer of CLA can down-regulate *Scd1* mRNA in 3T3-L1 adipocytes in a dose-dependent manner without affecting differentiation of these cells (Choi *et al.*, 2000); however, this fatty acid does not appear to have the same effects in the liver (Hwang & Kang, 2007).

Cholesterol up-regulates *SCD1* expression (Garg *et al.*, 1986; Garg *et al.*, 1988; Landau *et al.*, 1997). LXRs are activated by cholesterol, which may up-regulate *SCD*

via up-regulation of SREBP1c (Repa *et al.*, 2000). Furthermore, cholesterol's ability to up-regulate *SCD* in the liver may be overridden by PUFAs: up-regulation of *SREBP1c* mRNA by cholesterol may be thwarted by a PUFA-mediated decrease in SREPB1c maturation (Kim *et al.*, 2002).

1.5.2.4. Carbohydrates

Glucose up-regulates SCD in 3T3-L1 adipocytes independently from insulin action (Jones *et al.*, 1998). Carbohydrate overfeeding (of mono- and disaccharides) up-regulates lipogenic genes including SCD with a concomitant up-regulation of SREBP1c (Minehira *et al.*, 2004). Identification of a carbohydrate response element-binding protein (ChREBP), a transcription factor up-regulated by carbohydrates, may also provide another means by which carbohydrates may up-regulate *SCD* gene expression (Yamashita *et al.*, 2001; Iizuka *et al.*, 2004). Interestingly, it has been proposed that ChREBP is activated by xylulose 5- phosphate, a product of the pentose phosphate pathway (Dentin *et al.*, 2005).

1.5.2.5. Thiazolidinediones

TZDs are a group of PPARγ agonists used in the treatment of type 2 diabetes and insulin resistance. They act as insulin sensitizers although their precise mechanism of action remains unclear. There have been conflicting reports on their effects on SCD; some researchers report up-regulation (Singh Ahuja *et al.*, 2001; Risérus *et al.*, 2005; Yao-Borengasser *et al.*, 2008), while others report down-regulation of *SCD1* mRNA in response to TZDs (Kurebayashi *et al.*, 1997; Kakuma *et al.*, 2002).

1.5.3. SCD and disease

The detrimental effects of an overabundance of intracellular saturated fatty acids (SAFAs) has been well documented (Vessby *et al.*, 2001; Summers *et al.*, 2002; Lu *et al.*, 2003; Lee *et al.*, 2006; Wei *et al.*, 2006; Guo *et al.*, 2007). Maintenance of cell membrane fluidity and function relies on the ratio of saturated to monounsaturated fatty acid (SAFA:MUFA) within the phospholipid (PL) membrane (section **1.6.3**). Therefore, SCD would appear to be crucial to the preservation of cell function. There have, however, been many reports of SCD's contribution to states of disease.

High levels of SCD activity have been associated with metabolic diseases and disorders such as type 2 diabetes, insulin resistance, hypertriglyceridaemia, abnormal fatty acid partitioning in skeletal muscle and atherosclerosis (Attie *et al.*, 2002; Ntambi *et al.*, 2002; Hulver *et al.*, 2005; Gutierrez-Juarez *et al.*, 2006; Sjögren *et al.*, 2008). Increased SCD activity has also been linked with certain cancers (Scaglia *et al.*, 2005; Morgan-Lappe *et al.*, 2007; Scaglia & Igal, 2008).

However, the literature surrounding the involvement of SCD with various diseases and disorders is highly contradictory, and while many authors report adverse effects of SCD, there are many opposing reports. Increased SCD levels have also been shown to be protective against atherosclerosis, type 2 diabetes, fatty liver and insulin resistance (Risérus *et al.*, 2005; Pinnamaneni *et al.*, 2006; Peter *et al.*, 2008; Stefan *et al.*, 2008). Furthermore, the fact that increased SCD is observed in some cancer cell types stresses its importance in cell survival.

1.5.4. SCD inhibition as a target for obesity and insulin resistance

The generation of the *Scd1* knockout mouse sparked interest in this enzyme as a potential target for the treatment of obesity and related disorders (Ntambi *et al.*, 2002; Dobrzyn & Ntambi, 2005). Loss of *Scd1* was shown to have profound effects on metabolism in mice, as they were protected against high-fat diet-induced obesity, had increased insulin sensitivity compared with wild-type mice and were leaner. This was coupled with increased energy expenditure in these animals. Subsequent studies into this mouse model substantiated these initial findings and strengthened the theory of *Scd1* being an ideal pharmaceutical target (Dobrzyn *et al.*, 2004; Dobrzyn *et al.*, 2005a; Jiang *et al.*, 2005; Sampath *et al.*, 2007), initiating the development of SCD inhibitors (Liu *et al.*, 2007; Zhao *et al.*, 2007).

SCD inhibition in the human adipocyte and its consequences on DNL and insulin sensitivity will be addressed in **Chapter 6**.

1.6. THE ROLE OF FATTY ACIDS IN THE ADIPOCYTE MEMBRANE

Although the majority of the mature adipocyte is composed of fat in the form of TG, this is not the only lipid species to play a significant role in this cell. Lipids are also a major constituent of cell membranes and lipid composition can influence membrane fluidity and function.

1.6.1. Phospholipids

PLs are the main component of all cell membranes. They comprise a hydrophobic fatty acid tail, containing two fatty acyl chains, attached to a glycerol-phosphate backbone and an organic group, such as choline, inositol, ethanolamine or serine, attached by a phosphate group. Phosphatidylcholine is the most abundant PL in the outer leaflet of the plasma membrane of many cells (Schwartz *et al.*, 1985). The fatty acid moiety can vary, and chain length and degree of saturation can affect cell membrane fluidity and function (section **1.6.3**).

1.6.2. Cholesterol

Cholesterol is another major component of cell membranes, making up around 20 to 40 mol %. Cholesterol is distributed amongst the phospholipids where it helps to maintain membrane integrity and fluidity (Mouritsen & Zuckermann, 2004). Cholesterol is also present in the plasma membrane within highly structurally organised microdomains interspersed throughout the membrane, called lipid rafts, described in section **1.2.4.2**.

1.6.3. Cell membrane fluidity

The cell membrane hosts a variety of proteins, acting as transporters for goods in and out of the cells, as well as ion pumps and receptors. Some of these are continually expressed, whereas others are up-regulated and recruited as required. It is imperative that the structure of the membrane allows movement of these vital components of the membrane to maintain cell wellbeing (Stubbs & Smith, 1984).

The melting point of a fatty acid is determined by both its chain length and degree of saturation. The longer and more saturated a fatty acid is, the higher its melting point will be. For example, short chain fatty acids (C8-12) will have lower melting points than the long chain fatty acids (C13-20), just as saturated fatty acids will have higher melting points than unsaturated. Furthermore, melting point decreases with increasing number of double bonds. For example, palmitate (16:0) has a melting point of 63 °C and is solid at room temperature, whereas oleate (18:1 *n-9*) has a melting point of 13 to 14 °C and is liquid at room temperature (Moffitt *et al.*, 2005). Membrane fluidity can be affected by fatty acid composition of the PLs within the membrane (Stubbs & Smith, 1984). If all the PL fatty acids were saturated they would line up and form a rigid structure. The inclusion of a *cis* double bond introduces a kink into the fatty acid structure preventing the fatty acids from packaging neatly, and gives irregularity to the overall structure. As unsaturated fatty acids are more fluid in structure than SAFAs, this introduces movement into the membrane, allowing movement of intermediates within the membrane.

PL composition of the plasma membrane is dynamic and changes can be brought about by external influences such as diet. Alterations in cell membrane composition have been associated with diseases such as type 2 diabetes. For example, adipocyte membrane changes can cause insulin resistance and type 2 diabetes (Field *et al.*, 1988; Field *et al.*, 1990), a decrease in PUFAs in skeletal muscle PLs has been linked with insulin resistance (Borkman *et al.*, 1993), and macrovascular complications of type 2 diabetes are associated with decreased platelet membrane fluidity (Caimi *et al.*, 1995).

1.7. ADIPOSE TISSUE MODIFICATIONS IN OBESITY

1.7.1. Causes of obesity

Obesity arises as a result of an imbalance between energy intake and energy expenditure and is characterised by an excess of adipose tissue. It is associated with a number of complications including an increased risk of type 2 diabetes mellitus (T2DM) and cardiovascular disease, and is an increasing problem worldwide (Barness *et al.*, 2007; Hussain *et al.*, 2007).

It was once believed that we were born possessing all the adipocytes we would ever have. However, nowadays obesity is known to be associated with adipocyte hypertrophy and hyperplasia (Drolet *et al.*, 2008). Adipocyte hypertrophy occurs as the adipocyte increases its lipid content, and has been shown to be associated with metabolic disturbances such as insulin resistance, a risk factor for T2DM (Weyer *et al.*, 2000; Lundgren *et al.*, 2007). A recent study by Spalding *et al.* (Spalding *et al.*, 2008) stated that total adipocyte number is set during adolescence, and that there is a continuous turnover of adipocytes in adults. Although the total number of adipocytes renewed each year is greater in obese than lean subjects (due to there being a greater abundance), fat cell turnover is the same between the two groups. The author calculated that half of the total number of adipocytes is renewed every 8.3 years, with the rate of turnover remaining constant throughout life.

1.7.2. The effects of obesity on adipose tissue

As adipocytes expand, their ability to accommodate excess fat in an already lipid-rich cell diminishes. It can be said that the adipocyte becomes "overloaded" with fat and

its capability to buffer circulating plasma fatty acid concentrations dwindles (Frayn, 2002). Consequently, this can lead to ectopic deposition of lipids in non-adipose tissues. Fat deposition around visceral organs can lead to complications such as insulin resistance, hyperlipidaemia, cardiovascular disease and hepatic steatosis (Goossens, 2008; van Herpen & Schrauwen-Hinderling, 2008; Szendroedi & Roden, 2009).

As obesity progresses it is believed to induce a state of inflammation within the adipose tissue, as marked by infiltration of macrophages and an increase in adipokines (Weisberg *et al.*, 2003). Increased release by adipocytes of factors such as the proinflammatory adipokines TNF-α and IL-6, as well as hormones such as leptin, is associated with increased fat cell size and has also been linked with insulin resistance (Kern *et al.*, 2001; Maachi *et al.*, 2004; Skurk *et al.*, 2007). Conversely, secretion of adiponectin, which is thought to be protective against insulin resistance and atherosclerosis, decreases with adipocyte enlargement in the obese (Hulthe *et al.*, 2003). Therefore, as the adipocyte reaches its storage capacity, the potential for adverse metabolic consequences heightens.

1.8. AIMS OF THE THESIS

The significance of, and ability for DNL in the human adipocyte is still unclear despite attempts to determine its role in adipose tissue (Shrago *et al.*, 1969; Strawford *et al.*, 2004). SCD is known to be an important enzyme in fatty acid desaturation and may be linked to DNL (Chong *et al.*, 2008). Furthermore, recent interest in SCD as a target for the treatment of obesity has led to loss-of-function studies, although these

studies have mainly focussed on SCD's action in the liver (Ntambi *et al.*, 2002; Yee *et al.*, 2008).

The aims of this thesis were as follows:

1. To study the ability for *de novo* lipogenesis in the human adipocyte and to determine the main precursor for this process.
2. To explore regulation of DNL by an exogenous source of the end product of DNL, the saturated fatty acid palmitate, as well as palmitate's actions on fatty acid modification by SCD and other enzymes, such as elongases.
3. To assess the effects of knocking down SCD on DNL, cell membrane fluidity and insulin sensitivity in the human adipocyte.

Chapter 2

Method Development

2.1. PREADIPOCYTE ISOLATION

2.1.1. *In vitro* models used to study adipose tissue

Previously, much research focussed on rodent models to study adipose tissue. In 1964, Rodbell first described the isolation and culture of mature adipocytes from rat epididymal fat pads (Rodbell, 1964). Much early work was done using the epididymal fat pads of male rats (Frayn, 1992). In the 1970s, established cell lines such as 3T3-L1 murine preadipocytes (Green & Kehinde, 1975) became widely used models of adipose tissue. Although rodent models can be easily accessible and results reproducible, occurrences in these models may not translate to the same situation in humans, one example being the role of the adipokine resistin, released by the adipocytes of obese mice and linked with insulin resistance, but not produced by human adipocytes (Arner, 2005). Importantly, as discussed in **Chapter 1**, (section **1.4.1**), there may be significant differences in extent of DNL in rodent and human adipose tissue.

Human models have also been developed. Adipose tissue explants have been studied but have their disadvantages as changes in gene expression, increased TNF-α release and increased lipolysis have been shown with time in culture (Gesta *et al.*, 2003). Mature human adipocytes can also be cultured, but are fragile and prone to damage during isolation, are buoyant and do not adhere to flasks, and can only be cultured for short periods. Isolation of human preadipocytes from adipose tissue and their subsequent differentiation *in vitro* provides another means by which the adipocyte may be studied (Hauner *et al.*, 2001). Commonly, preadipocyte isolation from adults uses large amounts of adipose tissue taken during surgery, but the use of smaller

samples (0.2 to 0.5 g) taken from children during surgery has also been described (Grohmann *et al.*, 2005; Sabin *et al.*, 2006). As surgery is invasive and potentially a limited source of adipose tissue, I sought to isolate preadipocytes from smaller amounts of adipose tissue acquired by needle biopsy, taken under local anaesthetic. The biopsy technique was already established within our group and provided a readily available source of adipose tissue for preadipocyte isolation (Tan *et al.*, 2005). It has been shown that preadipocytes differentiated *in vitro* retain the characteristics of the adipose depot from which they were taken (Tchkonia *et al.*, 2006). Since I wished to study adipose tissue metabolism in samples taken from a variety of donors, I further developed this approach.

2.1.2. Isolation procedure

The taking of human adipose tissue samples was approved by the Oxfordshire Clinical Research Ethics Committee and all subjects gave written, informed consent. Adipose tissue biopsies were taken from abdominal subcutaneous adipose tissue of healthy volunteers using a 12 gauge needle and syringe. Adipose tissue was mechanically minced using scissors, washed twice with Hank's buffered salt solution (HBSS) to remove contaminating blood, then enzymatically digested in 1mg/ml collagenase (Roche, Burgess Hill, UK) in HBSS in a shaking water bath (90 rpm) at 37 °C for 45 minutes. The digested tissue was centrifuged at 1000 rpm for 5 minutes at 4 °C. The buoyant mature adipocytes and supernatant were removed, and the pellet containing the stromal-vascular cells resuspended in growth medium (Dulbecco's Eagle's Medium Nutrient Mixture (DMEM)/F12 HAM (v/v, 1:1), 10% foetal calf serum (FCS) (Invitrogen, Paisley, UK), 1 µl/100 ml fibroblast growth factor (FGF), 100 U/ml penicillin and 0.1 mg/ml streptomycin). The resuspended cells were filtered

twice through nylon mesh (SEFAR, Bury, UK), firstly with pore size 250 μm, then through 100 μm to remove any large cells. The filtered cells were centrifuged again at 1000 rpm for 5 minutes at 4 °C, the supernatant removed and resuspended in growth medium. Cells were plated in tissue culture flasks. After one day, contaminating red blood cells were washed off with phosphate buffered saline (PBS) and medium replaced. Preadipocytes were passaged up to five times before being used for experiments.

2.1.3. Preadipocyte differentiation

Confluent preadipocytes were differentiated for 14 days in standard differentiation medium adapted from the method of Hauner *et al.* (Hauner *et al.*, 2001), consisting of Dulbecco's Modified Eagle's Medium/Nutrient Mixture F-12 Ham (DMEM/F12 HAM) (1:1) containing 2 mM glutamine, 17 μM pantothenate, 100 nM human insulin, 1 nM triiodo-$_L$-thyronine (T_3), 33 μM biotin, 10 μg/ml transferrin, 1 μM dexamethasone and 1 ml/L gentamycin. 3-Isobutyl-1-methylxanthine (IBMX) (250 μM) and Troglitazone (2 μM, as determined from experiments in section **2.2**) were added for the first 3 days.

2.1.4. Confirmation of preadipocyte isolation

Preadipocyte factor 1 (Pref-1) is expressed in the preadipocyte and its presence inhibits adipogenesis (Wang *et al.*, 2006) (**Chapter 1**, section **1.3.1**). Upon induction of differentiation, Pref-1 expression is reduced and is inhibited as differentiation progresses.

Differentiating preadipocytes were stained at different stages of differentiation: days 0, 2, 4 and 12. Pref-1 staining used a horseradish peroxidase-linked antibody visualised with diaminobenzidine and cells were counterstained with haematoxylin (**Appendix 1**, section **A1.8.2**). Negative controls of no primary antibody were included and non-specific, background staining accounted for.

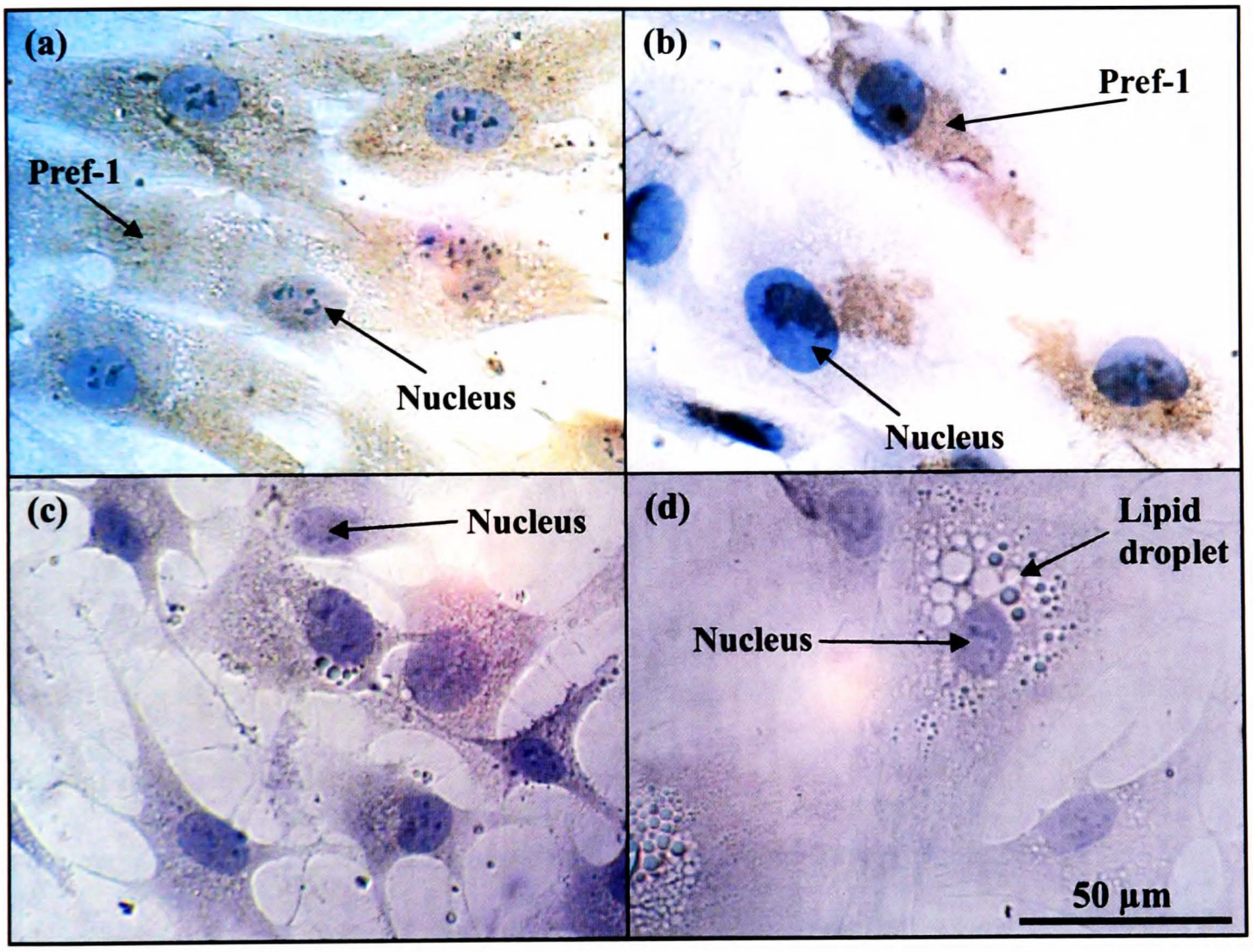


Figure 2-1 Adipocytes stained for Pref-1 expression (x40 magnification) (a) day 0, (b) day 2, (c) day 4, (d) day 12 (x40 objective)

Pref-1 was down-regulated as the preadipocytes differentiated. At day 0, Pref-1 was highly expressed, by day 2, pref-1 was less abundant and was only present around the nucleus, and from day 4 onwards pref-1 was undetectable (**Figure 2-1**).

The presence of Pref-1 and its subsequent down-regulation during differentiation, accompanied by the emergence of lipid droplets, verifies that these cells are preadipocytes.

2.2. TROGLITAZONE OPTIMISATION

The PPARγ agonist Troglitazone (Sigma, UK) was added to the differentiation medium to further promote adipogenesis. Whereas the other constituents of the differentiation medium are commonly used and their concentrations optimized (Hauner *et al.*, 2001; Hemmrich *et al.*, 2005), the optimum concentration of Troglitazone needed to be determined.

2.2.1. Results

Lipid droplet accumulation was visualised by oil red O (ORO) staining (**Appendix 1**, section **A1.8.1**) (**Figure 2-2(a)**). The average number of cells with lipid droplet accumulation was calculated by counting firstly, the number of nuclei and secondly, the number of cells with visible lipid droplets. This was repeated using 10 different fields of view for each Troglitazone concentration tested. Lipid droplet accumulation was taken as the average of the 10 fields and was greatest with 2 μM Troglitazone (**Figure 2-2(b)**). The higher concentrations (6 and 8 μM) had a less stimulatory effect on lipogenesis.



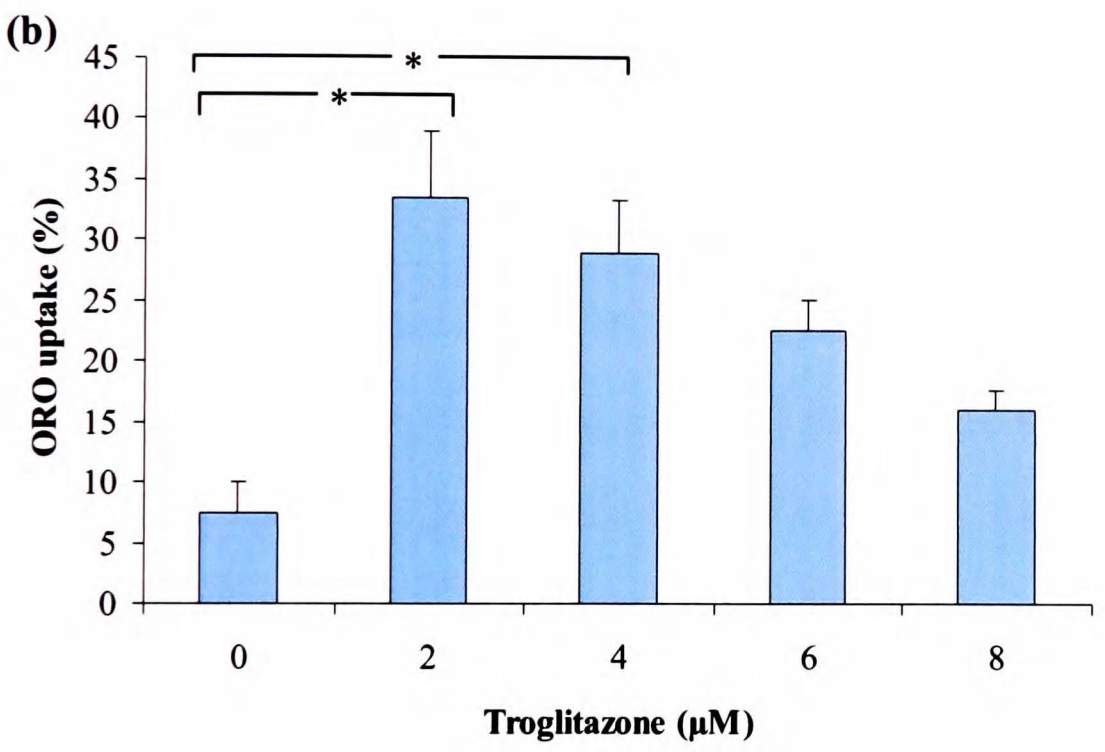


Figure 2-2 (a) ORO-stained adipocytes counterstained with haematoxylin (x10 objective) and (b) mean % oil red O uptake in adipocytes with 0-8 µM Troglitazone. Data are represented as mean ± SEM (n=9) * P<0.05

Fatty acids in the TG fraction were measured using gas chromatography (GC) (**Appendix 1**, section **1.3**) and total TG calculated from the sum of all the fatty acids (**Figure 2-3**). In agreement with the ORO data, 2 µM Troglitazone showed the highest TG accumulation.

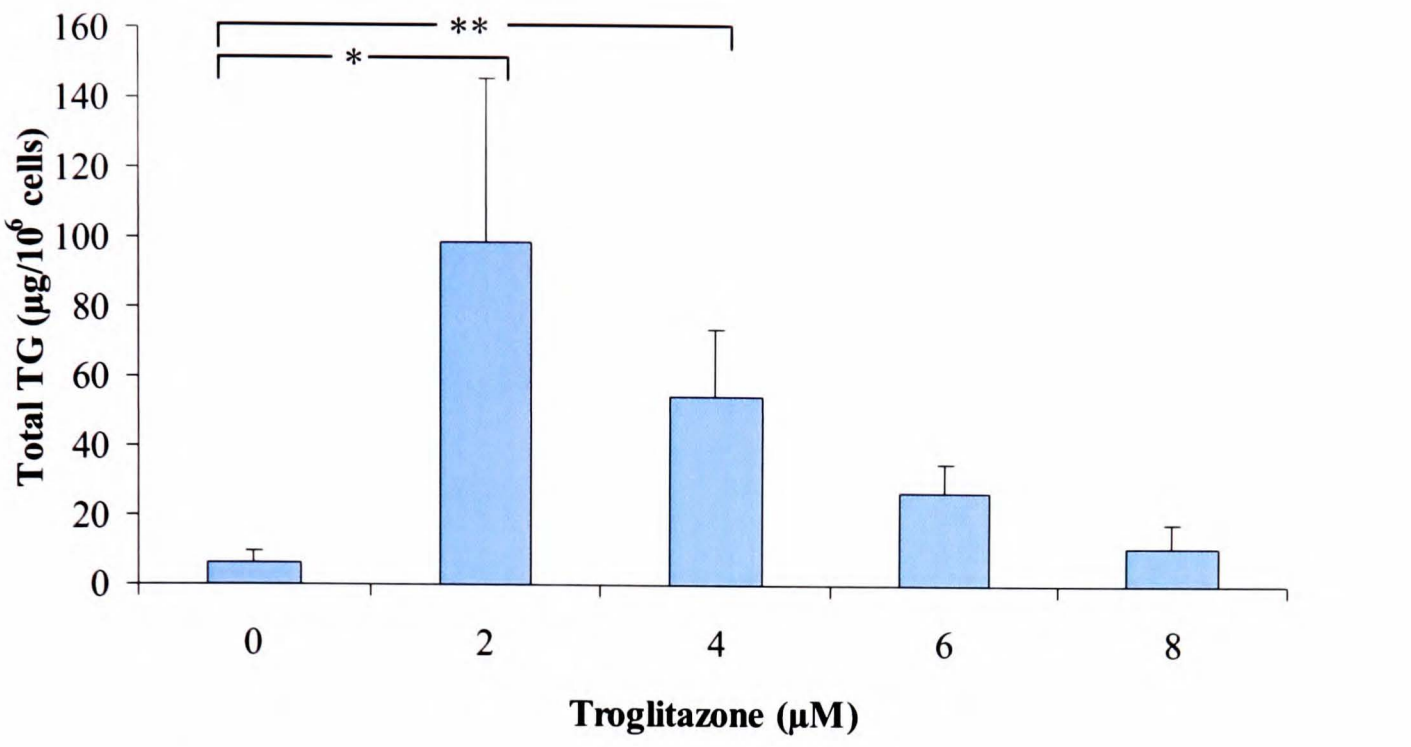


Figure 2-3 Total TG in cells treated with Troglitazone. Data are represented as mean ± SEM (n=8) * P=0.009, ** P=0.030

The SCD desaturation index can be calculated from the product/precursor ratio, i.e. 16:1 *n-7*/16:0 and 18:1 *n-9*/18:0, and can act as a proxy measure of SCD activity. Using this ratio it was seen that there was an overall increase in 16:1 *n-7*/16:0 and 18:1 *n-9*/18:0 ratios (P = 0.000 for both, repeated measures ANOVA). A Tukey's least significant difference *post hoc* test for pairwise comparisons showed 2, 4 and 6 µM Troglitazone significantly increased SCD indices compared with the 0 µM Troglitazone control (P = 0.000, 0.001 and 0.000 for 2, 4 and 6 µM Troglitazone, respectively, for the 16:1 *n-7*/16:0 ratio and P = 0.000, 0.005 and 0.013 for the 2, 4 and 6 µM Troglitazone, respectively, for the 18:1 *n-9*/18:0 ratio) (**Figure 2-4**).

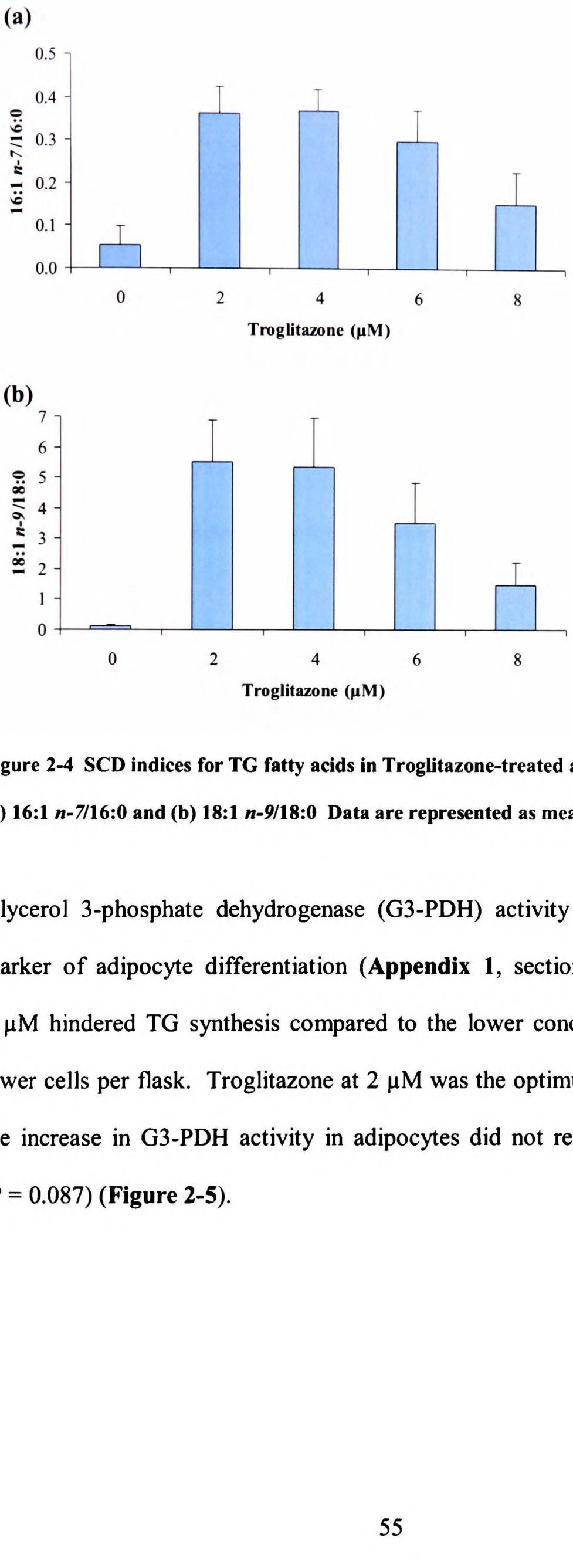


Figure 2-4 SCD indices for TG fatty acids in Troglitazone-treated adipocytes

(a) 16:1 *n-7*/16:0 and (b) 18:1 *n-9*/18:0 Data are represented as mean ± SEM (n = 8)

Glycerol 3-phosphate dehydrogenase (G3-PDH) activity was also measured as a marker of adipocyte differentiation (**Appendix 1**, section **A1.9**). Troglitazone at 8 µM hindered TG synthesis compared to the lower concentrations and there were fewer cells per flask. Troglitazone at 2 µM was the optimum concentration although the increase in G3-PDH activity in adipocytes did not reach statistical significance (P = 0.087) (**Figure 2-5**).

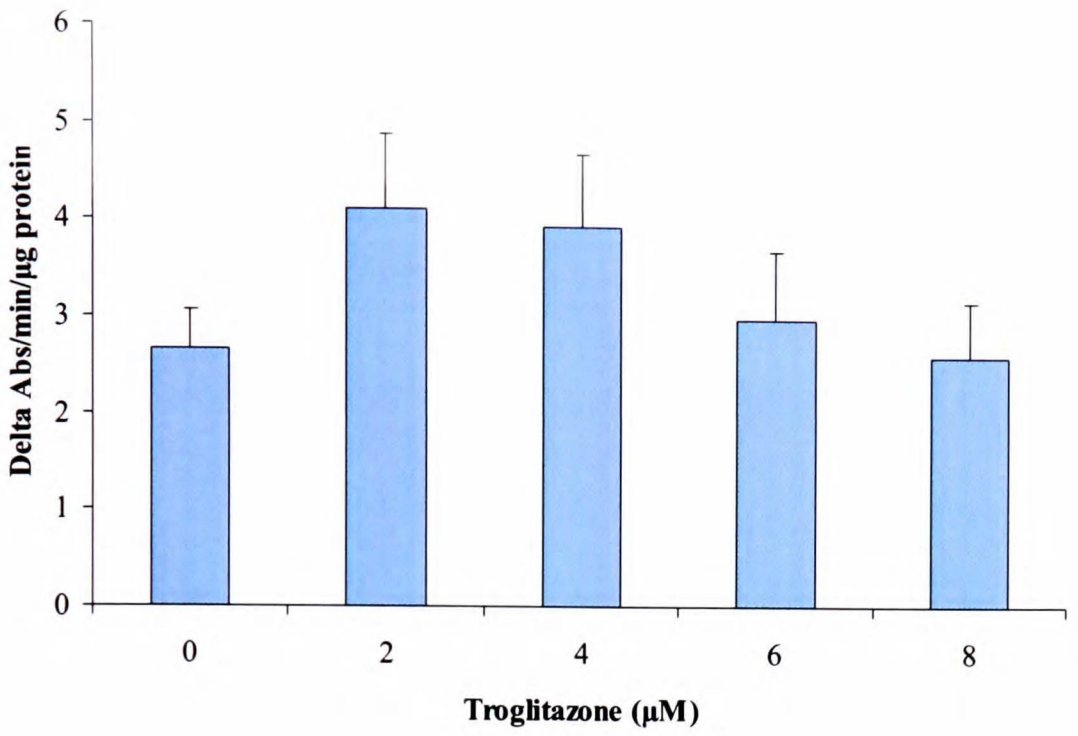


Figure 2-5 G3-PDH activity in Troglitazone-treated adipocytes . Data are represented as mean ± SEM (n = 9)

mRNA levels of five genetic markers of adipogenesis were measured: *PPARG* (PPARγ), *LPL* (lipoprotein lipase), *FABP4* (fatty acid binding protein 4), *SCD* (stearoyl-CoA desaturase) and *CEBPA* (C/EBPα). Compared with the control (0 µM), 2 µM Troglitazone showed the greatest up-regulation of *PPARG* and *LPL* mRNA ($P < 0.05$), whereas *FABP4* and *SCD* mRNA was up-regulated optimally with 2 µM and 4 µM ($P < 0.05$). Up-regulation of *CEBPA* mRNA did not reach statistical significance with any concentration. From the gene expression data, it can be concluded that 2 µM Troglitazone is optimal for adipogenesis in human adipocytes. Studies in 3T3-L1 preadipocytes and rodent models have suggested that Troglitazone down-regulates *Scd1* gene expression (Kurebayashi *et al.*, 1997; Kakuma *et al.*, 2002). However, up-regulation of *SCD* mRNA expression was observed in human adipocytes(**Figure 2-6**).

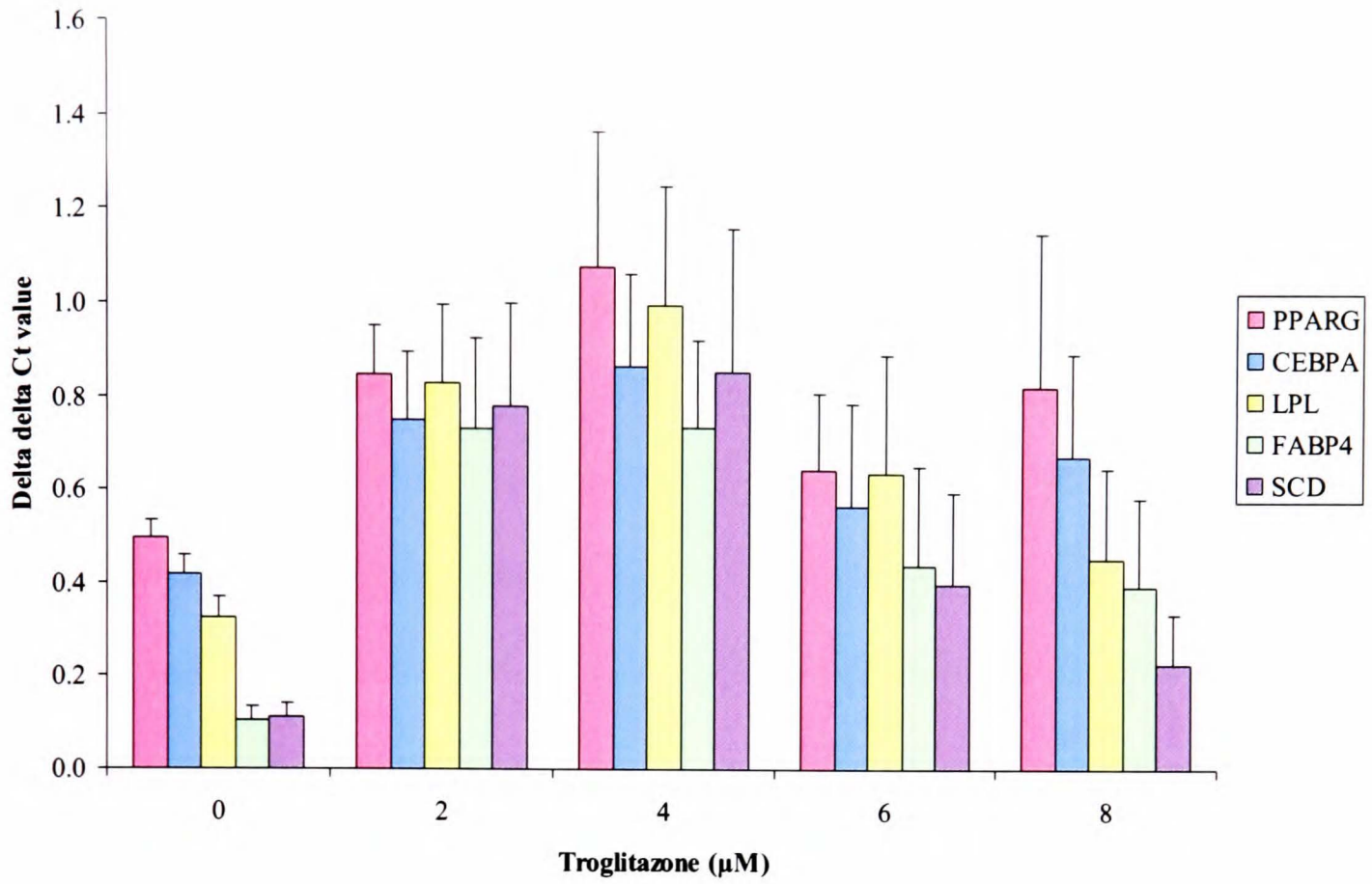


Figure 2-6 mRNA expression of *PPARG*, *CEBPA*, *LPL*, *FABP4* and *SCD* in Troglitazone-treated adipocytes. Data are represented as mean ± SEM (n = 9) Delta delta Ct value = Gene of interest/housekeeping gene (taken as the geometric mean of three separate housekeeping genes. Refer to Appendix 1, section A1.6.2 for details.)

2.2.2. Summary

The extent of preadipocyte differentiation in the presence of Troglitazone (0-8 μM) was determined by total ORO uptake, TG accumulation, SCD activity, G3-PDH activity and mRNA expression of *PPARG*, *CEBPA*, *LPL*, *FABP4* and *SCD*. At high concentrations of Troglitazone (6 to 8 μM) there were adverse effects on the cells resulting in reduced lipogenesis. From these results, it was concluded that the optimum Troglitazone concentration is 2 μM as it yielded maximum adipogenesis and did not inhibit cell growth.

2.3. THE USE OF STABLE ISOTOPES TO TRACE FATTY ACID METABOLISM

^{13}C is a stable isotope of native carbon, ^{12}C. The carbon composition of a compound can be measured using gas chromatography-mass spectrometry (GC-MS) (**Appendix 1**, section **A1.4**). By labelling either non-lipid precursors to fatty acid synthesis or exogenous fatty acids with this carbon isotope, their fate in cells can be traced. Stable isotopes have been used previously in our group in whole body, *in vivo* studies (Chong *et al.*, 2007; Evans *et al.*, 2008). Here, I have adapted their use for *in vitro* studies.

Uniformly labelled palmitate ([U-^{13}C]palmitate) was added, bound to albumin, to differentiating adipocytes. This enabled me to distinguish exogenous from endogenously-produced palmitate in the differentiating human adipocyte, since endogenously-produced palmitate would contain only unlabelled carbon (^{12}C). Palmitic acid was added to the medium during differentiation as follows. A stock was prepared of human albumin (10 g /100 ml) to which was added palmitic acid, 10 mM. This was diluted into the differentiation medium to produce the desired concentration of palmitic acid (50, 200 or 400 μM).

Non-esterified fatty acids are transported through plasma bound to albumin (Spector, 1975). Each molecule of albumin has a number of binding sites for fatty acids. A small proportion of non-bound fatty acids, in equilibrium with the bound fraction, is thought to be relevant for cellular uptake (Abumrad *et al.*, 1998; Stremmel *et al.*, 2001). Direct measurements of this fraction in human serum suggest concentrations in the 5 - 10 nM range (Richieri & Kleinfeld, 1995). Human plasma albumin

concentrations are typically 4 g/100 ml units, which equates to 0.6 mmol/l; with a typical NEFA concentration of 0.5 – 1.0 mmol/l, this would represent a NEFA:albumin molar ratio of around 1:1. The palmitate:albumin molar ratio in the medium prepared as above was 6.6. Although this might appear unphysiological, the situation in vivo is complex, as albumin is not present at plasma concentrations throughout the interstitial space, and also there may be direct presentation of fatty acids to the adipocytes via the lipoprotein lipase pathway (the normal route for adipocytes to take up fatty acids in vivo), since it has been shown that fatty acids derived from the action of lipoprotein lipase are taken up more efficiently than are plasma NEFA (Bickerton *et al.*, 2007). Similar ratios of fatty acid:albumin has been used in several previous cellular studies (for example, (Kharroubi *et al.*, 2004; Moffitt *et al.*, 2005)).

Additionally, the use of stable isotopes was used to assess the contribution of precursors to fatty acid synthesis using [U-^{13}C]glucose and [U-^{13}C]glutamine, and tracing ^{13}C incorporation into TG fatty acids (**Chapter 3**). As there is naturally occurring ^{13}C, all samples were corrected for this natural enrichment. These calculations are described in detail in **Appendix 1**, section **A1.4**.

2.4. siRNA-MEDIATED GENE SILENCING

The RNA interference (RNAi) pathway targets mRNA for degradation in a sequence-specific manner, thus preventing protein synthesis (Fire *et al.*, 1998; Fire, 1999). This pathway is employed in response to double-stranded (ds) RNA viral invasion (Bagasra & Prilliman, 2004). Following invasion, the virus releases long dsRNA

which is cleaved by an RNase enzyme, Dicer, to form shorter dsRNA of 21-23 base pairs (bp), termed small interfering RNA (siRNA). The siRNA then associates with RNA-induced silencing complexes (RISCs) and the double-stranded siRNA unwinds, leaving the anti-sense strand within the RISCs. The anti-sense siRNA-RISC then recognises and binds to the target mRNA, targeting it for cleavage by the components of RISCs, which include endonucleases, and protein synthesis is prevented (Leung & Whittaker, 2005) (**Figure 2-7**).

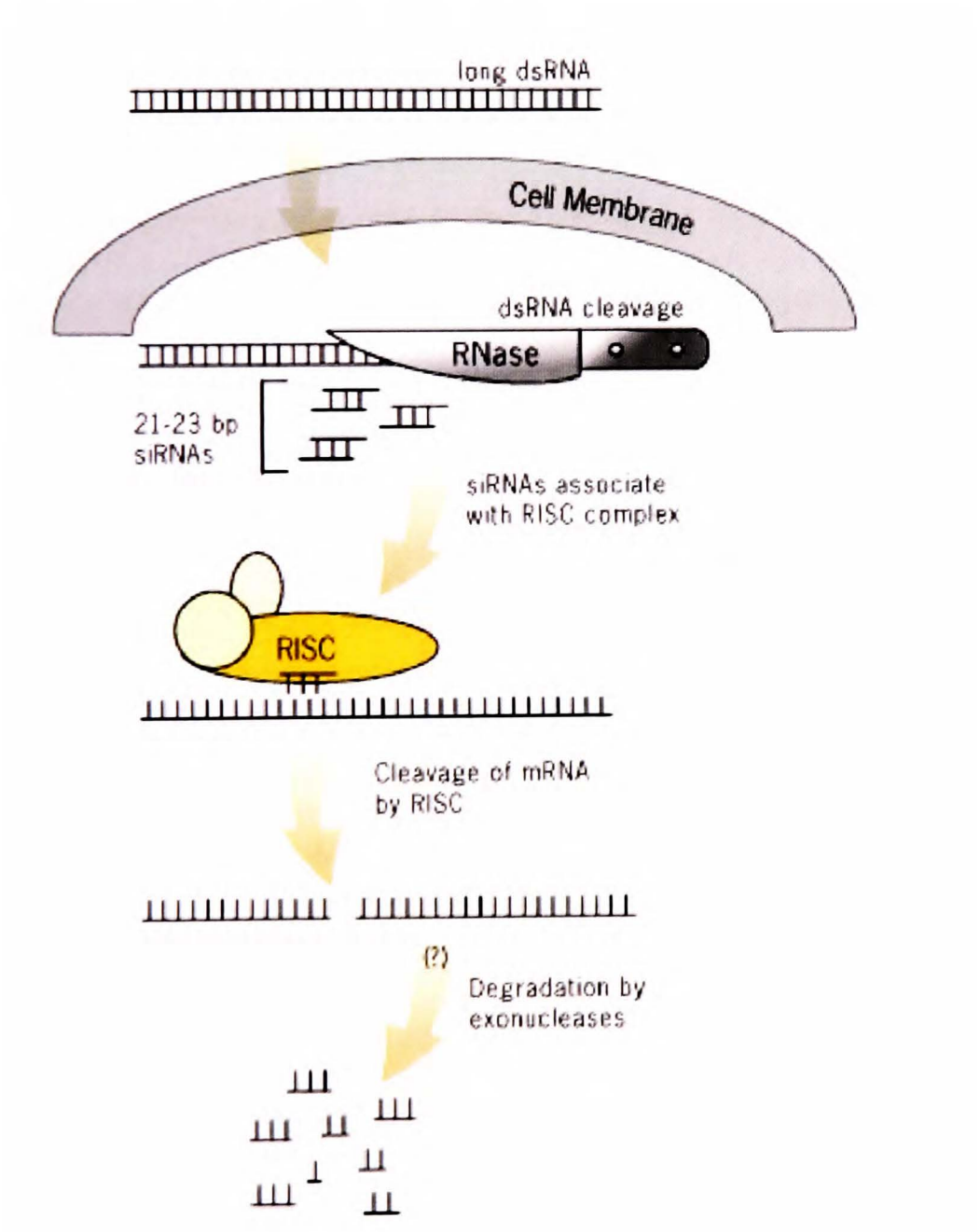


Figure 2-7 Pathway of RNAi

(taken from http://www.ambion.com/techlib/resources/RNAi/overview/index.html)

The RNAi pathway has been exploited as a tool to assess gene function by post-translationally "knocking down" or silencing a target gene, creating a loss-of-function situation within cells (Fire *et al.*, 1998; Maine, 2001). In mammalian cells, the introduction of dsRNA greater than 30 bp elicits an anti-viral response. Therefore, by introducing small interfering RNA (siRNA), short dsRNA of 21-25 bp that are complementory to the gene of interest, into cells the anti-viral response can be overcome whilst still bringing about targeted gene silencing.

2.4.1. siRNA uptake

There are various methods for delivering siRNA to the cell. siRNA can be introduced into the cell either as siRNA directly or as short hairpin RNA (shRNA). siRNA can be delivered to the cell using electroporation or lipid- or peptide-based carriers to bring about transient gene silencing. On the other hand, shRNA delivery requires a vector-based transfection, such as a plasmid or viral vector, the latter resulting in stable gene silencing. The use of plasmid vectors for shRNA delivery to the cell is problematic in primary cells, and commonly used vectors include viral vectors such as lentivirus and adenovirus (Leung & Whittaker, 2005). An RNA polymerase III promoter is used to initiate transcription of the shRNA, and to ensure its expression within the cell. The long shRNA hairpin structures are cleaved by Dicer to form siRNAs that facilitate target mRNA degradation. Selection of cells expressing shRNA can be achieved by incorporating an antibiotic resistance gene into the transfection vector and adding the antibiotic to the culture medium to ensure complete knockdown within the cell population. Although the use of shRNA ensures long-term transfection, successful delivery of the vector can be difficult.

Direct siRNA transfection is usually a simpler method than shRNA, in that it involves either electroporation or creating an siRNA-carrier complex that can be taken up by the cell via the culture medium. However, this method of transfection is only transient (Leung & Whittaker, 2005).

My initial experiements aimed to target *SCD* mRNA for siRNA-mediated silencing in differentiated adipocytes. As I set out to achieve a short-term knockdown, I chose to transfect the adipocytes using Lipofectamine™ 2000 (Invitrogen, Paisley, UK), a lipid-amine transfection reagent recommended for transfection of a broad range of cell types. Furthermore, I chose to use a lipid-based transfection reagent as adipocytes are lipid storage cells and are well-equipped to take up lipids.

Assessment of transfection was achieved using a fluorescently labelled non-specific siRNA, BLOCK-iT ™ (Invitrogen, Paisley, UK), and assesssing siRNA uptake. Recommended reagent volumes and concentrations of Lipofectamine™ 2000 and siRNA (**Table 2-1**) were tested and fluorescence was measured using a fluorescein-5-isothiocyanate filter set (λ_{ex} = 494 nm, λ_{em} = 519 nm).

		Media		RNAi transfection	
Culture vessel	**Surface area per well**	**Vol. of plating medium**	**Vol. of dilution medium**	**siRNA**	**Lipofectamine**
96 well	0.3 cm^2	100µl	2 x 25µl	5pmol	0.25µl
24 well	2 cm^2	500µl	2 x 50µl	20pmol	1µl
12 well	4 cm^2	1ml	2 x 100µl	40pmol	2µl
6 well	10 cm^2	2ml	2 x 250µl	100pmol	5µl

Table 2-1 Recommended reagent volumes and concentrations for RNAi from Invitrogen

Uptake of BLOCK-iT ™ was estimated to be around 90 %, as determined by overlay of fluorescent image with light micrograph. **Figure 2-8** shows preadipocytes transfected with BLOCK-iT ™ siRNA.

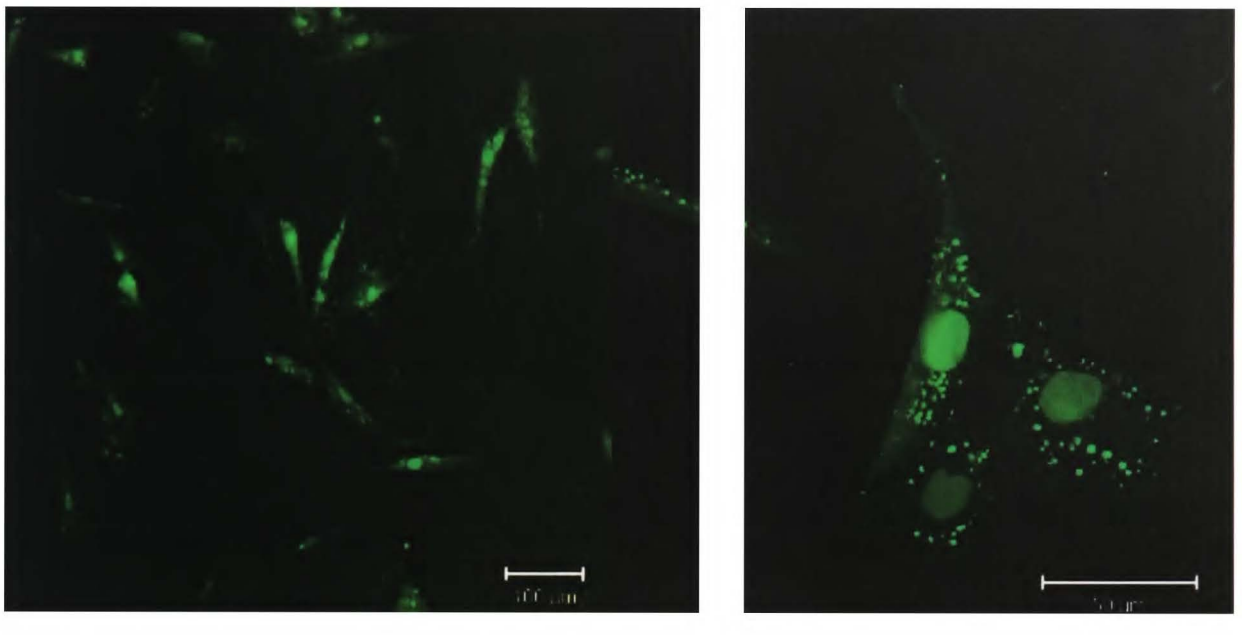


Figure 2-8 Preadipocytes fluorescing due to Block-iT siRNA uptake (x10 and x60 objective)

2.4.2. Protocol for siRNA-mediated knockdown

The protocol for siRNA-mediated gene silencing was adapted from that of Xu *et al.* (Xu *et al.*, 2006), who used this technique to silence *PPARG* expression in human preadipocytes (section **2.4.3**). Preadipocytes were differentiated for 14 days in a culture medium without antibiotics. On day 14, cells were transfected in 6-well plates. The final concentration of siRNA on the cells was 80 nM, therefore, 10 µl of a 20 µM stock solution of siRNA was diluted with 240 µl of antibiotic-free culture medium. For each well, 5 µl Lipofectamine™ 2000 was diluted with 245 µl of antibiotic-free culture medium, gently mixed and left to equilibrate for 5 to 25 minutes. The Lipofectamine™ 2000 and siRNA were combined, gently mixed and left to incubate at room temperature for 20 minutes. The 500 µl siRNA-

Lipofectamine™ 2000 complexes were then added to a well containing 2 ml differentiation medium. Knockdown could be assessed 24 hours after transfection.

2.4.3. *PPARG* mRNA knockdown as proof-of-concept

PPARG mRNA knockdown was performed as a proof-of-concept trial for siRNA gene knockdown. This had already been done in human subcutaneous preadipocytes successfully (Xu *et al.*, 2006) and I used the same siRNAs (Ambion 5636 and 5731 PPARγ siRNA (Ambion, Texas, USA)) to knock down *PPARG* mRNA expression in preadipocytes.

Preadipocytes were transfected (when 50 % confluent) with 80 nM *PPARG*-targeted siRNA using Lipofectamine™ 2000 as a carrier. Controls of no treatment and a negative (scrambled) siRNA (Ambion Negative control #1) were used. After 24 hours, cells were washed with PBS and harvested. mRNA was extracted and cDNA synthesised for real-time (quantitative) PCR quantitation of *PPARG* gene expression (**Appendix 1**, section **A1.6**). Compared with the scrambled siRNA, *PPARG* mRNA expression showed that around 55 to 70 % knockdown was achieved (**Figure 2-9**).

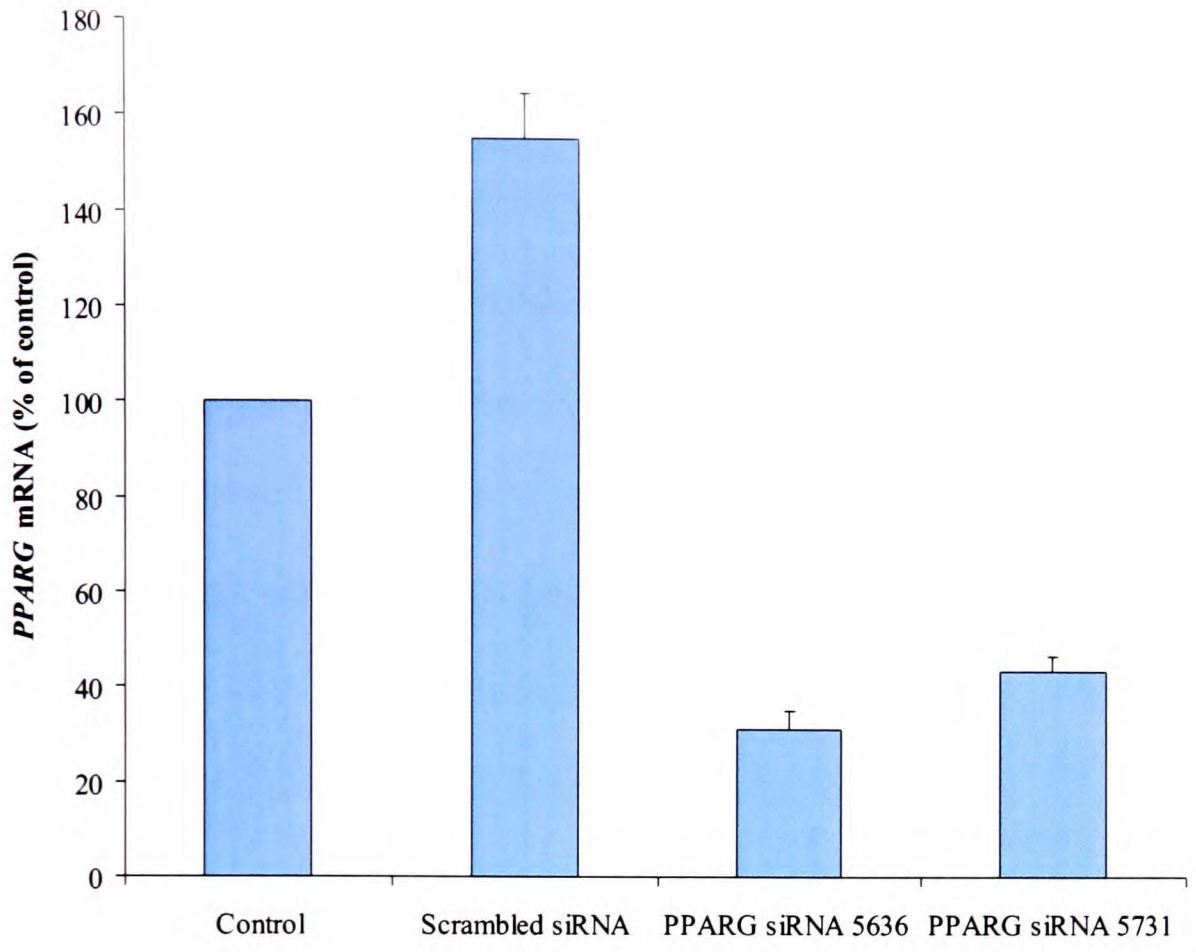


Figure 2-9 *PPARG* mRNA expression in human preadipocytes using siRNA targeted to *PPARG* (Ambion 5636 and 5731) 24 h post-transfection. *PPARG* mRNA is expressed as a comparison with the control. Data are represented as mean ± SEM (n = 3).

Off-target effects of non-specific siRNA may be a potential limitation of siRNA techniques. In a paper by Xu *et al*, the off-target effects of the Ambion Negative Conrol siRNA #1 (used in the *PPARG* knockdown experiments) were shown to up-regulate *PPARG* compared with control cells and mock transfection (Lipofectamine-treated cells) (Xu *et al.*, 2007). This was achieved even at low siRNA concentrations (10 nM) and was increased with higher concentrations. I also saw an up-regulation of *PPARG* mRNA with the Ambion Negative Control #1 and decided not to use it for future experiments.

2.4.4. SCD knockdown using siRNA

I initially set out to knock down SCD after differentiating preadipocytes for 14 days to look at the effects of SCD on cell function and insulin sensitivity. I also wanted to incubate SCD-deficient adipocytes with isotopically-labelled palmitate to look at the effects of SCD on DNL. The original experimental design would not allow easy distinction between DNL-derived fatty acids made prior to SCD knockdown and those made after. My approach therefore changed to attempt to knock down SCD over the 14 days using siRNA and Lipofectamine™ 2000. As siRNA-mediated silencing is a transient knockdown, it would not remain active for 14 days. However, transfection of cells can potentially lead to cytotoxicity and it is not recommended to frequently retransfect. Whereas *PPARG* is known to be expressed during the early stages of differentiation, expression of *SCD* occurs later. Documentation of gene expression during human adipocyte differentiation is sparse. Therefore, I had to determine when to target SCD for siRNA-mediated silencing.

Confluent preadipocytes were differentiated for 14 days (as previously described) and cells harvested every 3 days during the course of differentiation. mRNA expression of various genes involved in adipocyte differentiation was measured (**Figure 2-10**).

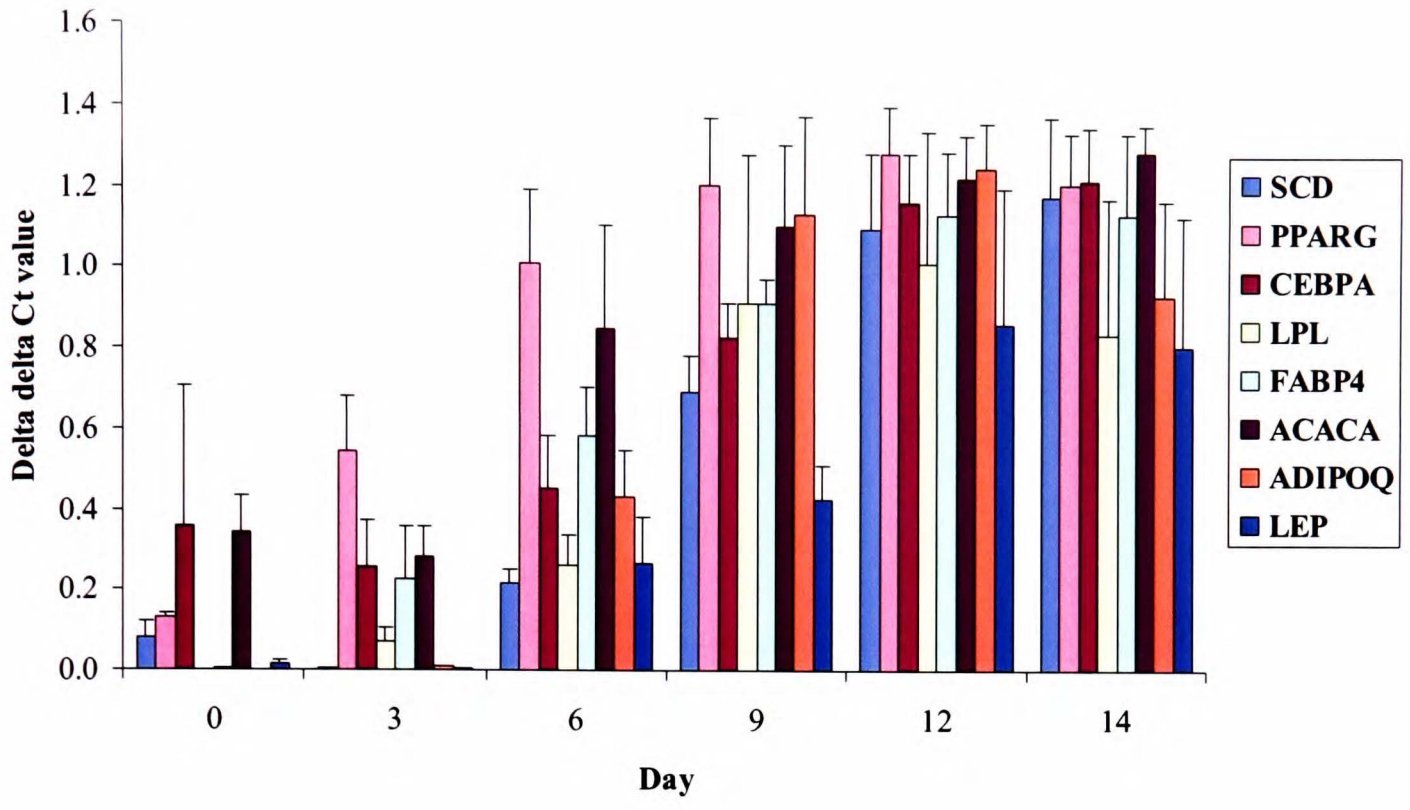


Figure 2-10 mRNA expression of genes expressed during adipocyte differentiation. Gene names: *SCD* = Stearoyl-CoA desaturase, *PPARG* = PPARγ, *CEBPA* = C/EBPα, *LPL* = lipoprotein lipase, *FABP4* = fatty acid binding protein 4, *ACACA* = acetyl-CoA carboxylase, *ADIPOQ* = adiponectin and *LEP* = leptin. Data are represented as mean ± SEM (n = 4)/

Based on the findings of this experiment, day 6 was chosen as the optimum day to target SCD for knockdown. In order to minimise the number of transfections, yet maintain knockdown of SCD, cells were transfected on days 6, 9 and 12 before being harvested on day 14. The results of this procedure are shown in **Chapter 6**.

2.5. MEASUREMENT OF ADIPOCYTE INSULIN SENSITIVITY VIA LABELLED 2-DEOXYGLUCOSE UPTAKE

Uptake of radiolabelled 2-deoxyglucose (2-DOG) is an established method for assessing the insulin sensitivity of adipocytes (Olefsky, 1975; Tanti *et al.*, 2001; Dey *et al.*, 2007). 2-DOG ($C_6H_{12}O_5$) is taken up by the adipocyte by glucose transporters

and is phosphorylated but not further metabolised. Radiolabelling of 2-DOG with ^{3}H (2-deoxy-D-[^{3}H]glucose) allows uptake in response to insulin to be determined using a scintillation counter. Three different insulin concentrations were used to establish a dose-response (0, 10 and 100 nM).

2.5.1. Protocol for 2-DOG uptake in adipocytes

Following differentiation in 6-well plates, adipocytes were washed 3 times in warm PBS. Adipocytes were incubated at 37 °C for 2 hours in Krebs Ringer HEPES (KRH) buffer[2] with 5 mM glucose. After 2 hours, the 5 mM glucose KRH buffer was removed and adipocytes were incubated for 30 minutes at 37 °C with 1.8 ml KRH buffer containing either 0, 10 or 100 nM insulin (Invitrogen, Paisley, UK). After 30 minutes, 200 µl of 2-DOG mixture (containing 37 kBq ^{3}H (2-deoxy-D-[^{3}H]glucose and 2 mM unlabelled 2-DOG) was added for a further 10 minutes. Wells were then carefully washed 3 times with ice cold PBS and harvested in 1 ml Triton X-100 lysis buffer[3]. Cell lysates were transferred to scintillation vials and 7 ml scintillation fluid (OptiPhase 'Safe', Fisher, Leicestershire, UK) added, then counted on a scintillation counter (LSs 6500 Multi-Purpose Scintillation Counter, Beckman, California, USA).

2.5.2. Correction of data for stage of differentiation

Exposure of Ob1771 preadipocytes to palmitate was shown to increase differentiation (Amri *et al.*, 1991; Amri *et al.*, 1994). Furthermore, the extent of differentiation of 3T3-L1 preadipocytes has been associated with changes in insulin-stimulated 2-DOG

[2] KRH buffer consisted of 119 mM NaCl, 4.75 mM KCl, 5 mM $NaHCO_3$, 1.2 mM $MgSO_4$, 1.18 mM $KH_2.PO_4$, 2.54 mM $CaCl_2$ and 20 mM HEPES, pH 7.4 plus 0.01 % bovine serum albumin (BSA).
[3] Triton X-100 lysis buffer consisted of 1 % Triton X-100, 20 nM Tris and 150 mM NaCl.

uptake (Gomez *et al.*, 2002). Therefore, to correct for state of differentiation, all measurements of 2-DOG uptake were corrected for *FABP4* mRNA expression, a marker of adipocyte differentiation. *FABP4* mRNA was chosen as a denominator rather than TG for three reasons. Firstly, *FABP4* mRNA is expressed as *FABP4*/HKG, using the geometric mean of three housekeeping genes (HKGs) measured within the same sample, whereas total TG would be expressed per 10^6 cells. Whereas the HKGs were measured within the same sample, thus correcting for possible differences in starting material (mRNA) or sample loss, cell counting was performed using cells from a separate well with identical cell seeding. Although this acts as a good representation of the number of cells present, it could not be as accurate as the mRNA HKG within-sample measurements. Secondly, the calculation of total TG involves the summation of all the fatty acid peaks as determined by GC, which may factor in error. Thirdly, as will be discussed in **Chapter 4** (section **4.4.4**), *FABP4* mRNA does not increase with palmitate in a dose-dependent manner, whereas TG accumulation does. As *FABP4* mRNA expression is an established marker or differentiation, its expression may also reflect other stages of development within the adipocyte.

2.6. MEASUREMENTS OF CELL MEMBRANE FLUIDITY

2.6.1. Phospholipid fatty acid composition

Total fatty acids were extracted from adipocytes using the method originally described by Folch *et al.* (1957). Individual lipid fractions were then separated using the solid phase extraction technique (**Appendix 1**, section **A1.2**). Using this

technique, PLs, specifically non-acidic PLs, that is, phosphatidylcholine and phosphatidylethanolamine are isolated. Previously, the PL species composition of preadipocytes was determined using thin layer chromatography, and the predominant species present were , phosphatidylcholine and phosphatidylethanolamine (data not shown).

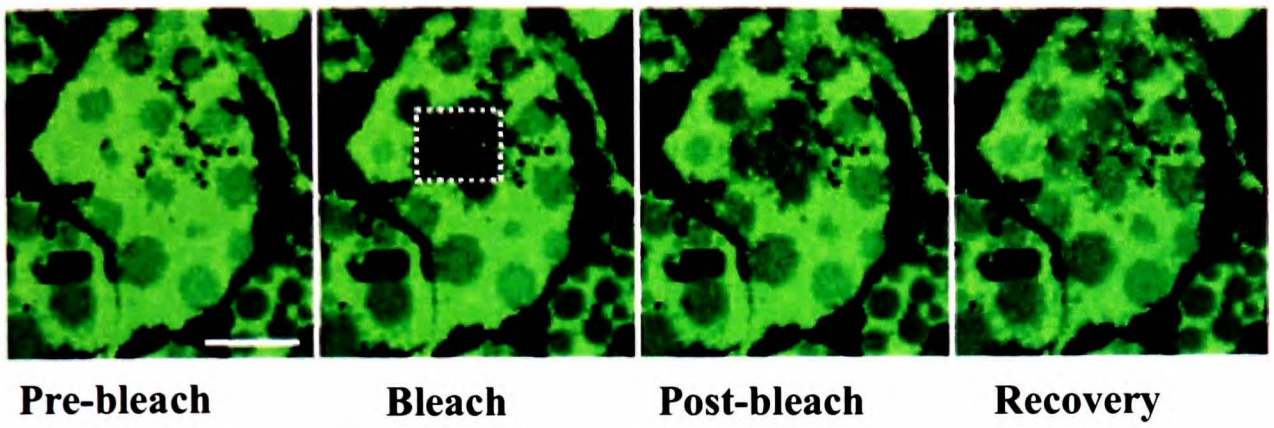
Using GC analysis of the PL fatty acid content within the cells, changes in the ratio of SAFA:MUFA following manipulation of cells was calculated. The ratio of saturated to monounsaturated fatty acids (SAFA:MUFA) in PLs can act as an indicator of cell membrane fluidity, and changes in this ratio can have profound influences on function (Stubbs & Smith, 1984).

2.6.2. Fluorescence recovery after photobleaching (FRAP)

2.6.2.1. Overview

Fluorescence recovery after photobleaching (FRAP) is a method commonly used to assess cell membrane fluidity by studying the mobility of a fluorophore attached to a molecule (in this case a lipid) within the membrane. The bottom of the cell or "footprint", just above the glass coverslip, is scanned using a confocal microscope. A small area of the footprint is photobleached using a laser that delivers pulses of high intensity light on the fluorescent molecules only within the specified area, thus overexciting the fluorophores causing them to go dark or to "bleach". The remaining fluorescently labelled lipid molecules are still free to move. Therefore, if the membrane is fluid they will diffuse and exchange with the bleached molecules, thus restoring fluorescence. The time taken to half maximal recovery from bleaching ($T_{1/2}$) is calculated as $(F_{(\infty)} - F_{(0)}) / 2$ (where F represents fluorescence intensity), and

can be translated to a measurement of membrane fluidity since the speed at which equilibrium is reached between bleached and fluorescent molecules relies on diffusion (Chen *et al.*, 2006) (**Figure 2-11**).



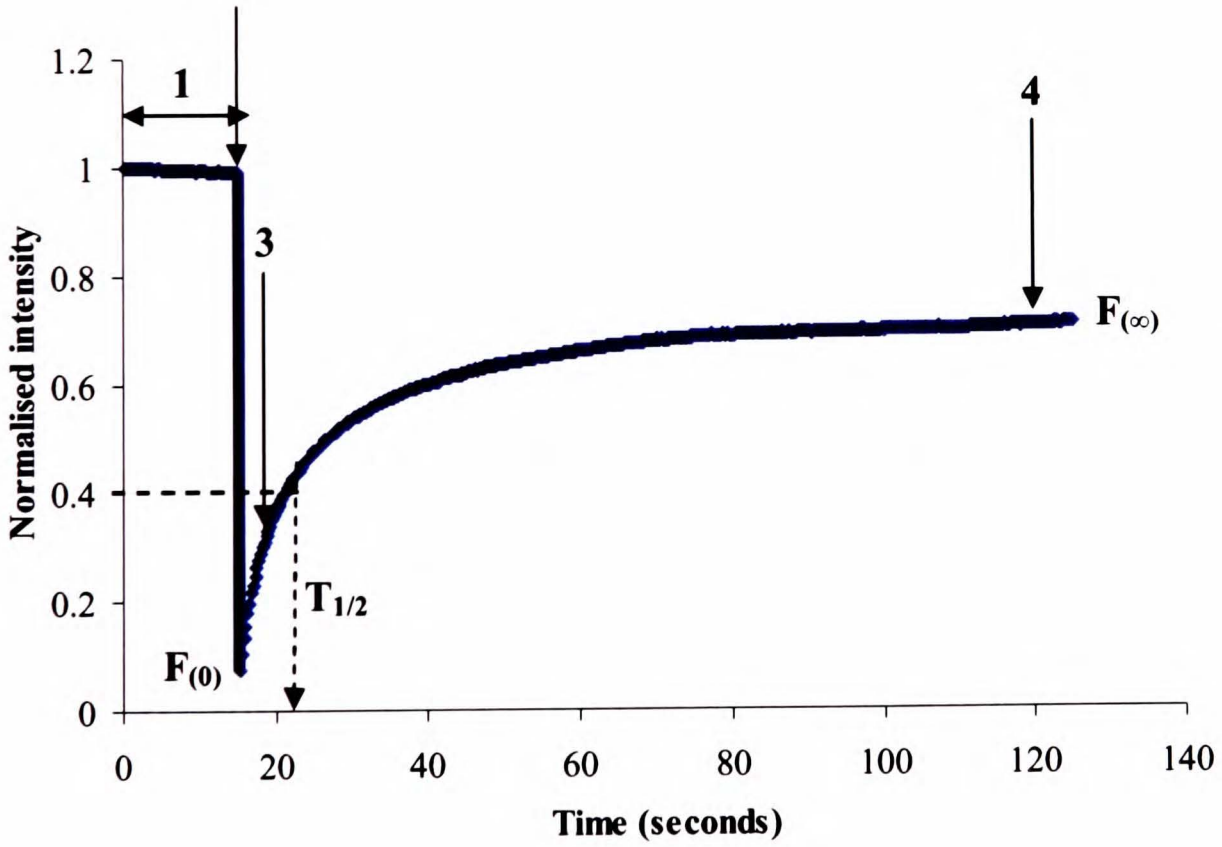


Figure 2-11 Fluorescence recovery after photobleaching (FRAP) (a) Fluorescent micrograph images of the main stages of FRAP in the adipocyte (x63 objective) and (b) and example of a raw data curve of fluorescence intensity (normalised to first frame), showing 1 = pre-bleach, 2 = bleach, 3 = post-bleach and 4 = maximum recovery.

$T_{1/2}$ = time to half-maximal recovery

2.6.2.2. FRAP measurements in human adipocytes

Human preadipocytes were grown on glass coverslips and differentiated for 14 days. Before FRAP analysis, cells were washed in PBS (room temperature) then incubated with 0.5 µl/ml 100 mM BODIPY® 500/510 C_1, C_{12} (4,4-difluoro-5-methyl-4-bora-3a,4a-diaza-*s*-indacene-3-dodecanoic acid) (Invitrogen, Paisley, UK) for 2 minutes at 37 °C. Cells were washed with PBS and the coverslip placed on the confocal microscope for analysis.

Images were acquired using an LSM510 confocal microscope and software (Zeiss, Hertfordshire, UK) using a 488 nm argon ion laser for excitation and x63/1.4 NA (numerical aperture) objective with light collected through a 515 nm longpass filter. Imaging frames were acquired at 4 Hz (4 frames/second) with an image depth of 8 bit. Background fluorescence was assessed by measurements taken 15 seconds prior to bleaching. For each condition, measurements were made on 15 different cells.

Data was analysed using the Metamorph (version 7.1) software package. All intensities were normalised to the intensity at frame 1, and recovery was calculated as the time taken to half the maximum recovery.

2.7. MICROARRAY DATA ANALYSIS

2.7.1. Overview

Microarrays were used as a tool to assess global changes in gene expression in adipocytes in response to palmitate (**Chapter 5**). RNA from adipocytes was used as a template to create cDNA, which, in turn, was used to generate secondary strand cDNA. Double-stranded cDNA then acted as a template from which biotinylated cRNA could be synthesised. Labelled cRNA was fragmented then hybridised to the microarray slide (Codelink (GE Healthcare), Amersham, UK). cRNA binding was visualised using a secondary fluorescent label of Cy5-streptavidin conjugate. Each slide contains approximately 55,000 probes, or "spots", each containing a representative oligonucleotide sequence specific for each gene in the human genome, plus a number of predicted transcripts. Binding of cRNA to each spot was measured using a GenePix 4000 scanner (Molecular Devices, California, USA), and intensities were determined, in order to assess overall changes in gene expression.

2.7.2. Probe intensity normalisation

Microarray probe intensities were determined and the data extracted using the Codelink Expression analysis software (version 5.0). Background correction and normalisation of probe intensities was performed in order to correct for variance between samples and slides, so that an accurate comparison between microarray slides could be made to determine regulation of genes in response to different treatments. There are several methods of microarray normalisation. The most commonly used are global median, cyclic loess and quantile. Briefly, global median normalisation is a within-slide normalization calculated around the median probe intensity for each

slide; cyclic loess uses a pairwise approach of slide comparison to analyse all pairwise combinations which are then used to generate a set of adjustments that are applied to the data set; and finally, the quantile normalization method is a between-slide comparison that aims to make the distribution of the probe intensity of each slide the same (Bolstad *et al.*, 2003). A comparison of these three methods using Codelink data showed the quantile method to be the most sensitive (personal communication with Matt Neville). Probe intensities were log-transformed then quantile-normalised in R, an open source statistical scripting language (http://www.r.project.org) using the Codelink 1.8.1 package (Diez *et al.*, 2007).

2.7.3. Statistical analyses

Detailed statistical analyses were performed on the quantile-normalised data using GeneSifter™ Analysis Edition (www.genesifter.net), a web based microarray analysis software package. Statistically significant changes in gene expression were analysed using 2-way ANOVA and paired *t* test analysis.

2.7.4. Analysis of significant changes in gene expression

To refine the list of changing genes, Genesifter™ can classify genes into groups of common biological pathways based on the Kyoto Encyclopaedia of Genes and Genomes (KEGG) and the Gene Ontology Consortium, databases of genes and their functions. Genesifter™ can list changes in pathways according to *z*-score. The *z*-score is a measure of the likelihood of whether or not the changes in gene expression could have happened by chance alone, and a *z*-score greater than 2, or less than -2, is

generally accepted as representing pathways that have changed significantly and not by chance (Pan *et al.*, 2008).

Genes shown to be changing significantly were listed according to pathway and a shortlist of genes was made based on pathways of interest and the statistical significance of change. Verification of microarray findings was achieved by quantitative PCR of a subset of genes.

Chapter 3

Characteristics of DNL in the human adipocyte

3.1. INTRODUCTION

The main end product of *de novo* lipogenesis (DNL) is the saturated fatty acid palmitate. This process requires cytosolic acetyl-CoA generated from non-lipid precursors and uses NADPH as an energy source, as described in section **1.4.1**. The human adipocyte acts primarily to store excess circulating fat, usually dietary fat, as triglycerides (TGs), so the need for *de novo* fatty acid synthesis in these cells, therefore, may be questionable. Rodent adipocytes are known to be capable of DNL; however, the role of this process in human fat cells is not clear. It has been argued that human adipocytes have low activity of the enymes crucial to lipogenesis, such as fatty acid synthase and acetyl-CoA carboxylase, and may even completely lack ATP-citrate lyase (Shrago *et al.*, 1969; Shrago *et al.*, 1971). Conversely, others have shown human adipose tissue is able to synthesise fatty acids, though neither the significance nor the capacity of human adipocyte DNL are well understood (Sjöstrom, 1973; Angel & Bray, 1979; Guo *et al.*, 2000).

Adipose tissue DNL is thought to be minimal during normal feeding (Mellati *et al.*, 1970; Diraison *et al.*, 2003) but is increased in situations of carbohydrate overfeeding (Chascione *et al.*, 1987; Aarsland *et al.*, 1997). This process has been viewed as a means to dispose of excess carbohydrate, occurring as a last resort, that is, when glycogen stores are saturated (in liver and muscle) and when glucose disposal via oxidation is insufficient (Acheson *et al.*, 1988; Minehira *et al.*, 2003). However, Strawford *et al.* (Strawford *et al.*, 2004) measured DNL in human adipose tissue over nine weeks under normal feeding conditions and concluded that 20 % of newly-deposited TG-palmitate in adipose tissue had been synthesised endogenously, showing that this process may not just be limited to times of carbohydrate excess.

Studies in our group have suggested a role for DNL in the mature human adipocyte, and that small adipocytes have a higher expression of DNL-associated genes than large adipocytes (Roberts *et al.*, 2009).

Insulin release from the pancreas is increased after feeding, in response to glucose, and promotes the uptake of glucose into insulin-responsive tissues. Insulin is known to be lipogenic and promotes fatty acid synthesis. In adipocytes, adipogenic genes such as fatty acid synthase and acetyl-CoA carboxylase are up-regulated by insulin (Girard *et al.*, 1994; Moustaid *et al.*, 1996). Up-regulation of DNL by insulin may be due to an increase in levels of the transcription factor SREBP1c.

The main substrate for DNL in the human adipocyte has not been fully identified. Early *in vitro* experiments tracing the fate of radiolabelled glucose towards triglyceride fatty acid synthesis in isolated mature human adipocytes concluded that only a small proportion of glucose, around 5 to 15%, was converted to fatty acids whereas the majority, 85 to 95%, was channelled towards TG-glycerol synthesis (Gries & Steinke, 1967; Galton, 1968; Shrago *et al.*, 1971). These findings propose that glucose utilisation in the mature adipocyte is primarily for TG-glycerol synthesis and not for DNL. This does not mean that when DNL occurs, glucose is not the primary precursor, but also does not rule out other substrates. A recent study in brown adipocytes highlighted glutamine as a precursor for fatty acid synthesis (Yoo *et al.*, 2004). Glutamine has also been shown previously to be a substrate for glyceroneogenesis (Ballard *et al.*, 1967; Reshef *et al.*, 1970) making it a likely candidate for fatty acid synthesis in the human adipocyte.

Throughout this thesis, the established method of *in vitro* differentiation of human preadipocytes described by Hauner *et al.* (2001) has been used. This method uses a chemically-defined, serum-free medium with no added fatty acids to achieve differentiation and results in the formation of lipid droplets within the cells. This suggests instantly that fatty acids synthesised within these cultured adipocytes originate from an endogenous source. Interestingly, preadipocytes differentiated using this fatty acid-free method appear similar to those differentiated with an exogenous fatty acid supply (**Figure 3-1**).

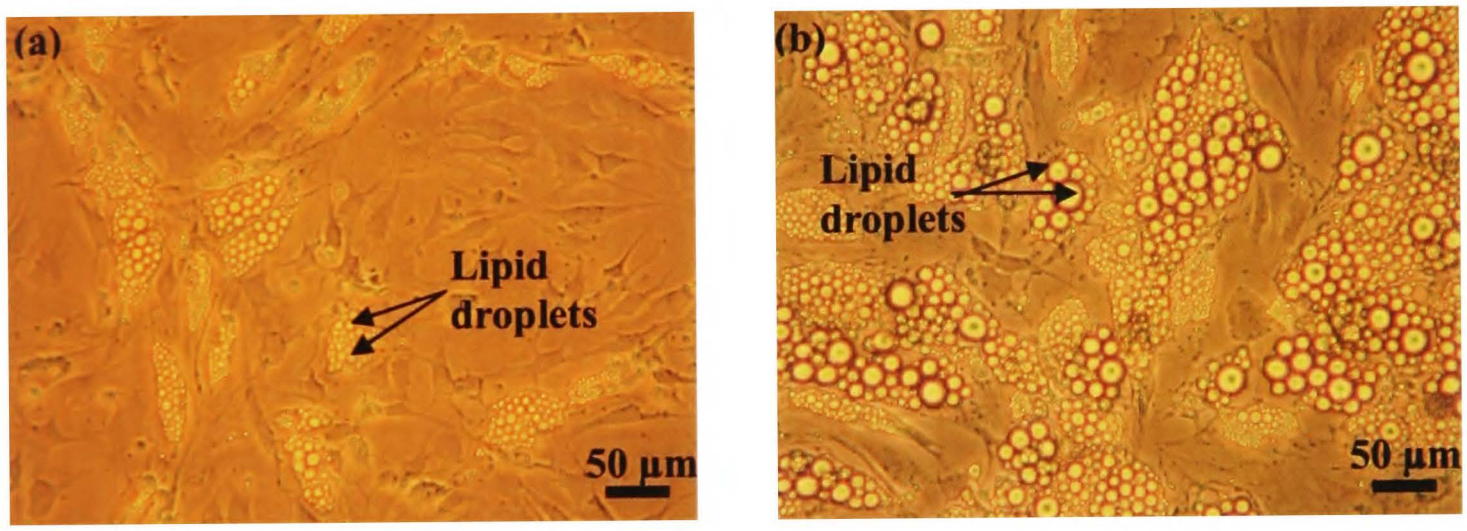


Figure 3-1 Human adipocytes differentiated in the absence of fatty acids (a) and with a combination of different exogenous fatty acids (b) (x10 objective)

An over-abundance of palmitate has been shown to have lipotoxic effects in cells; for example, in pancreatic β-cells, incubation with palmitate led to an accumulation of tripalmitin, a TG molecule comprising three palmitate chains with a melting point of around 65 °C, in the endoplasmic reticulum (ER). This led to morphological distortions of the ER and impairment of cellular function (Moffitt *et al.*, 2005). Therefore, if DNL were the sole source of fatty acids in preadipocytes differentiated with no exogenous source of fatty acids, the TG fatty acids would be expected to be

composed exclusively of palmitate which may have adverse effects on cell function. As cells appeared healthy, this prompted investigation into the fatty acid composition of the TG and of the pathways involved in their creation.

3.2. AIMS

The aims of this chapter were to define the characteristics of DNL within the differentiating human preadipocyte *in vitro*, with a specific focus on both the capacity for DNL within these cells in the absence of an exogenous fatty acid source, and on the fatty acid composition of intracellular TG. The pathway of DNL has been shown to operate in concert with SCD (Chong *et al.*, 2008); therefore, metabolic modification of palmitate was studied. As glucose may not be the sole precursor for DNL-derived fatty acids, the role of glutamine as a precursor was also investigated. The carbon contribution of glucose and glutamine to TG-glycerol was also explored.

3.3. METHODS

3.3.1. Adipose tissue sample collection

The taking of human adipose tissue samples was approved by the Oxfordshire Clinical Research Ethics Committee and all subjects gave written, informed consent. Subcutaneous adipose tissue biopsies were taken and preadipocytes isolated as described in **Chapter 2**, section **2.1.2**.

Volunteers for the experiments described in this chapter consisted of 30 males and 39 females.

3.3.2. Fatty acid analysis

Total lipids were extracted and the TG fraction isolated as described in **Appendix 1**, section **A1.2**. TG fatty acid composition was analysed using GC (**Appendix 1**, section **A1.3**).

3.3.3. Isotopic tracer incorporation

Preadipocytes were differentiated in the presence of isotopically (^{13}C)-labelled substrates in order to determine the major precursors for DNL. 1 mM [1-^{13}C]Acetate (CK gas, Hampshire, UK; 98 % purity) was added to the medium throughout differentiation. No unlabelled acetate was present in the medium at the start of differentiation. In separate experiments, [U-^{13}C]glucose and [U-^{13}C]glutamine (both from CK gas, Hampshire, UK; 98 % purity) were added to the medium. In the case of [U-^{13}C]glucose, glucose-free medium was purchased (Sigma Aldrich, UK), and [U-^{13}C]glucose was added to a concentration of either 5 mM ('low glucose') or 17.5 mM ('high glucose'). The [U-^{13}C]glutamine experiments were conducted by replacing glutamine (which was normally added separately to the incubation medium) with [U-^{13}C]glutamine, at a concentration of 2 mM. The glutamine experiments were carried out at a glucose concentration of 17.5 mM, the concentration present in standard differentiation medium.

After 14 days of differentiation in the presence of the various isotopically enriched media, cells were harvested and lipid extracted as described in **Appendix 1**, section **A1.2**. Fatty acid methyl esters (FAMEs) prepared from the TG fraction were analysed using gas chromatography-mass spectrometry (GC-MS) (**Appendix 1**, section **A1.4**). This produced a 'mass spectrum' for each fatty acid. For 16:0, for instance, the mass

of the all-^{12}C variant (isotopomer) of methyl-palmitate is 270.3 (denoted M+0 for native mass). The abundance of each mass isotopomer up to mass 286.3 (denoted M+16) was quantified by GC-MS. This was done for each of the fatty acids (14:0, 16:0, 16:1 *n-7*, 18:0, 18:1 *n-9* and 18:1 *n-7*) that were present in easily detectable amounts. A typical mass spectrum for palmitic acid, from cells differentiated in the presence of [U-^{13}C]glucose, is shown in **Figure 3-2**.

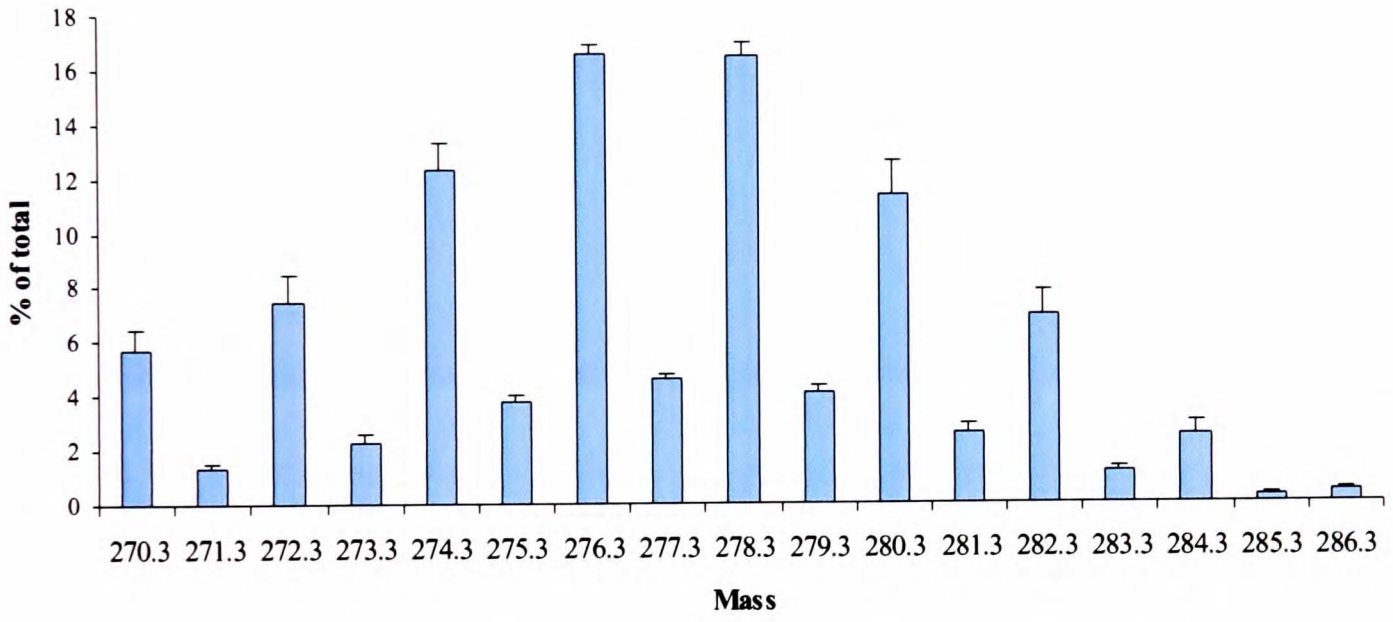


Figure 3-2 Mass spectrum of palmitate showing isotopomers (M to M + 16). Data are represented as mean ± SEM (n = 6)

The glycerol component of the TG was also isolated and subjected to GC-MS analysis after preparation of the tert.-butyldimethylsilyl derivative (**Appendix 1**, section **A1.5**).

The data were used in two ways: mass isotopomer distribution analysis (MIDA) and quantitative mass spectral analysis.

The results were sent to Dr Dirk-Jan Reingoud, Dr Theo van Dijk and Professor Folkert Kuipers at the University Medical Centre Groningen of the University of

Groningen, the Netherlands, for MIDA. MIDA was developed for studying the synthesis of polymeric molecules, such as fatty acids, and has been applied extensively to the analysis of DNL *in vivo* (Hellerstein & Neese, 1992; Hellerstein & Neese, 1999). This analysis uses the pattern of labelling amongst the mass isotopomers to give information about the synthetic pathways, and also about the level of enrichment of the immediate substrate (in this case acetyl-CoA) to enable calculations of the rate of synthesis (Hellerstein, 1999). The latter aspect was not important in the present case, because, as will be described below, essentially all the TG-fatty acids were derived from DNL and the rate of synthesis was simply reflected in the total TG content.

The simpler approach of quantitative mass spectral analysis was based on the method described by Tayek and Katz (1996). First, all relative abundance values were corrected for the natural abundance of ^{13}C. The presence of ^{13}C in all natural carbon sources (around 1.1%) will lead to significant abundances of M+1 through to M+3. These natural abundance values were obtained from measurements made in cells with no added labelled substrate. The corrected values then represent carbon atoms that have been labelled from the labelled precursor.

The (corrected) distribution of mass isotopomers was then used as follows. The abundance of all the mass isotopomers found for a given fatty acid was scaled so that their sum was 100 %. The relative abundance of each mass isotopomer (denoted M+n) was then multiplied by the excess mass compared with M; for example, for the M+4 peak, the relative abundance of that peak was multiplied by 4. The sum of all these products

$$\sum_{n=16}^{n=0}(M+n)$$

is called, by Tayek & Katz, the molar enrichment. Tayek & Katz state that these molar enrichment values are 'exactly equivalent to the relative specific activity with radioactive tracers'. This molar enrichment can then be compared with that of the precursor, but allowing for the different numbers of carbon atoms in precursor and product. For [U^{13}C]glucose, the precursor 'molar enrichment' calculated in the same way is 600 %.

We devised a simpler treatment (which gave the same results). The molar enrichment calculated as above is equivalent to the number of labelled (^{13}C) carbon atoms in 100 molecules of the fatty acid (in this case palmitic acid). Given that all carbons in the substrate (e.g. [U^{13}C]glucose) were ^{13}C (this assumption was tested, as described later in the chapter), it was then possible to say that the percentage of the palmitic acid that had been synthesised from glucose in the medium was:

$$(\sum_{n=16}^{n=0}(M+n))*100/(total_carbon_atoms_in_100_molecules_of_product)$$

Or, in the case of palmitic acid,

$$(\sum_{n=16}^{n=0}(M+n))*100/(16*100)$$

Exactly the same calculations could be made for other fatty acids, for the TG-glycerol, and also for TG-fatty acids and TG-glycerol produced in the presence of [U-^{13}C]glutamine.

3.3.4. Statistical analyses

Relationships between SCD indices and mRNA expression were made tested using the Spearman non-parametric coefficient, r_s. Comparisons between low and high glucose groups and their contributions to fatty acid mass were made using repeated measures analysis of variance (ANOVA). All statistical analyses were performed using SPSS, version 15.

3.4. RESULTS

3.4.1. Preadipocyte differentiation in the absence of exogenous fatty acids

Adipocytes differentiated in differentiation medium containing no fatty acids formed lipid droplets as seen by oil red O staining (**Figure 3-3**). The fatty acid composition of the stored TG showed the products of DNL, myristate (14:0) and palmitate (16:0), providing evidence for DNL (**Figure 3-4**). The TG fatty acid profile also showed palmitate elongation to stearate, and desaturation of these saturated fatty acids to form the monounsaturated fatty acids palmitoleate (16:1 *n-7*) and oleate (18:1 *n-9*), respectively. The presence of vaccenate (18:1 *n-7*) implied elongation of palmitoleate. These fatty acids suggest activity of fatty acid elongase (elongation of very long chain fatty acids-like 6 (Elovl6)) and stearoyl-CoA desaturase (SCD). Interestingly, adipocytes lacked detectable linoleate (18:2 *n-6*), an essential fatty acid,

and all fatty acids present in the TG appeared to have been made endogenously. A typical gas chromatogram displaying the fatty acids seen in these cells is in **Appendix 1**, section **A1.3 (Figure A1-1)**.

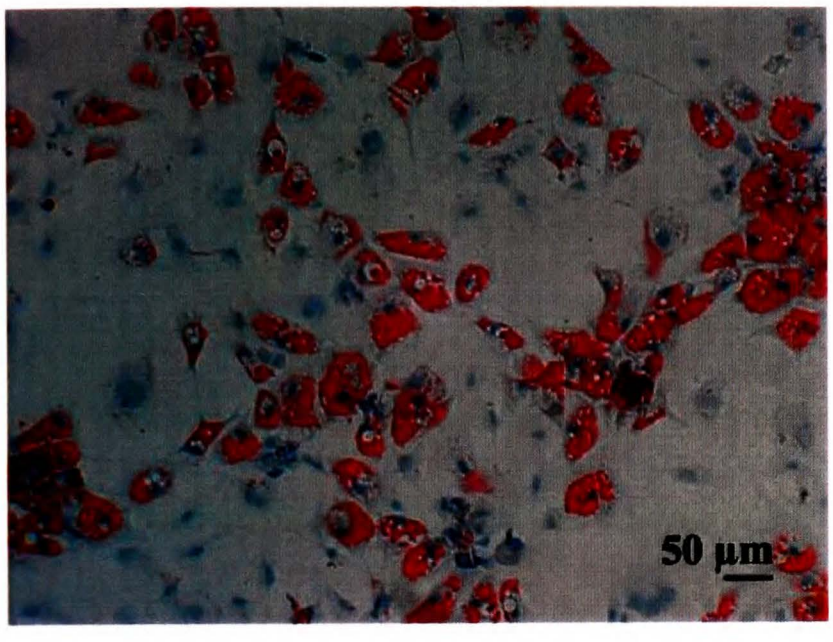


Figure 3-3 Oil red O stained adipocytes, counterstained with haematoxylin (x10 objective)

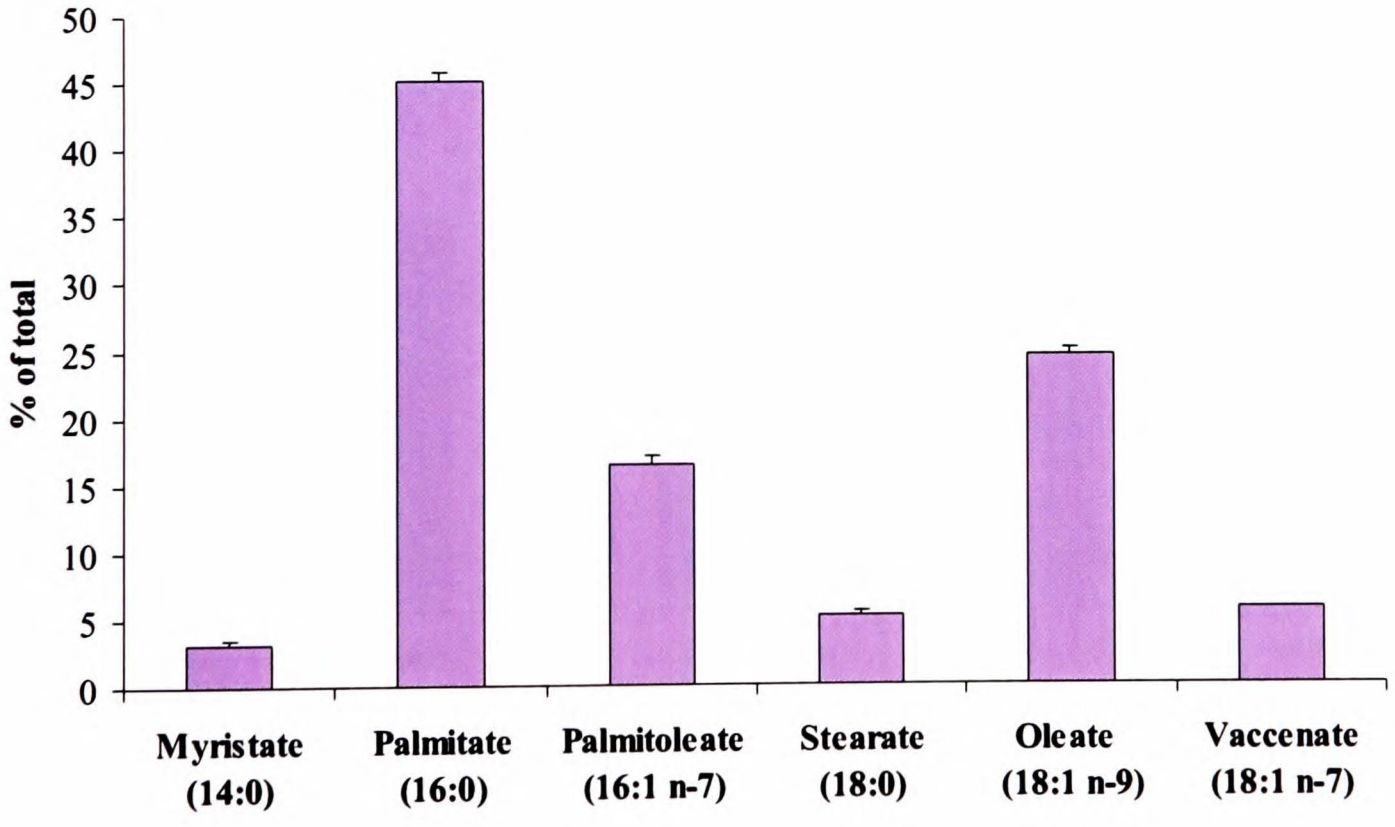


Figure 3-4 Fatty acid profile of adipocyte TG. Data are represented as mean ± SEM (n = 69)

To provide further evidence of DNL and subsequent desaturation and elongation in the differentiated preadipocytes, mRNA expression of DNL-associated genes was measured. Expression of glucose 6-phosphate dehydrogenase (*G6PD*), acetyl-CoA carboxylase (*ACACA*), ATP-citrate lyase (*ACLY*), fatty acid synthase (*FASN*), stearoyl-CoA desaturase (*SCD*) and diacylglycerol acyltransferase 2 (*DGAT2*) as well as the pro-lipogenic transcription factors CCAAT-enhancer binding protein α (*CEBPA*), peroxisome proliferator-activated receptor γ (*PPARG*) and sterol regulatory element binding protein 1c (*SREBF*) supported TG fatty acid data (**Figure 3-5**). *ELOVL6* was also expressed but at lower levels than the other genes, perhaps suggesting a comparatively minor role for this enzyme. Therefore, the TG fatty acid profiles, together with the expression of DNL-associated genes, provided solid evidence for not only the occurrence of DNL within the human adipocyte but also for post-DNL fatty acid modification.

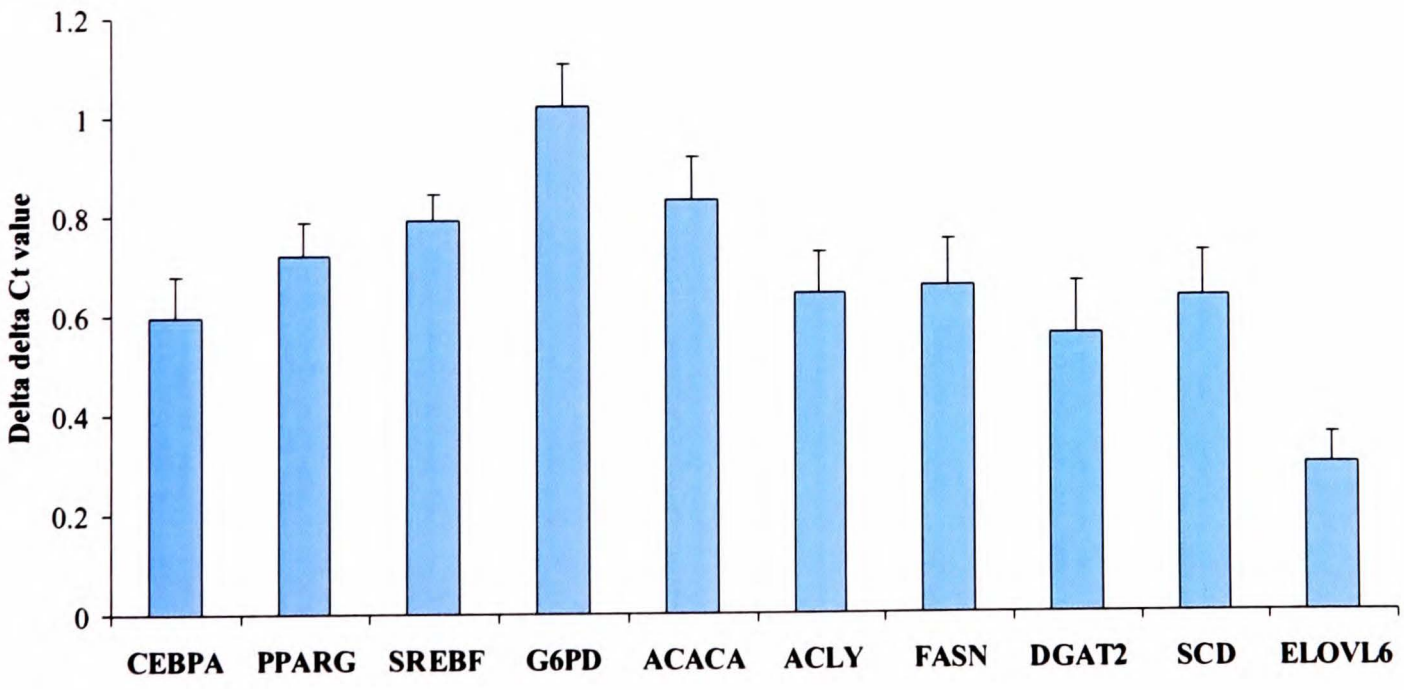
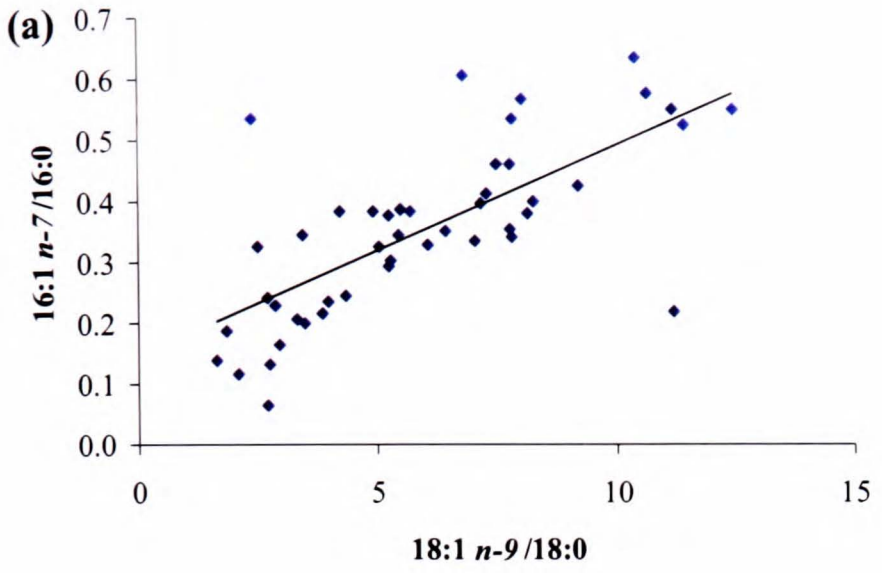
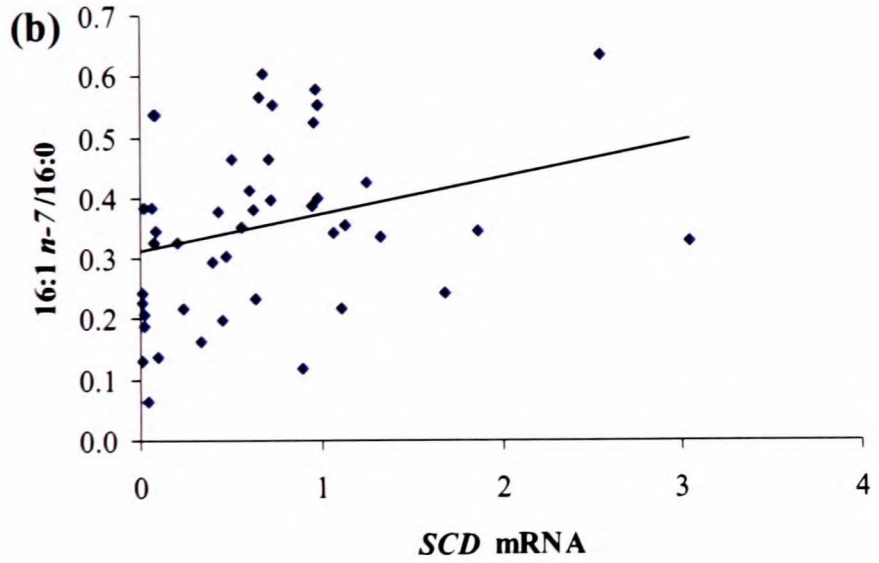


Figure 3-5 Relative mRNA expression of DNL-associated genes in differentiated preadipocytes. Delta delta Ct value = Gene of interest/housekeeping gene (taken as the geometric mean of three separate housekeeping genes. Refer to Appendix 1, section A1.6.2 for details). Data are represented as mean ± SEM (n = 50).

The SCD index is a proxy measure of SCD activity and is calculated using product-to-precursor ratios, that is, 16:1 *n-7*/16:0 and 18:1 *n-9*/18:0. **Figure 3-6** shows the correlation between the SCD indices and *SCD* mRNA expression. Both 16:1 *n-7*/16:0 and 18:1 *n-9*/18:0 ratios correlated positively with each other (r_s = 0.724, P = 0.000) and with *SCD* mRNA expression (r_s = 0.347, P = 0.017 and r_s = 0.648, P = 0.000, respectively). This is in agreement with Sjögren *et al.* (2008) who also showed a correlation between *SCD* mRNA and 16:1 *n-7*/16:0 and 18:1 *n-9*/18:0 in subcutaneous adipose tissue.





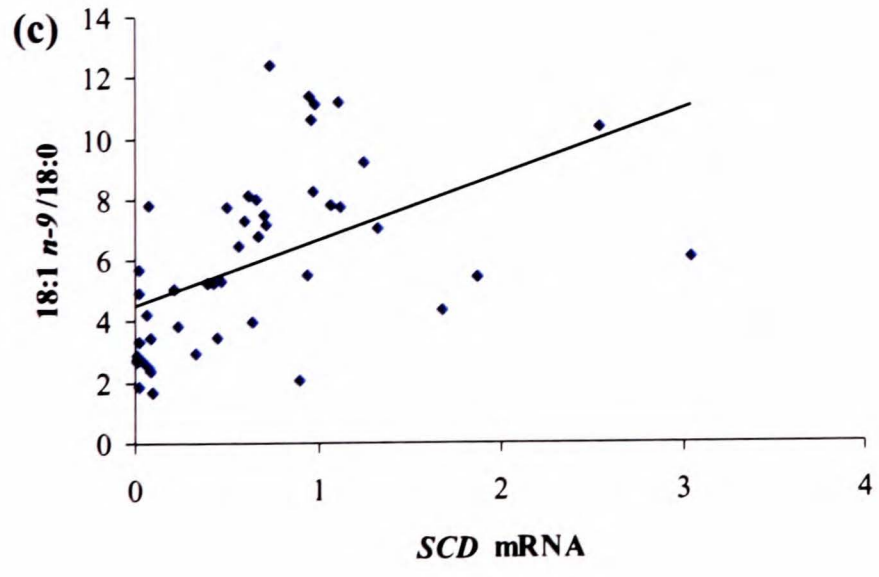


Figure 3-6 Correlations between (a) 16:1 *n-7*/16:0 and 18:1 *n-9*/18:0 SCD indices and (b) 16:1 *n-7*/16:0 and *SCD* mRNA expression and (c) 18:1 *n-9*/18:0 and *SCD* mRNA expression (n = 47)

3.4.2. The relationship between total TG accumulation and characteristics of the fat donor

Studies in mice and humans have shown that age reduces the ability for preadipocytes to differentiate *in vitro* (Kirkland *et al.*, 1990; van Harmelen *et al.*, 2003). Van Harmelen *et al.* (2003) reported that whereas BMI and age of women were positively correlated, there was a negative correlation between BMI (but not age) and differentiation capacity of isolated preadipocytes. In agreement with van Harmelen's study, there was a positive correlation between age and BMI ($r_s = 0.770$, $P = 0.000$). **Figure 3-7** shows there was a negative correlation between total TG accumulation during adipocyte differentiation and age of the fat donor. There was no significant correlation between donor BMI and TG accumulation. There was also no difference between TG accumulation in adipocytes from males and females ($P = 0.768$, Student's *t* test).

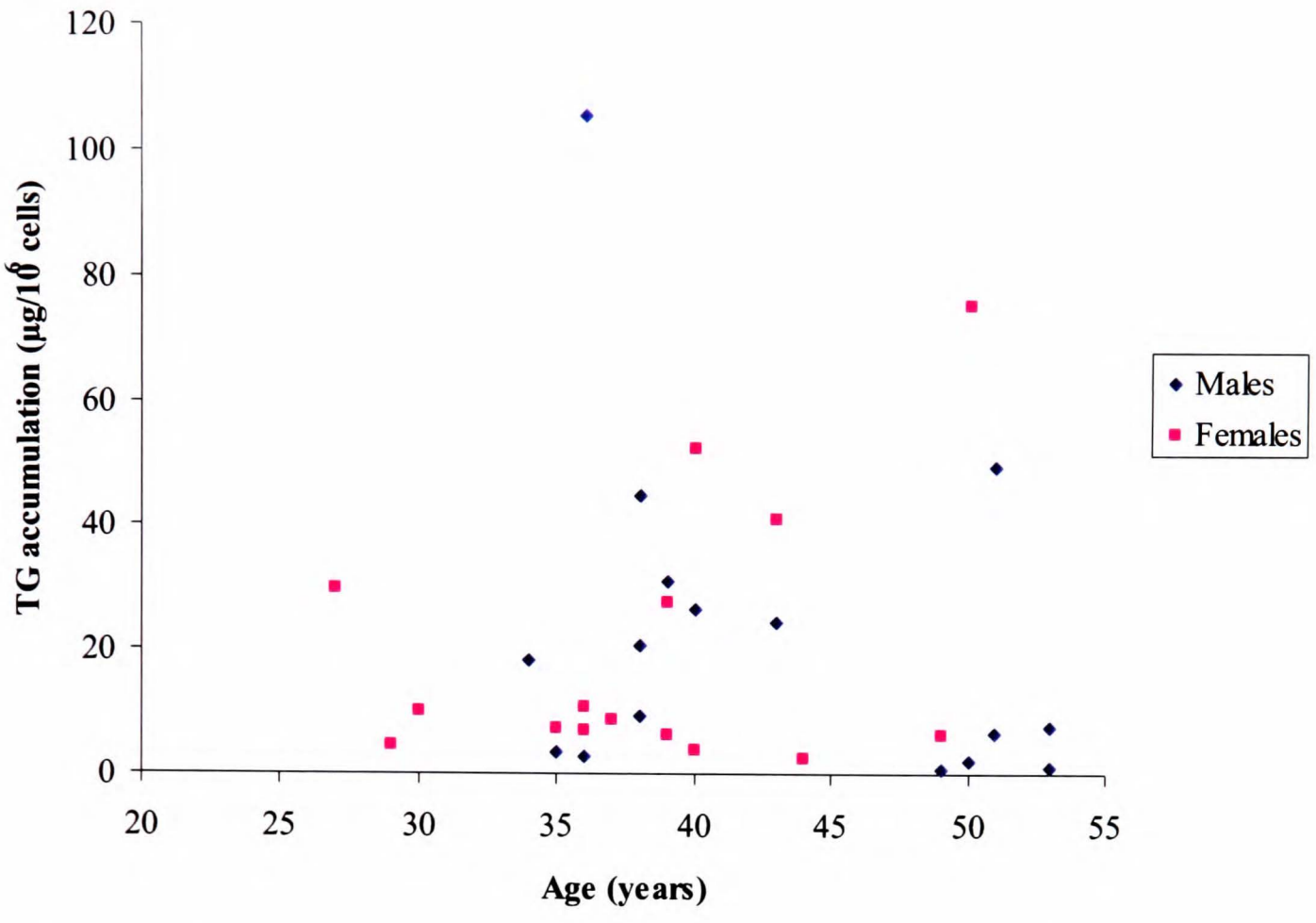


Figure 3-7 Correlation between total TG accumulation in differentiated preadipocytes and age of donor (n = 31) r_s = -0.356, P = 0.046 for males (n = 15) and females (n = 16) together

3.4.3. Acetate incorporation into newly-synthesised fatty acids

A classical MIDA technique is to measure incorporation of isotopically-labelled acetate into newly-synthesised fatty acids, usually to determine rate of synthesis (for an overview of MIDA, refer to **Appendix 1**, section **A1.4.1**). The rate of synthesis in this case was taken as the total enrichment at day 14 of differentiation. Our collaborators suggested that differentiation of preadipocytes with labelled acetate would provide a valuable insight into the fatty acid biosynthetic pathway.

Preadipocytes were differentiated in standard differentiation medium supplemented with 1 mM [1-^{13}C]acetate and incorporation into TG fatty acids was measured using GC-MS. This was measured by calculating the area under the curve for each

isotopomer of each fatty acid, and expressing this as a percentage of the total. **Figure 3-8** shows the incorporation of acetate into each of the TG fatty acids. The labelling of the TG fatty acids emphasised how the pathways of fatty acid synthesis, elongation and desaturation operate within the adipocyte in the absence of exogenous fatty acids. It is worth noting that the maximum possible amount of labelling in each fatty acid would be 50 % due to the fact that two-carbon acetate contained only one ^{13}C label.

MIDA was performed by Dr Dirk-Jan Reingoud and colleagues. His analysis was as follows:

> "The classical MIDA approach does not fit the data at all. One model, which gives at least a better fit, starts from the assumption that intermediates of fatty acid oxidation are substrates in chain elongation. Experimental support of substrate cycling between de novo lipogenesis and fatty acid oxidation at the level of acetyl-CoA have been presented in intact muscle ex vivo (Dulloo *et al.*, 2004). However, substrate cycling at the level of intermediates of fatty acid oxidation might not have been considered before, because incubation conditions were not favourable for this mechanism to show up."

And later, following further analysis:

> "The data of ^{13}C-acetate can only be fitted when we speculate that all possible unlabeled fragments of chain shortening from C2-C14 could be used to make C16. The acetate used in this process comes from a single pool of labeled ^{13}C-acetate. In this calculation the enrichment of the [$^{13}C_1$]-acetate was around 70%, reasonable in view of the near 100% enrichment in the medium. However, the source of these fragments remains obscure. For the glucose data we need to use a model with all possible unlabelled fragments to be used for palmitate synthesis. Added to this, the pool of acetate also contains [$^{13}C_1$]-acetate, besides [$^{13}C_2$]-acetate. This means that for each unlabeled fragment C2-C14 two binomial frequency distributions have to be multiplied to explain the full mass isotopomer spectrum. At this moment, we have no ability to solve this complex mathematical problem yet. The same is true for the [U-^{13}C]-glutamine data. (It resembles somewhat the calculation of mass spectra of compounds with natural isotopic labeling.)"

(Reingoud D-J and colleagues, personal communications, 5th December 2008 and 9th February 2009)

This analysis suggests that pathways of fatty acid synthesis in the human adipocyte are not as straightforward as often believed. The suggestion of concomitant fatty acid oxidation seems unlikely given the high insulin concentration and strongly lipogenic conditions, but led to the investigation of whether myristic acid, not usually thought of as a major product of DNL, might be produced by ß-oxidation (chain-shortening) of palmitic acid: these data will be presented in **Chapter 4**. Further analysis was therefore confined to mass spectral analysis.

Mass spectral analysis of the data from the [1-^{13}C]acetate incorporation experiments showed that 70 % of the palmitate arose from labelled acetate in the medium (**Figure 3-8**). Since 100 % of the palmitate was presumably synthesized from acetyl-CoA, this suggests dilution of the intracellular acetyl-CoA pool with unlabelled molecules coming, for instance, from glucose metabolism. As these experiments did not provide extensive information on DNL precursors in human adipocytes, experiments to investigate [U^{13}C]glucose and [U^{13}C]glutamine incorporation were undertaken.

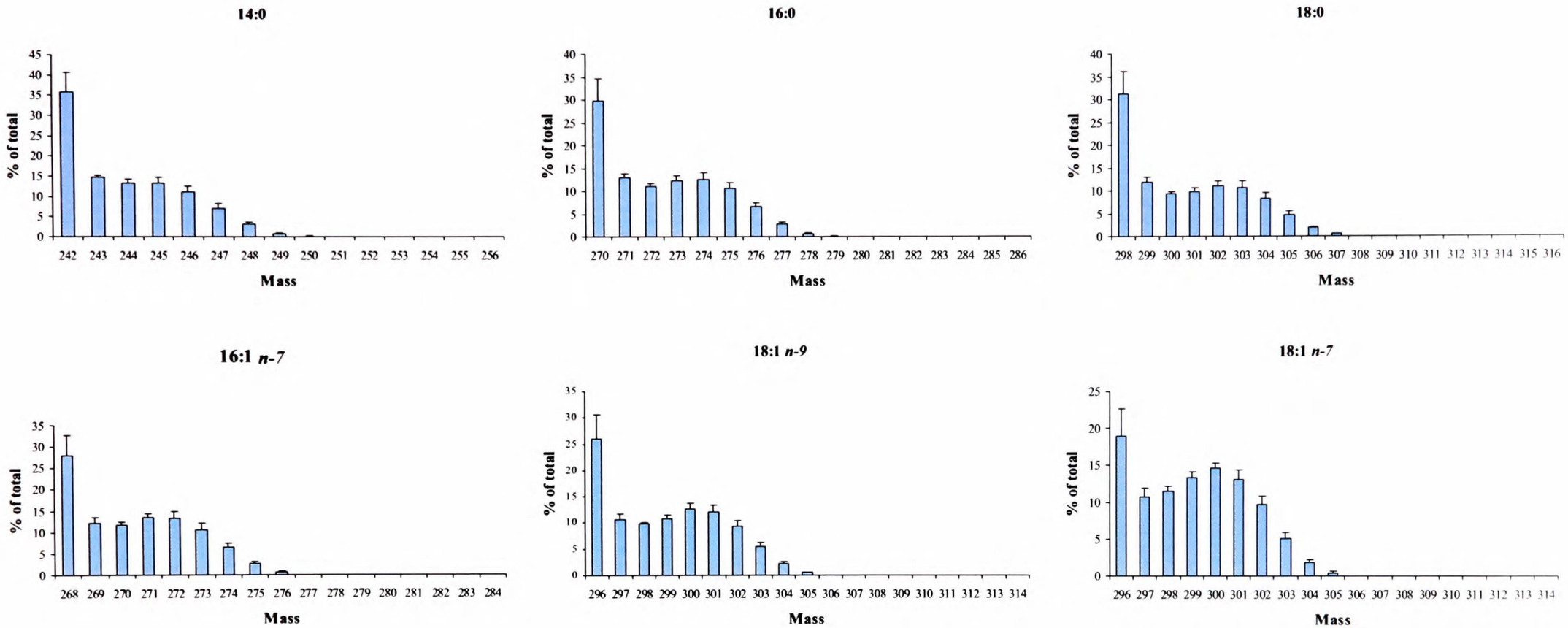


Figure 3-8 Acetate incorporation into TG fatty acids. The x-axes show the isotopomer masses of the fatty acid methyl esters (FAMEs), showing incorporation of the ^{13}C label from the [1-^{13}C]acetate in the culture medium. In each case the scale runs from the native mass (all ^{12}C, M) to the [U-^{13}C] mass (M + 14, M + 16 or M + 18). Data are represented as mean ± SEM (n = 6).

3.4.4. Glucose contribution to fatty acid synthesis

The contribution of glucose to the carbon source of fatty acid synthesis was determined by replacing all glucose in the medium, throughout the differentiation process, with a labelled glucose and tracing fatty acid enrichment. Human adipocytes were differentiated in either 5 mM [U-^{13}C]glucose (to represent a physiological glucose level, termed "low") or 17.5 mM [U-^{13}C]glucose (termed "high"). Incorporation of the labelled glucose into TG fatty acids was measured using GC-MS. The masses of the unlabelled and labelled fatty acids (as methyl esters) are listed in **Table 3-1**, where lack of ^{13}C denotes no involvement of [U-^{13}C]glucose in fatty acid synthesis (M+0). An increase of one in mass from that of the unlabelled mass indicates the presence of one ^{13}C (M+1), an increase of two indicates two ^{13}Cs (M+2), and so on.

Fatty acid	Native mass (M+0)	Uniformly labelled mass
Myristic acid (14:0)	242.3	256.3
Palmitic acid (16:0)	270.3	286.3
Palmitoleic acid (16:1 *n-7*)	268.3	284.3
Stearic acid (18:0)	298.3	316.3
Oleic acid (18:1 *n-9*)	296.3	314.3

Table 3-1 Masses of fatty acid methyl esters in their native and uniformly-^{13}C labelled forms

There was an increase in total TG accumulation with high, 17.5 mM, glucose compared with low, 5 mM, glucose, although this did not reach statistical significance

(P = 0.123) (**Figure 3-9**). This implies that glucose concentration does not have a major influence on TG accumulation in adipocytes.

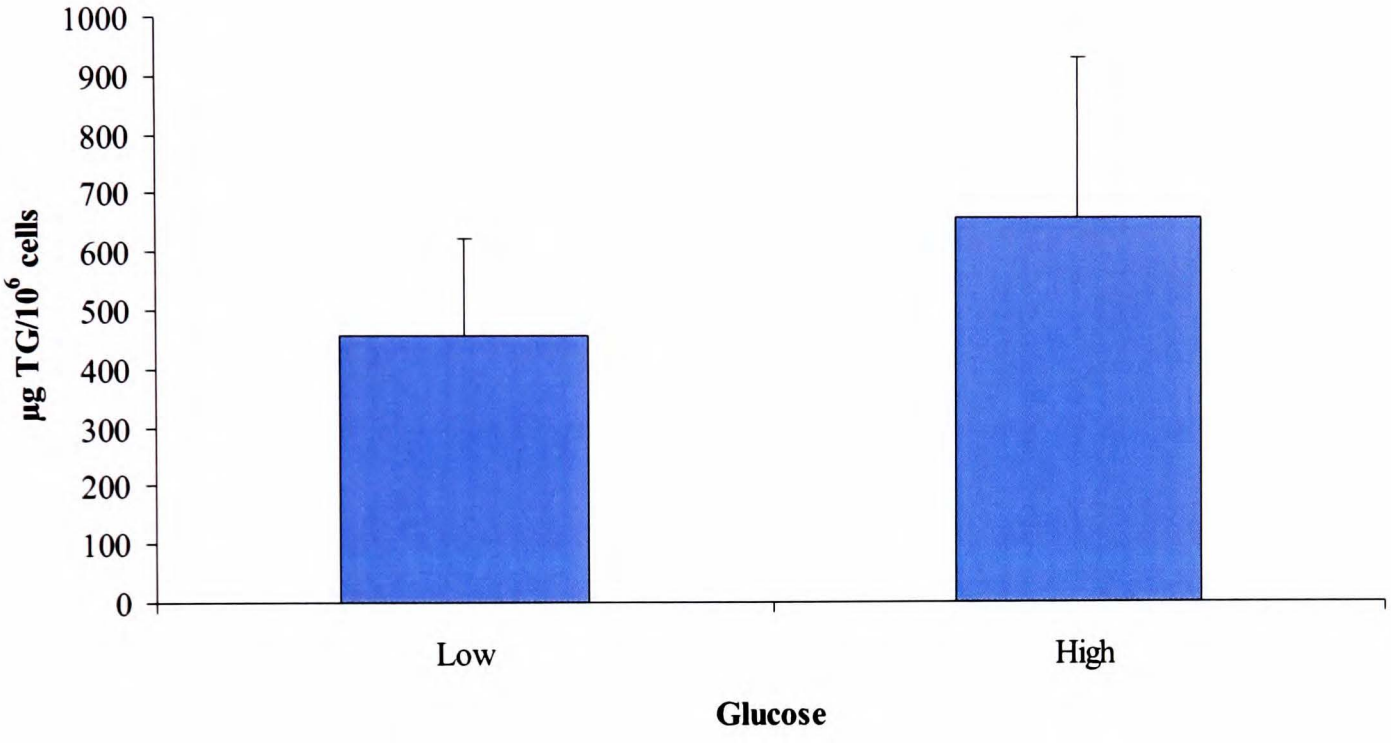


Figure 3-9 Total TG accumulation with high and low glucose. Data are represented as mean ± SEM. Data are represented as mean ± SEM (n = 6).

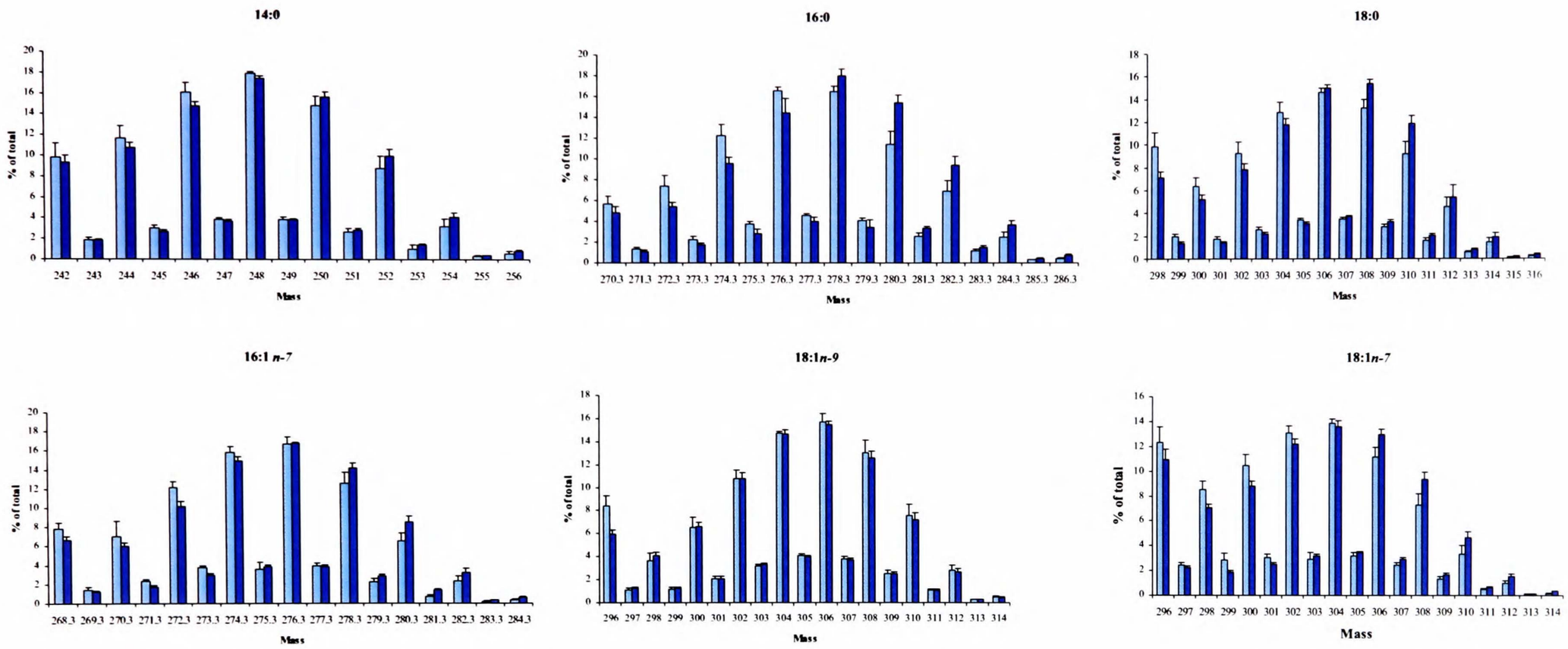


Figure 3-10 Isotopomer masses of TG fatty acids showing carbon composition and incorporation of ^{13}C from low glucose (light blue) and high glucose (dark blue). The x-axes show the isotopomer masses of the fatty acid methyl esters (FAMEs), showing incorporation of the ^{13}C label from the [1-^{13}C]glucose in the culture medium. In each case the scale runs from the native mass (all ^{12}C, M) to the [U-^{13}C] mass (M + 14, M + 16 or M + 18). Data are represented as mean ± SEM (n = 6).

The data reveal that neither myristic acid nor palmitic acid, the end products of DNL, were made exclusively from acetyl-CoA derived from [U-^{13}C]glucose (**Figure 3-10**). The most abundant isotopomer of palmitate was that with a mass of 278 (M+8), containing equal numbers of native and ^{13}C. At low and high glucose concentrations, [U-^{13}C]palmitate only accounted for 0.40 and 0.71 % of total palmitate synthesised, respectively.

Figure 3-11 shows the quantitative mass spectral analysis of contribution of glucose to fatty acid synthesis in human adipocytes at both low and high glucose concentrations. There was a greater contribution of glucose to fatty acid synthesis with the high glucose concentration (P = 0.024). The range of glucose contribution towards the carbon for fatty acid synthesis was 39.1 to 42.1 % with low glucose, and 39.3 to 47.0 % with high glucose.

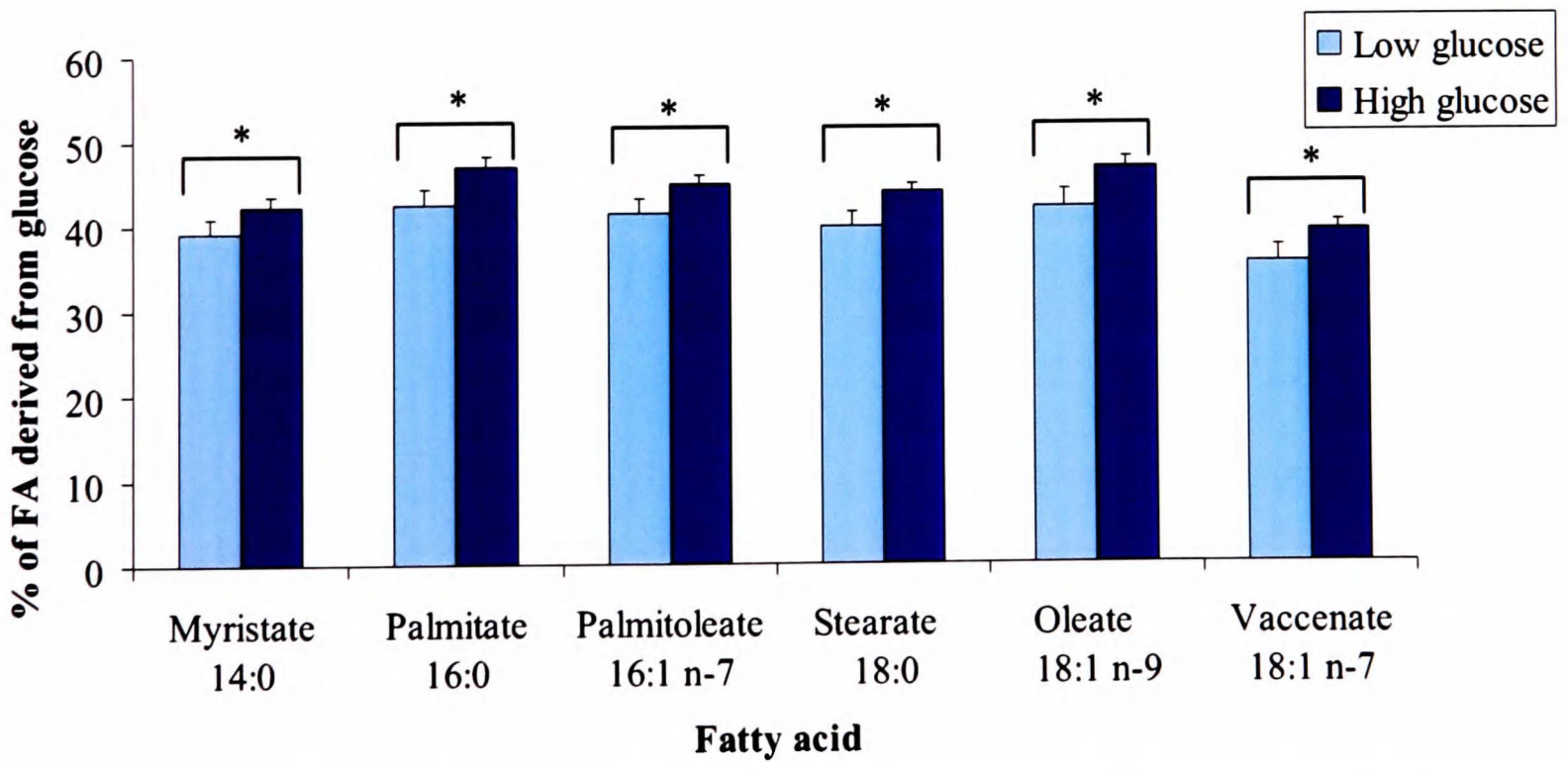


Figure 3-11 The percentage contribution of low and high glucose to adipocyte TG fatty acids

Data are represented as mean ± SEM (n = 6). * P > 0.035

3.4.5. ^{13}C-glutamine incorporation into fatty acids

To assess the carbon contribution of the amino acid glutamine to DNL, human preadipocytes were differentiated in differentiation medium containing 2 mM [U-^{13}C]glutamine. Again, incorporation of the labelled glutamine into TG fatty acids was measured using GC-MS.

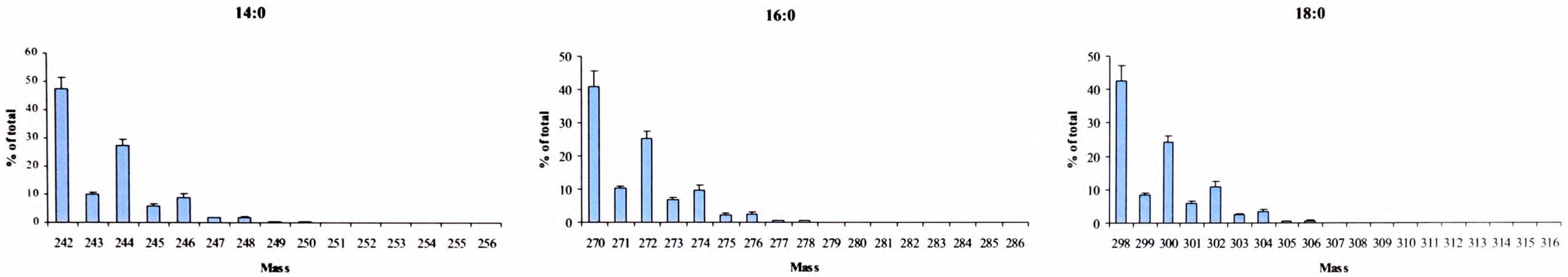


Figure 3-12 Isotopomer masses of TG fatty acids showing carbon composition and incorporation of ^{13}C from glutamine. The x-axes show the isotopomer masses of the fatty acid methyl esters (FAMEs), showing incorporation of the ^{13}C label from the [1-^{13}C]glutamine in the culture medium. In each case the scale runs from the native mass (all ^{12}C, M) to the [U-^{13}C] mass (M + 14, M + 16 or M + 18). Data are represented as mean ± SEM (n = 6).

The native forms of myristate and palmitate accounted for 48 and 41%, respectively, of these fatty acids (**Figure 3-12**). This implied that just over 50% of the total of each of these fatty acids had used glutamine as a precursor for DNL. Quantitative mass spectral analysis of contribution of glutamine to fatty acid synthesis in human adipocytes is shown in **Figure 3-13**. Around 10 % of each fatty acid measured had derived its carbon from glutamine.

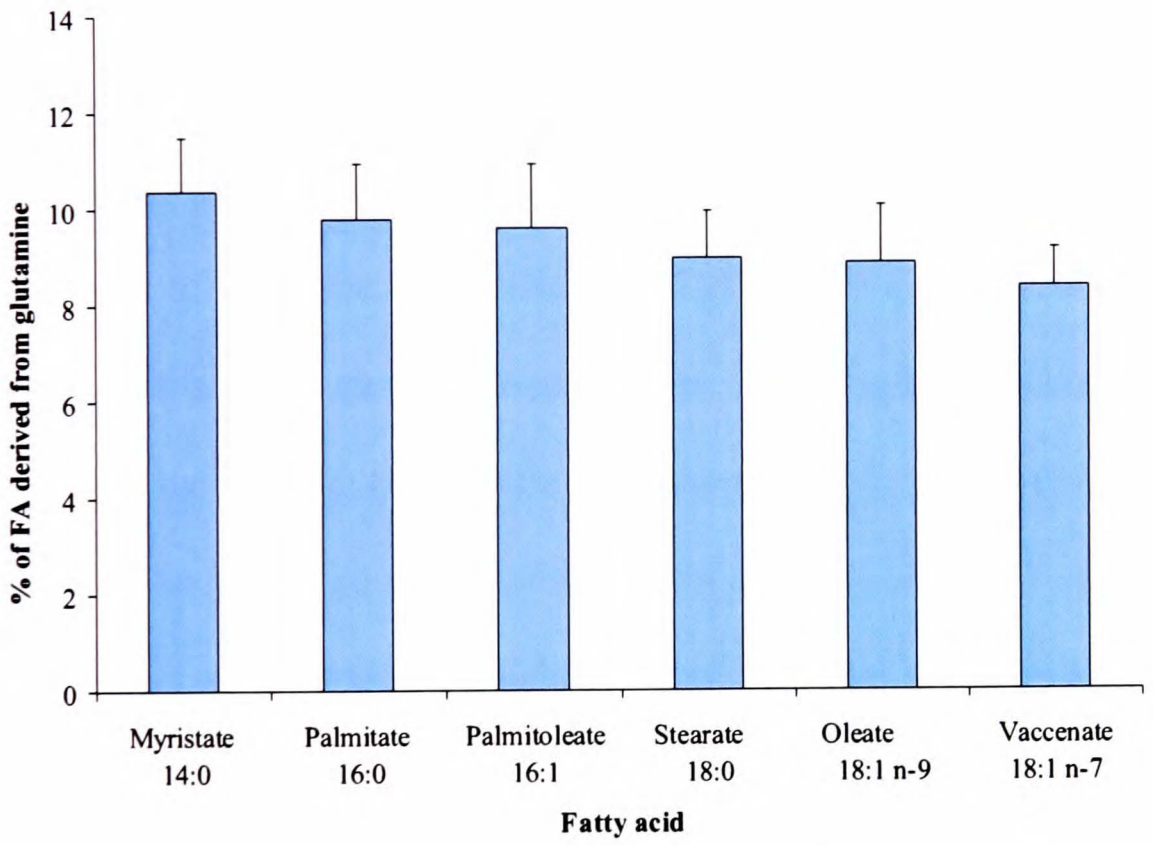


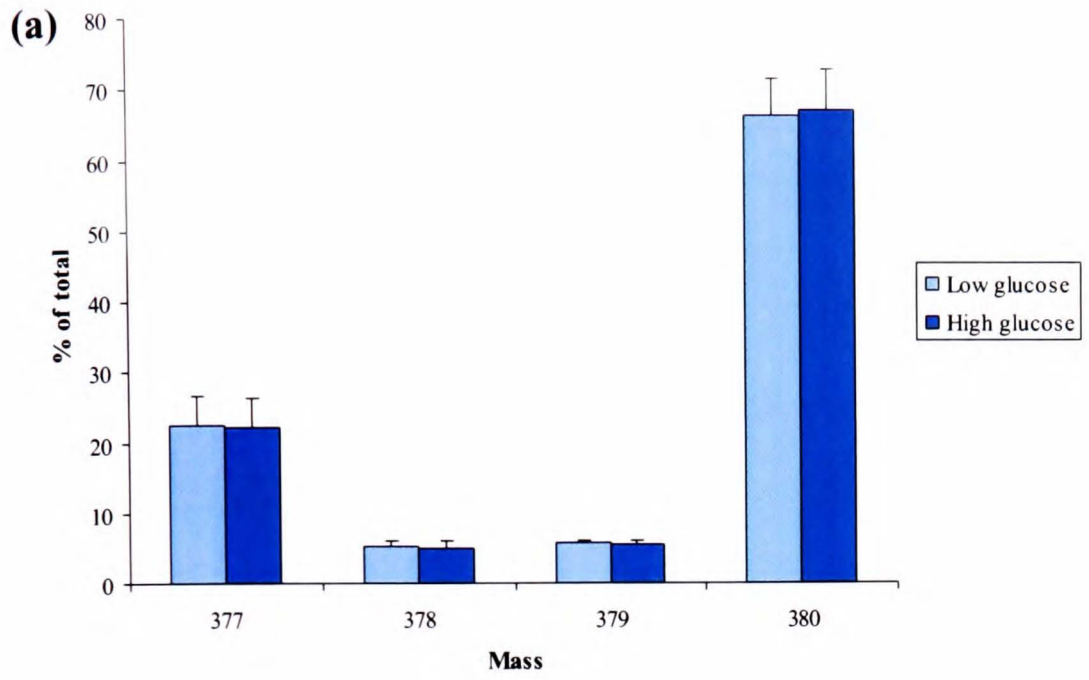
Figure 3-13 The percentage contribution of glutamine carbon to fatty acid synthesis in human adipocytes as determined by quantitative mass spectral analysis. Data are represented as mean ± SEM (n = 6).

3.4.6. Glycerol synthesis from glucose and glutamine

As TG synthesis requires the generation of both fatty acids and glycerol 3-phosphate, ^{13}C enrichment of the glycerol moiety of TGs was also measured. As the glycerol precursors (glucose or glutamine) in the media were uniformly labelled with ^{13}C,

glycerol derived exclusively from these ([U-^{13}C]glycerol) will have a mass of 380 (M+3). Glycerol with a mass of 377 therefore contains no ^{13}C (M+0), i.e. derived none of its carbons from the labelled precursor, whereas a mass of 378 (M+1) and 379 (M+2) implies that one and two of the carbons, respectively, are labelled.

The data show that TG-glycerol production is not affected by glucose concentration ($P = 0.975$) (**Figure 3-14(a)**). [U-^{13}C]glycerol was around 3-fold greater than native, that is, that the majority of TG-glycerol (almost 70 %) was derived from [U-^{13}C]glucose. The unlabelled glycerol was made from a source other than [U-^{13}C]glucose and could possibly have come from amino acids. Interestingly, a small proportion of the glycerol had masses of 378 and 379, having derived one or two of their carbons from glucose, respectively. The purity of the [U-^{13}C]glucose was measured by GC-MS (**Appendix 1**, section **A1.4.2**) and was found to be close to 100 %; therefore, contamination of the glucose with ^{12}C was not a concern. Quantitative mass spectral analysis showed the total contribution of glucose to TG-glycerol synthesis to be 72.1 and 72.6 % with low and high glucose, respectively (**Table 3-2**), emphasising that glucose concentration does not affect glycerol synthesis.



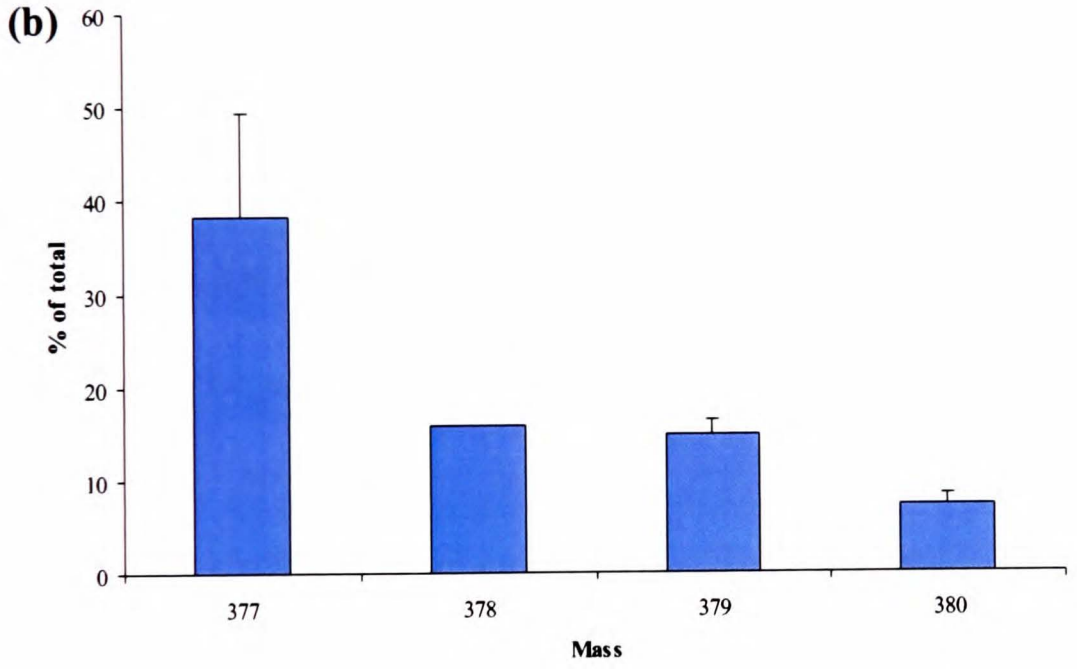


Figure 3-14 TG-glycerol derived from (a) [U-^{13}C]glucose and (b) [U-^{13}C]glutamine. Data are represented as mean ± SEM (n = 6).

Glutamine's contribution to glyceroneogenesis was also measured and seemed low from the isotopomer enrichment (**Figure 3-14(b)**). Quantitative mass spectral analysis showed the total contribution of glutamine to TG-glycerol synthesis to be 15.8 % (**Table 3-2**).

Glycerol precursor	% contribution to TG-glycerol
Glucose (5 mM)	72.1 ± 11.4
Glucose (17.5 mM)	72.6 ± 12.5
Glutamine	15.8 ± 0.2

Table 3-2 Contribution of glucose and glutamine to TG-glycerol synthesis in human adipocytes (n = 6)

Together these data imply that glyceroneogenesis plays a minor role in the synthesis of the TG-glycerol backbone in the differentiating preadipocytes *in vitro* in lipogenic culture conditions. **Figure 3-15** shows that in lipogenic culture conditions, there is very low mRNA expression of cytosolic PEPCK (*PCK1*) compared with glucose 6-phosphate dehydrogenase (*G6PD*).

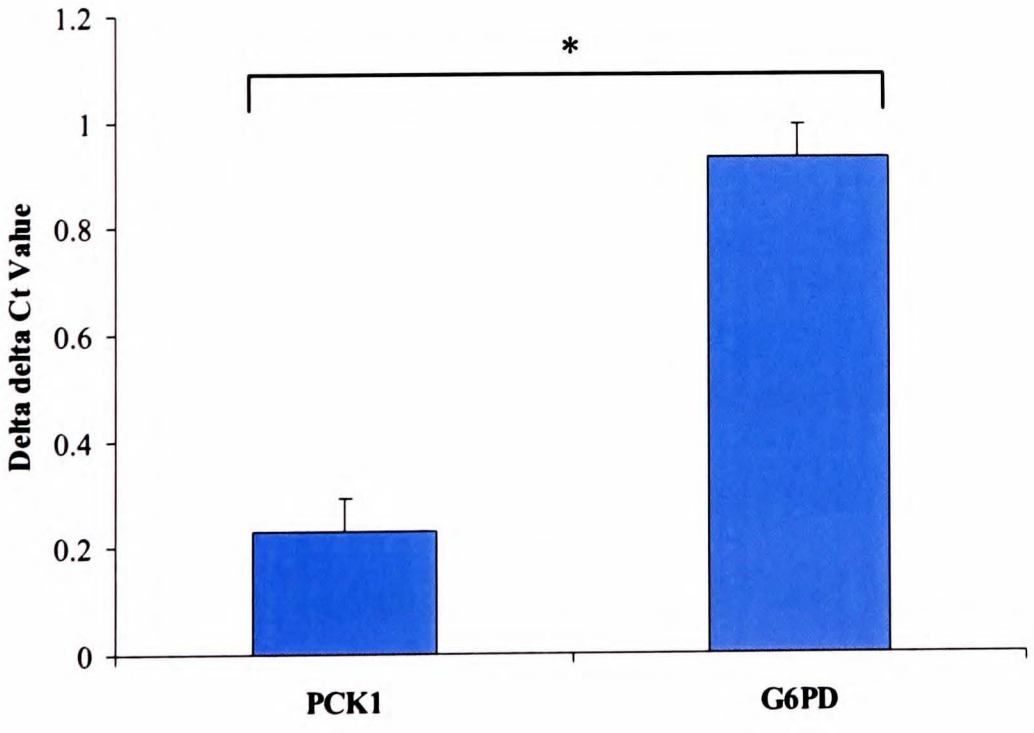


Figure 3-15 mRNA expression of *PCK1* and *G6PD* in adipocytes cultured with high (17.5 mM) glucose. Data are represented as mean ± SEM (n = 15). * P < 0.001 (Student's *t* test)

3.5. DISCUSSION

There is great debate as to the significance, and even occurrence, of DNL within the human adipocyte. The data presented here show clear evidence for the occurrence of DNL within the differentiating human adipocyte *in vitro*, with appropriate hormonal stimulation. In a standard fatty acid-free differentiation medium, high in glucose and containing pyruvate and various amino acids, the expression of genetic markers of fatty acid synthesis, in conjunction with lipid droplet formation and acetate incorporation into TG fatty acid, demonstrates *de novo* lipogenesis in this cellular model. Contrary to Shrago's reports (Shrago *et al.*, 1969; Shrago *et al.*, 1971) of human adipose tissue lacking the necessary enzymes, specifically ATP-citrate lyase, for DNL, this chapter shows the mRNA expression of the genes for these enzymes. Martin and Denton (Martin & Denton, 1970) showed that ATP-citrate lyase is fundamental to fatty acid synthesis in the cytosol of adipocytes, suggesting that this enzyme must have been functioning in order to create fatty acids. The TG-fatty acid spectra and gene expression seen in adipocytes differentiated without an exogenous source of fatty acids, provides evidence for coordinate regulation of DNL with other pathways for fatty acid metabolism.

Early studies investigating TG synthesis from glucose in the adipocyte concluded that glucose was used predominantly as a substrate for TG-glycerol synthesis and very little glucose was incorporated into TG fatty acid (Gries & Steinke, 1967; Galton, 1968; Shrago *et al.*, 1971). These studies used isolated mature adipocytes and short-term incubation with radiolabelled glucose. The stable isotope method described in this chapter has provided a different approach, by studying the incorporation of [U-^{13}C]glucose into fatty acids over a long-term period in pro-adipogenic conditions.

In this situation, glucose contributed to the formation of 42.4 and 47 % of total palmitate with low and high glucose, respectively. As discussed in **Chapter 1** (section **1.4.2**), adipocytes cannot readily recycle glycerol for TG synthesis as they lack the necessary enzyme, glycerol kinase. Therefore, in the mature adipocyte, glucose may be prioritised as a substrate for TG-glycerol to facilitate fatty acid (re-) esterification of fatty acids either released by lipolysis or supplied post-prandially.

In the experiment with [1-^{13}C]acetate, 30 % of the palmitate made via DNL was unlabelled, demonstrating an endogenous pool of intracellular acetyl-CoA. Possible sources of unlabelled acetyl-CoA could include glucose, pyruvate or amino acids, known to be present in the medium. Pyruvate present in the medium used for the acetate and glutamine experiments was at a concentration of 0.5 mM, and was 1 mM for the glucose experiment (slightly different media were used as there was no commercially available glucose-free DMEM/F12 HAM, therefore, glucose-free DMEM was used as the most similar alternative available). In the labelled acetate and glutamine experiments, the pyruvate concentration may have been further increased by the unlabelled glucose present at a high concentration, providing a source of not only acetyl-CoA but also NADPH necessary for fatty acid synthesis.

In rat adipocytes, acetate stimulated glucose incorporation into fatty acids (Saggerson, 1972a). Additionally, in the same study, pyruvate was also shown to increase glucose incorporation into TG fatty acids, providing an effective way of increasing the rate of fatty acid synthesis. The opposite is also true, glucose can stimulate pyruvate incorporation into TG fatty acids (Halperin, 1971). These findings highlight the possibilities that the contribution of glucose and glutamine to the carbon source of

DNL may have been under-estimated due to dilution of the labelled pyruvate precursor pool by (unlabelled) puruvate already present in the medium. Additionally, other metabolites within the medium may have acted to enhance glucose or glutamine incorporation.

In brown adipocytes, glucose and glutamine contributed equally to the carbon source of newly synthesised fatty acids, accounting for 60 % of the total lipids (Yoo *et al.*, 2004). Interestingly, in the absence of glucose, glutamine's contribution decreased and total TG accumulation was greatly reduced. This was attributed to a requirement for glucose for the synthesis of glycerol 3-phosphate, and hence for fatty acid esterification to form TG. In the differentiated preadipocytes in this chapter, glutamine contributed around 10 % of the carbon source of each fatty acid. Glutamine may act to produce fatty acids by being metabolised to glutamate in the mitochondrion and feeding into the Krebs cycle via α-ketoglutarate (**Figure 3-16**). This may also be a route for fatty acid production from other amino acids. Glutamate, proline, histidine and arginine are all metabolised in the mitochondrion to form α-ketoglutarate, and methionine, valine and isoleucine are metabolised to succinyl-CoA, also an intermediate in the Krebs cycle. The production of citrate from the metabolism of these amino acids yields acetyl-CoA for fatty acid synthesis and can also produce NADPH from oxaloacetate metabolism to pyruvate, via malic enzyme.

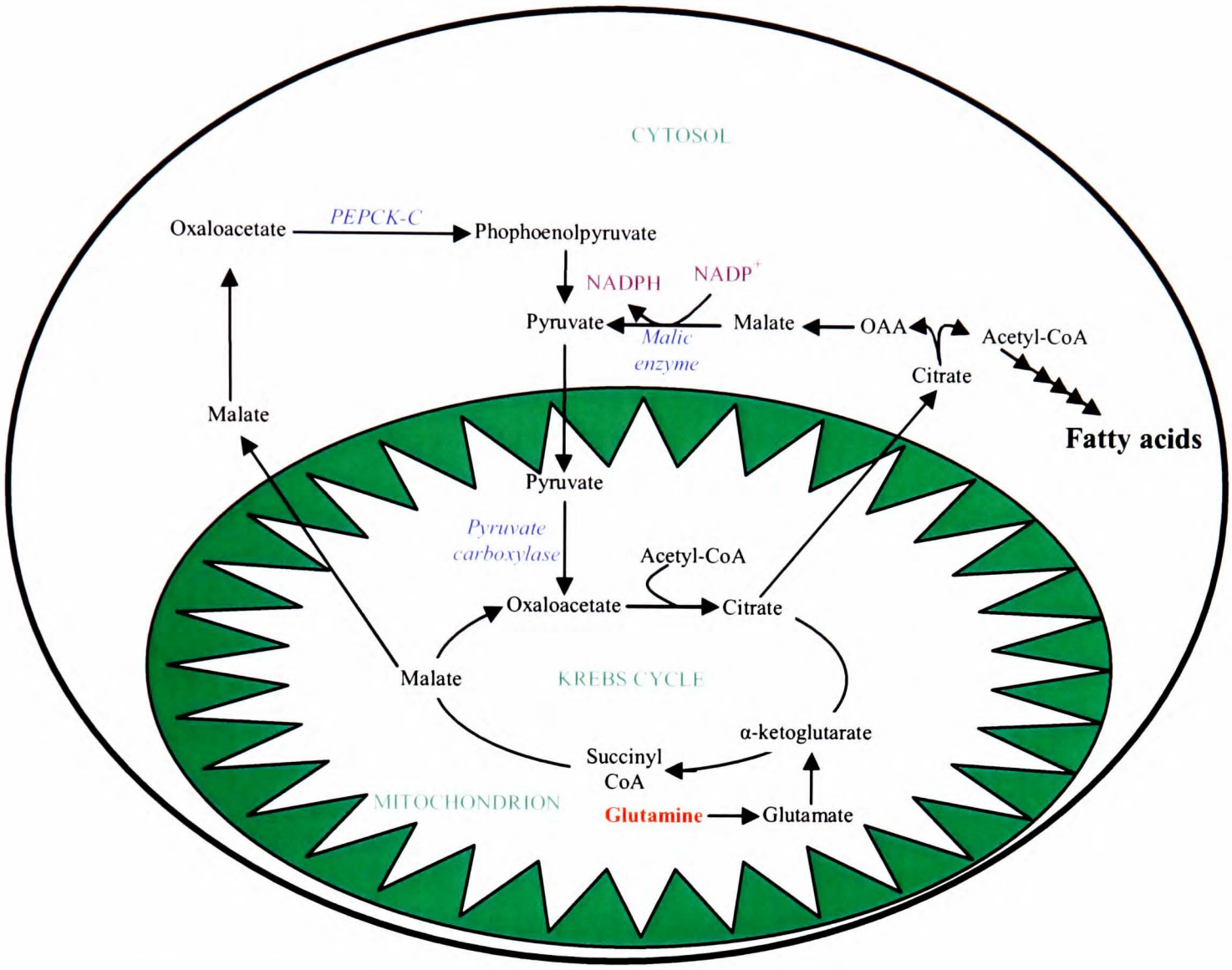


Figure 3-16 Fatty acid production from glutamine.

Yoo *et al.* (2004) calculated glucose incorporation into TG-glycerol in brown adipocytes to be 75 %, similar to the findings in this chapter in white adipocytes. Similarly, Bederman *et al.* (2008) showed that around 69 % of glucose makes TG-glycerol in the adipose tissue of mice fed a high carbohydrate diet. The findings in this chapter show glucose to contribute to around 72 % of TG-glycerol showing that the contribution of glucose to the glycerol moiety of TG remains consistent between studies.

It is perhaps not surprising that glutamine did not contribute a major proportion of TG-glycerol in this study. Glyceroneogenesis is up-regulated only during periods of low glucose (Botion *et al.*, 1998; Hanson & Reshef, 2003) and PEPCK, its rate-limiting enzyme, is down-regulated by insulin (Tilghman *et al.*, 1974; Hanson &

Reshef, 1997) and glucocorticoids in adipose tissue (Nechushtan *et al.*, 1987; Olswang *et al.*, 2003). As the contribution of glutamine towards the TG-glycerol backbone of TG was measured in a medium containing both glucocorticoids and high glucose, this is likely to account for the low incorporation of glutamine into TG-glycerol. Nutritional state may be important to the carbon source for TG synthesis. Mice fed a high-carbohydrate diet (containing labelled glucose) synthesised more than 2-fold more TG-glycerol from glucose than mice fed a carbohydrate-free diet (Bederman *et al.*, 2008). The same study also showed glucose to be the main carbon source for fatty acid synthesis with high carbohydrate feeding.

Pyruvate is thought to be a contributor to liver TG-glycerol (Kalhan *et al.*, 2001). This may provide an explanation as to the source of the unlabelled glycerol seen in the experiment with labelled glucose.

In conclusion, at high glucose concentrations, around 50 % of fatty acid carbon of newly-synthesised fatty acids is derived from glucose, and around 10 % from glutamine. The remaining 40 % could be synthesised from acetyl-CoA derived from pyruvate or from other amino acids. In this high-insulin environment, glucose dominates as the main carbon provider for TG-glycerol synthesis.

Chapter 4

The effects of exogenous palmitate on *de novo* lipogenesis, fatty acid metabolism and insulin sensitivity of human adipocytes

4.1. INTRODUCTION

In **Chapter 3**, evidence was presented showing the capacity for *de novo* lipogenesis (DNL) within the differentiating human preadipocyte *in vitro*. The observation that DNL within the human adipocyte is up-regulated *in vivo* in subjects on a high-carbohydrate diet implies regulation of this process by dietary macronutrients. DNL operates in the differentiating preadipocyte in the absence of exogenous fatty acid. Therefore, it would seem logical to hypothesise that addition of exogenous palmitate would down-regulate this process. The aim of this chapter was to test this hypothesis and to search for the mechanisms involved in palmitate regulation of DNL. Palmitate regulation of DNL was of particular interest as it is both the end product of DNL and a substrate for SCD; furthermore, there have been many reports in the literature on the regulation of DNL by polyunsaturated fatty acids (PUFAs) but comparatively fewer by saturated fatty acids (SAFAs).

An early study of PUFA regulation of lipogenesis showed that when mice were fed a fat-free, linoleate-deficient diet, hepatic fatty acid synthesis was up-regulated. This could be reversed by linoleic acid or corn oil supplementation but not by coconut oil, comprising mainly palmitic and oleic acids (Allmann & Gibson, 1965). Since then, more studies have also shown suppression of lipogenesis by *n-3* and *n-6* PUFAs, including the fish oils eicosapentaenoic acid and docosahexaenoic acid, and conjugated linoleic acid (CLA) (Sessler & Ntambi, 1998; Dentin *et al.*, 2005; Jose *et al.*, 2008; Li *et al.*, 2008; Perez-Echarri *et al.*, 2008). The precise mechanism of action of PUFA down-regulation of lipogenesis is not fully understood but may be due, in part, to down-regulation of sterol regulatory element binding protein-1c

(SREBP-1c) expression (Kim *et al.*, 1999) or to increased fatty acid oxidation (Aarsland *et al.*, 1990).

SCD is also prone to down-regulation by PUFAs, such as arachidonic acid, linoleic acid, linolenic acid and the *trans*-10,*cis*-12 isomer of CLA, as well as the plant fatty acid, sterculic acid (Sessler *et al.*, 1996; Ntambi, 1999; Choi *et al.*, 2000; Park *et al.*, 2000; Choi *et al.*, 2002; Gomez *et al.*, 2003). As with PUFA regulation of lipogenesis, the mechanism of regulation of SCD is not yet clearly understood. Studies have shown the existence of a PUFA response element (PUFA-RE) within the promoter region of the SCD gene which may act to prevent transcription upon PUFA binding (Waters *et al.*, 1997). PUFAs may also act to prevent the maturation of SREBP-1c protein (Ntambi, 1999).

Contrary to regulation by PUFAs, SAFAs may act to up-regulate DNL. Early studies in rats showed palmitate to up-regulate DNL. Palmitate stimulated glucose incorporation into TG fatty acids but inhibited acetate, pyruvate and lactate incorporation (Saggerson & Tomassi, 1971; Saggerson, 1972a). Furthermore, palmitate-induced incorporation of glucose into fatty acids was dependent upon dose; maximum incorporation was achieved with 0.5 mM palmitate, whereas higher concentrations had inhibitory effects (Saggerson, 1972b). In mice, dietary SAFA supplementation led to greater SCD activity in liver microsomes compared with PUFAs, but SCD activity was still lower than mice fed a control diet (Garg *et al.*, 1986). Recently, Warensjö *et al.* (2008) reported an increased SCD index (16:1 *n*-7/16:0) in serum phospholipid and cholesteryl esters in subjects fed a high saturated fat-diet compared with those fed a rapeseed oil-rich diet. Furthermore,

SAFAs up-regulate hepatic lipogenesis in mice, by a mechanism thought to be mediated by SREBP-1c and peroxisome proliferator-activated receptor co-activator-1β (Lin *et al.*, 2005; Sampath *et al.*, 2007).

Adipocytes function primarily as storage cells, removing excess circulating dietary fat and storing it as energy reserves. DNL may not be viewed as a large contributor to stored adipocyte fatty acids, but it is up-regulated during carbohydrate overfeeding. It would be logical to assume that DNL would be down-regulated by palmitate as it is the end-product of this process. However, the literature would suggest otherwise, at least in rodents. Therefore, an investigation of the regulation of DNL by an exogenous source of its major end product, palmitate, may assist in our understanding of the role of this seemingly minor process.

4.2. AIMS

The aim of this experiment was to determine the effects of exogenous palmitate on DNL regulation and SCD activity in the differentiating preadipocyte. Changes in cell morphology, TG and PL fatty acid composition and gene expression were assessed. Labelling of the exogenous palmitate allowed it to be distinguished from DNL-derived fatty acid, facilitating tracing the fate of the exogenous fatty acid. In addition, I also followed up the observations in **Chapter 3** of a close relationship between DNL and fatty acid desaturation, by testing the hypothesis that there may be specific channelling of fatty acids made via DNL into these pathways.

4.3. METHODS

4.3.1. Adipose tissue sample collection

The taking of human adipose tissue samples was approved by the Oxfordshire Clinical Research Ethics Committee and all subjects gave written, informed consent. Subcutaneous adipose tissue biopsies were taken and preadipocytes isolated as described in **Chapter 2**, section **2.1.2**. Volunteers for the experiments described in this chapter consisted of 7 males and 8 females.

4.3.2. Cell culture

Human preadipocytes were obtained from healthy volunteers and grown to confluence before differentiating for 14 days as described in **Chapter 2**, section **2.1.3**. [U-^{13}C]palmitate (99% isotopic purity) was added to the differentiation medium throughout differentiation at the following concentrations: 0 (control), 50, 100, 200 and 400 μM.

4.3.3. TG and PL fatty acid composition

TGs and PLs were extracted from harvested cells and fatty acid composition analysed using GC (**Appendix 1,** sections **A1.2 and A1.3**). The isotopic composition of the fatty acids was further examined by GC-MS (**Appendix 1,** section **A1.4**) to determine the fate of the exogenous palmitate.

4.3.4. Gene expression

Total mRNA was extracted using Tri-Reagent (Ambion, Texas, USA). This was then used to synthesise cDNA for real-time PCR analysis of gene expression using pre-designed, validated TaqMan® primers and probes from Applied Biosystems (Warrington, UK) (**Appendix 1**, section **A1.6**).

4.3.5. Cell membrane fluidity

Cell membrane fluidity was measured using fluorescence recovery after photobleaching. This method is described in detail in **Chapter 2**, section **2.6.2**.

4.3.6. Insulin sensitivity

Insulin-stimulated uptake of 2-deoxy-D-[1-^{3}H]glucose was measured as an indicator of insulin sensitivity (**Chapter 2**, section **2.5**). Cells differentiated with 0, 50 and 200 μM [U-^{13}C]palmitate were used in this experiment.

4.3.7. Statistical analyses

Changes seen with increasing exogenous palmitate were assessed using repeated measures analysis of variance (ANOVA). Correlations were tested using the Spearman non-parametric coefficient, r_s. Comparisons made between any two factors were analysed using a Student's *t* test. All statistical analyses were carried out using SPSS (version 15).

4.4. RESULTS

4.4.1. Initial investigations

Initial experiments were conducted using preadipocytes differentiated with 400 μM palmitate (chosen as a high, yet still physiological concentration). However, this concentration caused cell death in a sub-population of the cells. Lower concentrations of 50, 100 and 200 μM palmitate were used in experiments described in this chapter as they had no adverse effects on cell viability.

4.4.2. Adipocyte triglyceride storage

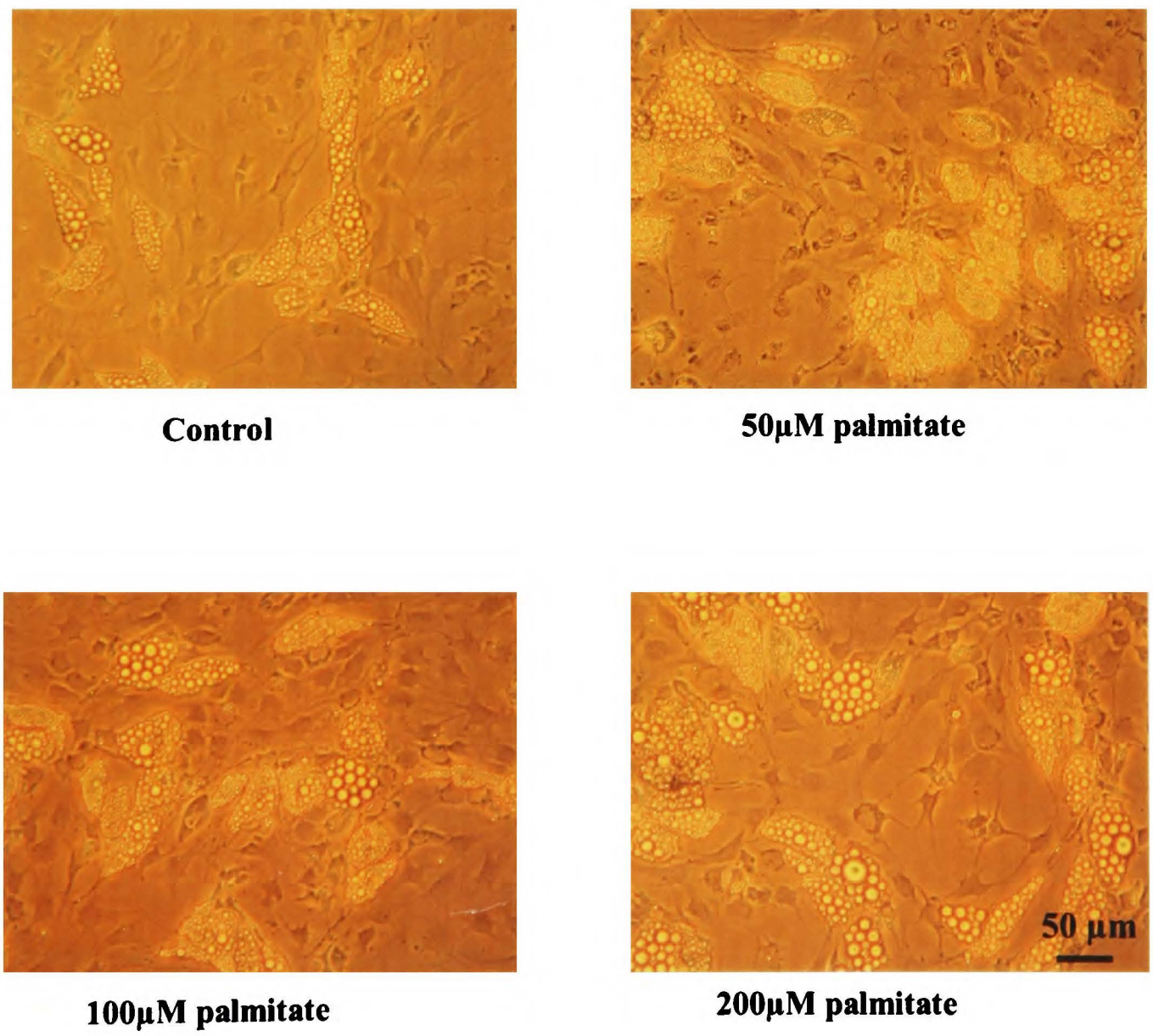


Figure 4-1 Light micrographs of preadipocytes differentiated with 0 to 200 μM exogenous palmitate (x 10 objective).

Initial observations indicated that lipid droplet size and accumulation increased with increasing palmitate concentration (**Figure 4-1**). This was quantified by measuring total TG, calculated as the sum of all the TG-fatty acids measured using gas chromatography. TG accumulation increased with exogenous palmitate concentration in a dose-dependent manner (**Figure 4-2**). Expression of mRNA for diacylglycerol acyltransferase 2 (DGAT2), the enzyme that catalyses the final step in TG synthesis, the addition of the third fatty acyl chain to diacylglycerol, was also up-regulated with palmitate (P = 0.016) (**Figure 4-3**).

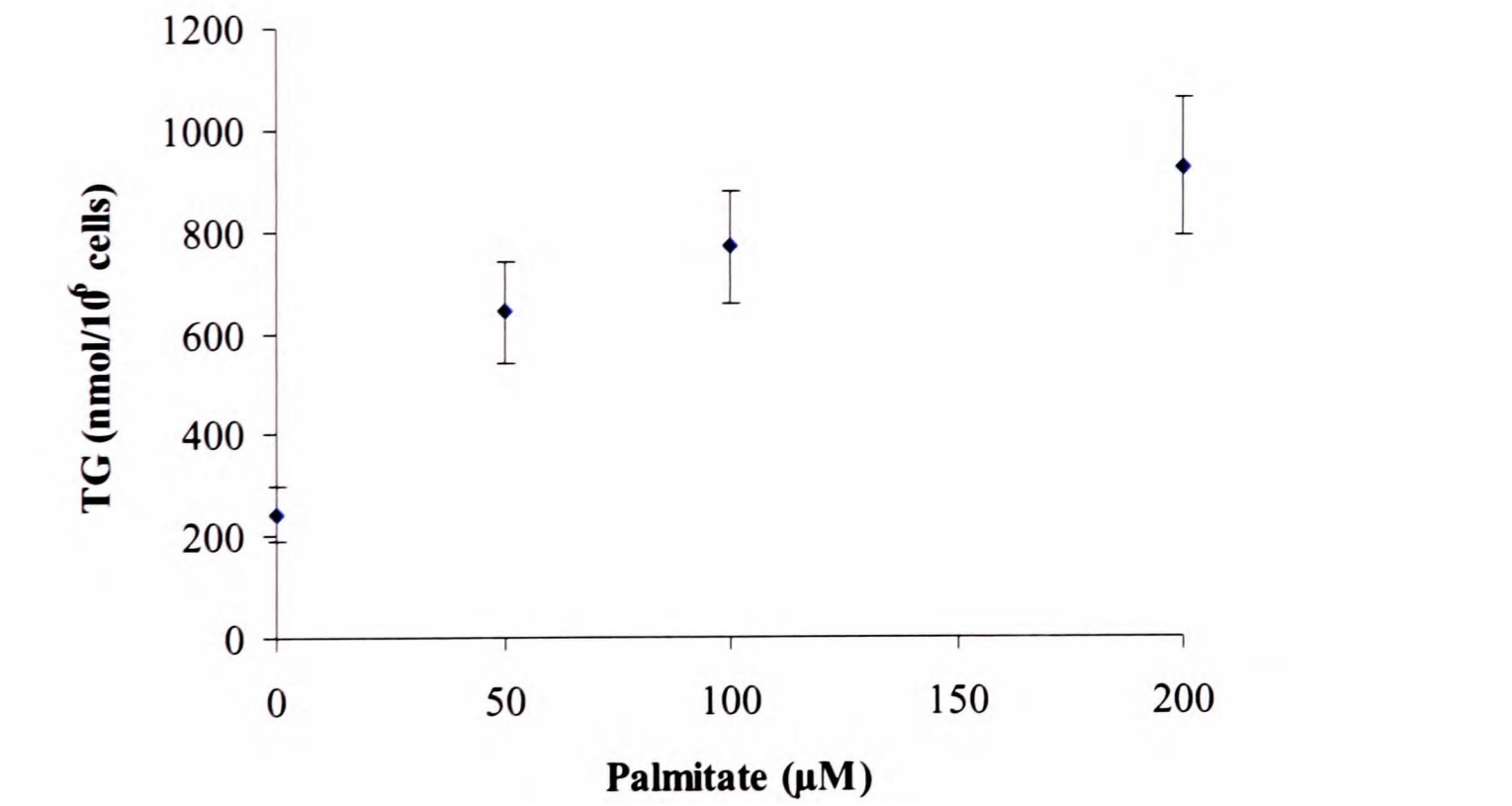


Figure 4-2 Total TG in adipocytes differentiated with 0, 50, 100 and 200 μM palmitate. Data are represented as mean ± SEM (n = 15). P = 0.000 (ANOVA)

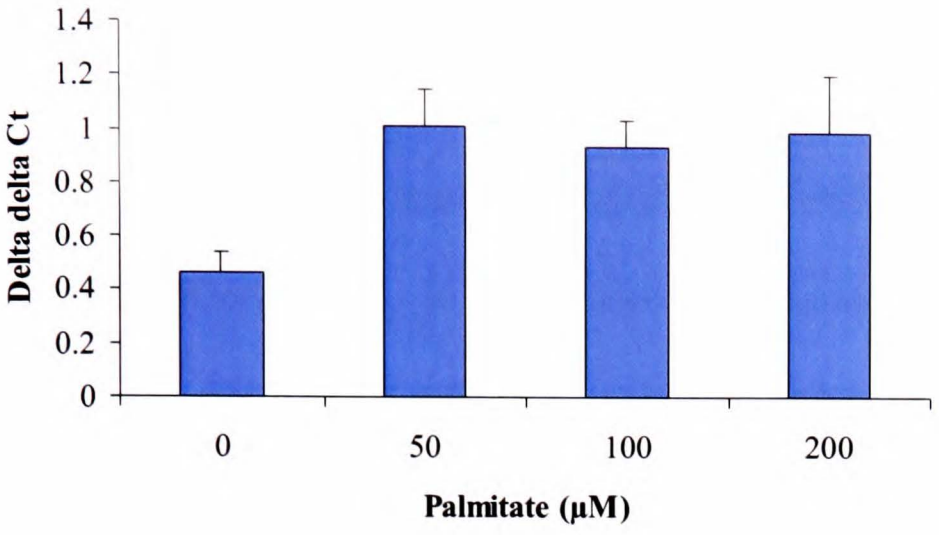


Figure 4-3 *DGAT2* mRNA expression in response to palmitate. Data are represented as mean ± SEM (n = 15).

4.4.3. Fatty acid composition of TG

The fatty acid composition of the TG fraction was analysed using GC and is summarised in **Table 4-1**. In accordance with the increase in TG in response to exogenous palmitate, there was also a corresponding increase of each fatty acid with increasing palmitate. The fatty acids present showed the products of DNL and desaturation by SCD as well as chain elongation, as described in **Chapter 3**.

	0 µM palmitate	50 µM palmitate	100 µM palmitate	200 µM palmitate	P value
14:0	21.8±6.7	50.8±10.8	57.3±12.7	58.6±14.6	0.099
16:0	354.6±86.6	931.3±143.5	1189.6±166	1557.4±216	0.000
16:1 *n-7*	137.2±36.7	375.3±71.9	451.6±76.2	557.3±83.2	0.001
18:0	28.7±4.8	71.3±9.4	84.0±11.5	91.3±14.6	0.001
18:1 *n-9*	168.1±34.3	448.7±83.5	473.1±90.5	452.3±100.3	0.031
18:1 *n-7*	21.37±4.2	47.8±10.8	54.8±10.4	71.3±10.9	0.005

Table 4-1 Composition of the fatty acid moiety of adipocyte TG expressed as nmol fatty acid/10^6 cells. Values shown as mean±SEM (n = 15). P values were calculated using ANOVA.

4.4.4. Adipocyte TG accumulation and differentiation

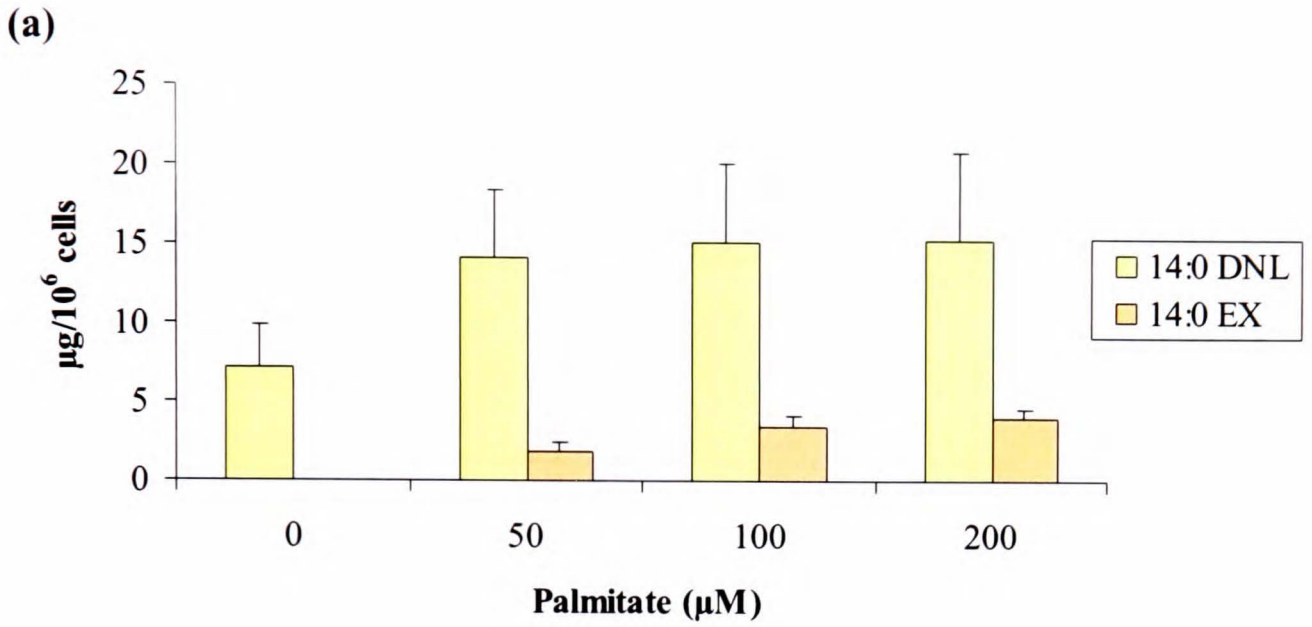
The relationship between TG accumulation and differentiation was determined by assessing the correlation between total TG and *FABP4* mRNA expression, a marker of adipocyte differentiation. In the absence of palmitate, there was a positive correlation between TG and *FABP4* mRNA expression (**Table 4-2**). The addition of palmitate increased *FABP4* mRNA but not in a dose-dependent manner.

Palmitate (μM)	TG	FABP4	r_s	P
0	65.8±14.3	0.4±0.1	0.79	0.001
50	173.4±25.7	1.2±0.2	0.03	0.911
100	207.4±28.3	1.0±0.1	0.12	0.681
200	249.0±34.0	1.1±0.3	0.40	0.159

Table 4-2 Spearman correlations between TG (μg/10^6 cells) and *FABP4* mRNA (delta delta Ct value). Values show mean±SEM (n = 15).

4.4.5. Effects of palmitate on DNL

The effects of differentiating adipocytes with exogenous palmitate on DNL was investigated. The exogenous palmitate was supplied in the form of [U-^{13}C]palmitate. GC-MS was then used as a tool to distinguish exogenous, ^{13}C-labelled palmitate from endogenously produced, unlabelled fatty acids in adipocyte-TG.



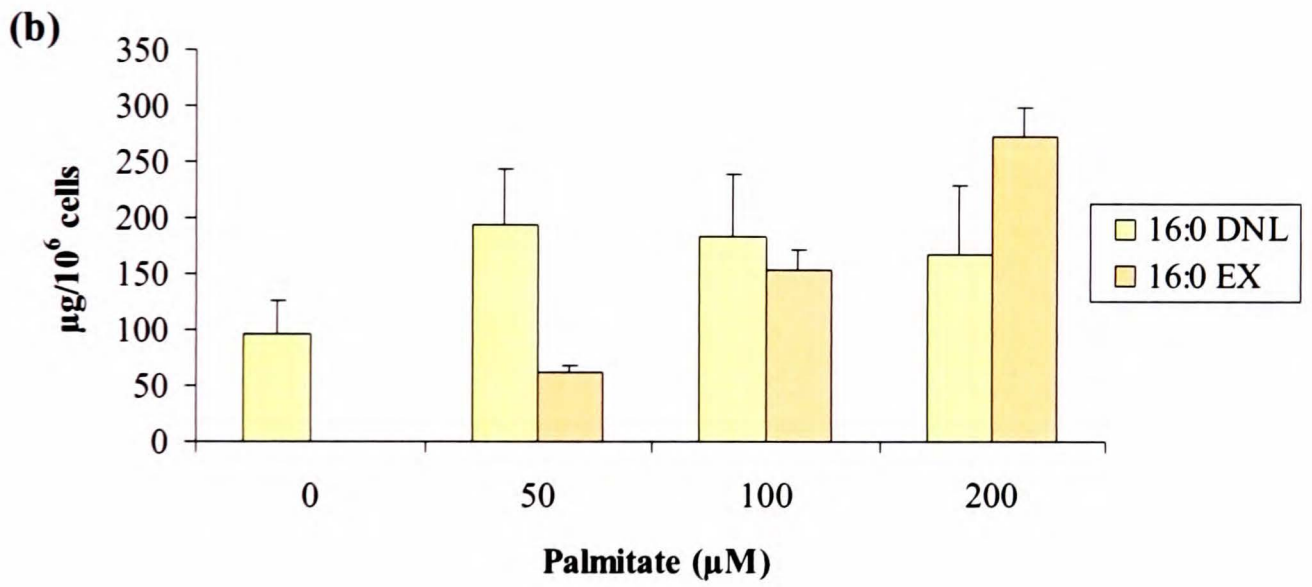


Figure 4-4 Effects of exogenous palmitate on DNL-derived myristate (a) and palmitate (b) in adipocyte-TG. 14:0 DNL and 16:0 DNL denotes DNL-derived TG fatty acid, and 14:0 EX and 16:0 EX denotes exogenously-derived TG fatty acids. Data are represented as mean ± SEM (n = 15).

DNL-derived myristate and palmitate were increased in response to addition of exogenous palmitate (50 to 200 µM) but did not increase in a dose-dependent manner (P = 0.349 and 0.242, respectively, ANOVA) (**Figure 4-4**). Not surprisingly, exogenously-derived palmitate increased with the addition of exogenous palmitate (P = 0.000, ANOVA). Exogenously-derived myristate, that is, a product of chain

shortening of exogenous palmitate, was also increased with exogenous palmitate (P = 0.000, ANOVA) in a dose-dependent manner. It was confirmed by analysis of the [U-^{13}C]palmitate added to the medium that there was no contamination with [U-^{13}C]myristate (**Appendix 1**, section **A1.4.2**).

mRNA expression of DNL-associated genes *ACACA* (acetyl-CoA carboxylase), *FASN* (fatty acid synthase), *ACLY* (ATP-citrate lyase) and *G6PD* (glucose 6-phosphate dehydrogenase) was measured using real-time PCR (**Figure 4-5**). In agreement with the fatty acid data, mRNA expression of DNL-associated genes was also up-regulated with exogenous palmitate, although only *ACACA* was seen to increase significantly (P = 0.039, 0.074, 0.053 and 0.150 for *ACACA*, *FASN*, *ACLY* and *G6PD* mRNA, respectively).

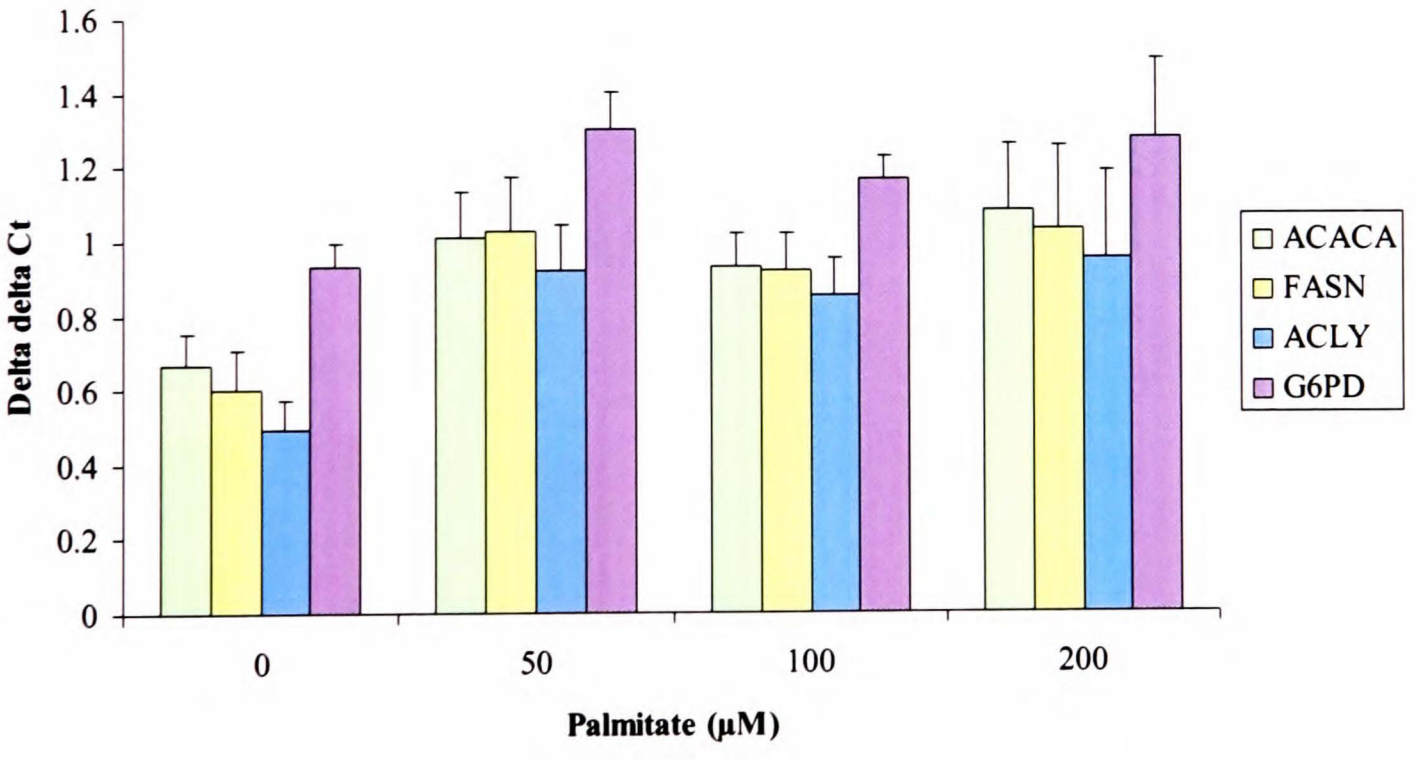


Figure 4-5 mRNA expression of DNL-associated genes in response to exogenous palmitate. Data are represented as mean ± SEM (n = 15).

4.4.6. Effects of palmitate on SCD activity

Using total (unlabelled and labelled) TG fatty acid measurements, product to precursor ratios of 16:1 *n-7*/16:0 and 18:1 *n-9*/18:0, indices of SCD activity, were calculated (**Figure 4-6**). As palmitate is a substrate for SCD, it would be logical to predict that SCD activity would be up-regulated upon supply of its substrate. There was a reduction in the 18:1 *n-9*/18:0 ratio with 200 μM but exogenous palmitate had no effect on this SCD index at other concentrations.

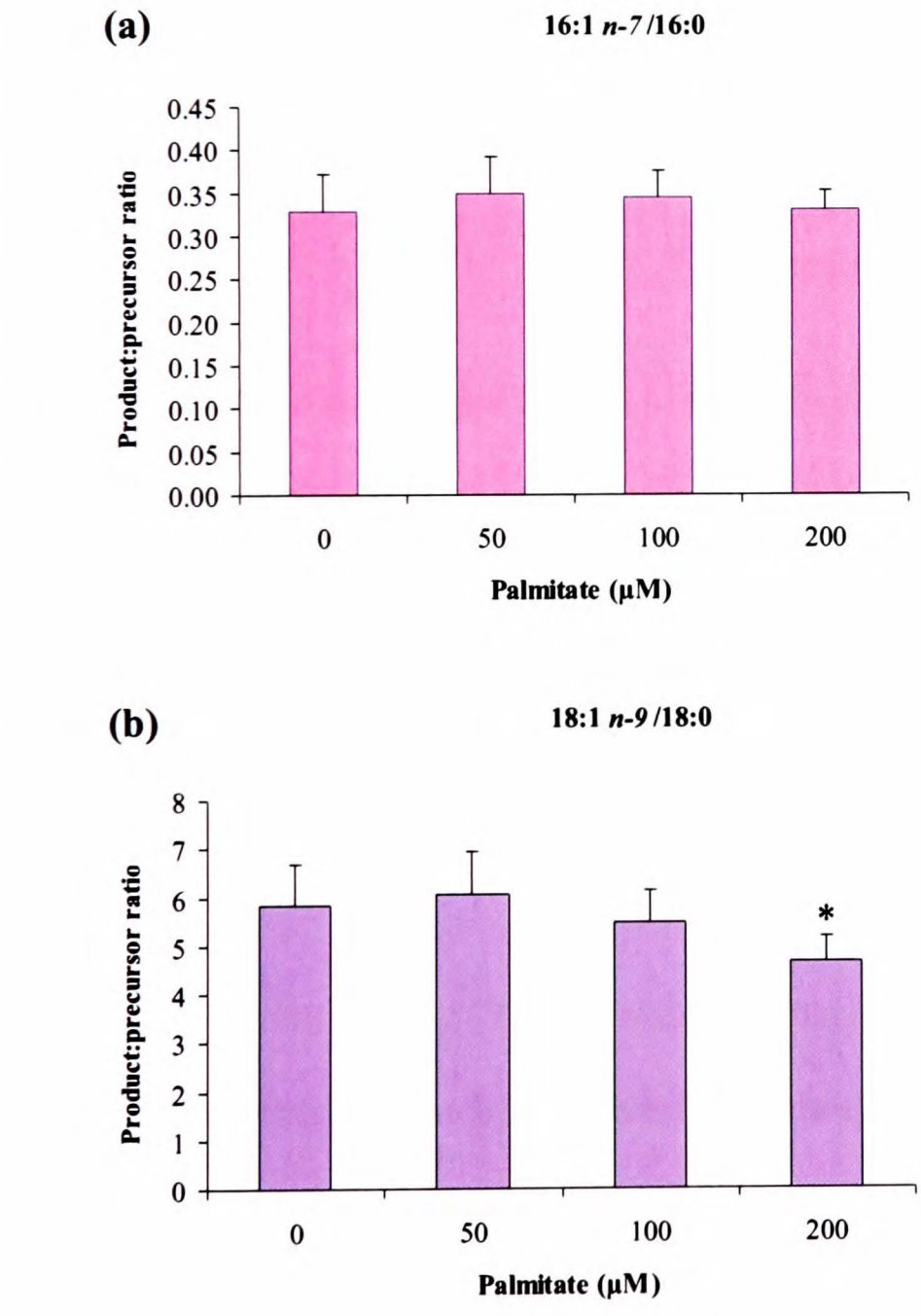


Figure 4-6 Effects of exogenous palmitate on SCD indices. Data are represented as mean ± SEM (n = 15). * P = 0.032 compared with control.

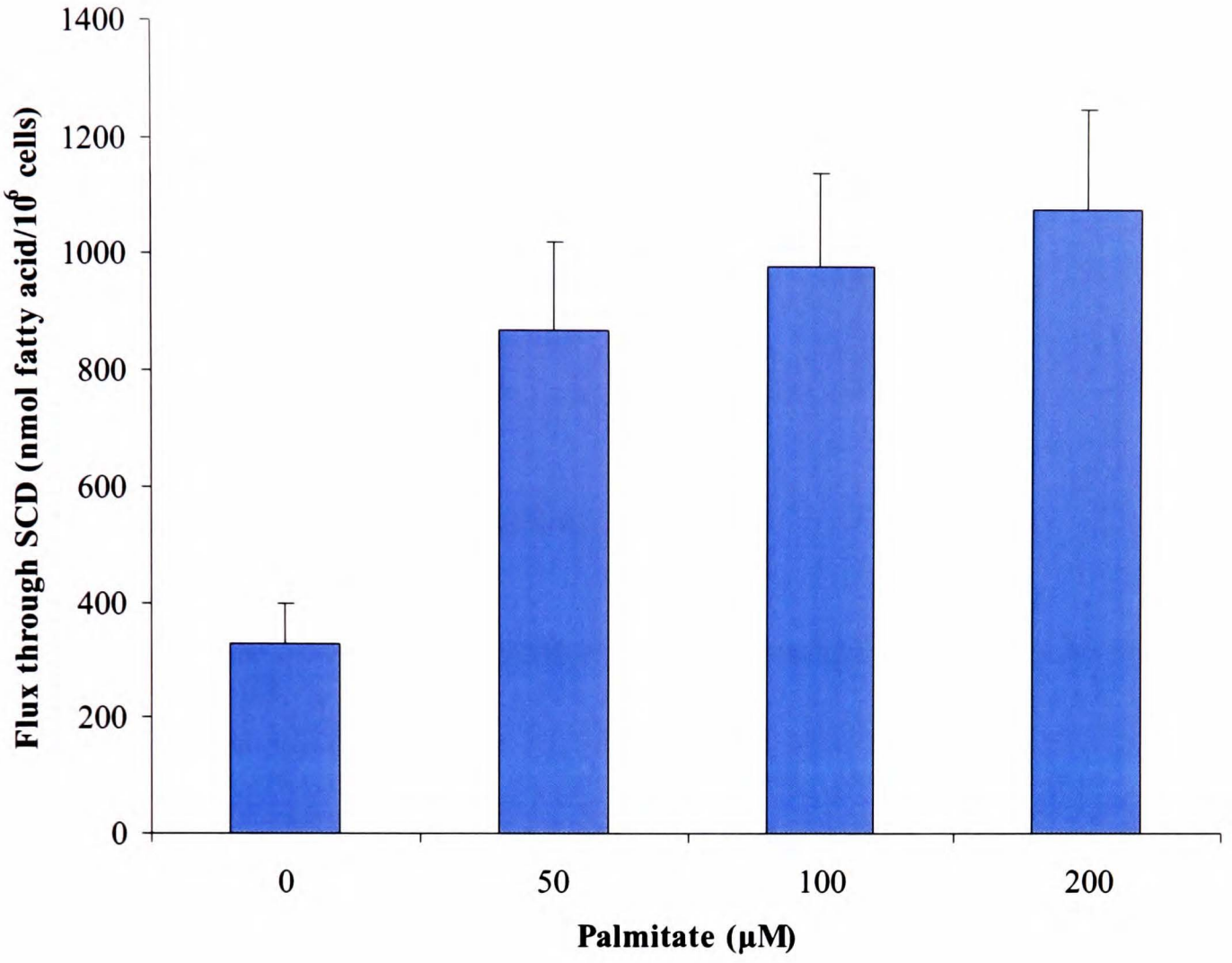


Figure 4-7 Total flux through SCD over 14 days. Data are represented as mean ± SEM (n=15)

There was, however, an increase in total flux through SCD (**Figure 4-7**). This was calculated as the sum of the products of the fatty acids directly and indirectly made via SCD action, that is, 16:1 *n-7*, 18:1 *n-7* and 18:1 *n-9* (**Figure 4-19**). Flux through SCD increased with increasing palmitate (P = 0.000, repeated measures ANOVA).

mRNA expression of *SCD* was measured using real-time PCR (**Figure 4-8**). SCD mRNA expression was up-regulated with exogenous palmitate (P = 0.022). These findings are consistent with the up-regulation of the DNL-associated genes.

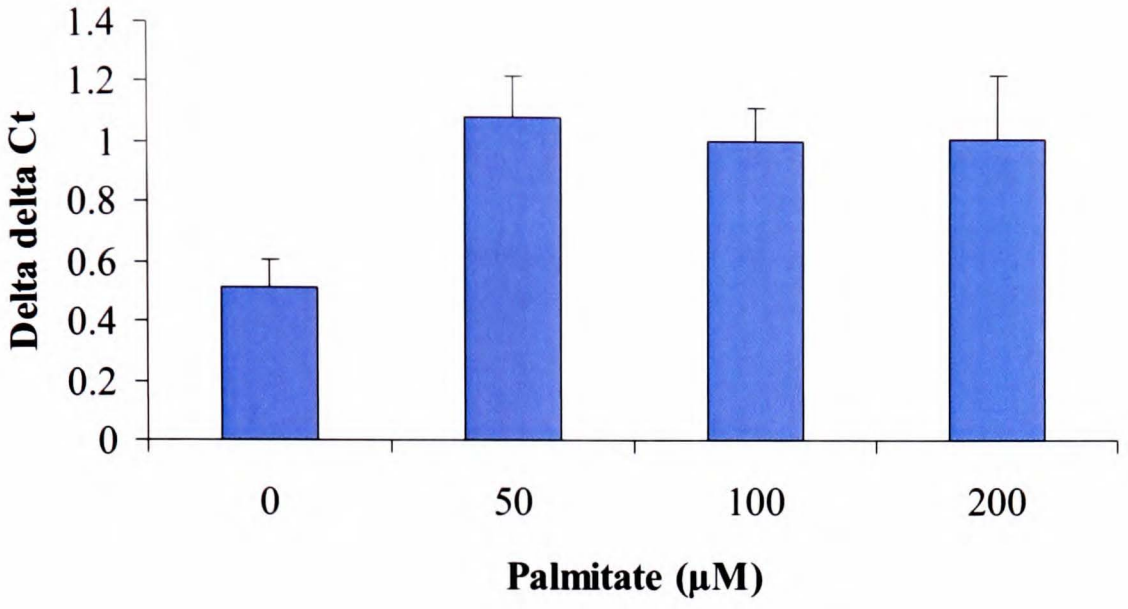
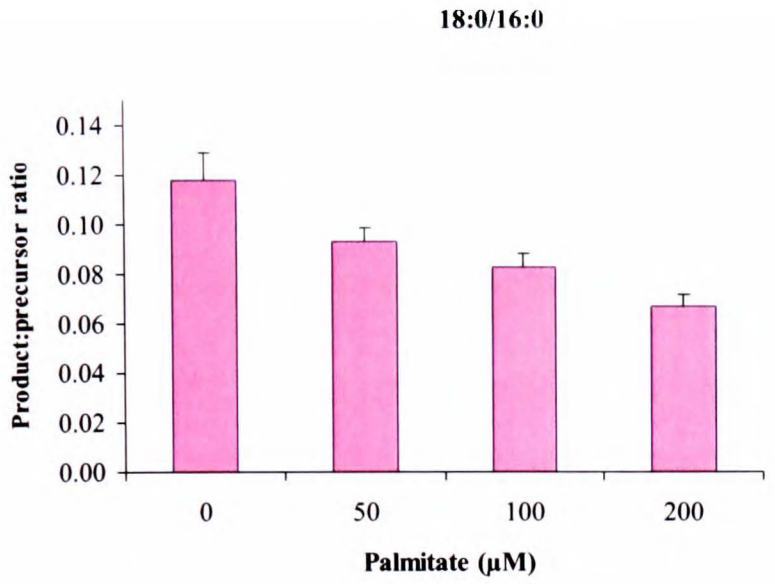


Figure 4-8 Changes in *SCD* mRNA expression with exogenous palmitate. Data are represented as mean ± SEM (n = 15).

4.4.7. Effects of palmitate on fatty acid elongation

The enzyme ELOVL6 (elongation of very long chain fatty acids-like 6) converts C16 to C18 fatty acids. Exogenous palmitate significantly reduced the 18:0/16:0 ratio (P = 0.001, ANOVA) and, although the18:1 *n-7*/16:1 *n-7* ratio was also reduced, this ratio did not reach statistical significance (P = 0.264, ANOVA) (**Figure 4-9**).



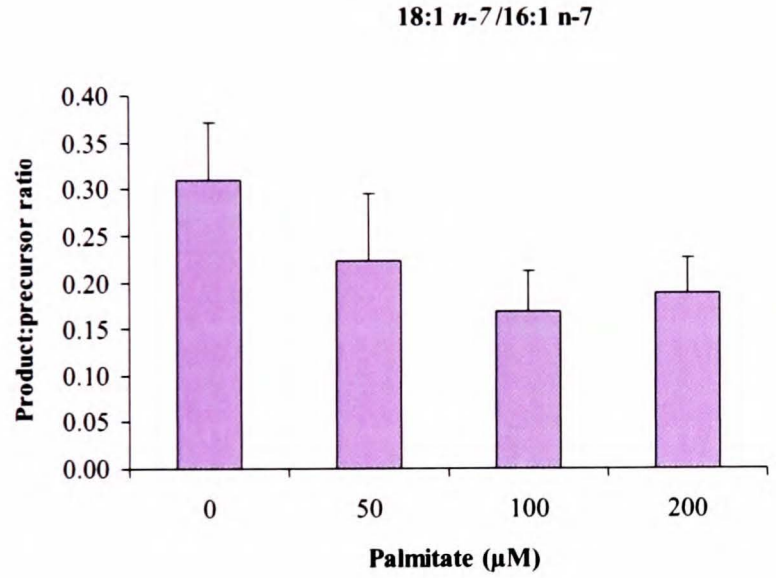


Figure 4-9 Changes in elongation indices with exogenous palmitate. Data are represented as mean ± SEM (n = 15).

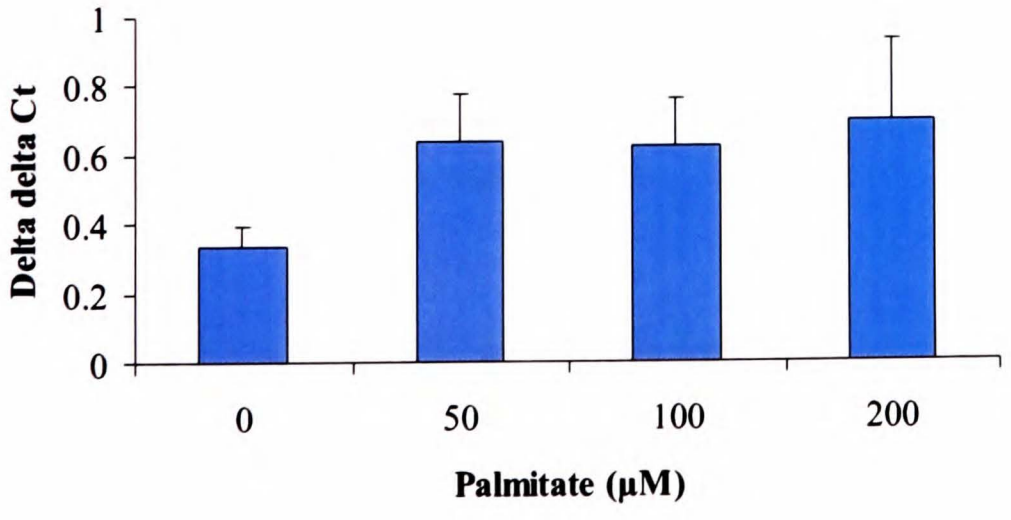


Figure 4-10 Changes in *ELOVL6* mRNA expression with exogenous palmitate. Data are represented as mean ± SEM (n = 15).

Despite a decrease in ELOVL6 enzyme indices, *ELOVL6* mRNA expression was up-regulated by exogenous palmitate (**Figure 4-10**), although this did not reach statistical significance (P = 0.130, ANOVA). Flux through ELOVL6 was calculated as the sum of the products of ELOVL6 action, that is, the sum of 18:0, 18:1 *n-9* and 18:1 *n-7* (**Figure 4-11**). Using this calculation, the flux through ELOVL6 agreed with the changes in *ELOVL6* mRNA and was increased in response to palmitate (P = 0.000).

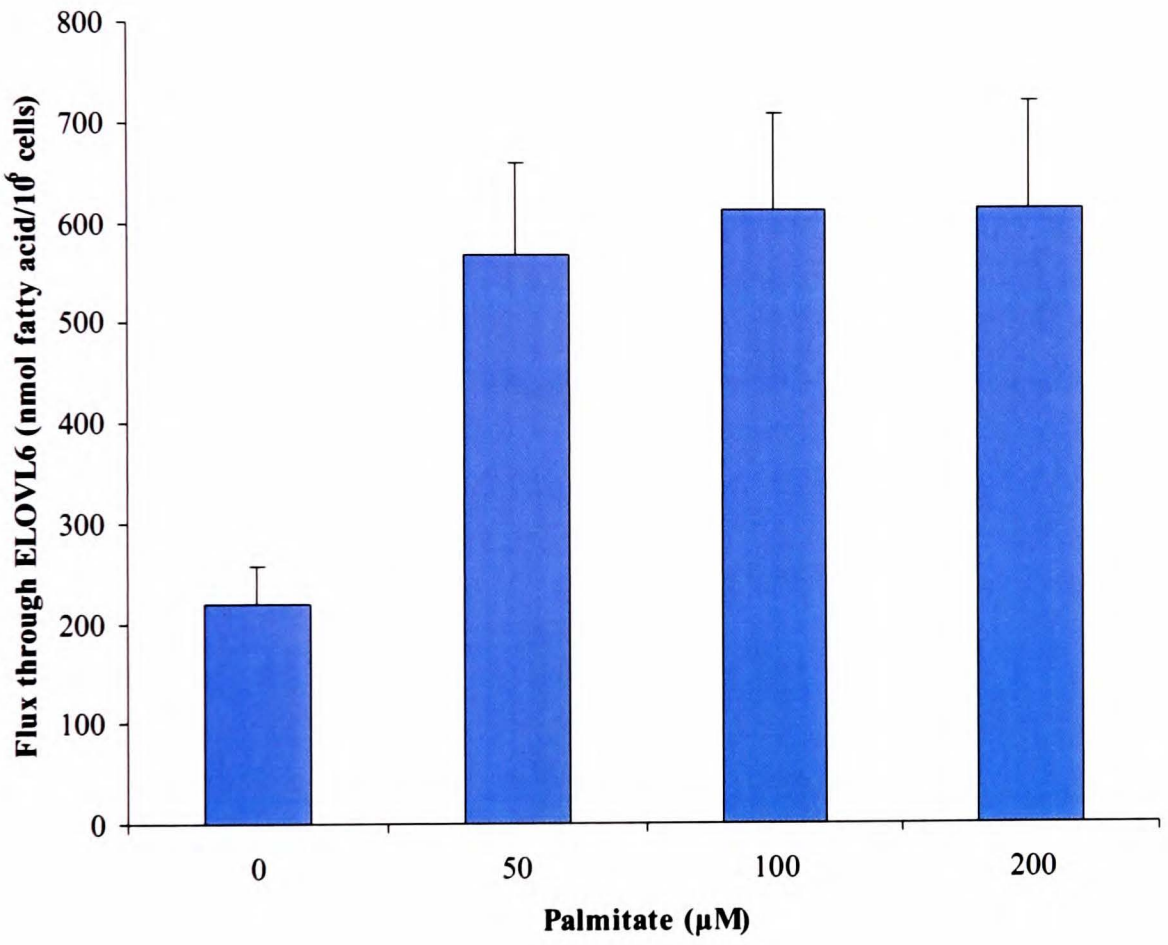


Figure 4-11 Total flux through ELOVL6 over 14 days.
Data are represented as mean ± SEM (n = 15).

4.4.8. Substrate channelling towards desaturation and elongation

The use of [U-^{13}C]palmitate enabled not only the detection of just this exogenous fatty acid, but also any fatty acids produced from it. Using these measurements, specific channelling of exogenous and endogenous fatty acids towards desaturation by SCD and elongation by ELOVL6 was measured.

4.4.8.1. Fatty acid channelling towards SCD desaturation

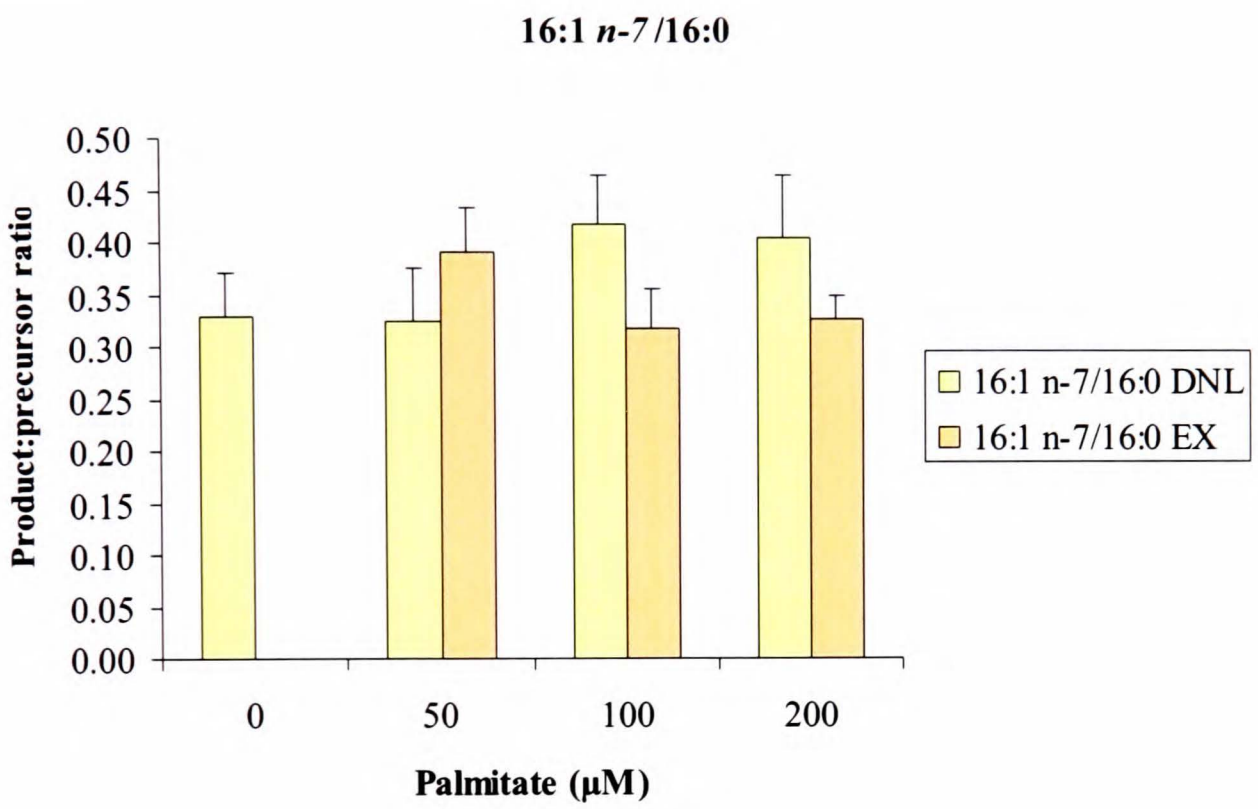


Figure 4-12 SCD indices for DNL-derived and exogenous TG-fatty acids (a) 16:1n-7/16:0 ratios and (b) 18:1n-9/18:0 ratios for TG fatty acids. Data are represented as mean ± SEM (n = 15). DNL represents DNL-derived fatty acid ratios and EX represents exogenous fatty acid ratios.

***P ≤ 0.004**

The source of palmitate, whether DNL-derived or exogenous, did not influence channelling towards desaturation by SCD (P = 0.361 repeated measures ANOVA) (**Figure 4-13(a)**). However, the 18:1 *n-9*/18:0 ratios for DNL-derived stearate were higher than those for exogenously-derived stearate (P = 0.000 repeated measures ANOVA) (**Figure 4-13(b)**), indicating preferential channelling of DNL-derived stearate towards SCD action.

4.4.8.2. Fatty acid channelling towards elongation

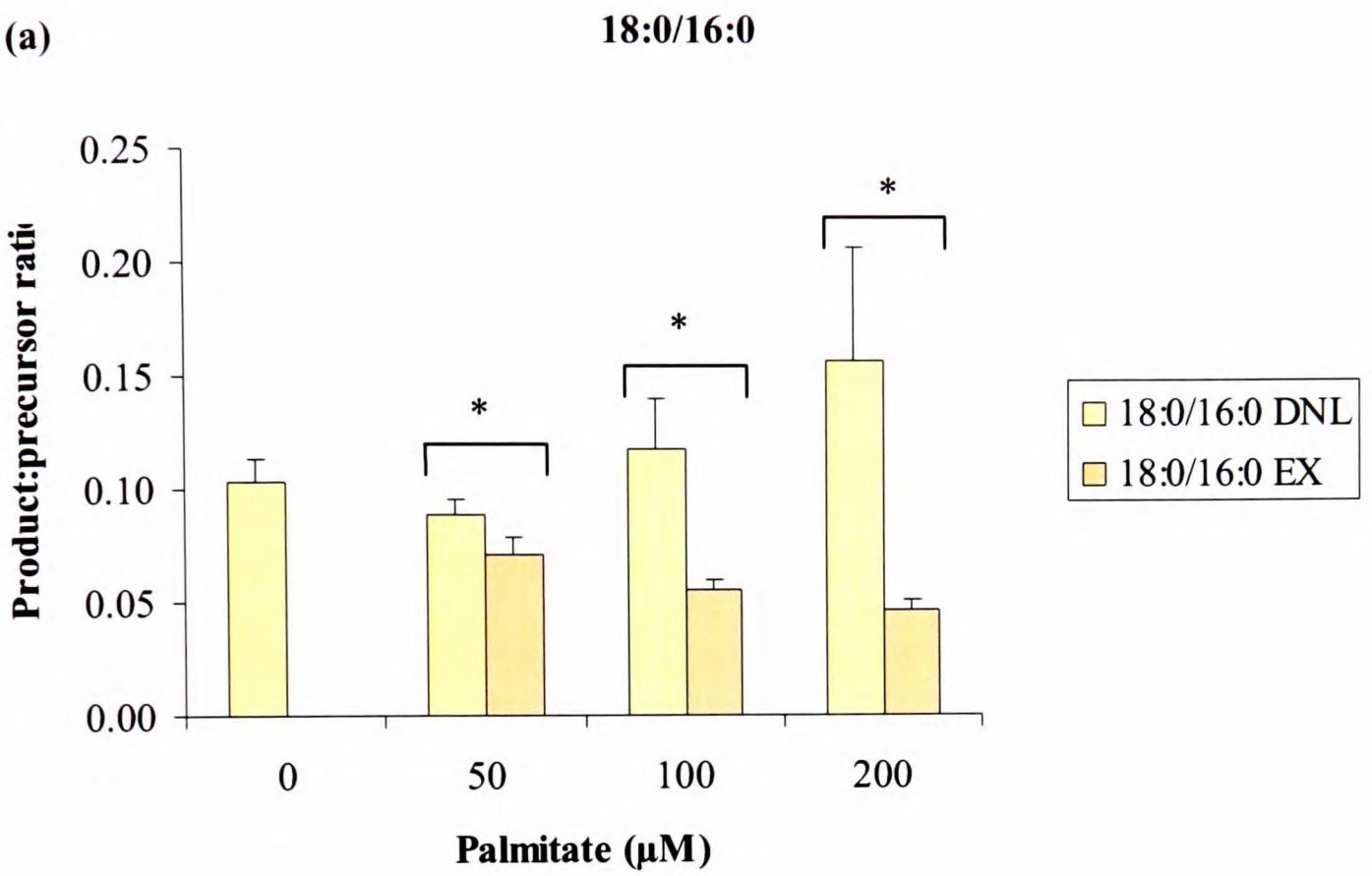


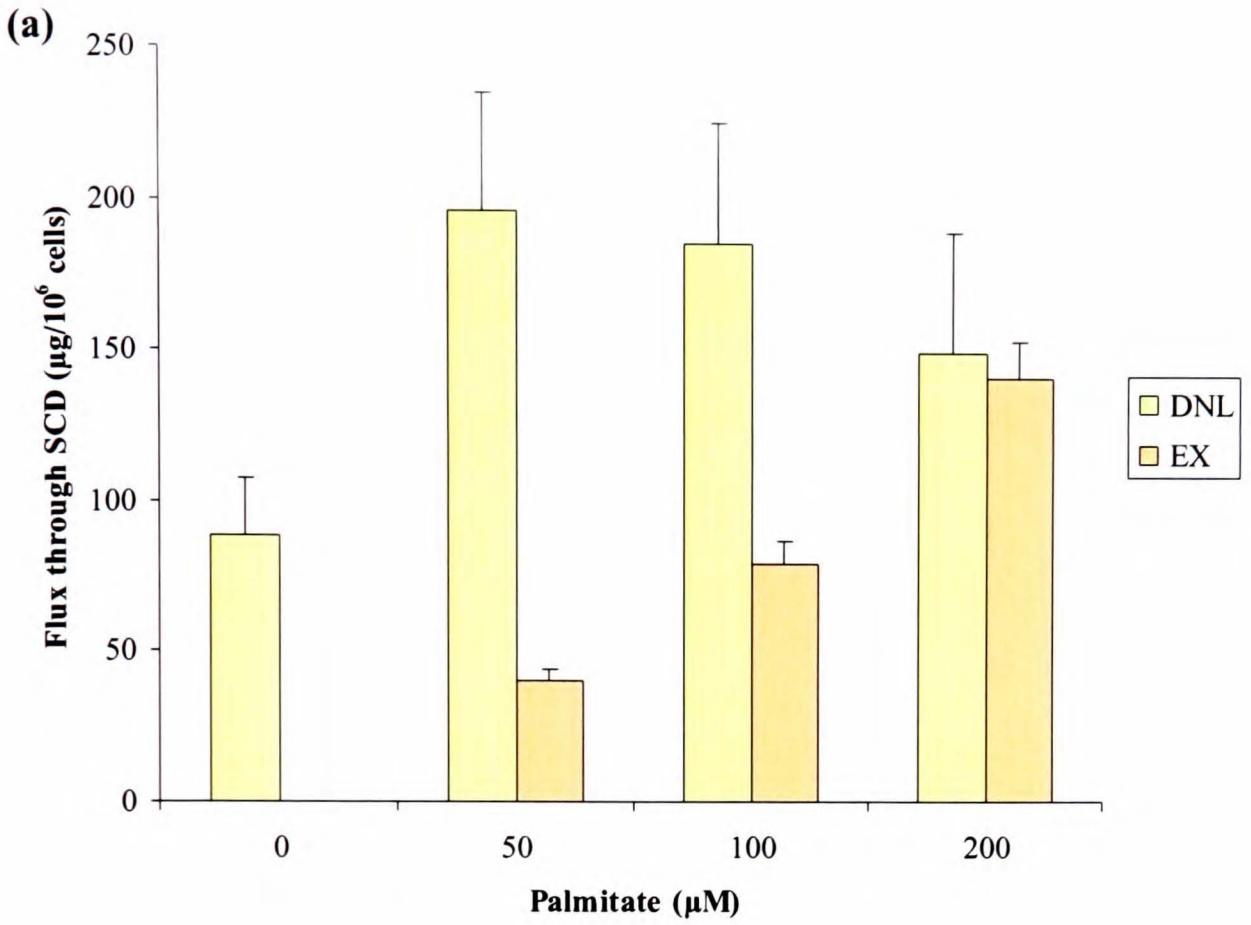
Figure 4-13 Elongation indices for DNL-derived and exogenous TG-fatty acids (a) 18:0/16:0 ratios and (b) 18:1 *n-7*/16:1 *n-7* ratios for TG fatty acids in palmitate tolerant and intolerant adipocytes. Data are represented as mean ± SEM (n = 15).

DNL represents DNL-derived fatty acid ratios and EX represents exogenous fatty acid ratios.

*** P < 0.05**

ELOVL6 appeared to preferentially elongate DNL-derived palmitate over exogenous palmitate (P = 0.022, repeated measures ANOVA) (**Figure 4-13 (a)**). There was no significant difference, however, between the DNL-derived and exogenous 18:1 *n-7*/16:1 *n-7* ratios (P = 0.963, repeated measures ANOVA).

Comparisons of flux of DNL-derived and exogenous fatty acids through both SCD and ELOVL6 showed that there was a preference for DNL-derived fatty acids through ELOVL6 (P = 0.014) but that there was no substrate specificity for SCD (P = 0.144) (**Figure 4-14**). Interestingly, there was an effect of an interaction of palmitate concentration and substrate source on SCD and ELOVL6 (P = 0.003 and 0.008, respectively, repeated measures ANOVA).



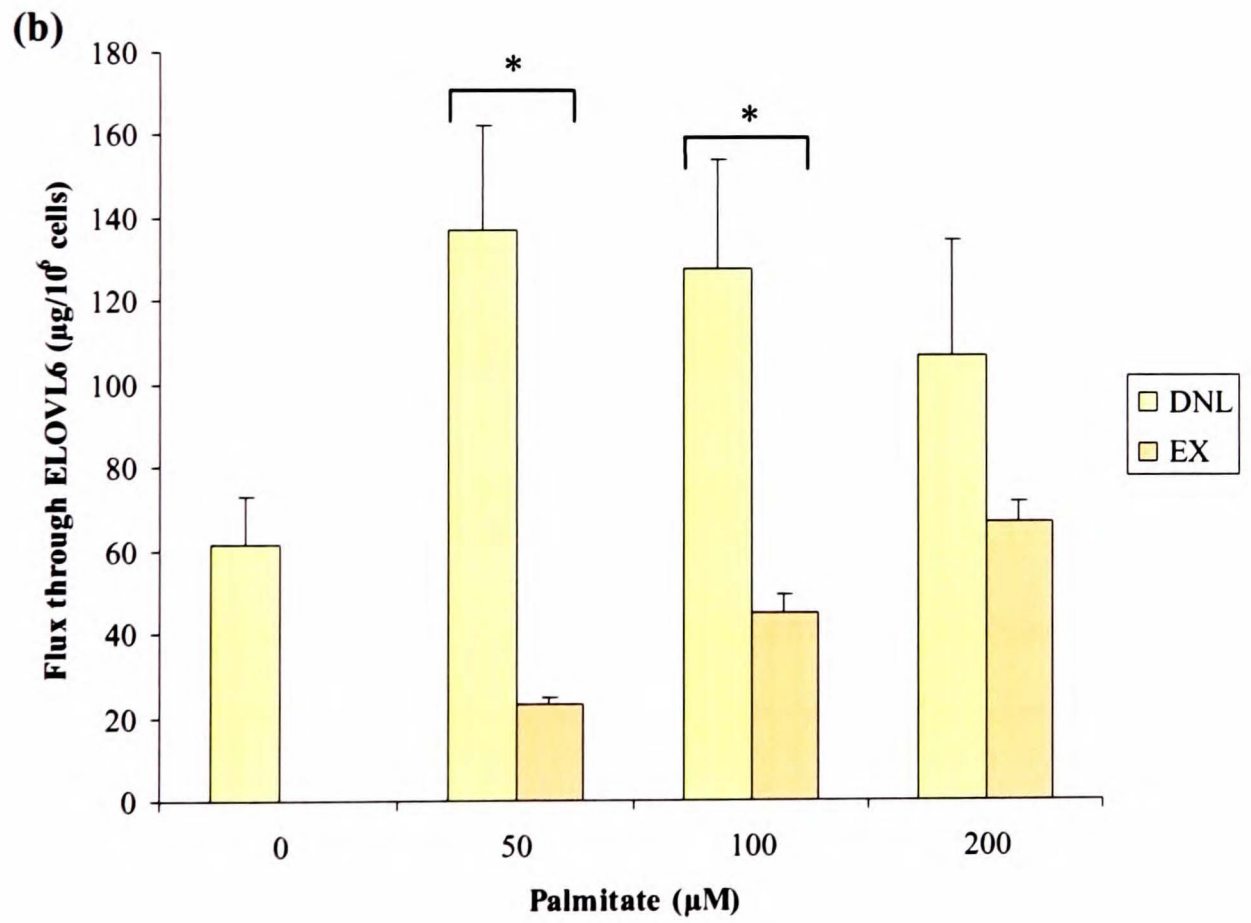


Figure 4-14 DNL and exogenous fatty acid flux through (a) SCD and (b) ELOVL6. Data are represented as mean ± SEM (n = 15). * $P \leq 0.030$

4.4.9. Palmitate chain shortening

In addition to elongation to stearate or desaturation to palmitoleate, one other possible fate of palmitate could be conversion to myristate. This could only be measured in the exogenous, labelled palmitate as unlabelled myristate originating from chain-shortening of DNL-derived palmitate could not be distinguished from DNL-derived myristate.

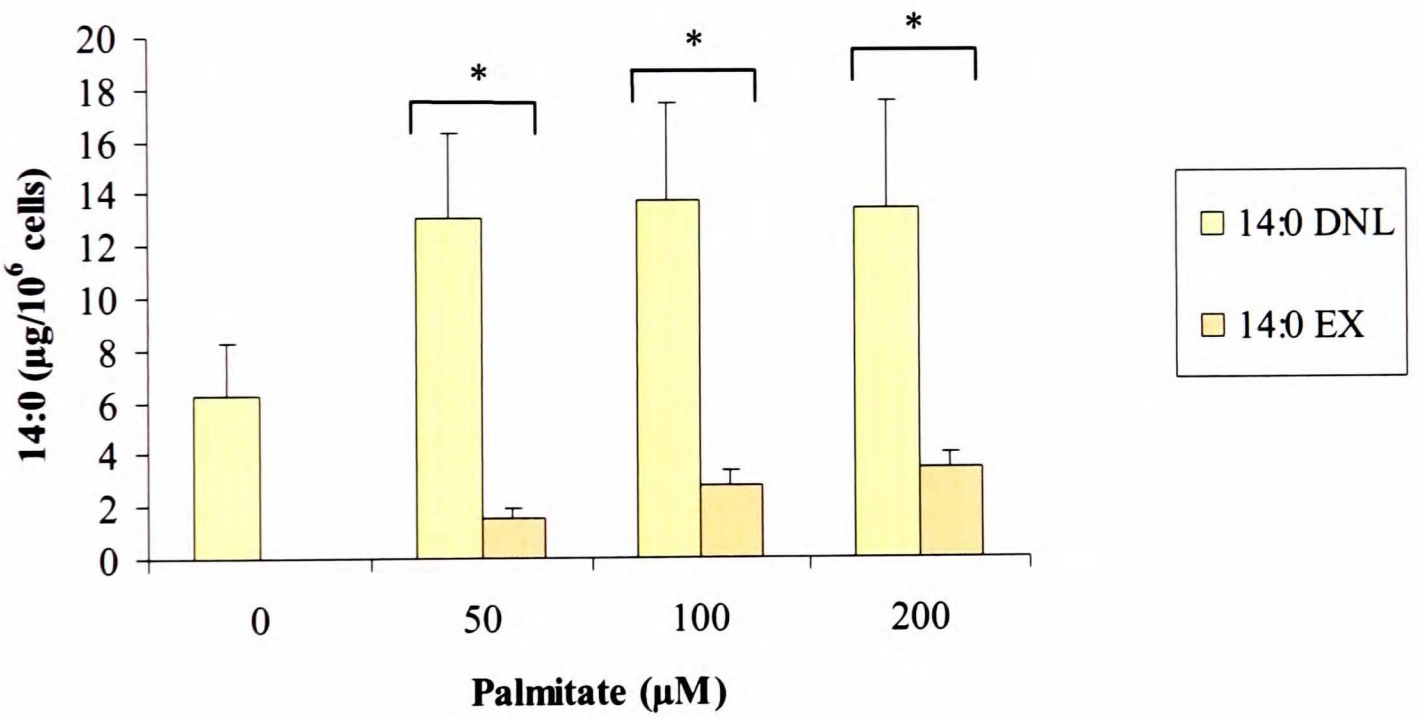


Figure 4-15 Myristate, formed by palmitate chain shortening, in exogenous palmitate-treated adipocytes. Data are represented as mean ± SEM (n = 15). * $P \leq 0.033$

The majority of myristate present in exogenous palmitate-incubated cells was DNL-derived ($P = 0.002$, repeated measures ANOVA). Palmitate chain shortening did contribute to the total myristate, and increased in response to increasing exogenous palmitate concentration ($P = 0.031$, ANOVA) (**Figure 4-15**).

4.4.10. Changes in the cell membrane

As discussed in **Chapter 1**, section **1.6.3**, the fatty acid composition of the plasma membrane can influence its fluidity, and the degree of unsaturation within these fatty acids is crucial to maintain function. Since the TGs produced by the adipocytes in the presence of exogenous palmitate are rich in SAFAs, particularly palmitate (**Table 4.1**), I investigated whether the PL pool of fatty acids was similarly affected and what implications this would have on cell membrane fluidity and insulin sensitivity.

4.4.10.1. Phospholipid fatty acid composition

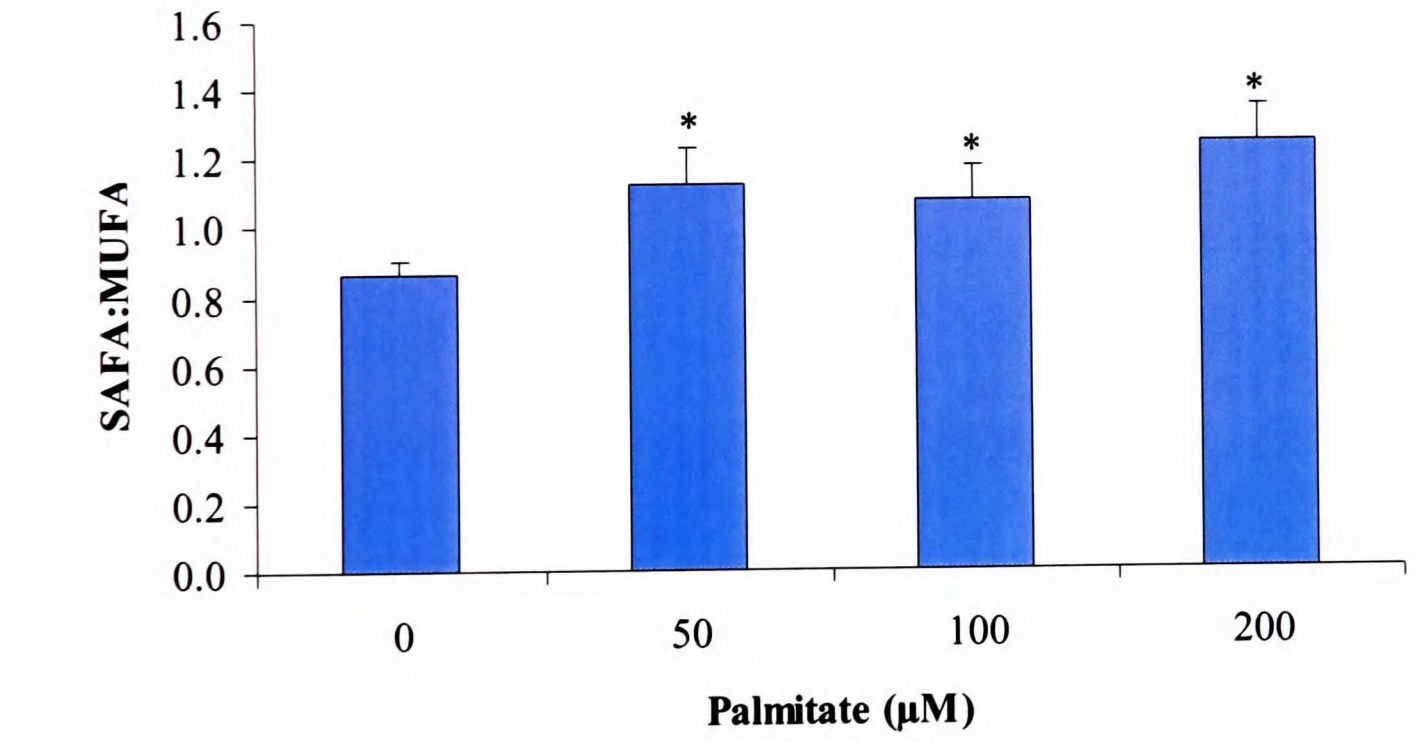


Figure 4-16 Phospholipid fatty acid SAFA:MUFA ratios. Data are represented as mean ± SEM (n = 15). *P ≤ 0.035 compared with 0 μM palmitate control

The SAFA:MUFA ratio of PL fatty acids was calculated and this ratio increased with exogenous palmitate in a dose-dependent manner (P=0.038, ANOVA) (**Figure 4-16**).

This implies that there may be a detrimental effect of palmitate on cell membrane fluidity and insulin sensitivity.

4.4.10.2. Fluorescence recovery after photobleaching (FRAP)

As the PL SAFA:MUFA ratio was increased by exogenous palmitate, the effect on cell membrane fluidity was determined by FRAP (described in **Chapter 2**, section **2.6.2**).

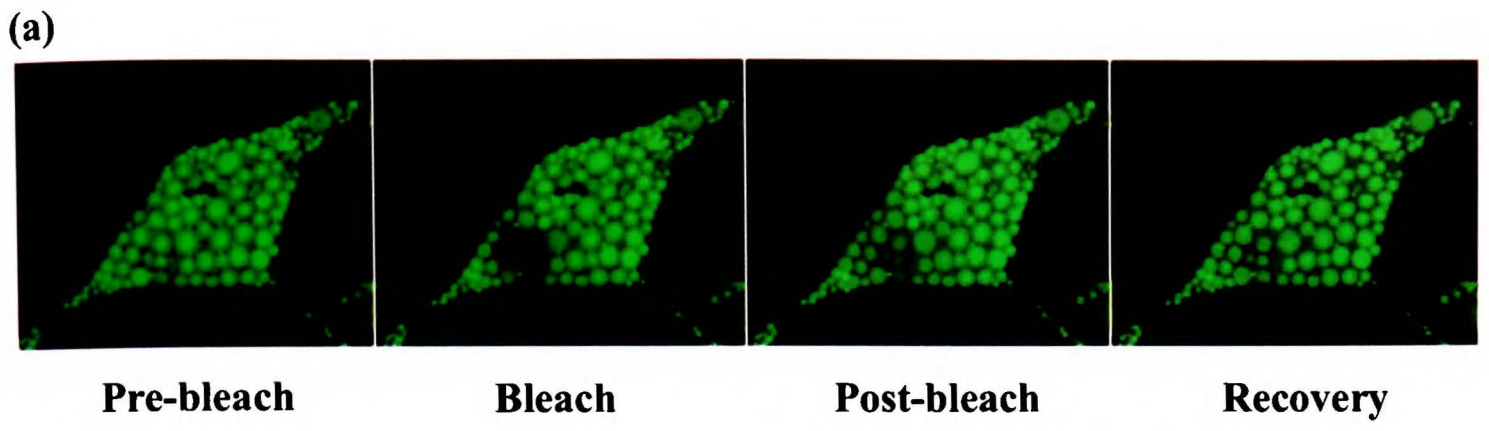


Figure 4-17 Changes in cell membrane fluidity as determined by fluorescence recovery after photobleaching (FRAP) analysis. (a) Fluorescent micrograph images of the main stages of FRAP in the adipocyte (x63 objective), (b) raw data curves of fluorescence intensity (normalised to first frame) and (c) calculated recovery times of adipocytes differentiated with [U-^{13}C]palmitate. Data are represented as mean ± SEM (n = 3 subjects)

The effects of 0, 50 and 200 μM palmitate on the cell membrane fluidity, assessed by FRAP, are shown in **Figure 4-17**. Neither 50 nor 200 μM palmitate changed the fluidity compared with the control cells (P = 0.426 and 0.254, respectively).

4.4.11. Effects of palmitate on adipocyte insulin sensitivity

A previous study looking at the effects of various SAFAs and MUFAs, at a concentration of 330 μM, on insulin sensitivity in differentiated 3T3-L1 preadipocytes showed SAFAs but not MUFAs to reduce both insulin binding and insulin-stimulated deoxyglucose uptake of these cells (Grunfeld *et al.*, 1981).

Figure 4-18 shows the effects of 50 and 200 μM palmitate on 2-deoxy-D-[1-^{3}H]glucose ([^{3}H]2-DOG) uptake in differentiated human preadipocytes. At all palmitate concentrations there was a significant dose-response to palmitate (P = 0.003, repeated measures ANOVA) and to insulin (P < 0.001, repeated measures ANOVA). The addition of exogenous palmitate reduced 2-DOG uptake. A Tukey's least significant difference *post hoc* test for comparing differences between the palmitate concentrations showed significant differences between 0 and 50 μM (P = 0.021) and 0 and 200 μM (P = 0.016) but not between 50 and 200 μM (P = 0.672).

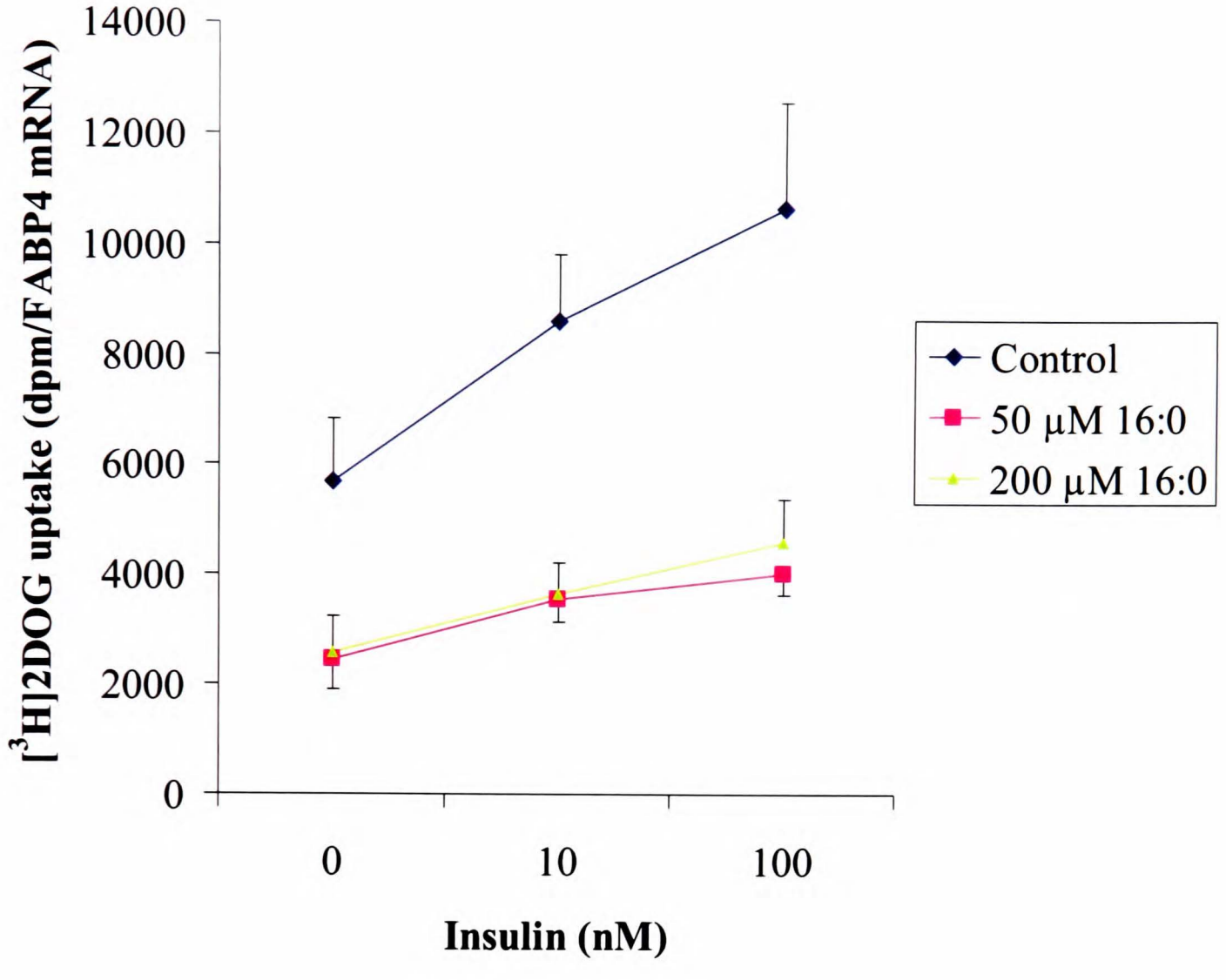


Figure 4-18 [^{3}H]2-deoxyglucose uptake in response to 0, 50 and 200 µM exogenous palmitate with dose-response to insulin. Data are represented as mean ± SEM (n = 5).

4.5. DISCUSSION

There was a clear correlation between total TG accumulation and exogenous palmitate concentration which also corresponded to a direct increase in each fatty acid. The TG fatty acid profiles provided evidence for desaturation and elongation within the adipocyte in the presence of exogenous fatty acid.

Amri *et al.* (1991; 1994) reported that incubating preadipocytes with fatty acids increased the number of differentiated cells and up-regulated genes involved in differentiation and TG synthesis. Here, there was a dose-dependent increase of TG

accumulation with the addition of palmitate and an increase in *FABP4* mRNA expression which was not dependent upon palmitate concentration. Although TG correlated with *FABP4* mRNA expression in control cells, this was not the case with palmitate-incubated cells. Therefore, in differentiated human preadipocytes, uptake and storage of exogenous palmitate increases TG accumulation but does not correspond to a dose-dependent increase in differentiation.

SCD indices correlated positively with *SCD* mRNA expression. However, there were discrepancies between *SCD* and *ELOVL6* mRNA expression and their respective product-to-precursor ratios. Both SCD indices are subject to alteration by the activity of ELOVL6 (**Figure 4-19**). As 16:1 *n-7* is a substrate for chain elongation, the measured 16:1 *n-7*/16:0 ratio may be artificially reduced due to elongation of 16:1 *n-7*. Additionally, 16:0 is also a substrate for ELOVL6, and elongation of this fatty acid could alter both 16:1 *n-7*/16:0 (by reducing product levels) and 18:1 n-9/18:0 ratios (by increasing product levels). ELOVL6 activity may also be miscalculated using the 18:0/16:0 ratio as this could be affected by SCD action; both the product and the precursor of this ratio are substrates for SCD. We know that 18:0 is the preferred substrate for SCD, so it is unlikely that there would be equal desaturation of 16:0 and 18:0, which could lead to an underestimation of 18:0/16:0 ratio. Therefore, measurement of flux through these enzymes, estimated as a sum of all the fatty acid products of the enzyme, along with the enzyme indices, may provide a clearer insight into enzyme activity. Furthermore, calculated total flux through SCD and ELOVL6 agreed with their respective enzyme mRNA expression.

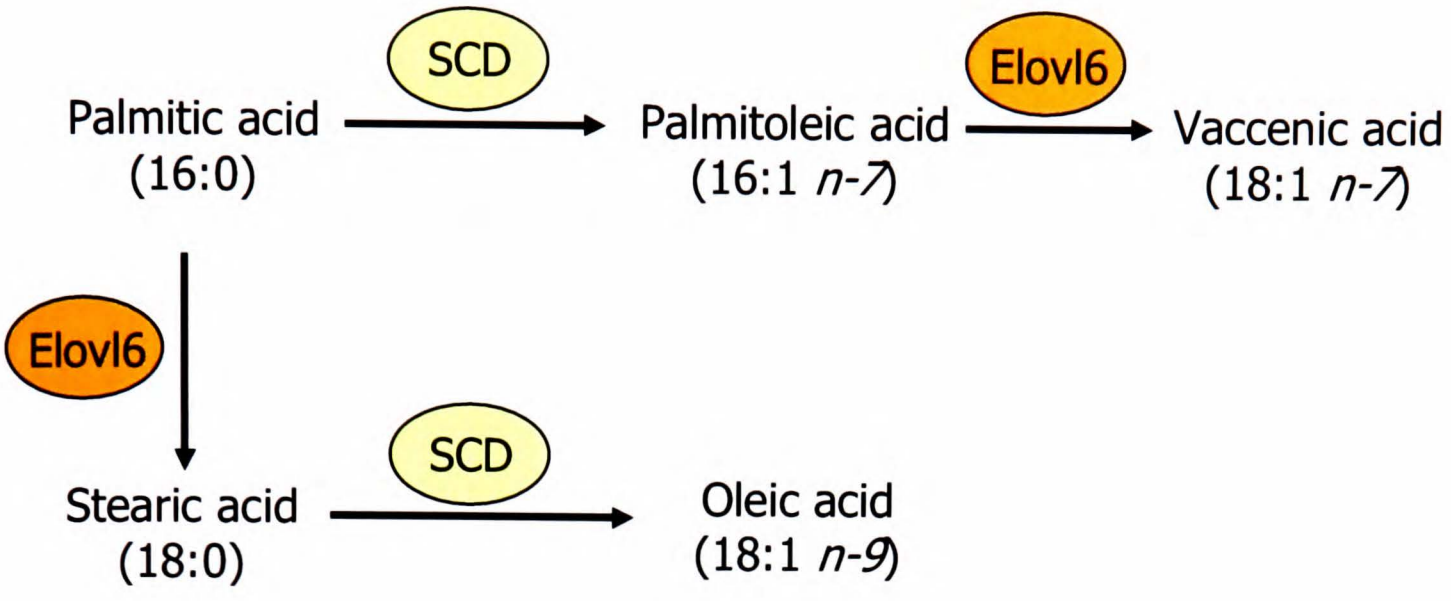


Figure 4-19 Fatty acid pathways showing how fatty acids acted upon by SCD and ELOVL6 may overlap and distort enzyme activity calculations using product-to-precursor ratios.

In agreement with previous findings of DNL up-regulation by palmitate, palmitate also up-regulated DNL in human adipocytes, although this was not in a dose-dependent manner. It seems counter-intuitive that increasing the end-product of DNL, palmitate, should up-regulate this process. SCD and ELOVL6 were also increased by palmitate and this increase was dose-dependent. This would seem logical as palmitate increased the supply of substrate for these enzymes. It has previously been shown that DNL and SCD are co-ordinately up-regulated in response to short-term high carbohydrate feeding in humans (Chong *et al.*, 2008). If SCD and DNL are synchronously regulated, one possible effect of up-regulating SCD could be to simultaneously up-regulate the pathway for DNL. Despite SCD being up-regulated in a dose-dependent manner, the lack of a dose-response to palmitate up-regulation of DNL could represent a limit in the absolute capacity for this process within the human adipocyte that has already been reached with lower palmitate concentrations.

In addition to an apparently synchronised, palmitate-induced up-regulation of SCD and DNL, measurements of substrate specificity of SCD, with respect to origin of the fatty acid, highlighted a preference for DNL-derived over exogenous stearate. There was no significant substrate preference for palmitate. Flux through ELOVL6 was also greater for DNL-derived fatty acids although this may have been influenced by a specific preference for elongation of DNL-derived palmitate. Taken together, these findings imply that newly synthesised palmitate is targeted for elongation to stearate, which is then desaturated to oleate. The potential importance of oleate within the cell is two-fold. Firstly, endogenously-derived oleate may be crucial for TG synthesis (Miyazaki *et al.*, 2001; Man *et al.*, 2006). Faced with an excess abundance of palmitate within the cell, the adipocyte may act to maximise its storage by up-regulating DNL and SCD, generating a source of endogenous oleate. Man *et al.* (2006) showed DGAT2 and SCD to be co-localised on the endoplasmic reticulum. Palmitate up-regulation of DGAT2 may occur as a knock-on effect of SCD up-regulation which could then act to enhance TG formation. Secondly, oleate is one of the most abundant fatty acids in the cell membrane and DNL may provide a source of this fatty acid for PL synthesis. Therefore, it could be that this mechanism of shunting endogenously-produced palmitate towards oleate synthesis has been engineered by the adipocyte to optimise TG storage and maintain cell membrane fluidity. Channelling of fatty acids will be discussed further in **Chapter 6**.

An interesting observation in the TG fatty acid composition of adipocytes differentiated with exogenous palmitate, was the presence of a small amount of labelled myristate. This could have arisen as a result of β-oxidation of palmitate. However, it is known that malonyl-CoA acts as a repressor of carnitine palmitoyl

transferase-1 (CPT-1), and hence β-oxidation (Ruderman *et al.*, 1999; Saggerson, 2008). In the highly lipogenic environment of the culture conditions, it would seem unlikely that fatty acid oxidation could occur, bearing in mind also, the already limited capacity of β-oxidation within the white adipocyte. One possibility may be that fatty acid oxidation occurred in another organelle, other than the mitochondria, such as the peroxisomes, in which fatty acid oxidation may not be regulated by malonyl-CoA (Saggerson, 2008).

Fatty acid composition of the plasma membrane is known to be important to maintenance of function. Changes in the SAFA:MUFA ratio may help to explain the decrease in insulin-stimulated 2-DOG uptake in the adipocytes, however, the FRAP data show that there was no deterioration of cell membrane fluidity with exogenous palmitate. This could suggest that while the fluidity *per se* is not affected by an increase in saturated fatty acids, function may be, for example, insulin receptor signalling with the cell membrane might be diminished. This would be in keeping with other reports of saturated fatty acids, particularly palmitate, being associated with insulin resistance (Schmitz-Peiffer *et al.*, 1999; Vessby *et al.*, 2002; Reynoso *et al.*, 2003; Dimopoulos *et al.*, 2006). Explanations for reduced insulin-stimulated 2-DOG uptake could include impairment of GLUT4 translocation to the cell membrane or changes in insulin receptor signalling. High fat diets are associated with insulin resistance and have been linked with reduced glucose transport (Boden *et al.*, 1994; Hansen *et al.*, 1998). In hepatocytes, palmitate induced insulin resistance by decreasing insulin receptor protein and preventing phosphorylation of intermediates of the insulin signalling pathway (Ruddock *et al.*, 2008).

In conclusion, the process of DNL has been dismissed by many as being insignificant in the human adipocyte. Whereas its contribution to fatty acid storage in the adipocyte may be minor, it may play a more subtle role in being a key regulator of other pathways within this cell. An over-abundance of palmitate has been linked with insulin resistance and metabolic dysregulation. Therefore, by acting in tandem, DNL and SCD may promote conversion of exogenous palmitate to monounsaturated fatty acids and storage within the adipocyte-TG, protecting the cell from its potentially damaging effects.

Chapter 5

The effects of a high concentration of palmitate on DNL and SCD and global changes seen in gene expression

5.1. INTRODUCTION

In **Chapter 4**, the effects of typical physiological concentrations of palmitate on the regulation of DNL, fatty acid metabolism and insulin sensitivity were described in differentiated human preadipocytes. This chapter will focus on the effects of a higher, yet still physiological, concentration of palmitate and look at how palmitate can disrupt cell function.

In many cell types, incubation with palmitate can have adverse effects. In pancreatic β-cells, palmitate has been reported to have adverse effects on cell function. Moffitt *et al.* showed that palmitate led to an accumulation of tripalmitin within the endoplasmic reticulum (ER), resulting in an abnormal morphology and reduced glucose-stimulated insulin secretion which may induce ER stress and apoptosis (Moffitt *et al.*, 2005). Increases in intracellular ceramide have been linked with palmitate, a precursor for ceramide biosynthesis. It has been proposed that palmitate conversion to ceramide is responsible for palmitate's ill-effects on cells, such as apoptosis and insulin resistance (Maedler *et al.*, 2003; Powell *et al.*, 2004; Sabin *et al.*, 2007). However, other investigations have shown palmitate-induced ER stress and apoptosis to occur independently of ceramide production (Listenberger *et al.*, 2001; Wei *et al.*, 2006). Although the mechanism of action has not yet been elucidated, the evidence exists for palmitate induction of ER stress and apoptosis in various cell types. Interestingly, palmitate-induced apoptosis can be rescued by the monounsaturated fats palmitoleate and oleate, preventing apoptosis and increasing fatty acid storage as TG (Listenberger *et al.*, 2003; Maedler *et al.*, 2003).

Many of the adverse effects of saturated fatty acids described are from studies in non-adipose cells, with a limited capacity for fatty acid storage. In my initial experiments, differentiating preadipocytes with a high concentration (400 μM) of palmitate led to cell death in a subpopulation of some subjects' adipocytes. As lower concentrations had no adverse effects on cell viability, the causes for cell death with this higher concentration were further investigated.

5.2. AIMS

The aims of the experiments in this chapter were to understand the effects of high concentrations of palmitate on adipose tissue and the mechanisms involved in cell toxicity. In order to gain a greater understanding of the key regulatory points of lipotoxicity, global changes in gene expression were investigated using microarray techniques.

5.3. METHODS

5.3.1. Adipose tissue sample collection

The taking of human adipose tissue samples was approved by the Oxfordshire Clinical Research Ethics Committee and all subjects gave written, informed consent. Subcutaneous adipose tissue biopsies were taken and preadipocytes isolated as described in **Chapter 2**, section **2.1.2**. Volunteers for the experiments described in this chapter consisted of 7 males and 8 females.

5.3.2. Cell culture

Preadipocytes were grown to confluence before differentiating for 14 days as described in **Chapter 2**, section **2.1.3**. [U-^{13}C]palmitate (99% isotopic purity) was added to the differentiation medium throughout differentiation at a concentration of 400 μM.

5.3.3. TG and PL fatty acid composition

TGs and PLs were extracted from harvested cells and fatty acid composition analysed using GC (**Appendix 1,** sections **A1.2 and A1.3**). The isotopic composition of the fatty acids was further examined by GC-MS (**Appendix 1,** section **A1.4**) to determine the fate of the exogenous palmitate.

5.3.4. Gene expression

Total mRNA was extracted using Tri-Reagent (Ambion, Houston, Texas, USA). This was then used to synthesise cDNA for real-time PCR analysis of gene expression as well as being used to create labelled cRNA for use on microarray slides to study global changes in gene expression (**Appendix 1,** section **A1.7**). Pre-designed, validated TaqMan primers and probes were obtained from Applied Biosystems, Warrington, UK (**Appendix 1,** section **A1.6**).

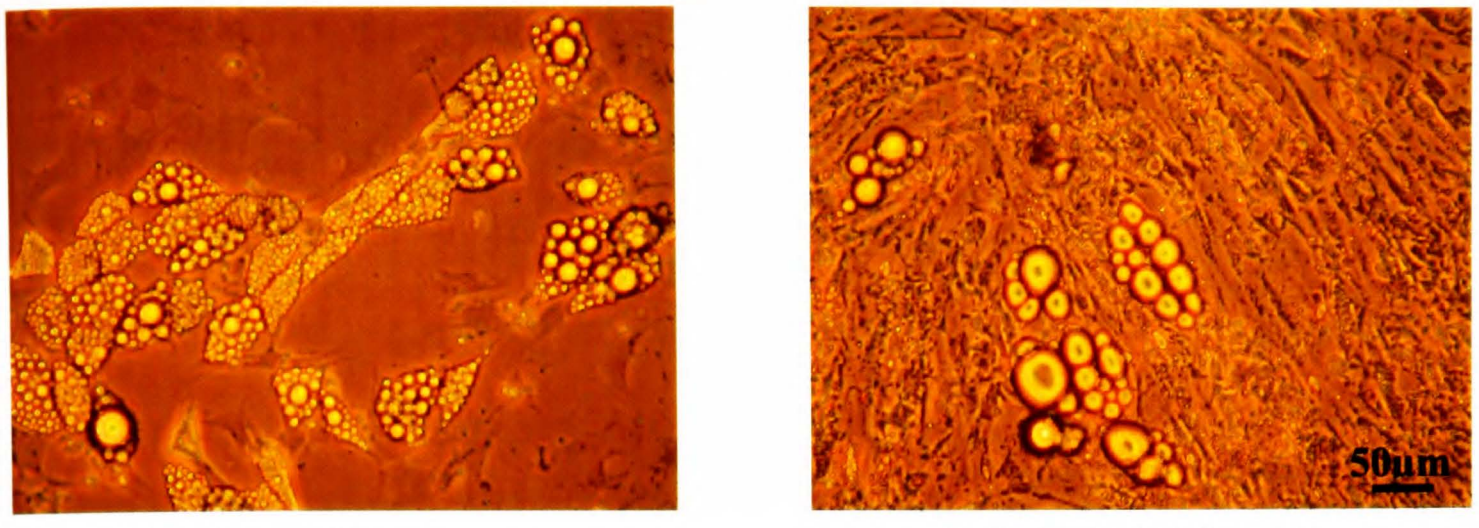
5.3.5. Statistical analyses

Comparisons made between palmitate-tolerant and intolerant groups were analysed using a Student's *t* test. Statistical analyses of microarray were made using the online Genesifter™ Analysis Edition, as described in **Chapter 2** section **2.7.3**.

5.4. RESULTS

5.4.1. Cell morphology and TG accumulation

Differentiation of preadipocytes with 400 μM palmitate revealed that the adipocytes from some donors showed reduced cell viability in a sub-population of the cells. As the adipocytes from each donor varied in their response to this higher concentration of exogenous palmitate, that is, adipocytes either thrived or showed partial cell death, the two populations were studied separately. Adipocytes that survived the high, 400 μM palmitate were classed as tolerant (n = 10) and those that did not were classed as intolerant (n = 5). Classification was determined solely by observation of significant cell death, as seen by large areas of cell debris interspersed with occasional, very large lipid droplets, in the presence of 400 μM pamitate (**Figure 5-1**).



Palmitate-tolerant **Palmitate-intolerant**

Figure 5-1 Cell morphology of palmitate-tolerant and palmitate-intolerant cells treated with 400 µM palmitate (x10 objective)

The morphological observations were supported by measurements of total TG, showing a decrease in total TG accumulation in the palmitate-intolerant cells (**Figure 5-2**).

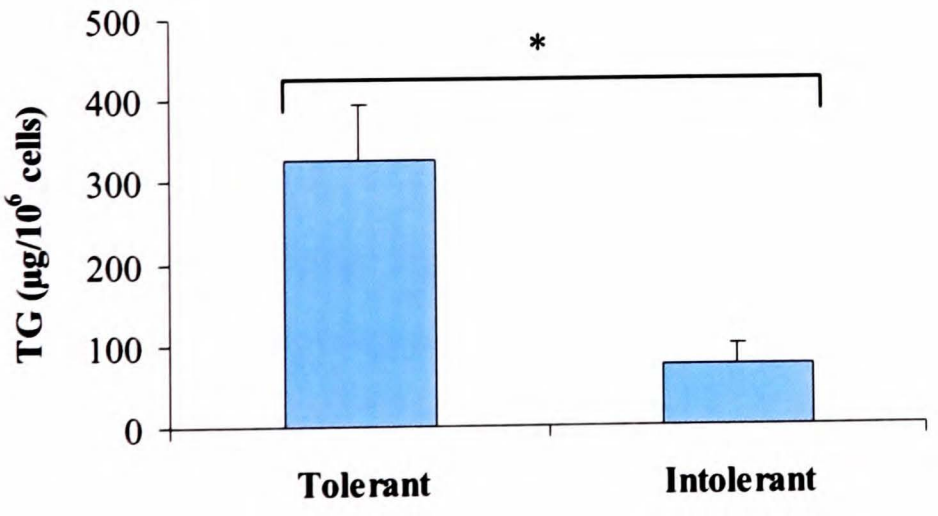


Figure 5-2 Total TG accumulation in palmitate-tolerant (n = 10) and intolerant (n = 5) adipocytes. Data are represented as mean ± SEM * P = 0.040

Acyl-coenzyme A:diacylglycerol acyltransferase 2 (DGAT2) is the enzyme that catalyses the terminal step of TG synthesis (**Chapter 1**, section **1.4.3**). In parallel with a decrease in TG accumulation in the palmitate-intolerant adipocytes, *DGAT2* mRNA expression was also reduced (**Figure 5-3**). In order to correct for cell death, the geometric mean of three separate housekeeping genes was used as a denominator when calculating mRNA expression.

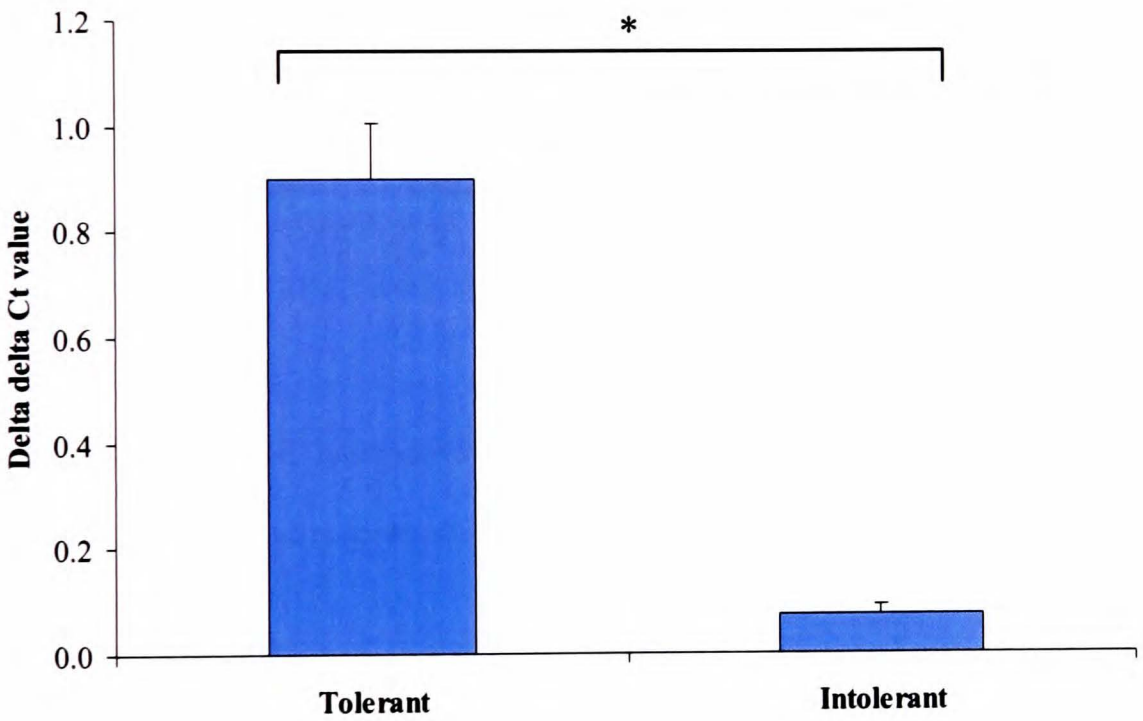


Figure 5-3 ***DGAT2*** **mRNA expression in palmitate-tolerant (n = 10) and intolerant (n = 5) adipocytes. Data are represented as mean ± SEM * P < 0.001**

The fatty acid composition of the TG differed between the palmitate-tolerant and intolerant groups (**Figure 5-4**). There were significantly higher proportions of the saturated fatty acids, palmitate and stearate, and lower proportions of the unsaturated fatty acids palmitoleate and oleate in the palmitate-intolerant adipocytes.

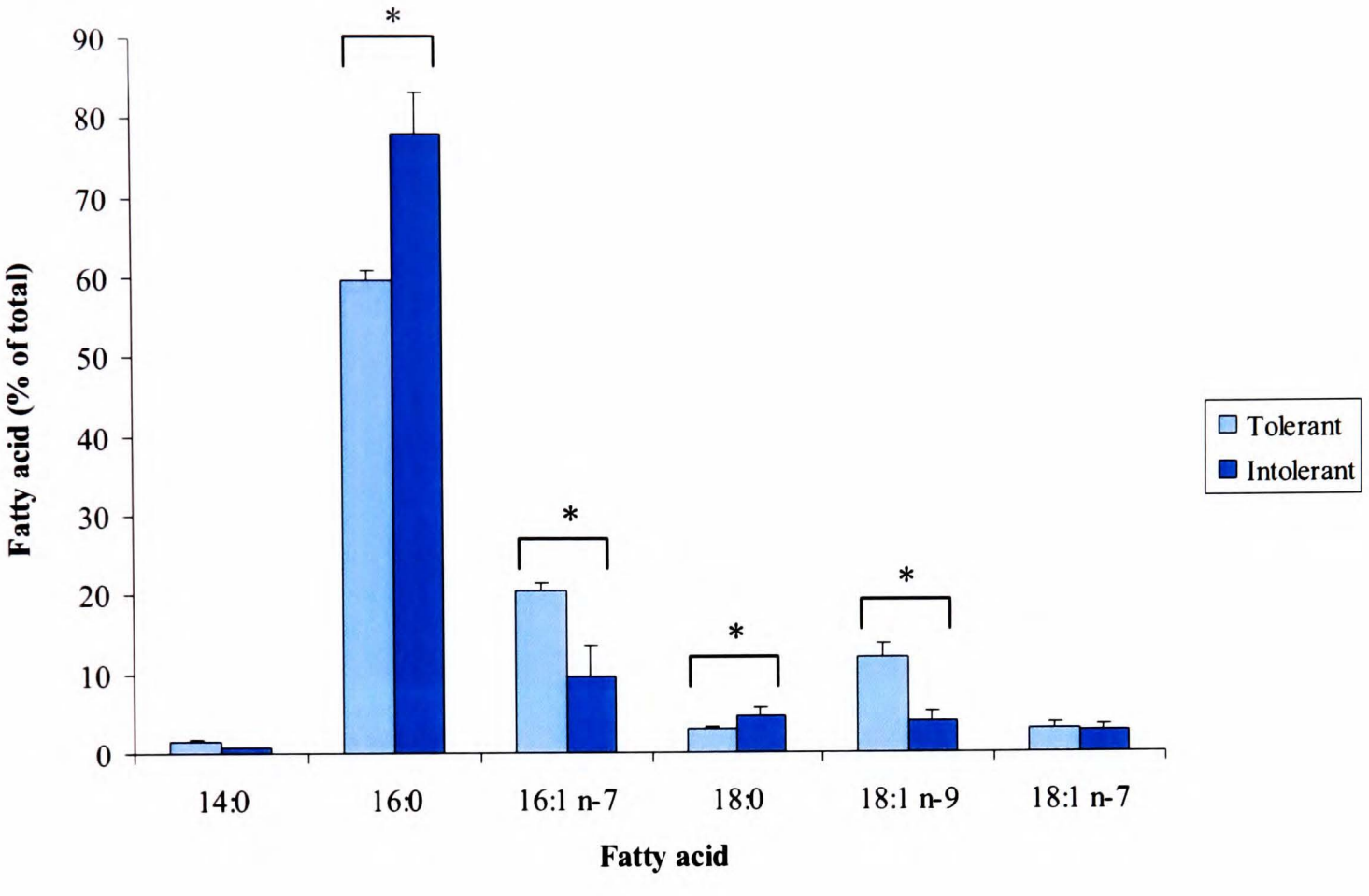


Figure 5-4 Fatty acid composition of TG in palmitate-tolerant (n = 10) and intolerant (n = 5) adipocytes. Data are represented as mean ± SEM. Data are represented as mean ± SEM

*** $P \leq 0.023$**

5.4.2. Changes in DNL

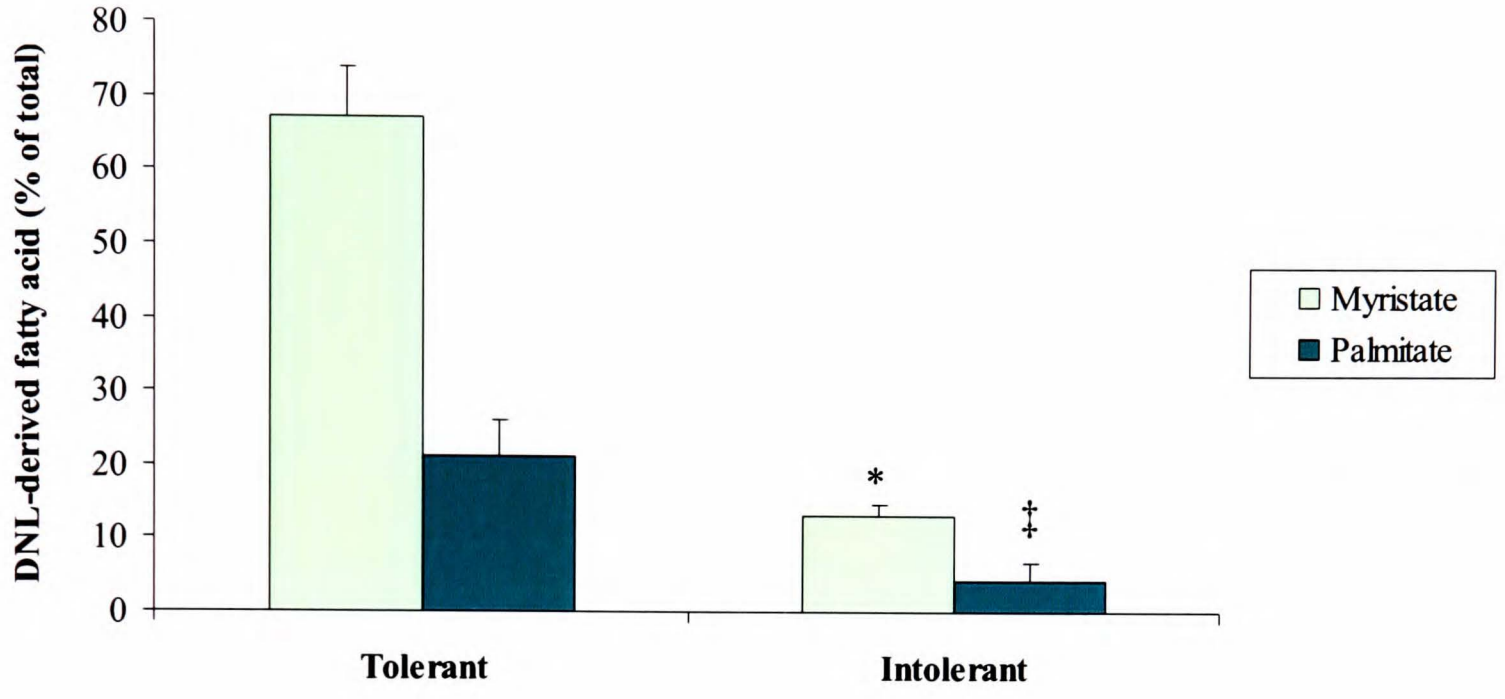


Figure 5-5 Differences in DNL-derived myristate and palmitate in palmitate-tolerant (n = 10) and intolerant (n = 5) groups. Data are represented as mean ± SEM. * P <0.001, ‡ P = 0.042 (tolerant vs intolerant)

Differences in regulation of DNL were measured between the two populations of adipocytes. The DNL-derived fatty acid content of adipocyte TG was reduced in the palmitate-intolerant compared with the palmitate-tolerant cells (**Figure 5-5**). Expression of mRNA for DNL-associated genes was significantly down-regulated and is summarised in **Figure 5-6**.

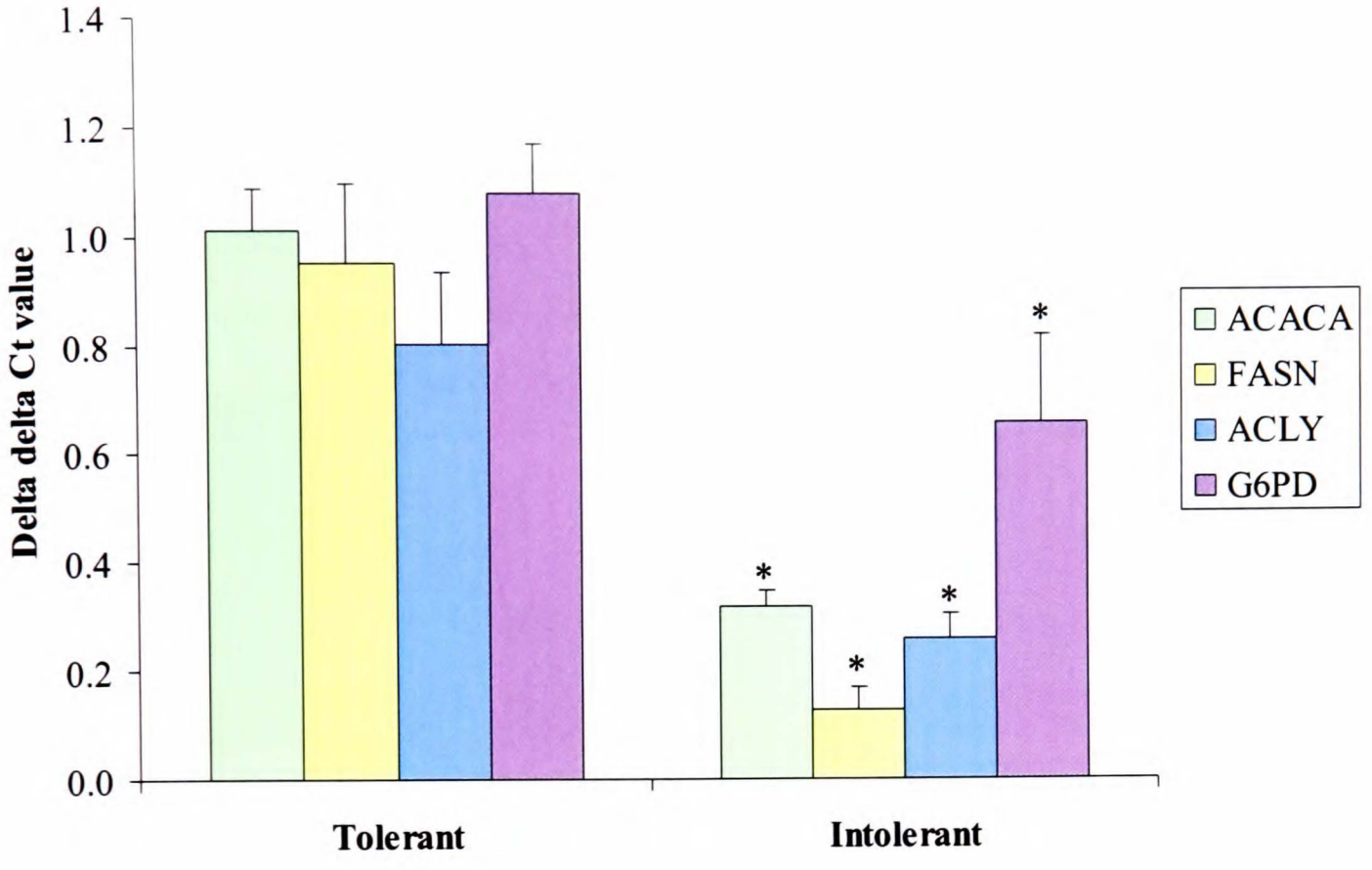
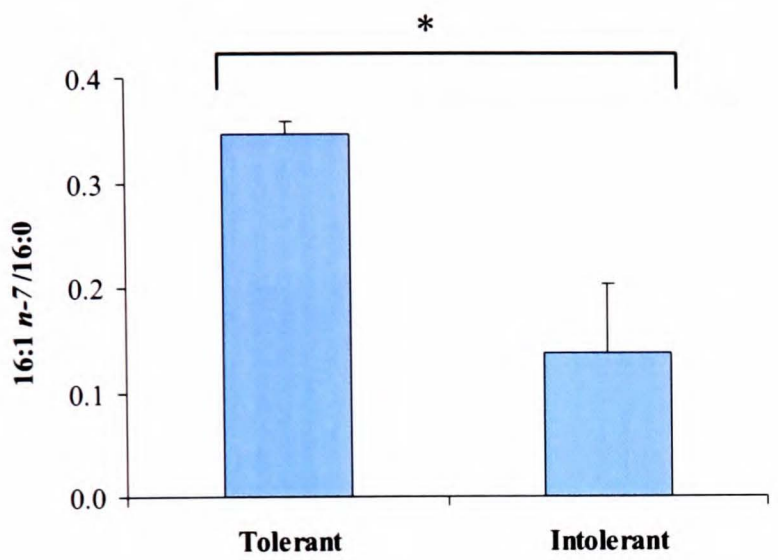


Figure 5-6 Expression of DNL-asssociated genes in palmitate-tolerant (n = 10) and intolerant (n = 5) adipocytes. Data are represented as mean ± SEM. * $P \leq 0.027$ (tolerant vs intolerant)

5.4.3. Intracellular modification of palmitate



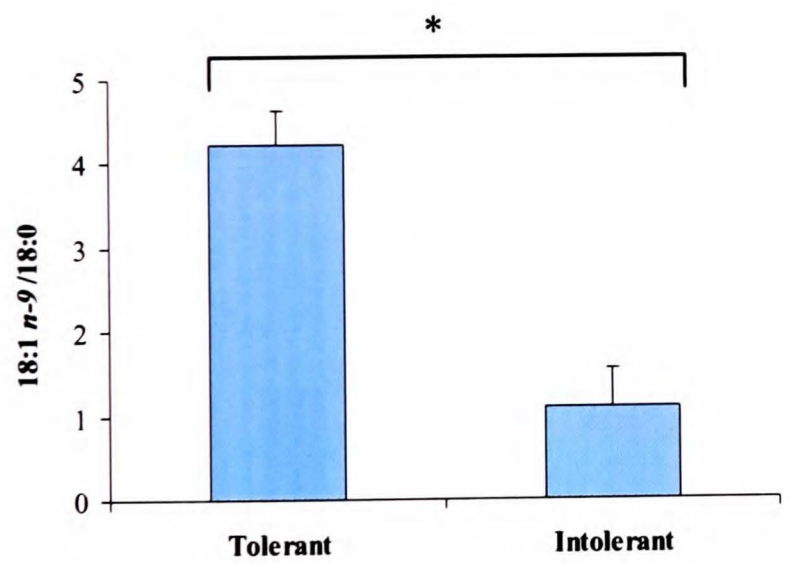


Figure 5-7 SCD indices for palmitate-tolerant (n = 10) and intolerant (n = 5) TG-fatty acids showing (a) 16:1 n-7/16:0 and (b) 18:1 n-9/18:0 * P < 0.001 Data are represented as mean ± SEM.

The proportions of saturated to monounsaturated fatty acids were different between the palmitate-tolerant and intolerant adipocytes suggesting a difference in handling of palmitate within the two groups (**Figure 5-4**). Therefore, modification of palmitate

was investigated. The SCD indices were lower in the intolerant than the tolerant group (**Figure 5-7**) and *SCD* mRNA expression was also reduced (**Figure 5-9**).

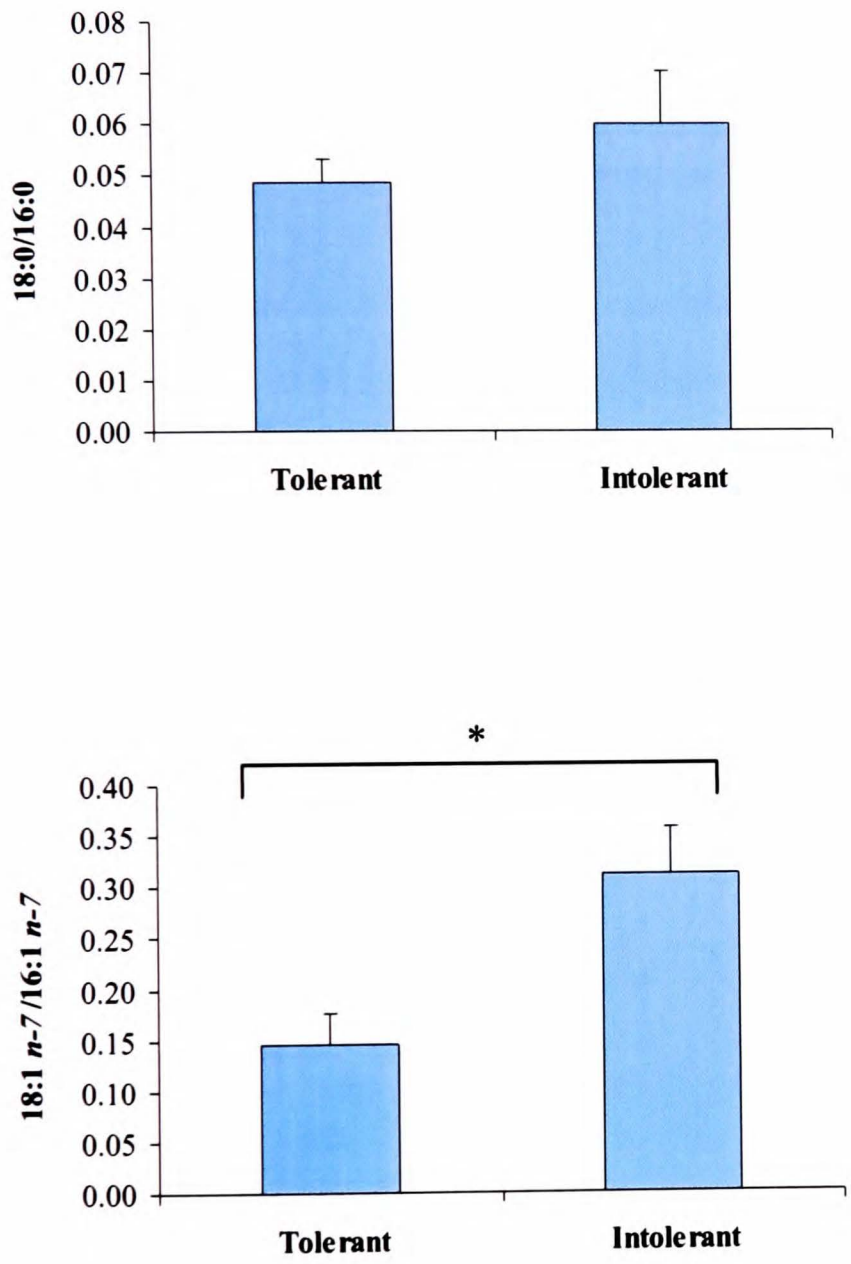


Figure 5-8 ELOVL6 indices in palmitate-tolerant (n = 10) and intolerant (n = 5) groups showing (a) 18:0/16:0 and (b)18:1 n-7/16:1 n-7 ratios. Data are represented as mean ± SEM. * P = 0.013

Interestingly, elongation was increased in the intolerant cells, as seen by an increase in 18:0/16:0 and 18:1 *n*-7/16:1 *n*-7 (**Figure 5-8**) although there was a decrease in *ELOVL6* mRNA (**Figure 5-9**).

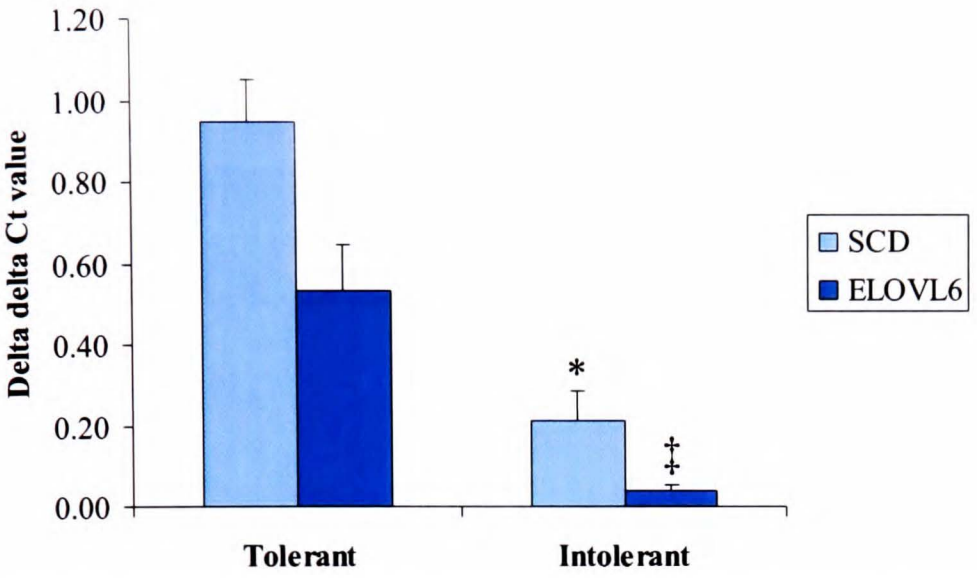


Figure 5-9 *SCD* and *ELOVL6* mRNA expression in palmitate-tolerant (n = 10) and intolerant (n = 5) adipocytes. Data are represented as mean ± SEM. * P = 0.001, ‡ P = 0.011

Calculation of total flux through SCD and ELOVL6 agreed with the observed down-regulation of mRNA for both of these enzymes (**Figure 5-10**). Both SCD and ELOVL6 were down-regulated in the intolerant group compared with the tolerant group of adipocytes.

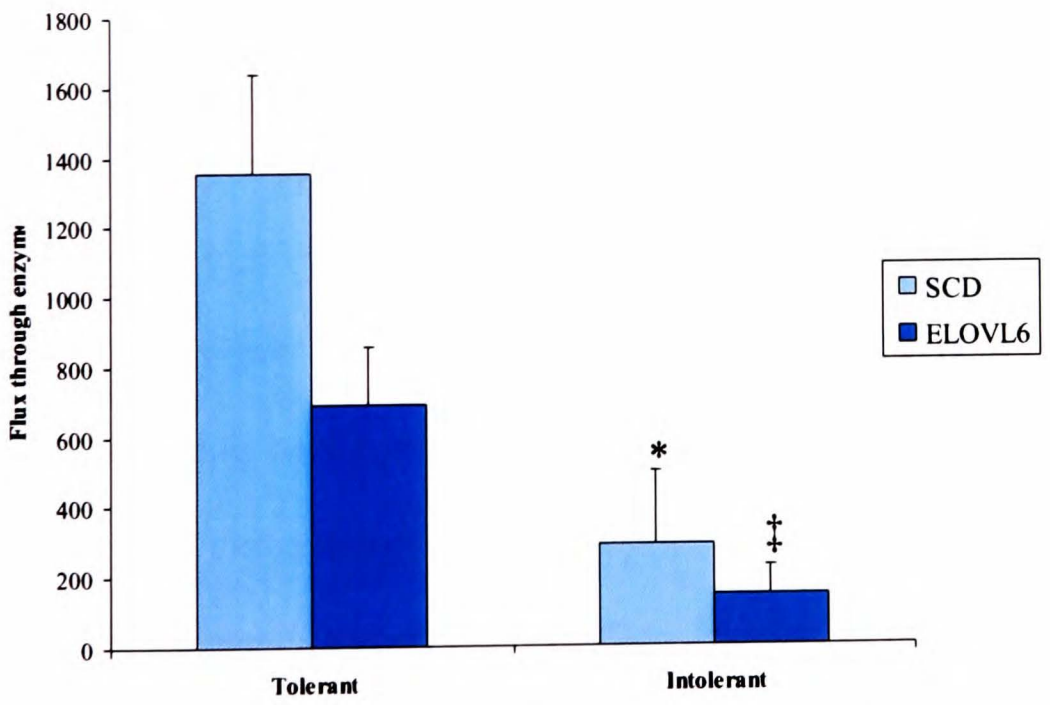


Figure 5-10 Flux through SCD and ELOVL6 over 14 days (nmol fatty acid/10^6 cells) in palmitate-tolerant (n = 10) and intolerant (n = 5) adipocytes. Data are represented as mean ± SEM. * P <0.001, ‡ P = 0.016

5.4.4. Palmitate chain shortening

In **Chapter 4**, chain shortening of palmitate was observed to occur in a dose-dependent manner in adipocytes incubated with 50 to 200 μM palmitate. This was also measured in the palmitate-tolerant and intolerant adipocytes with 400 μM palmitate.

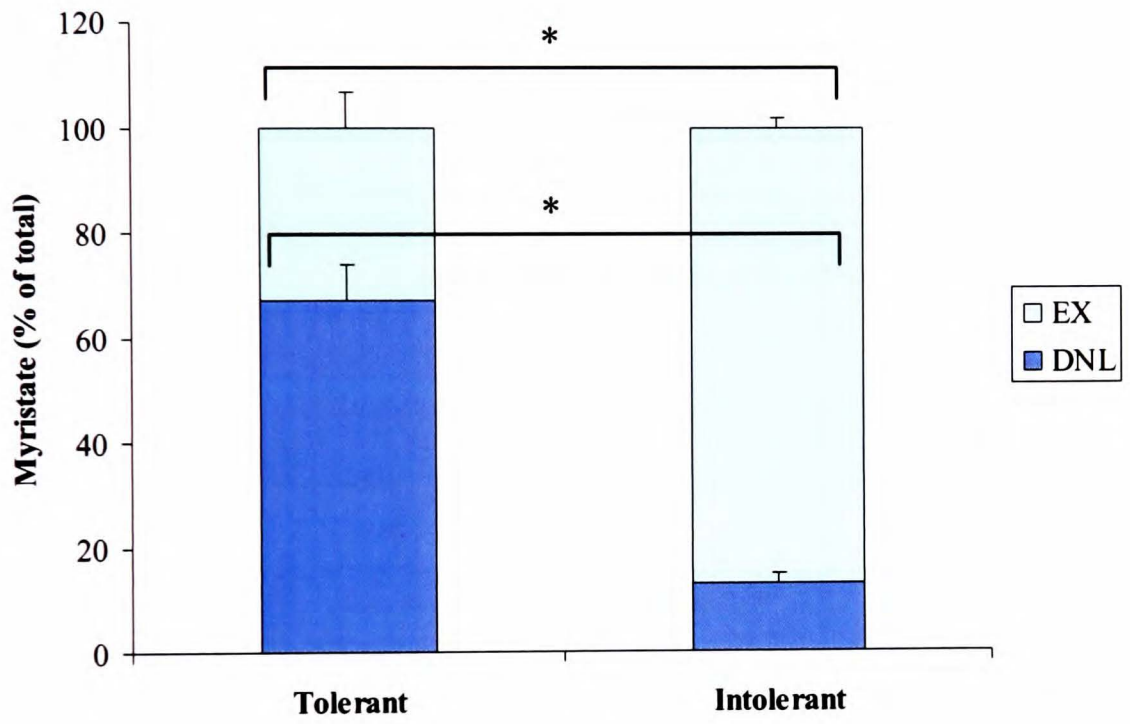


Figure 5-11 Source of TG myristate (DNL or exogenous (EX)) in palmitate-tolerant (n = 10) and intolerant (n = 5) adipocytes. Data are represented as mean ± SEM. * P < 0.01

The product-to-precursor ratio of total 14:0/16:0 showed no difference in palmitate chain shortening between groups (data not shown). However, there was a greater proportion of exogenously derived myristate in the palmitate-intolerant than in the tolerant adipocytes (**Figure 5-11**). This implies firstly, that DNL has been down-regulated in the palmitate-intolerant compared with the palmitate-tolerant adipocytes, and secondly, that there is an increase in chain shortening of exogenous palmitate in the palmitate-intolerant adipocytes.

5.4.5. Fatty acid channelling

5.4.5.1. Fatty acid channelling towards SCD desaturation

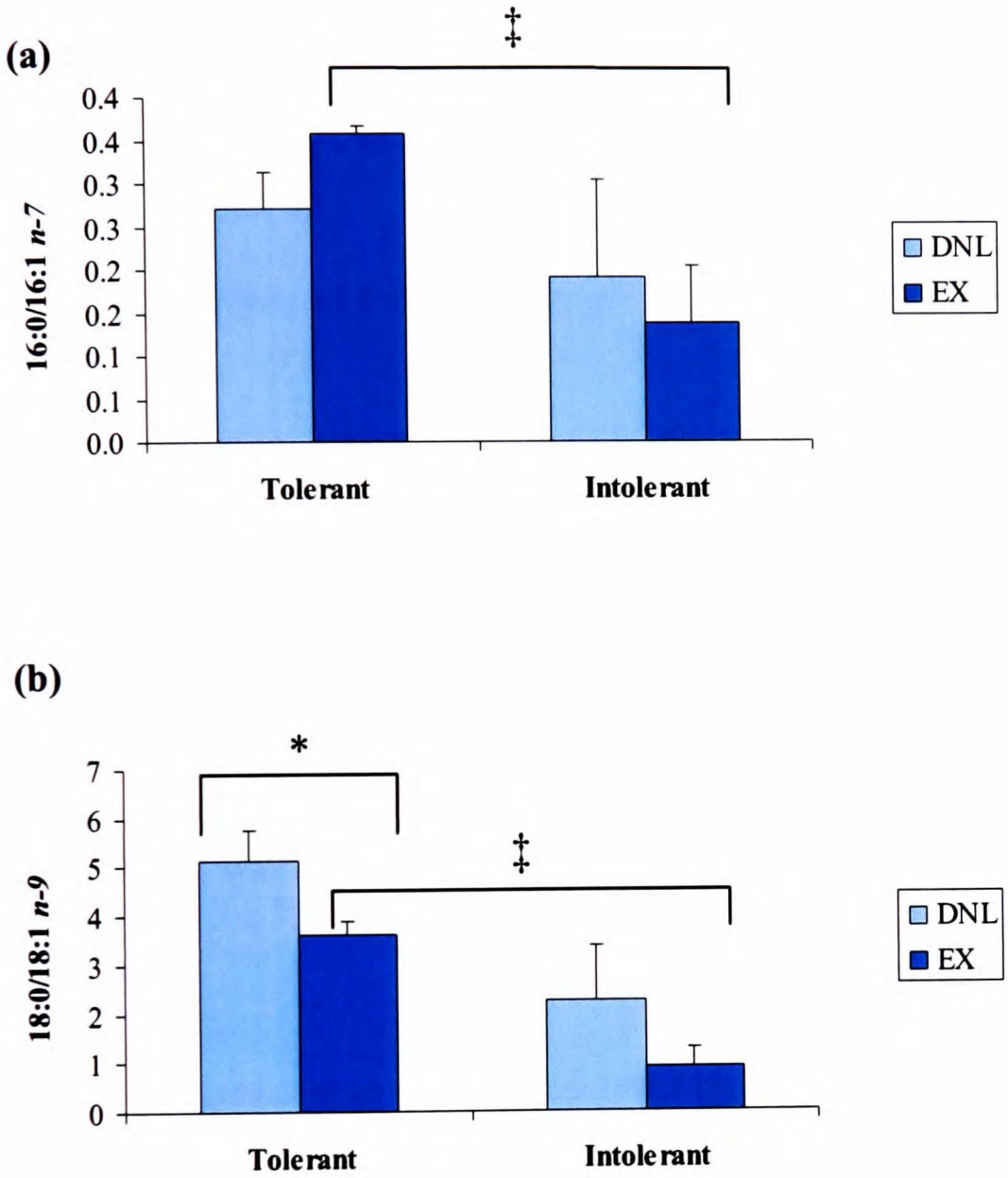


Figure 5-12 Channelling of DNL-derived (DNL) and exogenous (EX) fatty acids towards desaturation by SCD in palmitate-tolerant (n = 10) and intolerant (n = 5) adipocytes. Graph (a) shows the 16:0/16:1 *n-7* ratio and (b) shows the 18:1 *n-9*/18:0 ratio. Data are represented as mean ± SEM. * P = 0.008, ‡ P ≤ 0.036

As was shown in **Chapter 4**, the source of palmitate, whether DNL-derived or exogenous, did not influence channelling towards desaturation by SCD (P = 0.059 in tolerant adipocytes and 0.99 in intolerant adipocytes) (**Figure 5-12(a)**). Also in

agreement with the findings in **Chapter 4** was SCD's preference for DNL-derived stearate (**Figure 5-12(b)**), although this was only significant in the palmitate-tolerant group. The tolerant cells did, however, have higher SCD indices for exogenous 16:1 *n*-7/16:0 ($P = 0.036$) and 18:1 *n*-9/18:0 ($P < 0.001$), implying a difference in handling of exogenous palmitate between the two groups.

5.4.5.2. Palmitate channelling towards ELOVL6 elongation

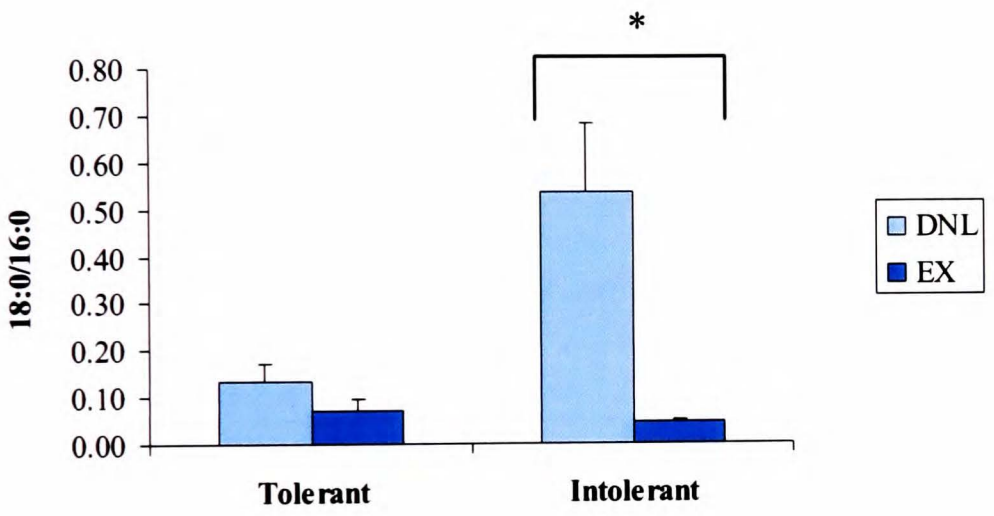


Figure 5-13 Channelling of DNL-derived (DNL) and exogenous (EX) palmitate towards elongation in palmitate-tolerant (n = 10) and intolerant (n = 5) adipocytes. Data are represented as mean ± SEM * P = 0.016

In both groups, there was preferential elongation of DNL-derived palmitate over exogenous palmitate, although this did not reach statistical significance in the tolerant cells (**Figure 5-13**). In the palmitate-intolerant group, elongation of DNL-derived palmitate was around 10-fold greater than exogenous palmitate. These findings imply that while there is preferential elongation of DNL-derived palmitate in the palmitate-tolerant cells, the fold-difference between elongation of DNL-derived and exogenous palmitate is not as great as in the palmitate-intolerant cells. Taken together with the

SCD data (**Figure 5-12**), this may suggest a limitation in the palmitate-intolerant cells to act upon the exogenous palmitate.

5.4.6. Changes in the cell membrane

The PL SAFA:MUFA ratio was more than 2.5-fold higher in the palmitate-intolerant adipocytes than in the tolerant group (**Figure 5-14**). The SAFA:MUFA ratio reached 1.43 in the palmitate-tolerant group whereas it was more than 3 in the intolerant adipocytes. This dramatic increase in SAFA in the phospholipids, which make up the cell membrane, could have contributed to the loss of cell viability.

5.4.6.1. Phospholipid fatty acid composition

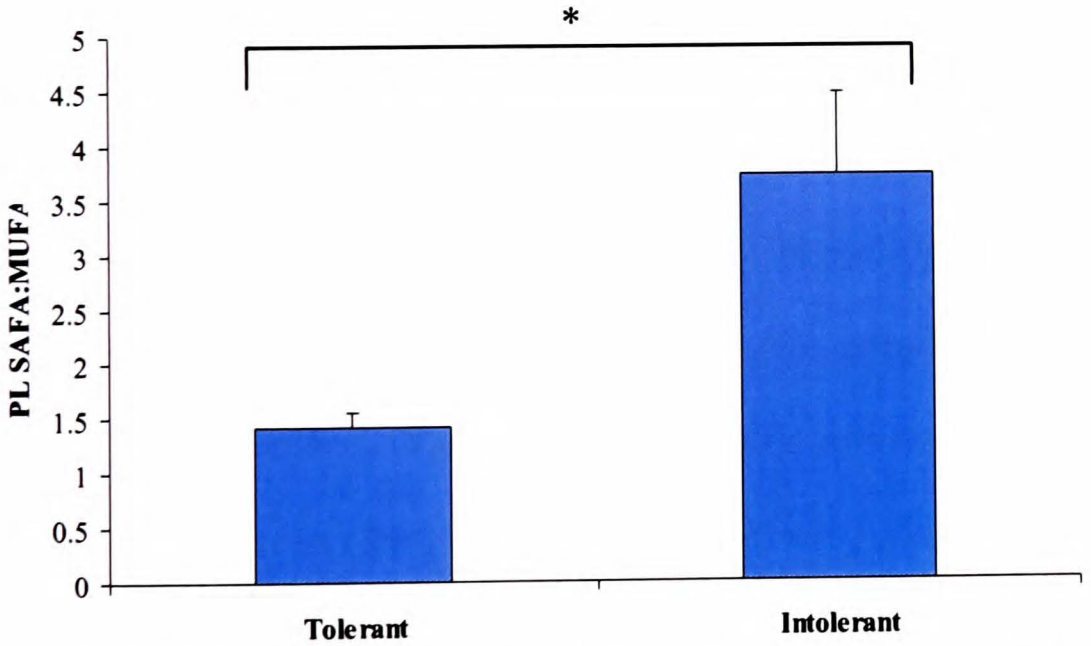


Figure 5-14 Phospholipid SAFA:MUFA in the palmitate-tolerant (n = 10) and intolerant (n = 5) groups. Data are represented as mean ± SEM. * P = 0.001

In the intolerant group, more exogenous palmitate was incorporated into the PL fatty acids than in the tolerant group (**Figure 5-15**). This may suggest that the intolerant cells have a different channelling mechanism for the exogenous palmitate.

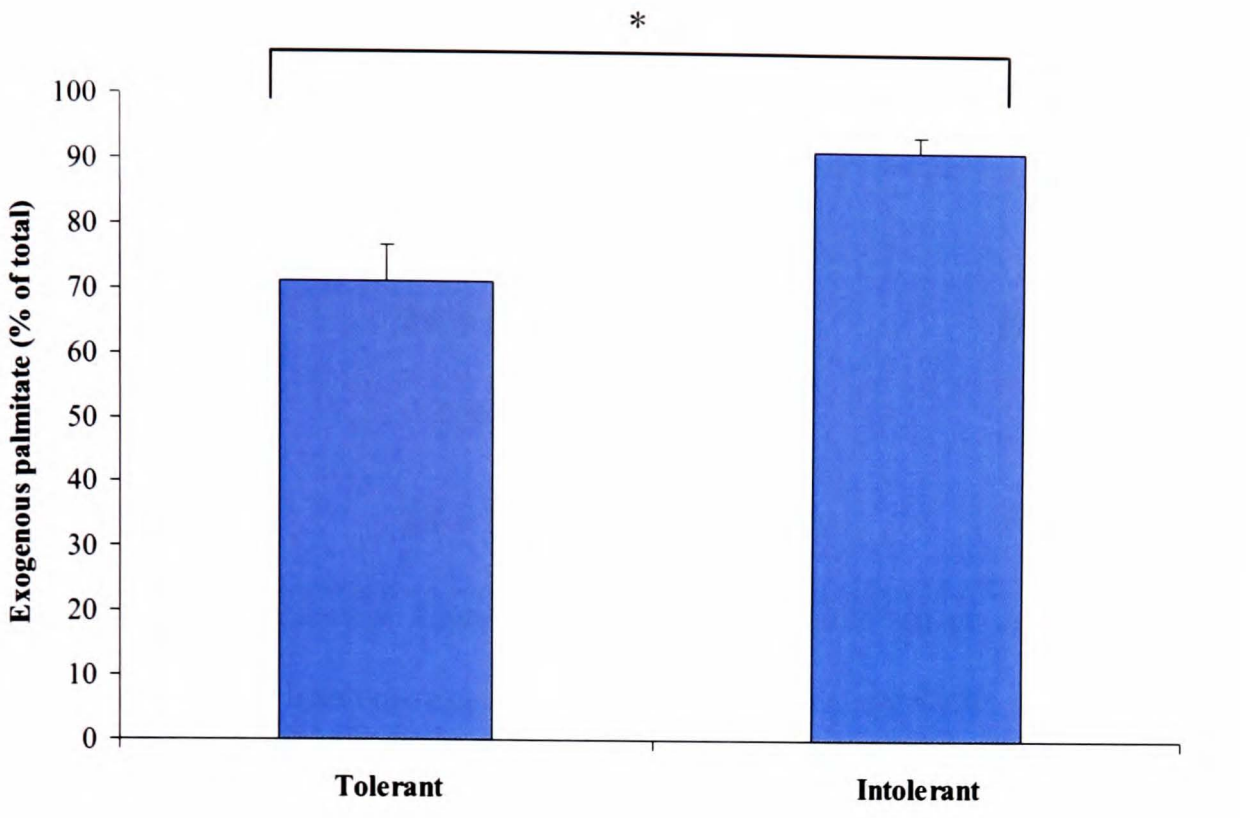


Figure 5-15 Incorporation of exogenous palmitate into phospholipid in palmitate-tolerant (n = 10) and intolerant (n = 5) adipocytes. Data are represented as mean ± SEM. * P = 0.051

5.4.7. Anthropometric details of subjects

The fact that adipocytes from different donors responded differently to 400 μM palmitate, that is, that they were either palmitate-tolerant or palmitate-intolerant, provoked an interest in the source of these cells, namely the volunteers from which they had been obtained. Various anthropometric measurements were compared (age, sex, body mass index (BMI), waist to hip ratio and percentage body fat) in an attempt to uncover a possible link between the fat donor and the tolerance to palmitate (**Table 5-1**). None of the parameters measured was statistically significantly different between the two groups, although the BMI of the palmitate-intolerant group was slightly higher and had a broader range in the palmitate-intolerant group (the highest BMI being 40.1 kg/m^2 compared with 30.9 kg/m^2 in the tolerant group).

Variable	Palmitate-tolerant group	Palmitate-intolerant group
Age (y)	**37.5** (27-53)	**31.5** (21-51)
Sex (M/F)	**4/6**	**3/2**
BMI (kg/m^2)	**24.6** (21.0-30.9)	**26.0** (24.0-40.1)
Waist:hip	**0.9** (0.7-1.0)	**0.9** (0.8-1.1)
% body fat	**28.6** (14.7-37.5)	**30.6** (13.9-39.0)

Table 5-1 Anthropometric measurements of the subjects whose cells were in the palmitate-tolerant (n = 10) and intolerant groups (n = 5). Values are expressed as median, with the range in parentheses.

5.4.8. Global changes in gene expression in response to palmitate

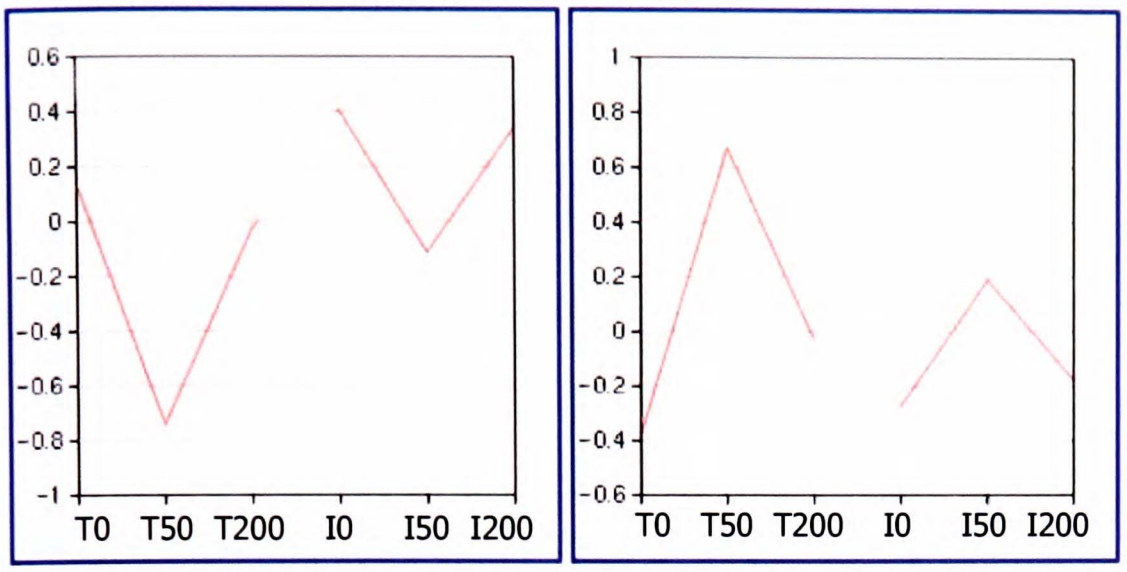
The differences in response to palmitate were further analysed using human whole genome microarrays to assess global changes in gene expression in response to palmitate. **Chapter 4** described the response of adipocytes to 0 to 200 μM palmitate, and this chapter has shown how the higher concentration of 400 μM had adverse effects on a sub-population of the adipocytes of some subjects. As the cells used for **Chapters 4** and **5** were all from the same subjects, and each subject's cells were differentiated with the range of exogenous palmitate (0, 50, 100, 200 and 400 μM) simultaneously, the results were pooled and treated as one bigger experiment. Although the differences between the two groups, palmitate-tolerant and intolerant, were only observed with 400 μM palmitate, data for each of the two groups were merged to form palmitate-tolerant and intolerant groups studied at a concentration range spanning 0 to 400 μM.

Due to the expense of each microarray slide, RNA from six subjects' adipocytes was analysed. Of the six, RNA from three subjects' adipocytes was picked at random from each group (palmitate-tolerant and intolerant), and was taken as representative for the subjects in that group. Also, only 0, 50 and 200 μM palmitate-treated samples were studied in order to limit the number of slides required, yet still capture changes.

Changes due to palmitate concentration, tolerance and "interaction", that is, changes due to an effect of both palmitate and tolerance together, were measured by 2-way ANOVA using Genesifter™ (**Chapter 2**, section **2.7**). The fold changes in either up- or down-regulation of genes significantly changing ($P < 0.05$) were recorded. Genes changing significantly were also assigned to pathways (KEGG or Ontology, as assigned by Genesifter™ (**Chapter 2**, section **2.7.4**)), thereby providing a link between changes in gene expression and possible functional regulation.

(a) Pamitate and tolerance (individually)

Mean silhouette width: 0.608



(b) Interaction

Mean silhouette width: 0.723

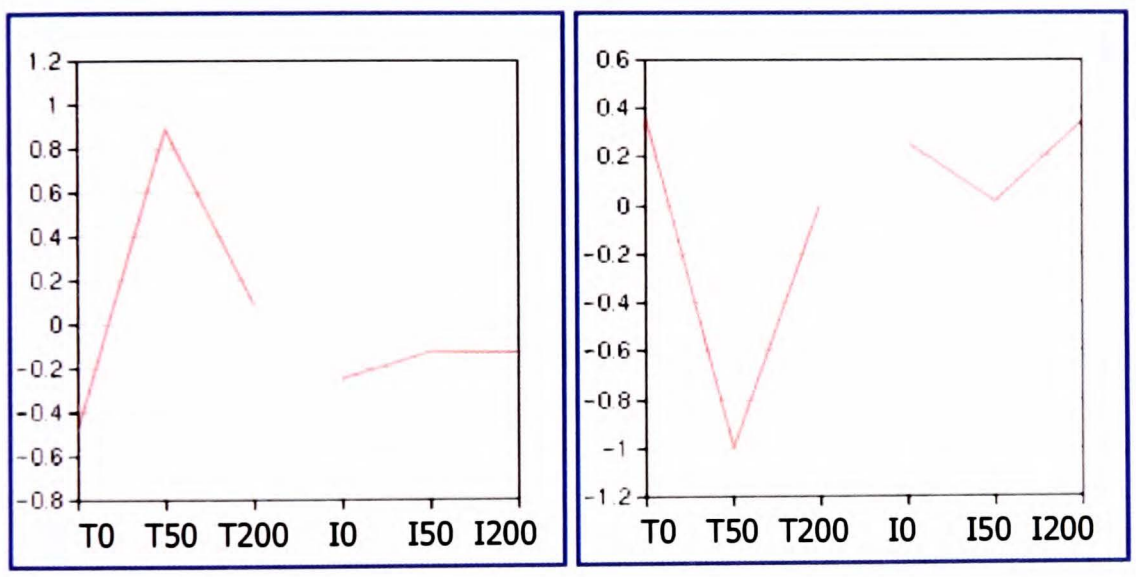


Figure 5-16 Changes in gene expression were assessed by 2-way ANOVA using the Genesifter™ software. The above graphs show hierarchical cluster analyses of genes changing significantly ($P < 0.05$) in response to (a) palmitate (136 genes) and tolerance (117 genes) and (b) interaction, that is, changes due to both palmitate and tolerance (58 genes).

Key to x-axes: T0, T50 and T200 = tolerant cells with 0, 50 and 200 µM palmitate, respectively, and I0, I50 and I200 = intolerant cells with 0, 50 and 200 µM palmitate, respectively.

Figure 5-16 shows gene cluster analyses according to changes in response to palmitate, tolerance and interaction (changes occurring due to both palmitate and tolerance). Changes due to palmitate concentration (**Figure 5-16 (a)**) had the greatest

effects, significantly changing the gene expression of 136 genes. Of these changes, there were two distinct patterns of regulation; genes were either up-regulated with 50 μM palmitate or down-regulated, returning to around the control values with 200 μM. The gene clusters in **Figure 5-16 (a)** indicated that the tolerant and intolerant groups behaved similarly, but that the magnitude of the response was less pronounced in the intolerant group. The number of genes changing to a significant level due to tolerance was slightly less than due to palmitate (117 genes). Of the genes changing with either palmitate or tolerance, 28 were common to both clusters.

Fewer genes significantly changed due to interaction of palmitate and tolerance **(Figure 5-16(b))**. Although 58 genes were shown to be changing, only 36 of these were previously identified genes. The others consisted of a mixture of hypothetical proteins (predicted genes), transcribed loci (potential genes predicted from expressed sequence tags) and GE identification numbers (potentially novel transcripts predicted by GE Healthcare) (**Figure 5-17**). It is unclear why this group comprised so many of these genes. In this cluster, the 50 μM palmitate-treated tolerant samples again showed the greatest differences from all the other samples.

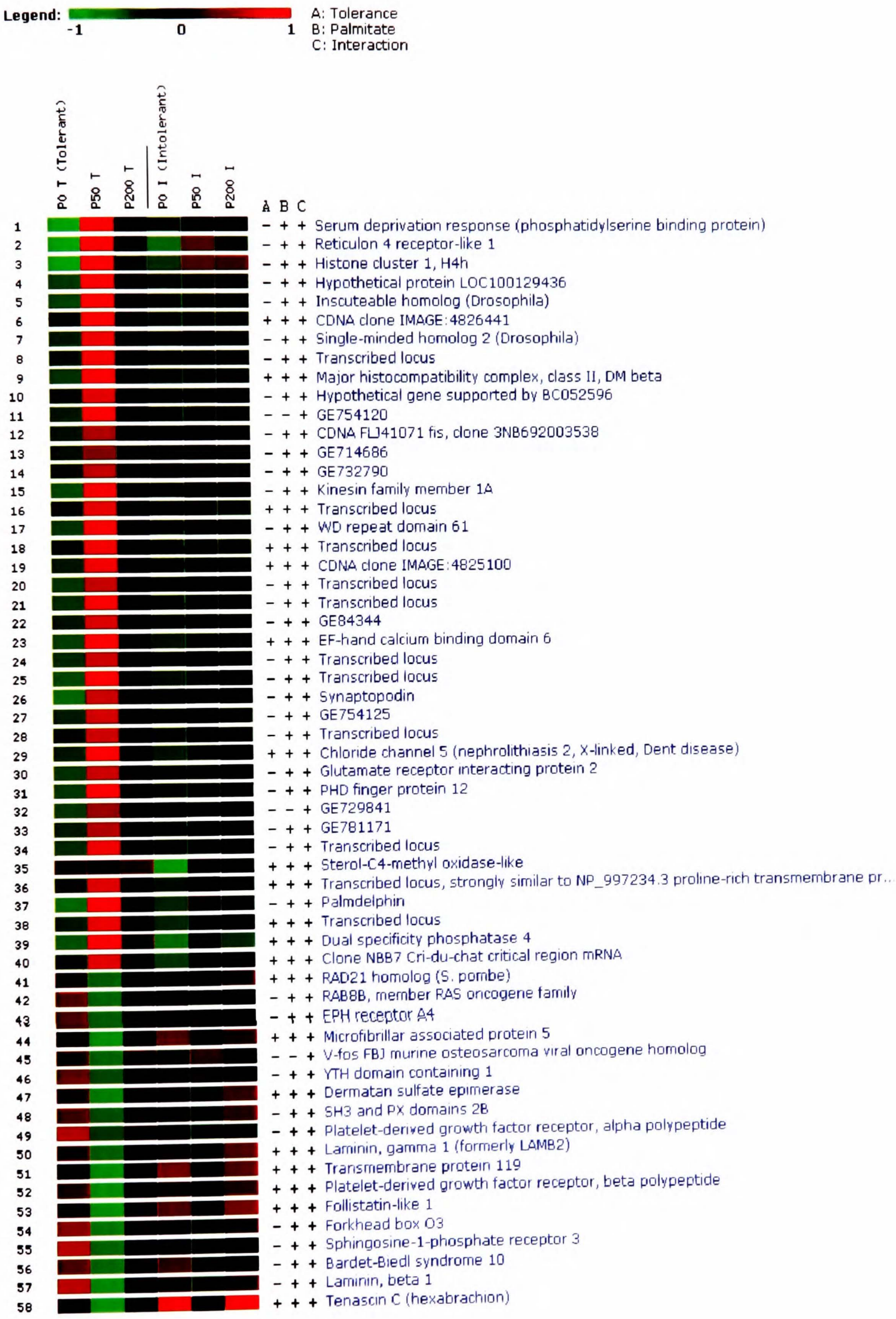
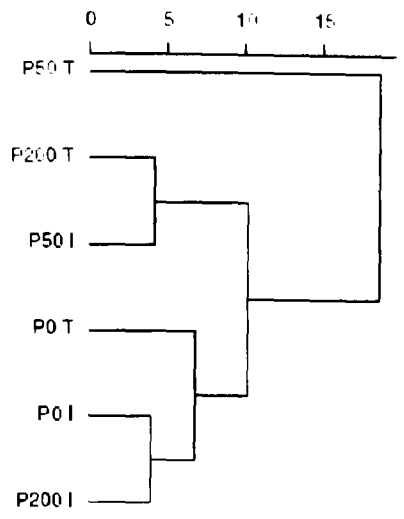


Figure 5-17 Heatmap showing changes in regulation of genes with "interaction" of palmitate and tolerance. Green indicates a down-regulation of a gene, and red indicates up-regulation.

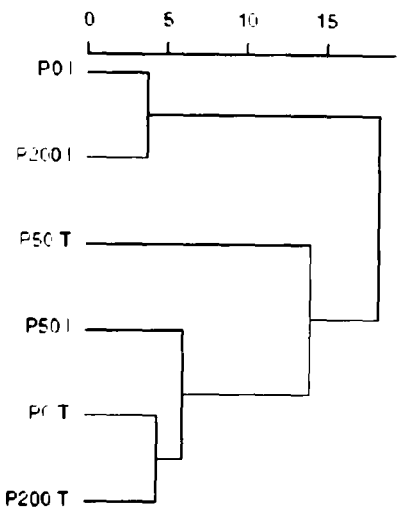
Cluster analyses of samples were also performed to look at how the samples from the tolerant and intolerant groups behaved at different palmitate concentrations. These are summarised in **Figure 5-18** and are shown as changes seen with palmitate, tolerance or interaction.

Sample cluster analysis revealed that treatment with 50 μM palmitate in the tolerant samples differed most from the 0 and 200 μM palmitate-treated samples, which were grouped closely together. These findings reflected the gene cluster patterns seen in **Figure 5-16**, that showed that treatment in the tolerant and intolerant groups with 50 μM palmitate resulted in the greatest changes in gene expression.

(a) Genes changing in response to palmitate



(b) Genes changing in response to tolerance



(c) Genes changing in response to interaction

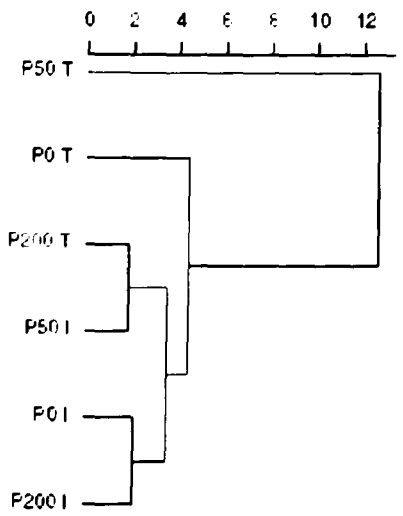


Figure 5-18 Sample hierarchical cluster analyses of genes changing in response to (a) palmitate, (b) tolerance and (c) interaction (palmitate and tolerance together) (n = 3 for each palmitate concentration) Key to sample names: P0 T, P50 T and P200 T = 0, 50 and 200 μM palmitate in tolerant group and P0 I, P50 I and P200 I = 0, 50 and 200 μM palmitate in the intolerant group.

As the patterns of gene regulation in response to palmitate were similar in the tolerant and intolerant groups (**Figure 5-16(a)**), differing only in magnitude of response, the two groups (palmitate-tolerant and intolerant) were combined to create one larger group (n = 6), and were compared, in Genesifter™, using a paired *t* test to further assess changes due to palmitate and to improve the statistical power. Changes in gene expression from 0 to 50 μM palmitate, 50 to 200 μM palmitate and 0 to 200 μM palmitate were compared. A list of genes changing significantly using the pairwise analysis was made, noting the direction of gene regulation (up or down) and the P value for each change (**Appendix 2,** section **A2-2**). These genes were also arranged according to significant changes in KEGG pathways and were ranked by *z* score. **Table 5-2** summarises pathways up- and down-regulated from 0 to 50 μM palmitate.

KEGG Pathway	List	Up	Down	Array	*z* score (up)	*z* score (down)
PPAR signalling pathway	7	7	0	54	**8.64**	-0.52
Vitamin B6 metabolism	1	1	0	4	**4.69**	-0.14
Pyruvate metabolism	3	3	0	40	**4.02**	-0.45
Insulin signalling pathway	5	5	0	125	**3.29**	-0.81
Urea cycle and metabolism of amino groups	2	2	0	30	**3.02**	-0.39
Glycosphingolipid biosynthesis – lactoseries	1	1	0	10	**2.77**	-0.22
Reductive carboxylate cycle (CO_2 fixation)	1	1	0	10	**2.77**	-0.22
Hematopoietic cell lineage	4	3	1	76	**2.5**	1.02
Glycosphingolipid biosynthesis – globoseries	1	1	0	12	**2.47**	-0.25
Cell Communication	5	1	4	105	-0.1	**4.9**
Focal adhesion	6	1	5	169	-0.6	**4.66**
ECM-receptor interaction	5	2	3	77	1.34	**4.29**
Arachidonic acid metabolism	2	0	2	45	-0.7	**3.79**
Cell adhesion molecules (CAMs)	6	3	3	114	1.68	**3.29**
TGF-beta signalling pathway	2	0	2	64	-0.83	**3.01**
Ether lipid metabolism	1	0	1	26	-0.53	**2.44**
Linoleic acid metabolism	2	1	1	29	1.27	**2.27**

Table 5-2 Changes in KEGG pathways from 0 to 50 µM palmitate ranked by *z* score. Key to headings: List = Number of genes within the pathway changing, Up = number of genes up-regulated, Down = number of genes down-regulated, Array = number of genes in pathway represented on microarray slide

From the lists of genes generated from the Genesifter™ paired *t* test comparison of samples changing due to palmitate, and from the 2-way ANOVA analysis of genes changing in response to palmitate, tolerance and interaction, a shortlist of genes was created. Genes in this list were selected based on the following criteria: statistical significance ($P < 0.05$, repeated measures ANOVA) and relevance of the pathways they were involved in. The final list comprised 45 genes (**Table 5-3**).

Gene name	Gene ID	Change with	Pathway/Process 1	Pathway/Process 2	Fold change 0 to 50	Fold change 50 to 200	Fold change 0 to 200	P value
ATP-binding cassette, sub-family A (ABC1), member 10	*ABCA10*	T	ABC transporters - General		2.13	1.46	1.45	0.0007
Adiponectin, C1Q and collagen domain containing	*ADIPOQ*	P	Adipocytokine signalling pathway		4.56	1.72	2.65	0.0151
Leptin	*LEP*	P/T	Adipocytokine signalling pathway		2.56	2.80	1.10	0.0074
Interleukin 33	*IL33*	P	Adipocytokine signalling pathway		3.45	2.17	1.61	0.0007
Interleukin 32	*IL32*	T/P	Adipocytokines	Cytokine activity	1.69	2.27	1.34	0.0023
DNA-damage-inducible transcript 4-like	*DDIT4L*	P	Apoptosis		2.64	2.63	0	0.0028
Apoptosis-inducing factor, mitochondrion-associated, 2	*AIFM2*	P/T	Apoptosis		2.15	1.92	1.12	0.0002
Sterol-C4-methyl oxidase-like [4]	*SC4MOL*	I	Biosynthesis of steroids	Fatty acid metabolic process	0	0	0	0.1960
Collagen, type XI, alpha 1	*COL11A1*	P	Cell Communication	Focal adhesion	4.17	4.59	1.11	0.0071
Collagen, type VIII, alpha 1	*COL8A1*	P	Cell interaction		1.34	2.83	2.12	0.0199
Activated leukocyte cell adhesion molecule	*ALCAM*	P	Cell interaction	Cell adhesion molecules	2.43	2.11	1.15	0.0027

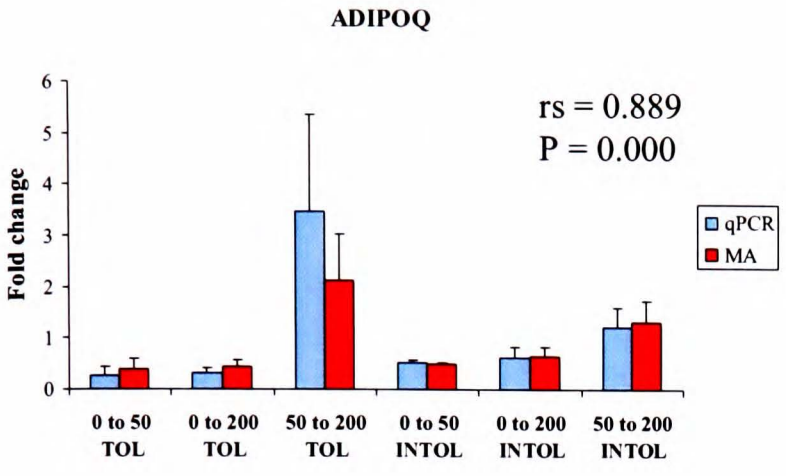
[4] This gene did not change significantly but was included in this table as its regulation was different to the other genes changing due to "interaction" (see heatmap in Figure 5-17, gene 35). For this reason, this gene was also verified by qPCR (**Figure 5-19**).

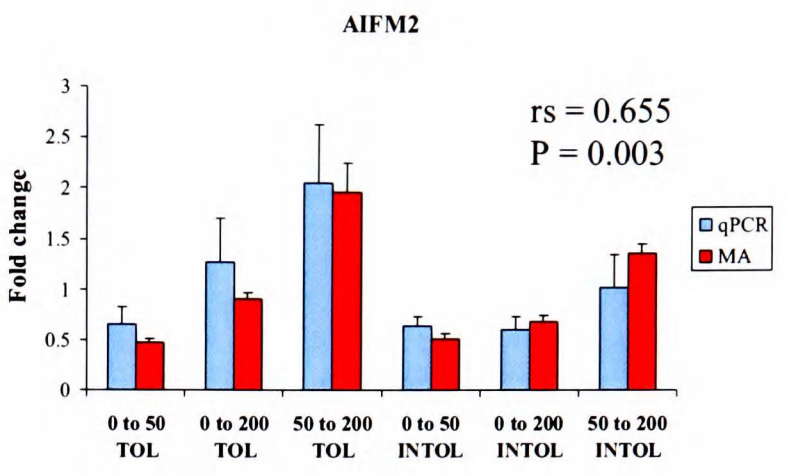
CD34 molecule	*CD34*	P/T	Cell interaction	Cell adhesion molecules	3.34	1.69	1.96	0.0001
Vascular endothelial growth factor C	*VEGFC*	P	Cell interaction	Focal adhesion	3.70	1.76	2.13	0.0108
Follistatin-like 1	*FSTL1*	I/T	Extracellular region		2.94	2.86	0	0.0002
Collagen, type XII, alpha 1	*COL12A1*	T	Extracellular region	Structural molecule activity	3.45	2.51	1.31	0.0001
Fatty acid binding protein 5 (psoriasis-associated)	*FABP5*	P	FA metabolism		5.03	2.5	2.02	0.0115
Aquaporin 7	*AQP7*	P	FA metabolism	PPAR signalling	3.96	1.56	2.53	0.0144
Fatty acid binding protein 4, adipocyte	*FABP4*	P	FA metabolism		3.48	1.85	1.89	0.0110
Glycerol-3-phosphate dehydrogenase 1 (soluble)	*GPD1*	P	FA metabolism		3.44	1.85	1.86	0.0165
Phosphoenolpyruvate carboxykinase 1 (soluble)	*PCK1*	P	FA metabolism	PPAR signalling	3.40	1.69	2.00	0.0174
Glycerol-3-phosphate acyltransferase, mitochondrial	*GPAM*	P	FA metabolism		2.92	1.72	1.68	0.0022
Nuclear receptor subfamily 1, group H, member 3	*NR1H3*	P	FA metabolism	PPAR signalling	2.83	2.70	0	0.0022
Perilipin	*PLIN*	P	FA metabolism	PPAR signalling	2.81	1.41	2.00	0.0154
CD36 molecule (thrombospondin receptor)	*CD36*	P	FA metabolism	PPAR signalling	2.69	1.64	1.65	0.0073
Acyl-CoA synthetase short-chain family member 2	*ACSS2*	P	FA metabolism	Pyruvate metabolism	2.14	1.41	1.52	0.0097

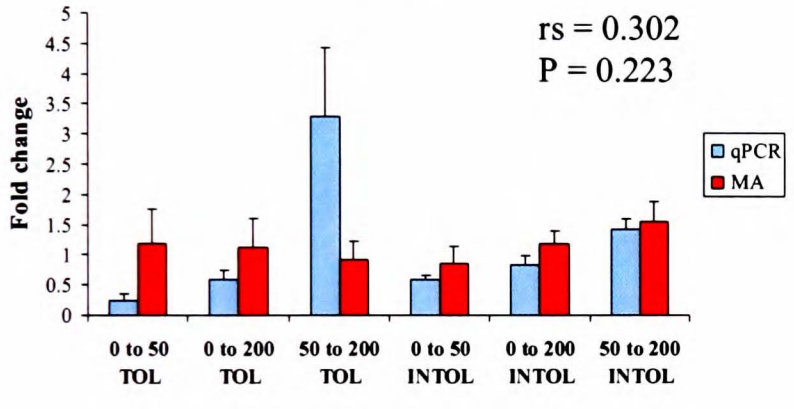
ELOVL family member 5, elongation of long chain fatty acids	ELOVL5	P	FA metabolism		1.88	1.30	1.45	0.0040
Malic enzyme 1, NADP(+)-dependent, cytosolic	ME1	P	FA metabolism	PPAR signalling	1.88	1.75	0	0.0015
Laminin, beta 1	LAMB1	P/I	Focal adhesion	ECM-receptor interaction	3.13	1.94	1.61	0.0064
Tenascin C (hexabrachion)	TNC	P/T/I	Focal adhesion	ECM-receptor interaction	6.67	5.55	1.23	0.0017
Protein tyrosine phosphatase, receptor type, F	PTPRF	P	Insulin signalling pathway	Cell adhesion molecules	2.32	1.56	1.48	0.0035
VAMP (vesicle-associated membrane protein)-associated protein A, 33kDa	VAPA	T	Membrane fusion	Tight junction	1.52	1.16	1.30	0.0004
Lysophosphatidic acid receptor 1	LPAR1	T	Plasma membrane	Signal transduction	1.78	1.82	0	0.0004
Sphingosine-1-phosphate receptor 3	EDG3	I	Plasma membrane	Lipid binding	2.63	1.72	1.52	0.0275
Nuclear receptor subfamily 1, group H, member 3	NR1H3	P	Signalling		2.83	2.70	0	0.0028
G protein-coupled bile acid receptor 1	GPBAR1	P	Signalling	G-protein coupled receptor protein signalling pathway	5.79	2.56	2.26	0.0135
Stearoyl-CoA desaturase (delta-9-desaturase)	SCD	P	Signalling	PPAR signalling pathway	2.3	1.45	1.60	0.0096

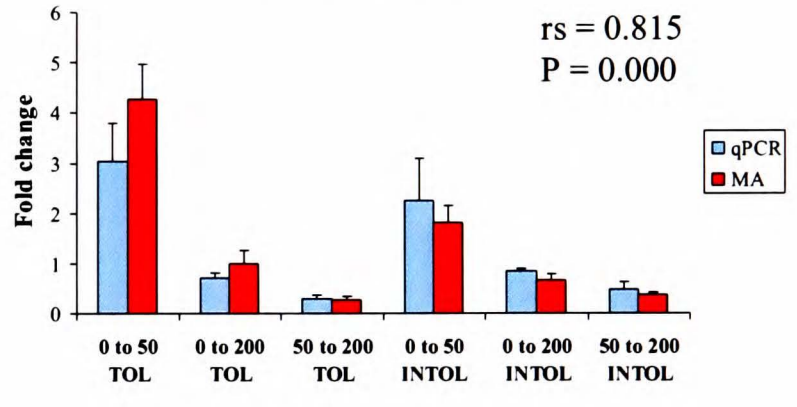
MAP kinase interacting serine/threonine kinase 2	MKNK2	P	Signalling	Insulin signalling pathway	2.28	2.08	0	0.0046
Nuclear receptor subfamily 1, group H, member 3	NR1H3	P	Signalling	PPAR signalling pathway	2.83	2.70	0	0.0028
Phosphodiesterase 3B, cGMP-inhibited	PDE3B	P	Signalling	Insulin signalling pathway	2.49	1.61	1.54	0.0110
Follistatin	FST	P/T	TGF-beta signalling pathway		2.70	2.09	1.30	0.0002
Indolethylamine N-methyltransferase	INMT1	P/T	Tryptophan metabolism		5.0	3.93	1.3	0.0001
TNF receptor-associated protein 1	TRAP1	T	Tumour necrosis factor receptor binding		1.29	1.45	1.12	0.0012
Naked cuticle homolog 2 (Drosophila)	NKD2	P	Wnt signalling pathway		3.11	1.89	1.65	0.0024
Secreted frizzled-related protein 1	SFRP1	P	Wnt signalling pathway		2.44	2.30	0	0.0022
WNT1 inducible signalling pathway protein 2	WISP2	P	Wnt signalling pathway		4.17	2.25	1.85	0.0013
Secreted frizzled-related protein 2	SFRF2	T	Wnt signalling pathway		1.92	1.51	1.27	0.0332

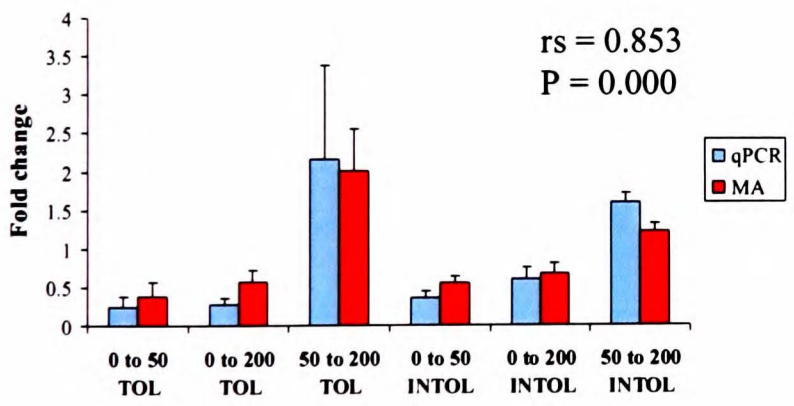
Table 5-3 Summary of genes changing significantly ($P < 0.05$, repeated measures ANOVA) with palmitate (P), tolerance (T) or interaction (I). Fold changes shown in red indicate up-regulation and green indicate down-regulation.

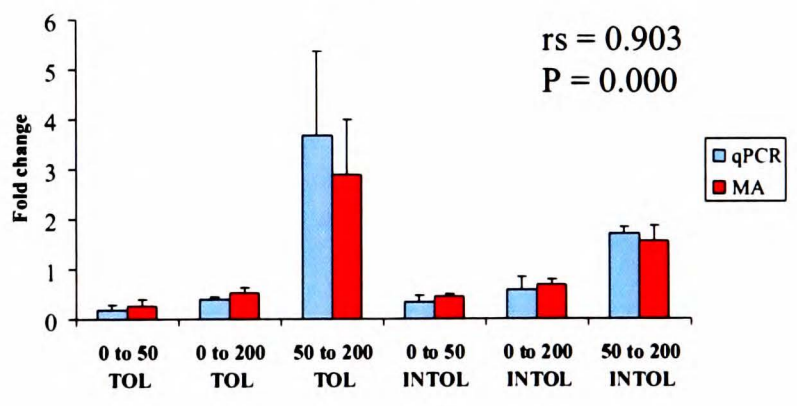

ADIPOQ
rs = 0.889
P = 0.000
Fold change
qPCR
MA
0 to 50 TOL
0 to 200 TOL
50 to 200 TOL
0 to 50 INTOL
0 to 200 INTOL
50 to 200 INTOL

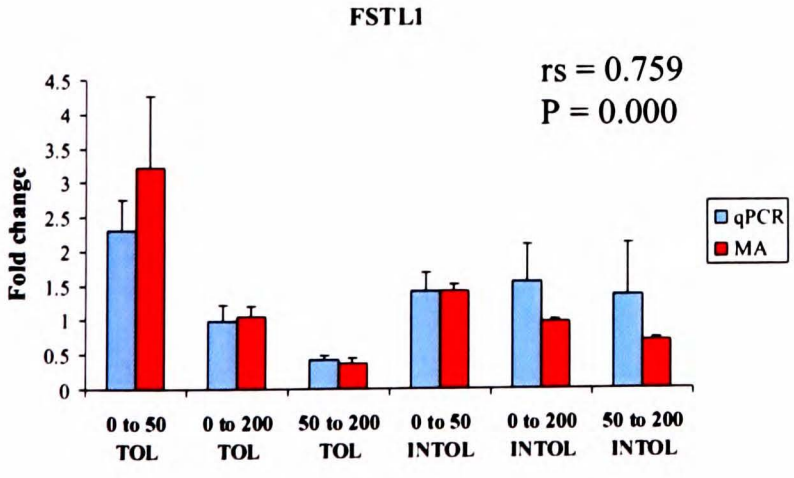

AIFM2
rs = 0.655
P = 0.003
Fold change
qPCR
MA
0 to 50 TOL
0 to 200 TOL
50 to 200 TOL
0 to 50 INTOL
0 to 200 INTOL
50 to 200 INTOL

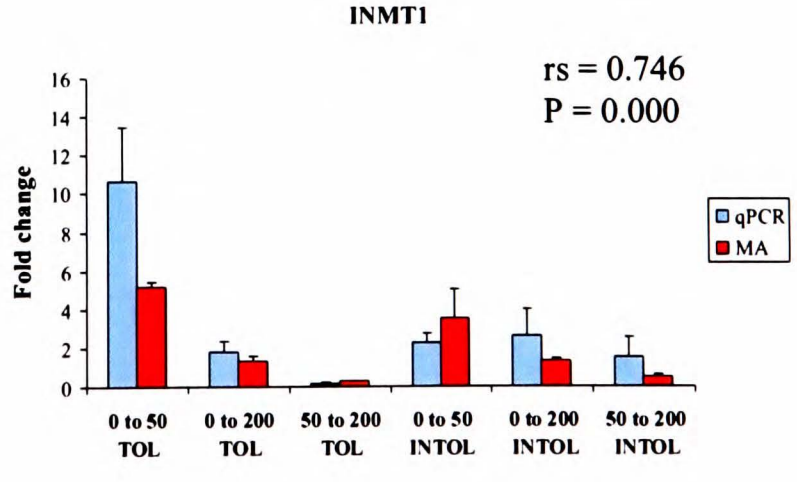

CD36
rs = 0.302
P = 0.223
Fold change
qPCR
MA
0 to 50 TOL
0 to 200 TOL
50 to 200 TOL
0 to 50 INTOL
0 to 200 INTOL
50 to 200 INTOL


COL11A1
rs = 0.815
P = 0.000
Fold change
qPCR
MA
0 to 50 TOL
0 to 200 TOL
50 to 200 TOL
0 to 50 INTOL
0 to 200 INTOL
50 to 200 INTOL


FABP4
rs = 0.853
P = 0.000
Fold change
qPCR
MA
0 to 50 TOL
0 to 200 TOL
50 to 200 TOL
0 to 50 INTOL
0 to 200 INTOL
50 to 200 INTOL


FABP5
rs = 0.903
P = 0.000
Fold change
qPCR
MA
0 to 50 TOL
0 to 200 TOL
50 to 200 TOL
0 to 50 INTOL
0 to 200 INTOL
50 to 200 INTOL


FSTL1
rs = 0.759
P = 0.000
Fold change
qPCR
MA
0 to 50 TOL
0 to 200 TOL
50 to 200 TOL
0 to 50 INTOL
0 to 200 INTOL
50 to 200 INTOL


INMT1
rs = 0.746
P = 0.000
Fold change
qPCR
MA
0 to 50 TOL
0 to 200 TOL
50 to 200 TOL
0 to 50 INTOL
0 to 200 INTOL
50 to 200 INTOL

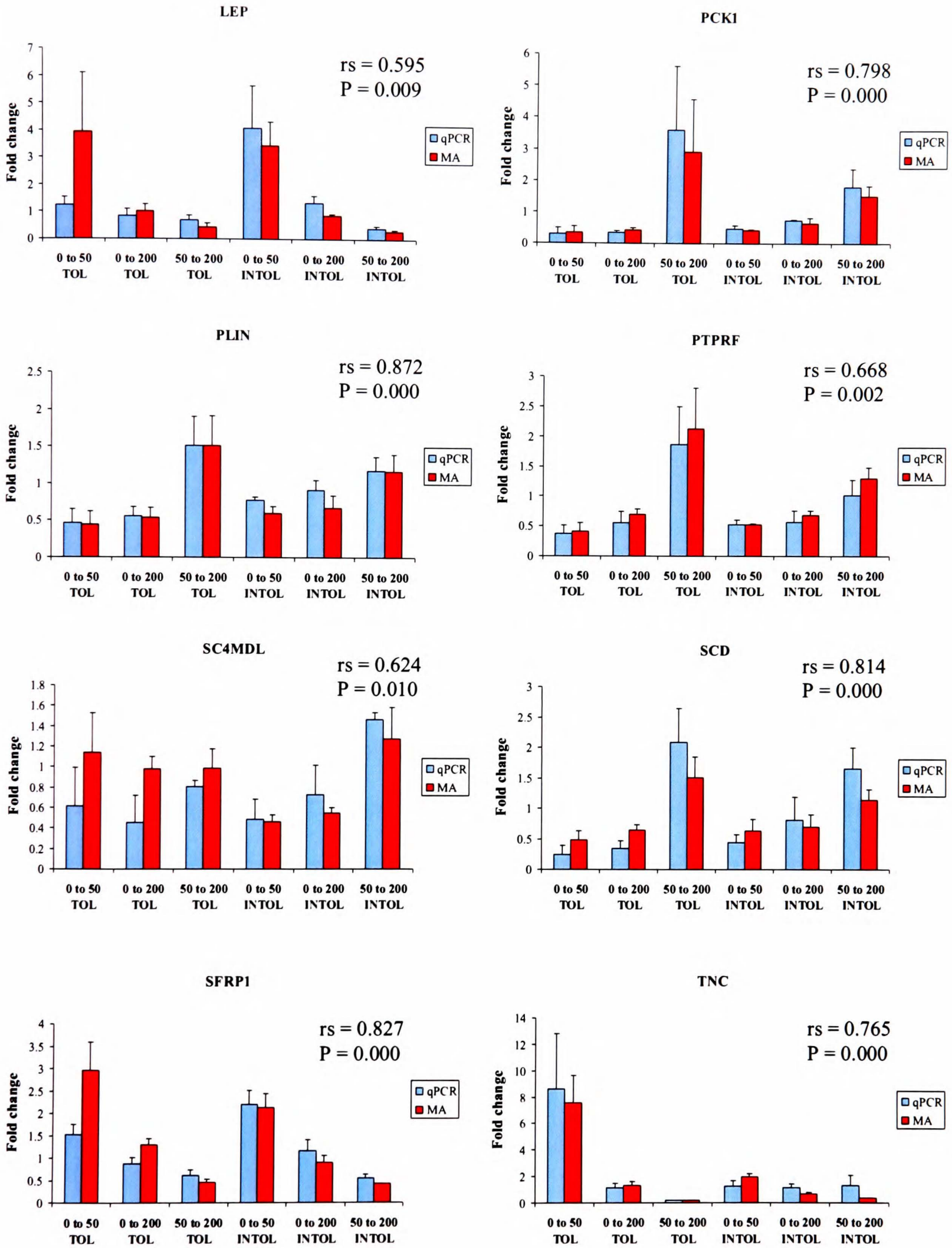


Figure 5-19 Comparisons of quantitative PCR (qPCR) and microarray (MA) results (n = 3 for tolerant and intolerant groups). Gene names are given in Table 5-3. Spearman correlations were performed and results are shown for each gene measured.

A sample of the genes changing in the microarrays (at least one gene per pathway listed in **Table 5-3**) was verified by quantitative PCR (qPCR). qPCR anaylsis of the same samples used for microarray analysis showed that the qPCR and microarray results were positively correlated (**Figure 5-19**). These comparisons verify that the changes in gene expression seen using microarray analysis are robust and can be assessed directly with a high degree of confidence.

Microarray analysis revealed changes in several different pathways with palmitate treatment in both palmitate-tolerant and intolerant groups (**Table 5-3**). Not surprisingly, fatty acid metabolism showed the most number of genes changing. Differentiation of adipocytes with 50 μM palmitate revealed up-regulation of genes involved in fatty acid synthesis, fatty acid uptake, lipid droplet proteins, desaturation and elongation, and up-regulation of insulin signalling. There was also general down-regulation of Wnt signalling molecules, adipocytokines and cell interaction/adhesion molecules. Taken together, these results may imply that a low concentration of exogenous palmitate acts to up-regulate lipid synthesis and storage and promote differentiation (by down-regulation of Wnt-signalling). Although the insulin signalling pathway was up-regulated with 50 μM of exogenous palmitate, results shown in **Chapter 4** (section **4.4.11**) showed that insulin-sensitivity was reduced by this concentration of palmitate.

A more detailed investigation of the palmitate-tolerant and palmitate-intolerant groups was carried out using larger sample sizes in each group: 10 subjects in the tolerant group and 5 subjects in the intolerant group.

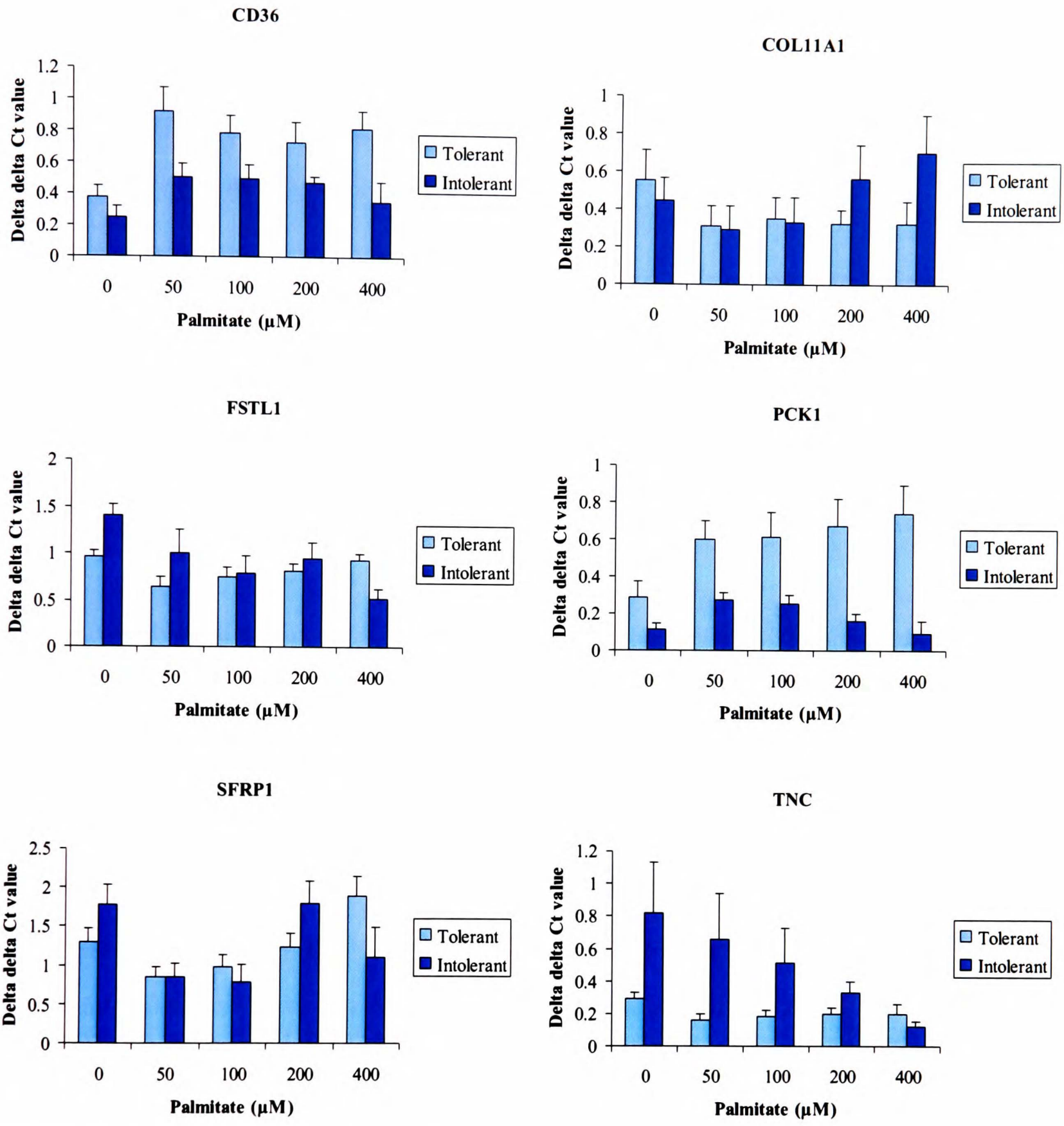


Figure 5-20 Genes changing significantly between palmitate-tolerant (n = 10) and palmitate-intolerant (n = 5) groups of adipocytes (analysed by qPCR).

Genes changing significantly in the smaller (n = 3) groups differed slightly from those changing in the larger groups of palmitate-tolerant (n = 10) and palmitate-intolerant (n = 5) adipocytes. Specifically, more changes were seen due to tolerance in the larger group (**Figure 5-20**). Genes showing differences between the palmitate-

tolerant and intolerant groups included *CD36*, *COL11A1*, *FSTL1*, *PCK1*, *SFRP1* and *TNC*. These are involved in the following pathways: fatty acid uptake, cell adhesion (collagen), extracellular pathway, PPAR signalling (lipid synthesis), Wnt signalling pathway and focal adhesion, respectively.

Microarray analysis showed that two markers for apoptosis, *AIFM2* and *DDIT4L* were significantly up-regulated with 50 μM palmitate. However, in the larger groups these genes were not significantly changed with either palmitate concentration or tolerance (data not shown).

Although not highlighted as a significantly changing pathway by microarray analysis, changes in genes relating to ER stress were investigated. This pathway was explored as non-adipose cells may suffer ER stress as a consequence of palmitate overloading (Moffitt *et al.*, 2005; Wei *et al.*, 2006), and this may have provided a possible explanation for the lipotoxic effects of 400 μM palmitate on the palmitate-intolerant adipocytes. Between the palmitate-tolerant and intolerant group, there were no significant differences seen in mRNA expression of markers of ER stress, *CALR*, *HSP90B1*, *HSP5A* or *XBP1* (**Figure 5-21**).

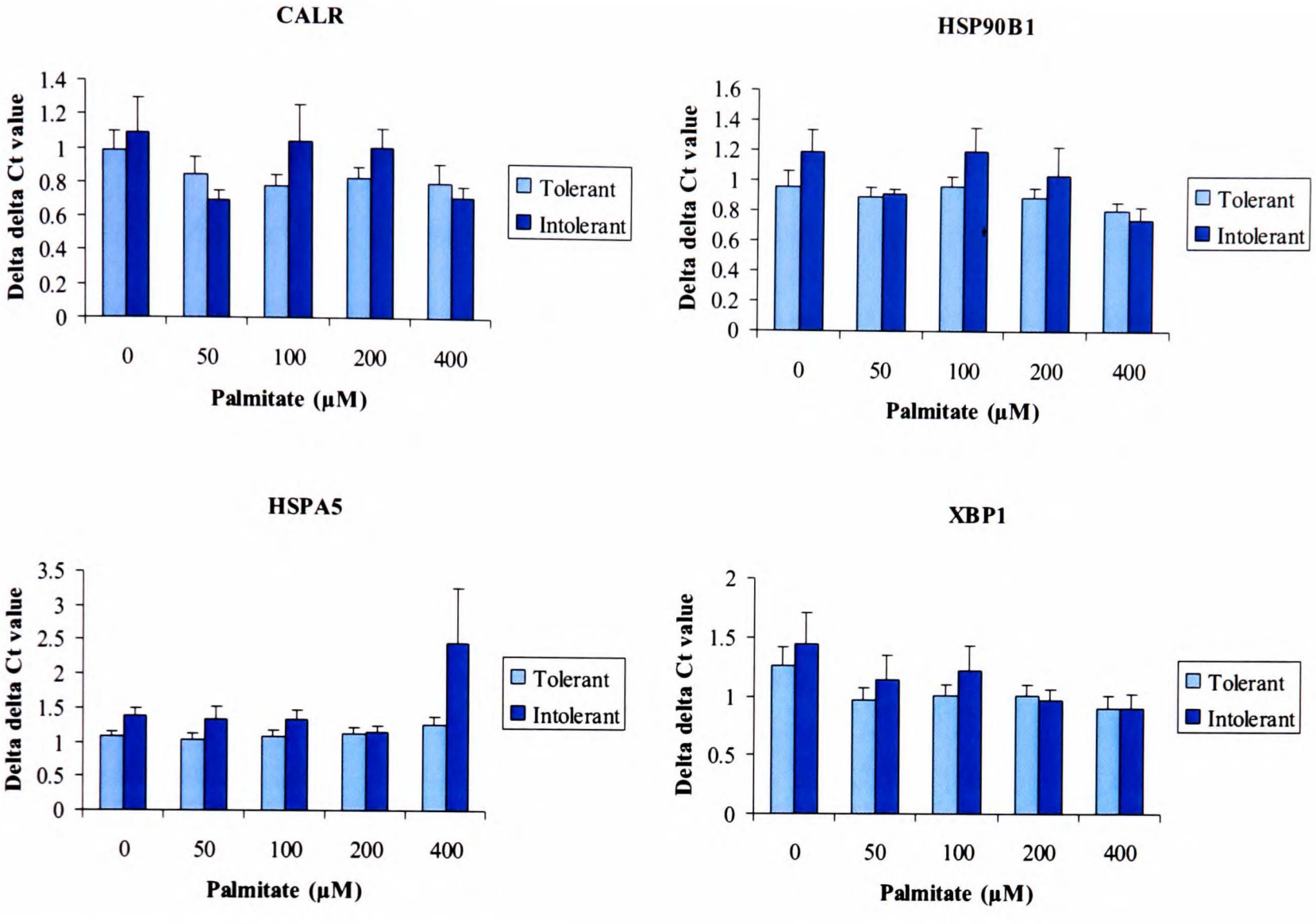


Figure 5-21 Changes in mRNA expression of ER stress-related genes

5.5. DISCUSSION

Adipocytes differentiated with a high concentration, 400 µM, of [U-^{13}C]palmitate revealed that adipocytes from different donors either thrived with this high dose of palmitate (palmitate-tolerant) or showed partial cell death (palmitate-intolerant). Definition of the groups was based on visual observations of cell death of adipocytes, as represented by apparent cell debris, with occasional large lipid droplets interspersed throughout, present in surviving cells. These visual observations were supported by a reduction in total TG accumulation.

Despite obvious cell death in the palmitate-intolerant group, the measurements made between the two groups are comparable. Prior to harvesting the cells, media was removed and cells were washed in PBS, thus removing any extracellular contaminants within the media, perhaps released by the cells. It can be assumed that all TG and mRNA measurements were taken from remaining viable cells. Furthermore, the fatty acid measurements made were reported as either ratios or percentage of the total of the fatty acid of interest, eliminating any differences in total amounts between the groups. All mRNA measurements were related back to the geometric mean of three separate housekeeping genes. This means that expression of mRNA has only been made in viable cells and also corrects for the differences in starting material of RNA between the two groups.

The pathways of DNL and SCD-mediated desaturation were down-regulated in the palmitate-intolerant group compared with the palmitate-tolerant group, and the proportion of TG SAFA was higher (and MUFA lower) in this group. The increase in SAFA may have occurred due to the reduction in SCD activity which may have caused SAFAs to accumulate within the cell. Furthermore, there was a higher proportion of exogenously-derived myristate in the TG fatty acid. It is possible that the reduction of SCD activity, and consequential reduced ability for desaturation of palmitate in the intolerant cells, may have caused these cells to seek other means to rid themselves of palmitate. Sampath *et al.* (2007) showed that high-stearate diet-induced up-regulation of lipogenesis in mice was dependent upon *Scd1* activation; knockdown of *Scd1* in these mice removed stearate's ability to induce lipogenesis. This emphasises a coordination of SCD and DNL regulation, and further supports the theory of a pro-lipogenic effect of saturated fatty acids.

Other studies have shown SCD to play an important role in aiding storage of palmitate as neutral lipid and protecting the cell from apoptosis (Listenberger *et al.*, 2003). Busch *et al.* (2005) identified a population of palmitate-resistant MIN-6 β-cells that were resistant to palmitate-induced apoptosis. These cells survived by storing palmitate as cholesteryl esters and by up-regulating fatty acid oxidation and *Scd1* mRNA expression. Interestingly, inhibition of *Scd1* in these cells abolished resistance to palmitate, showing fatty acid desaturation to be crucial to protection from palmitate-induced apoptosis.

Interestingly, in the palmitate-tolerant group, there was no preferential desaturation of exogenous palmitate over DNL-derived palmitate. In the palmitate-intolerant group, however, SCD preferentially acted upon DNL-derived palmitate. This is perhaps of importance, as DNL was down-regulated in the palmitate-intolerant cells; therefore, the amount of DNL-derived palmitate was reduced. Tolerance may be achieved partly by up-regulation of SCD action, and also by the fact that when the influx of exogenous palmitate increases, these cells are able to survive by converting the saturated to a monounsaturated fatty acid, which may help to promote its storage (Listenberger *et al.*, 2003). Flux through ELOVL6 was less in the palmitate-intolerant group than in the tolerant group, although there was greater stearate production from palmitate. This could be due to a down-regulation of *SCD*; if SCD does not act upon stearate synthesised from palmitate, there will be a build-up of stearate and the accumulation of SAFA will increase. Furthermore, there also appeared to be a greater proportion of exogenously-derived myristate in this group's cells, further adding to the intracellular concentration of SAFA. These findings hint at there being a

mechanism by which handling of exogenous palmitate is altered in the palmitate-intolerant cells.

Investigation of the fatty acid composition of the phospholipids also exposed differences between the palmitate-tolerant and intolerant groups. The ratio of PL SAFA:MUFA was more than 2.5-fold higher in the palmitate-intolerant cells compared with the tolerant group. Additionally, incorporation of the exogenous palmitate was greater in the palmitate-intolerant adipocyte PLs. Reduced TG storage, seen in the palmitate-intolerant adipocytes, was also accompanied by a corresponding reduction in *DGAT2* mRNA. One possibility for the higher incorporation of exogenous palmitate into the PL fatty acids could be a limited ability for storage as TG in the palmitate-intolerant cells. Channelling of exogenous palmitate into PLs could have caused an overwhelming rise in SAFAs within the cell membrane, and may have contributed to loss of membrane fluidity to such a great extent as to cause the cells to rupture.

Studies using non-adipose cells have shown saturated fatty acids to induce apoptosis (Artwohl *et al.*, 2004; Mishra & Simonson, 2005; Wei *et al.*, 2007). Microarray analysis indicated that there may have been an up-regulation of the apoptotic pathway in adipocytes in response to palmitate. However, when the sample sizes of the palmitate-tolerant and intolerant groups were increased these differences were no longer statistically significant. *In vitro* studies have shown incubation of cells with palmitate to induce ER stress (Moffitt *et al.*, 2005; Wei *et al.*, 2007); therefore, this pathway was investigated at the mRNA level. There were no significant differences between the palmitate-tolerant and palmitate-intolerant groups. This suggests that

neither increased ER stress nor apoptosis can account for the differences in cell viability seen between the two groups and shows that there must be a different mechanism responsible.

The main differences between the palmitate-tolerant and intolerant groups may have been in pathways concerning fatty acid metabolism, Wnt signalling or cell adhesion. The palmitate-tolerant adipocytes had greater *PCK1* expression than the intolerant cells. Cytosolic PEPCK, the enzyme encoded by the *PCK1* gene, is a key enzyme involved in glyceroneogenesis. Therefore, by increasing *PCK1* expression, the adipocyte may produce more glycerol 3-phosphate, thereby increasing fatty acid esterification, and storing the free fatty acids away safely as TG. Adipocyte-specific down-regulation of *Pck1* expression in mice resulted in reduced adipose tissue mass (Olswang *et al.*, 2002), whereas over-expression of *Pck1* caused adipocyte hypertrophy (Franckhauser *et al.*, 2002). These findings indicate the importance of *PCK1* in fat storage in the adipocyte. It is worth remembering, however, that in **Chapter 3**, it was noted that *PCK1* is expressed at low levels in adipocytes cultured in a highly lipogenic environment, and this pathway may not contribute greatly to overall glycerol 3-production in this situation.

Secreted frizzled-related proteins 1 and 2 are known endogenous inhibitors of the Wnt signalling pathway (Prestwich & Macdougald, 2007). *SFRP1* increased with 400 μM palmitate (compared with controls) in the tolerant cells but decreased in the intolerant cells. This could indicate a reduced capacity for adipogenesis in the palmitate-intolerant cells that further contributes to their inability to store fatty acids as TG at a time when there is a surge of exogenous palmitate influx into the adipocyte.

There were distinct differences in the expression of *TNC*, the gene that encodes tenascin C, involved with focal adhesion. The palmitate-intolerant adipocytes expressed far greater levels of *TNC* than the palmitate-tolerant adipocytes in the absence of exogenous palmitate. Whereas palmitate did not affect *TNC* mRNA expression in the palmitate-tolerant cells, there was a marked down-regulation in its expression in the palmitate-intolerant cells. The possible reasons for such great differences are not clear.

In conclusion, it would seem that the adipocytes from some subjects are capable of surviving high concentrations of exogenous palmitate, whereas those from others are not. The two groups, palmitate-tolerant and palmitate-intolerant, appear to differ in intracellular processing of exogenous palmitate. Palmitate intolerance is associated with a down-regulation of DNL and SCD, and an accumulation of intracellular saturated fatty acids. In the palmitate-intolerant adipocytes, TG storage is down-regulated, and fatty acids that are stored contain more SAFAs than in the tolerant cells. The reduced ability to store fatty acids may be caused by the down-regulation of SCD and may even be further exacerbated by low levels of cytosolic PEPCK, a source of additional glycerol 3-phosphate for esterification, or by a lack of inhibition of Wnt signalling, thus limiting adipogenesis and potential for storage. Cell death, seen in the palmitate-intolerant adipocytes, could not be explained by apoptosis or attributed to ER stress. The increased shunting of exogenous palmitate towards PLs caused an increase in PL SAFA content and possibly explains the rupturing of the cell membrane. The chain of events may have been initiated by the reduction of DNL and SCD, which could act in tandem to play a crucial role in the incorporation of

palmitate into the lipid droplet of the adipocyte, thus protecting the cell from loss of function and possible cell death.

Chapter 6

The effects of SCD silencing in human adipocytes

6.1. INTRODUCTION

SCD, or delta-9 desaturase, is a key enzyme in the conversion of saturated to monounsaturated fatty acids. Its preferred substrates, palmitoyl-CoA and stearoyl-CoA, are converted to palmitoleoyl-CoA and to oleoyl-CoA, respectively. These monounsaturated fatty acids comprise the majority of fatty acids found in triglycerides, phospholipids and cholesteryl esters. The adverse effects of an over-abundance of saturated fatty acids have been well documented (Vessby *et al.*, 2001; Summers *et al.*, 2002; Lu *et al.*, 2003; Lee *et al.*, 2006; Risérus, 2008). Therefore, it would seem plausible to assume that this enzyme plays a crucial role in maintaining the intracellular equilibrium of saturated and monounsaturated fatty acids.

In human studies, up-regulation of SCD protected human arterial endothelial cells from atherosclerosis (Peter *et al.*, 2008). Additionally, TZD (rosigitazone) treatment for type 2 diabetes was associated with an increase in SCD mRNA in adipose tissue and an increase in plasma TG fatty acid SCD indices, paralleled by an improvement in insulin sensitivity (Risérus *et al.*, 2005). Further supporting this, low SCD activity has been associated with increased hepatic insulin resistance and fatty liver (Stefan *et al.*, 2008).

Rodent studies have shown high-fat diet-induced obesity in normal Sprague-Dawley rats to cause an 80 % decrease in *SCD1* mRNA in the liver (Kakuma *et al.*, 2002), and high SCD expression to prevent hypercholesterolaemia (Lu *et al.*, 2003). Additionally, *SCD1* inhibition in rat myotubes reduced insulin sensitivity and increased DAG and ceramide production. Equally, over-expression of *SCD1* restored insulin sensitivity and diverted fatty acid esterification away from DAG towards TG

(Pinnamaneni *et al.*, 2006), suggesting a positive role for SCD1 in maintaining insulin sensitivity within muscle.

However, in many studies using murine models or cells lines, high SCD activity has been linked with various diseases and disorders, including obesity, insulin resistance, atherosclerosis and cancer (Scaglia *et al.*, 2005; Gutierrez-Juarez *et al.*, 2006; Morgan-Lappe *et al.*, 2007; Scaglia & Igal, 2008; Flowers & Ntambi, 2009). For example, high-fat feeding in obesity-prone mice was linked to an increase in hepatic *Scd1* mRNA expression (Hu *et al.*, 2004). Furthermore, the generation of the *Scd1* knockout mouse added weight to the argument that increased SCD activity may be associated with an unfavourable metabolic profile (Ntambi *et al.*, 2002).

The *Scd1* knockout mouse was shown to be leaner and more insulin sensitive than its wild-type littermates and resistant to high-fat diet-induced obesity. Loss of SCD1 function was also accompanied by increased energy expenditure and oxygen consumption as well as changes in gene expression; lipogenic genes, including fatty acid synthase and sterol regulatory element binding protein 1, were down-regulated, whereas those for fatty acid oxidation, such as carnitine palmitoyl transferase 1 and acyl-CoA oxidase, were up-regulated. *Scd1*-targeted antisense oligonucleotides have also been used to achieve *Scd1* loss-of-function in mice (Jiang *et al.*, 2005). In this study, treated mice were also challenged with a high-fat diet and again showed protection from obesity, reduced hepatic triglycerides and fatty acid synthesis, improved insulin sensitivity and increased fatty acid oxidation.

The asebia mouse is characterised by a naturally occurring homozygous mutation in the *Scd1* gene resulting in SCD1 deficiency. It was first identified by Gates and Karasek (1965) as a mutant of the BALB/c strain of mice, completely lacking sebaceous glands and suffering from alopecia, skin abnormalities and, eventually, blindness. The mutation was later identified as being autosomal recessive and attributed to a deletion in the *Scd1* gene, spanning exons 1 to 4, rendering the animal completely devoid of SCD1 protein (Zheng *et al.*, 1999). Further characterisation of this mouse revealed an inability to synthesise hepatic triglycerides and cholesteryl esters despite expression of normal activities of the enzymes glycerol phosphate acyltransferase and acyl-CoA:cholesterol acyltransferase (Miyazaki *et al.*, 2000).

Many human studies have also labelled SCD as a key player in the development of obesity and related disorders. Elevated SCD indices and mRNA expression have been associated with hypertriglyceridaemia, abnormal fatty acid partitioning in skeletal muscle and insulin resistance (Attie *et al.*, 2002; Hulver *et al.*, 2005; Chu *et al.*, 2006; Sjögren *et al.*, 2008) and desaturation indices have been shown to correlate positively with plasma TG levels (Attie *et al.*, 2002).

Whilst some research into SCD and its association with obesity and related disorders has highlighted SCD as an ideal target for obesity treatment, other studies have often produced contradictory and conflicting findings. The consideration that SCD could be a potential target for obesity treatment sparked the development of SCD inhibitors (Dobrzyn & Ntambi, 2005; Liu *et al.*, 2007; Zhao *et al.*, 2007). However, the literature is rife with inconsistencies as to whether or not SCD contributes to metabolic diseases such as type 2 diabetes and insulin resistance in humans.

Therefore, a clearer understanding of the tissue-specific roles of SCD is required before the benefits of SCD inhibition in man can be ascertained.

6.2. AIMS

Many studies into SCD have focussed on effects on the liver. Despite the adipocyte being a highly insulin-sensitive cell with primary functions in fatty acid metabolism, there has been little investigation into the effects of SCD in this cell. The aims of this study were to investigate the role of SCD in the adipocyte by knocking it down in the differentiating preadipocyte, and assessing the effects on SCD activity and consequences on TG and PL fatty acid composition, cell membrane fluidity and insulin sensitivity. Addition of labelled exogenous palmitate would also open up the opportunity to investigate the substrate specificity, with respect to fatty acid origin, of SCD in the human adipocytes following SCD knockdown.

6.3. METHODS

6.3.1. Adipose tissue sample collection

The taking of human adipose tissue samples was approved by the Oxfordshire Clinical Research Ethics Committee and all subjects gave written, informed consent. Subcutaneous adipose tissue biopsies were taken and preadipocytes isolated as described in **Chapter 2**, section **2.1.2**. Tissue donors for the experiments described in this chapter consisted of 5 males and 3 females, with a median age of 43.5 years (ranging from 33 to 53 years), and with a median BMI of 25.8 kg/m^2 (ranging from 24.0 to 37.9 kg/m^2).

6.3.2. Cell culture

Human preadipocytes were isolated from subcutaneous adipose tissue as described in section **2.2**. Differentiation of confluent preadipocytes was carried out for 14 days.

6.3.3. SCD knockdown

siRNA transfection of cells induces a transient knockdown of mRNA. Therefore, addition of siRNA to preadipocytes to knock down *SCD* mRNA at day 1 of the 14 required for differentiation would have little effect for two main reasons. Firstly, *SCD* mRNA expression is up-regulated during differentiation and would, therefore, be minimal at day one, as was shown in **Chapter 2** (**Figure 2-6**). Secondly, suppression of mRNA expression at day 1 would not be sustained throughout differentiation. For these reasons, siRNA was added to differentiating preadipocytes at day 6 of differentiation, when *SCD* mRNA would be expressed (**Figure 2-6**), and again at days 9 and 12 (a total of three times), in order to maintain knockdown. Two different *SCD*-specific siRNAs were used to achieve *SCD* mRNA knockdown, termed SCD siRNA1 and 2, (Stealth siRNA, HSS109499 and HSS109500, respectively, Invitrogen, Paisley, UK) with controls of lipofectamine only, scrambled siRNA negative control (Stealth Negative siRNA 12935-300 (GC content matched to SCD-specific siRNAs), Invitrogen, Paisley, UK) and one control with no transfection components, termed control.

6.3.4. Use of stable isotopes to study palmitate channelling

[U-^{13}C]palmitate was also added during differentiation to trace the fate of exogenous palmitate with SCD knockdown and to assess SCD substrate channelling and possible

compartmentalisation. No (0 μM) or 200 μM [U-^{13}C]palmitate was added throughout differentiation.

6.3.5. Statistical analyses

Differences between control and palmitate-treated cells were statistically analysed using repeated measures analysis of variance (ANOVA). Differences between scrambled siRNA controls and SCD-specific siRNAs were assessed using a Student's *t* test (paired). All statistical analyses were carried out using SPSS (version 15).

6.4. RESULTS

6.4.1. Cell morphology

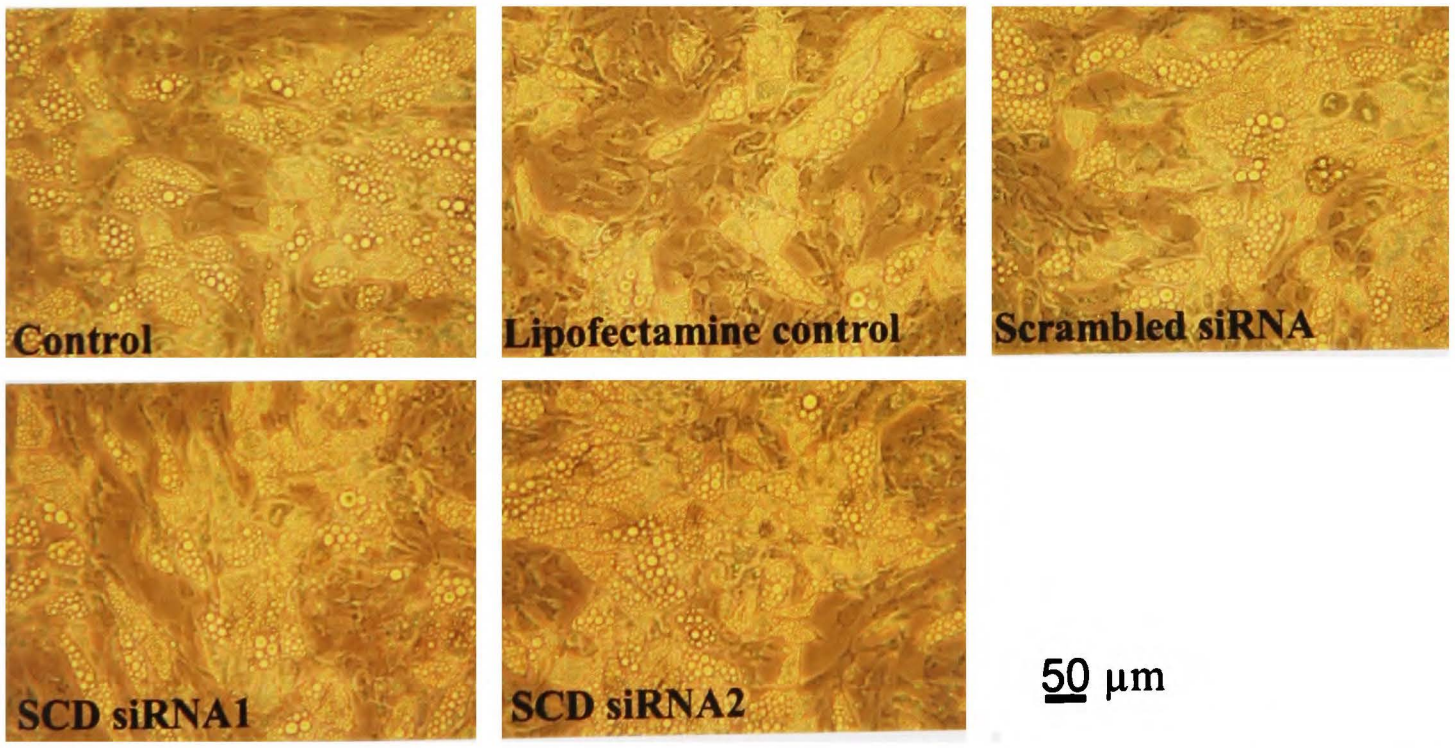


Figure 6-1 Micrographs of differentiated preadipocytes after treatment with SCD siRNA (x10 objective)

Knockdown of *SCD1* mRNA had no apparent effects on adipocyte morphology. Appearance of the adipocytes indicated that they remained viable and accumulated

similar-sized lipid droplets in the presence of both transfection agent and siRNA (**Figure 6-1**).

6.4.2. Maintenance of SCD knockdown

SCD-specific siRNA was added to the media of differentiating preadipocytes as described and cells were harvested 24, 48 and 72 hours post-transfection to assess *SCD* mRNA knockdown. Cells were harvested on days 13, 14 and 15, following their third dose of siRNA. **Figure 6-2** shows the percentage knockdown achieved with the two different siRNA oligonucleotides. Both siRNAs showed a consistent, stable knockdown over the 72 hour period following transfection although siRNA2 achieved a greater knockdown than siRNA1 ($P = 0.000$, repeated measures ANOVA).

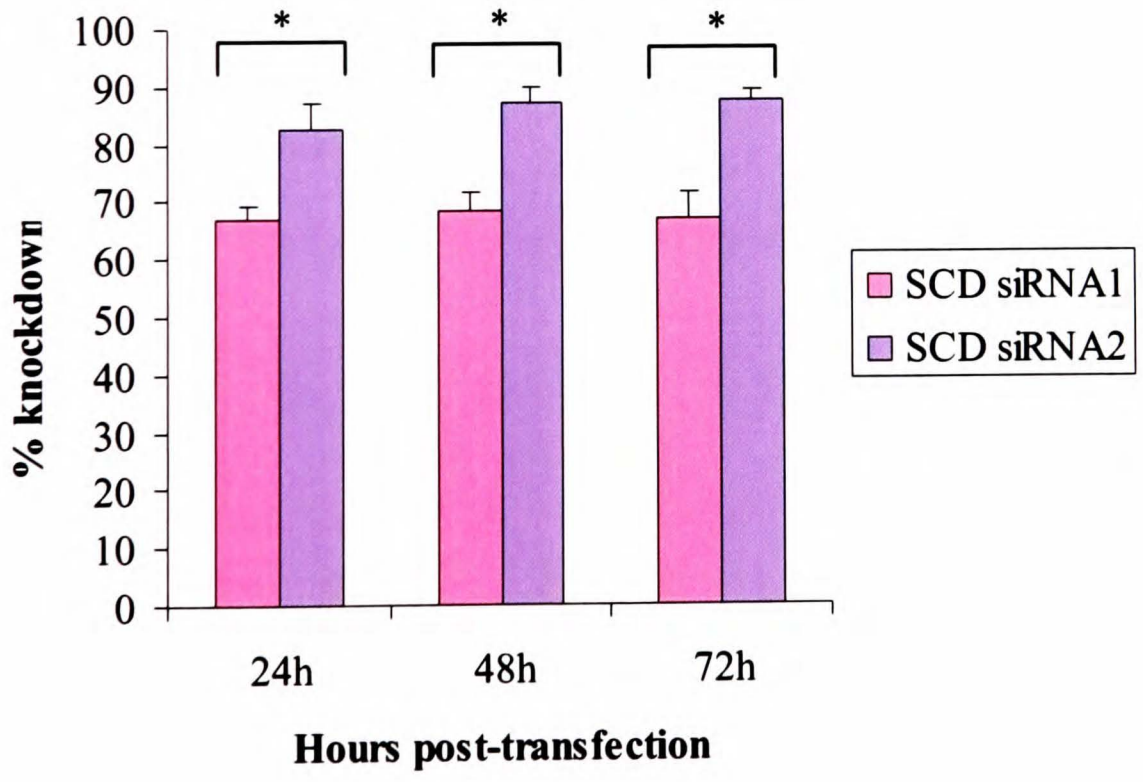


Figure 6-2 *SCD* mRNA knockdown expressed compared to *SCD* mRNA expression in scrambled siRNA samples. Data are represented as mean ± SEM (n=4). *P < 0.01

6.4.3. Effect of SCD knockdown on adipocyte TG accumulation

In cells with no added palmitate, *SCD* mRNA silencing slightly reduced total TG accumulation, although this reached only borderline significance with SCD siRNA2 (P = 0.056). When adipocytes were differentiated with 200 μM palmitate with simultaneous silencing of *SCD* mRNA, the result was a slight reduction in total TG accumulation (**Figure 6-3**), although this only reached statistical significance with one of the two SCD1 siRNAs used (P = 0.027 and P = 0.118 for SCD siRNA1 and 2, respectively). Addition of 200 μM palmitate resulted generally in more TG accumulation than those with no added palmitate but this did not reach statistical significance (P = 0.225 repeated measures ANOVA).

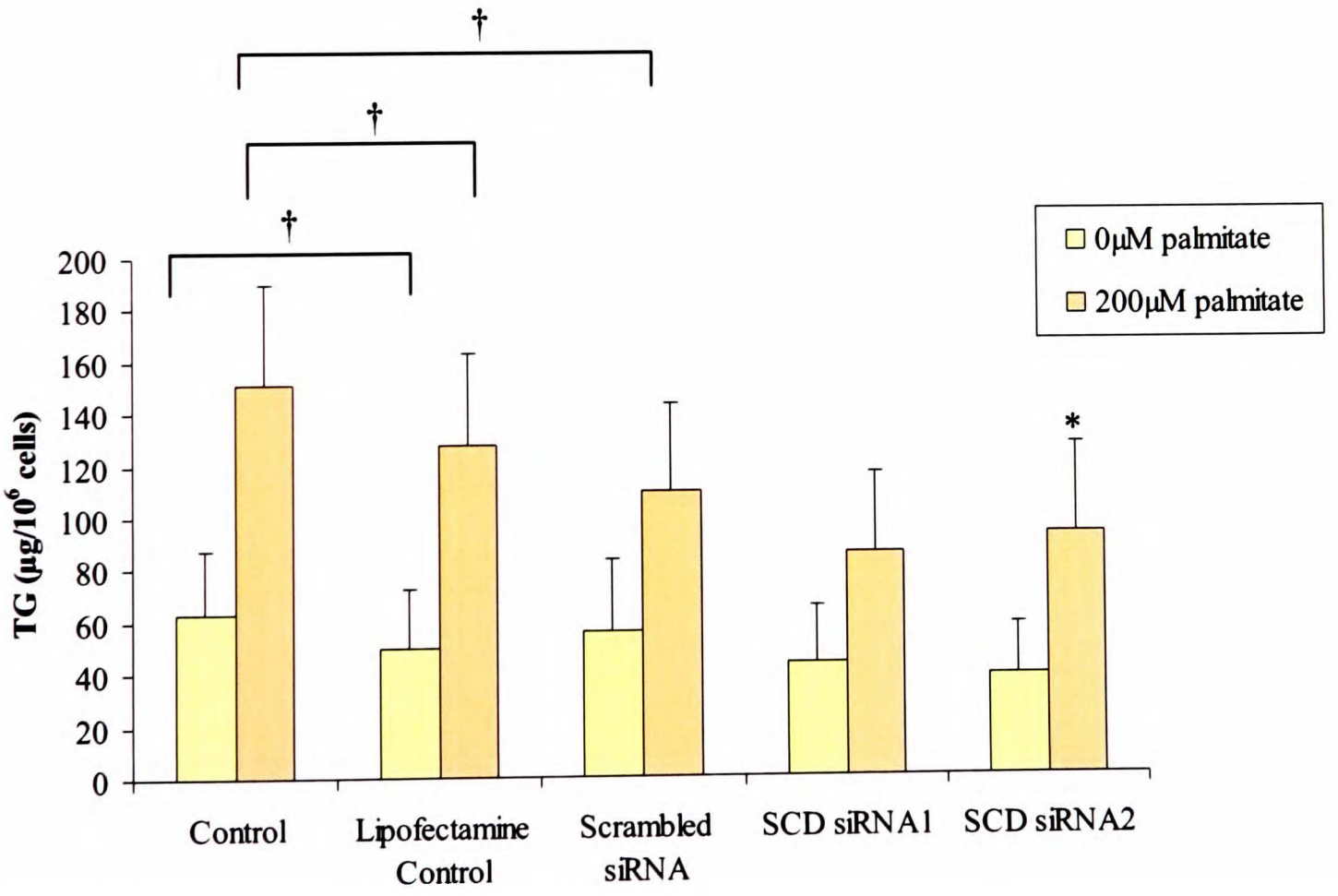
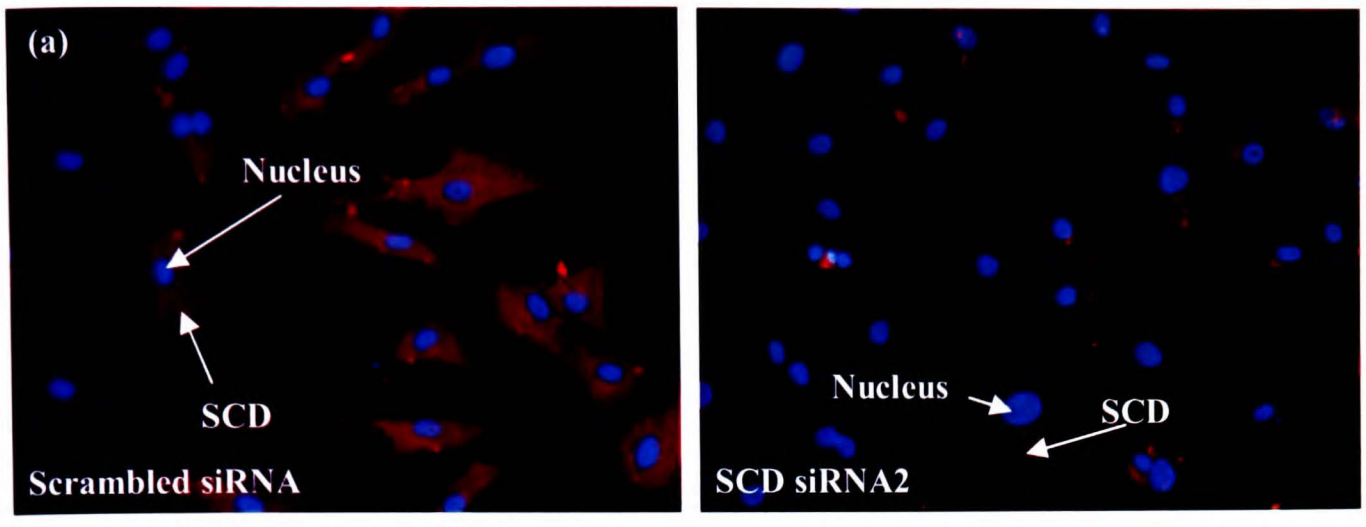


Figure 6-3 Total TG in adipocytes in response to siRNA-mediated silencing of SCD. Data are represented as mean ± SEM (n = 8). * P = 0.027 compared with scrambled siRNA † P ≤ 0.03 Differences between controls

6.4.4. SCD activity

SCD indices, used as a proxy measure of activity, were calculated using the product-to-precursor ratios of 16:1 *n-7*/16:0 and 18:1 *n-9*/18:0 in TG-fatty acids. Both SCD siRNA1 and 2 reduced SCD indices (**Figure 6-4**). *SCD* mRNA silencing had a more pronounced effect of reducing the desaturation of stearic acid than it did on palmitic acid ($P = 0.005$ for 0 μM palmitate and $P = 0.000$ for 200 μM palmitate-treated cells, repeated measures ANOVA). There were no differences in SCD indices between 0 μM and 200 μM palmitate-treated cells ($P = 0.170$, repeated measures ANOVA). Percentage down-regulation is summarised in **Table 6-1**.



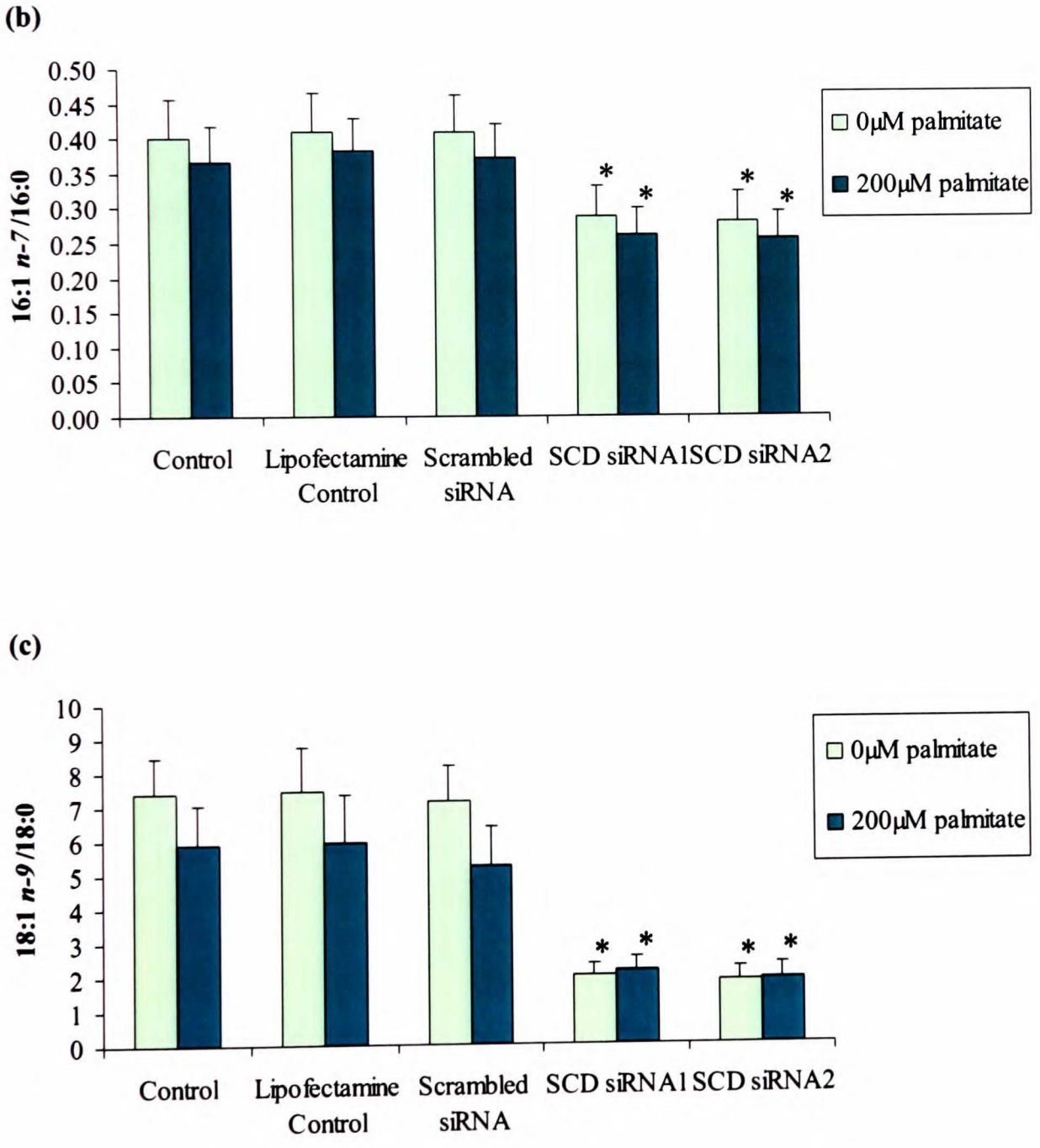


Figure 6-4 Effects of SCD siRNA on (a) SCD protein using TRITC and DAPI fluorescence staining for SCD protein and nuclei (x40 objective), respectively, and TG-fatty acid product-to-precursor ratios for (b) 16:1 *n-7*/16:0 and (c) 18:1 *n-9*/18:0 as a measure of SCD activity in adipocytes in response to siRNA-mediated silencing of SCD. Data are represented as mean ± SEM (n = 8). * $P \leq 0.003$ compared with scrambled siRNA

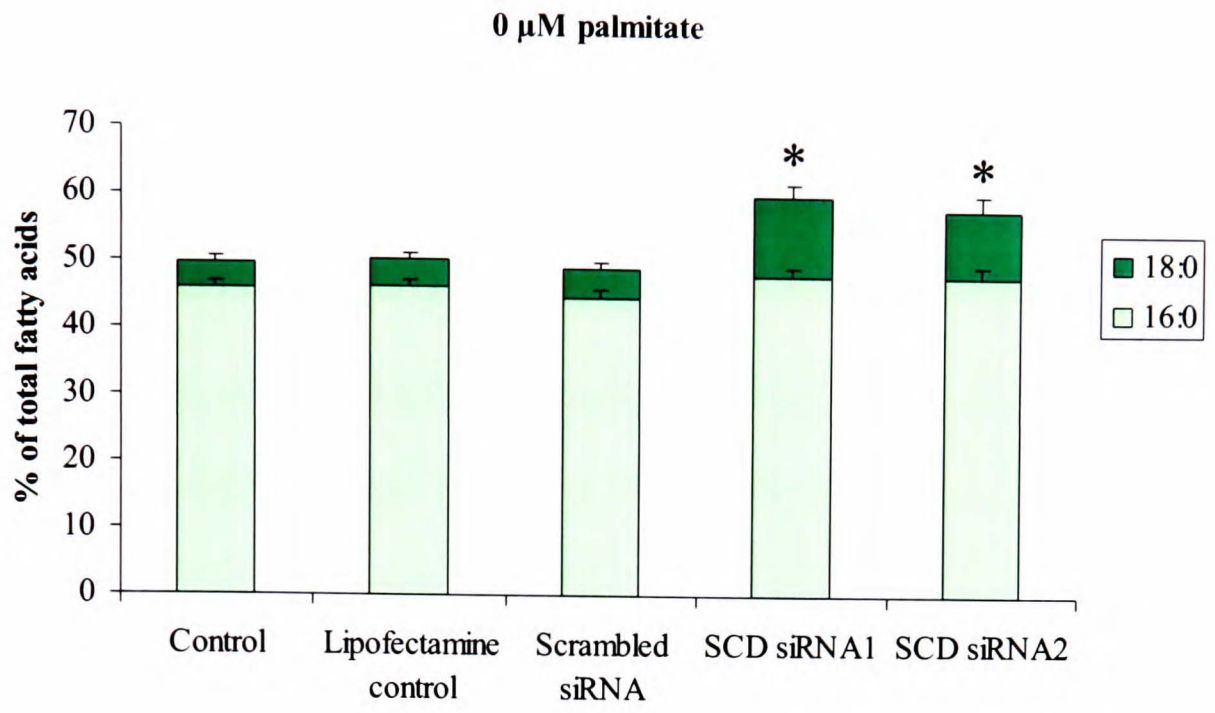
	0 μM palmitate		200 μM palmitate	
	16:1 *n-7*/16:0	18:1 *n-9*/18:0	16:1 *n-7*/16:0	18:1 *n-9*/18:0
SCD1 siRNA1	58.4±4.3	23.9±2.4*	61.3±6.1	35.3±6.2*
SCD1 siRNA2	50.5±10.4	32.6±6.1*	55.0±5.2	30.8±5.4*

Table 6-1 SCD indices in adipocytes shown as a percentage compared to scrambled siRNA.

Data are represented as mean ± SEM (n = 8)

*** P < 0.001 (difference between 16:1 *n-7*/16:0 and 18:1 *n-9*/18:0)**

SCD silencing affected TG-fatty acid composition. The reduced ability to desaturate palmitate and stearate led to a consequential increase in the accumulation of these fatty acids in both 0 μM and 200 μM palmitate-treated adipocytes (**Figure 6-5**).



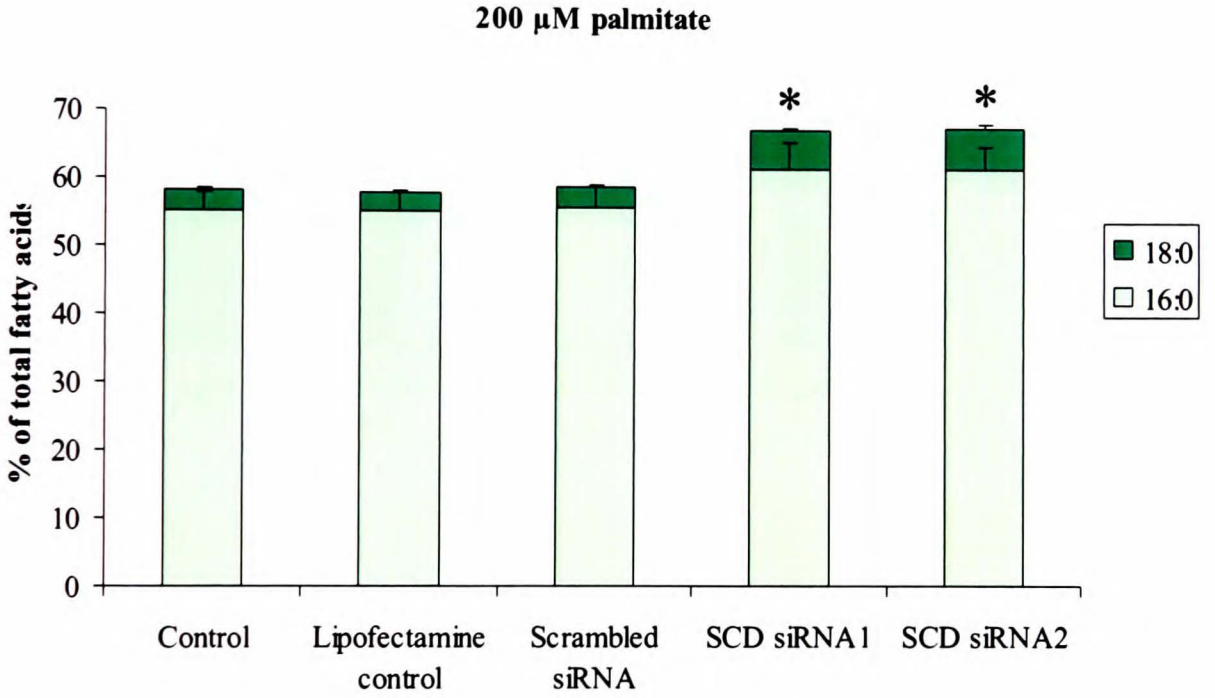


Figure 6-5 Changes in TG saturated fatty acid composition with SCD knockdown. Data are represented as mean ± SEM (n=8). *P ≤ 0.001 compared with scrambled siRNA

6.4.5. Channelling of fatty acids towards SCD desaturation

In preadipocytes differentiated with 200 µM [U-^{13}C]palmitate, channelling of substrates towards SCD was investigated. Using GC-MS, exogenous, i.e. labelled, palmitate could be distinguished from the DNL-derived palmitate, i.e. unlabelled. Labelled stearate and oleate indicated that these fatty acids were derived via

modification of exogenous palmitate. In agreement with the findings of **Chapter 4**, SCD's action on palmitic acid was not dependent upon the source of this fatty acid, whether from DNL or exogenously derived (**Figure 6-6 (a)**) (P = 0.856, repeated measures ANOVA). There was preferential channelling of DNL-derived stearic acid towards SCD, and substrate preference for DNL-derived stearate was not influenced by SCD knockdown (**Figure 6-6 (b)**) (P = 0.048, repeated measures ANOVA).

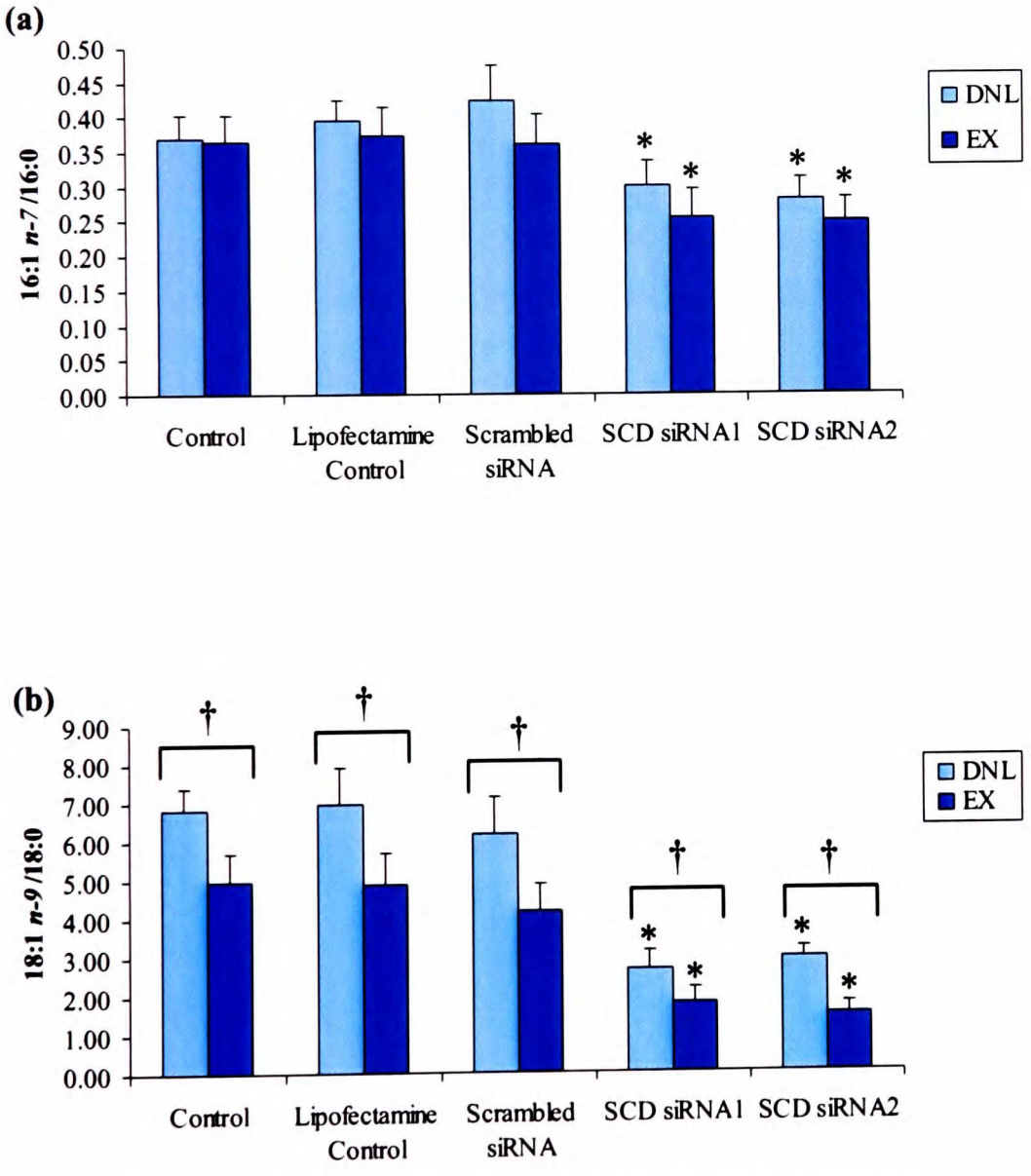


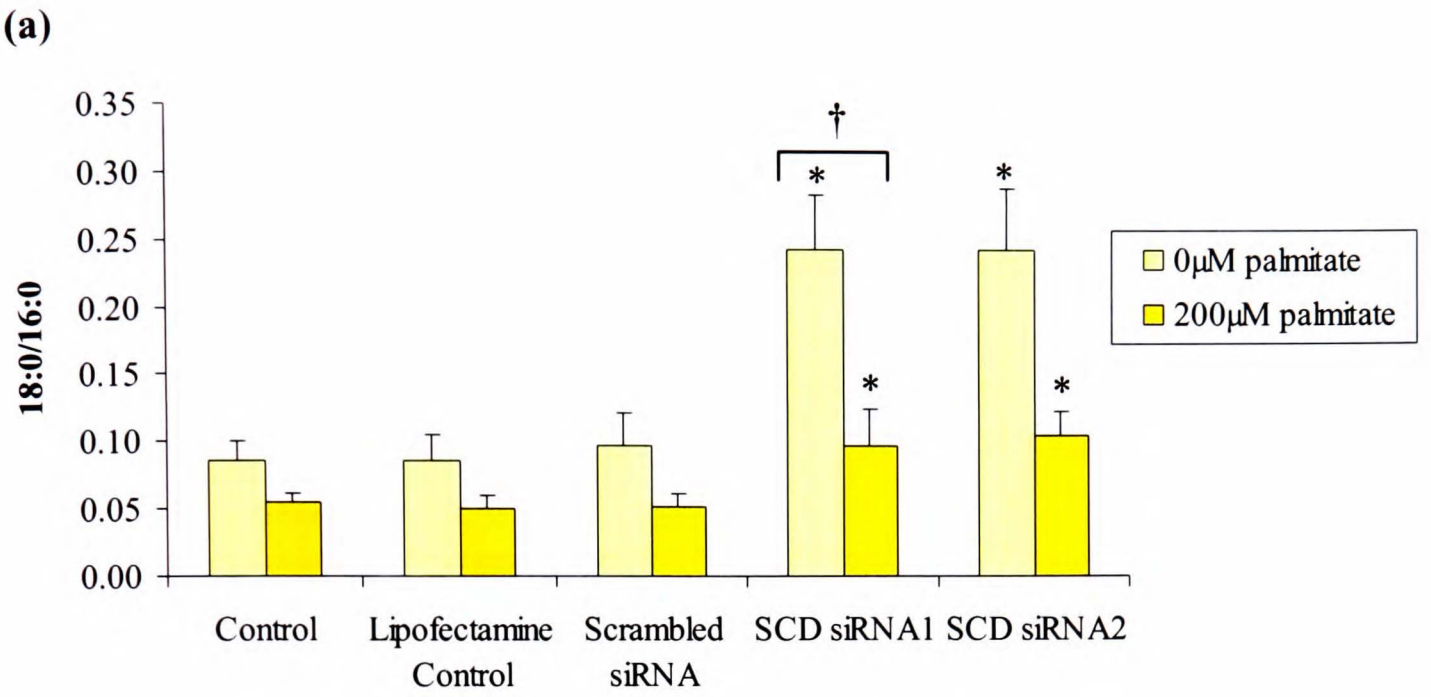
Figure 6-6 SCD indices showing (a) 16:1 *n*-7/16:0 and (b) 18:1 *n*-9/18:0 of DNL-derived and exogenous TG-fatty acids after siRNA-mediated silencing of SCD.

Data are represented as mean ± SEM (n = 8)† P > 0.05 between DNL and exogenous fatty acid indices

***P > 0.05 between scrambled and SCD siRNAs**

6.4.6. Fatty acid elongation

Elongase, specifically ELOVL6, activity was estimated using product-to-precursor ratios. Palmitate elongation was increased with *SCD* knockdown in both palmitate-free (0 μM) cells and palmitate-treated cells ($P \leq 0.02$). Cells differentiated without exogenous palmitate showed slightly more elongation of 16:1 *n-7*, and *SCD* knockdown had no effect on this ratio. Overall, the product-to-precursor ratios were higher in the palmitate-free (0 μM) cells than the 200 μM palmitate-treated cells (18:0/16:0 $P = 0.023$ and 18:1 *n-7*/16:1 *n-7* $P = 0.05$, repeated measures ANOVA) (**Figure 6-7**).



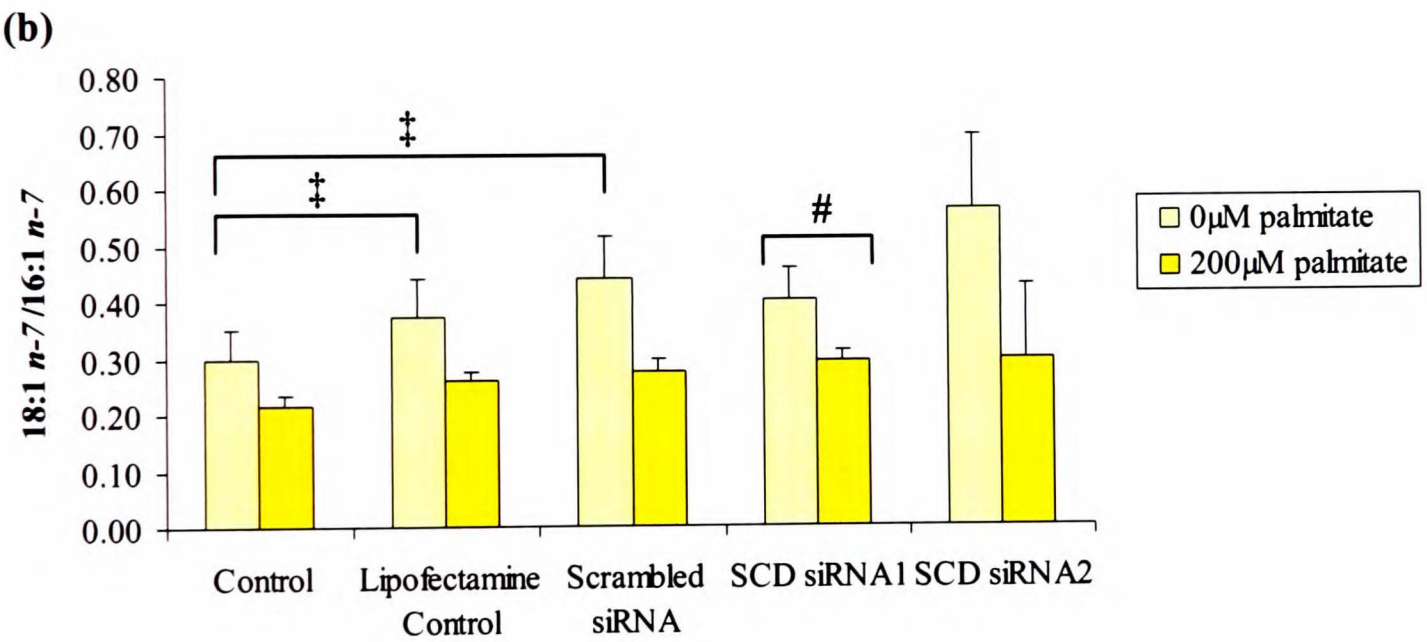


Figure 6-7 TG-fatty acid product-to-precursor ratios for (a)18:0/16:0 and (b) 18:1 *n-7*/16:1 *n-7* as a measure of ELOVL6 activity in adipocytes in response to siRNA-mediated silencing of SCD. Data are represented as mean ± SEM (n = 8).

*** P ≤ 0.02 vs scrambled siRNA, † P = 0.01, ‡ P < 0.01 # P = 0.035**

6.4.7. Channelling of fatty acids towards elongation

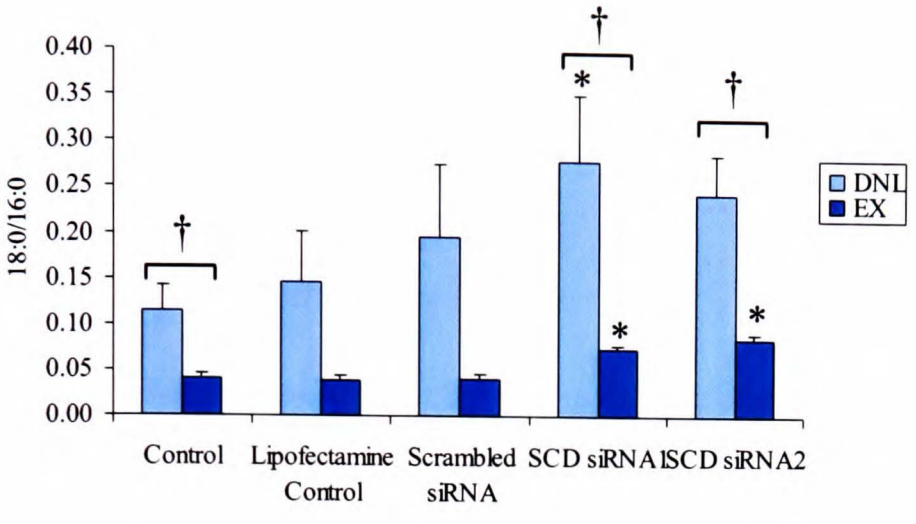


Figure 6-8 TG-fatty acid product-to-precursor ratios for ^{12}C16:0 to 18:0 (DNL) and ^{13}C16:0 to 18:0 (EX) fatty acid elongation. Data are represented as mean ± SEM (n = 8)

† P ≤ 0.04, * P ≤ 0.011

There was no statistically significant difference in elongation between control, lipofectamine control or scrambled siRNA for either DNL-derived or exogenous palmitate ($P > 0.05$). SCD siRNA1 increased elongation of DNL-derived palmitate ($P = 0.011$) but siRNA2 did not ($P = 0.328$). Elongation of exogenous palmitate was significantly increased by both SCD siRNA1 and 2 ($P = 0.000$ for both). There was preferential elongation of DNL-derived palmitate ($P = 0.022$, repeated measures ANOVA) (**Figure 6-8**).

6.4.8. Cell membrane fluidity

Changes in cell membrane fluidity in response to SCD knockdown were determined by two different methods. The phospholipid (PL) fatty acid composition was analysed and expressed as changes in the saturated to monounsaturated fatty acid ratio (SAFA:MUFA). A more direct measurement of cell membrane fluidity was also

made using fluorescence recovery after photobleaching (FRAP) techniques. A more detailed description of these measurements of cell membrane fluidity can be found in section **2.7**.

6.4.8.1. Phospholipids

SCD knockdown caused an increase in PL SAFA:MUFA ratios in both control and palmitate-treated cells. There was a borderline significant difference in SAFA:MUFA between the 0 μM and 200 μM palmitate-treated cells (P = 0.051, repeated measures ANOVA) (**Figure 6-9**).

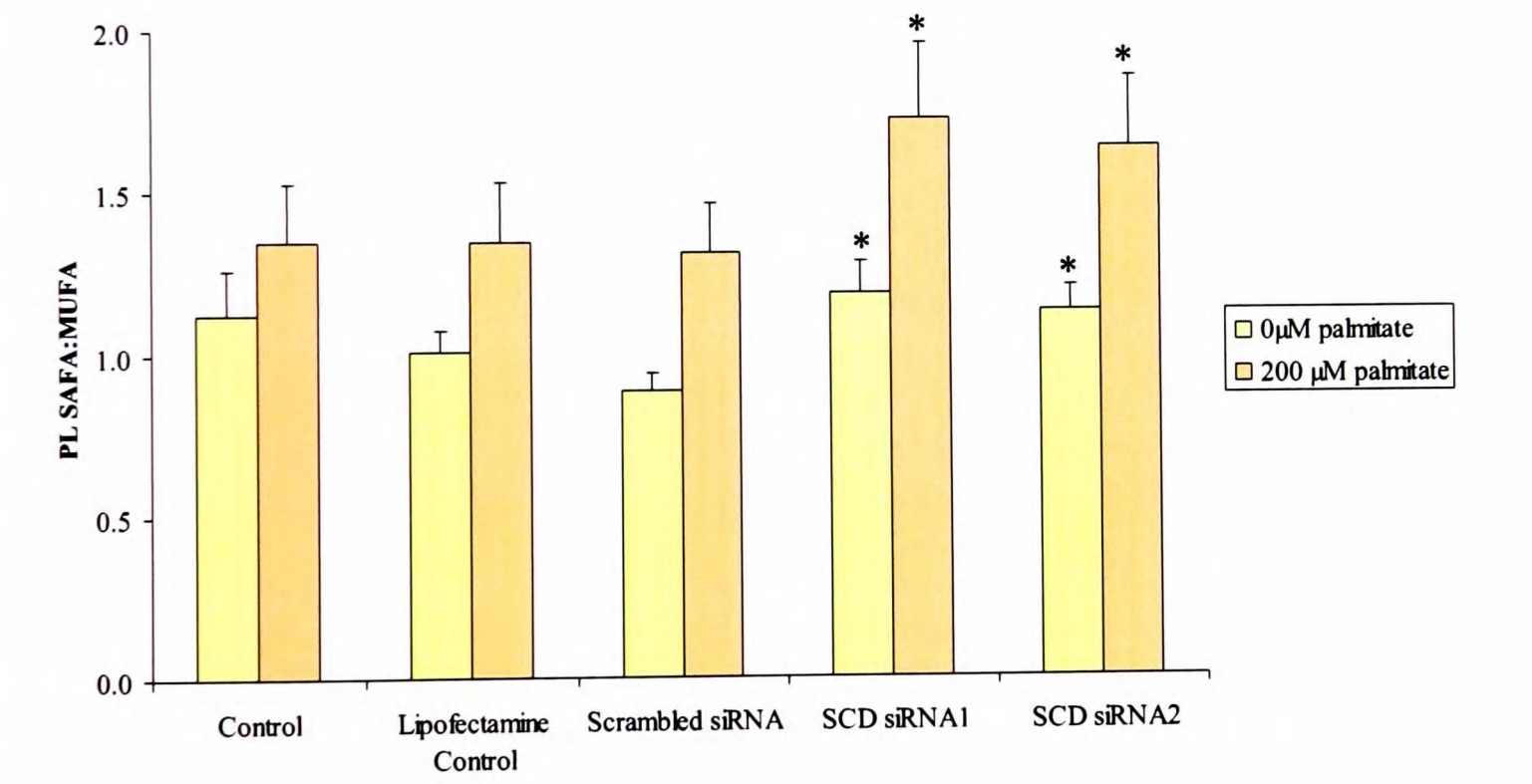


Figure 6-9 Phospholipid SAFA:MUFA ratios. Data are represented as mean ± SEM (n = 8)

***P ≤ 0.043 compared with scrambled siRNA**

There was also a reduction in 16:1 *n-7*/16:0 and 18:1 *n-9*/18:0 ratios with SCD knockdown, showing that PL fatty acids were also affected by inhibition of this enzyme. The reduction in 18:1 *n-9*/18:0 ratio did not reach statistical significance in

the palmitic acid-incubated cells (P = 0.091 and 0.123 for SCD siRNA1 and 2, respectively) (**Figure 6-10**).

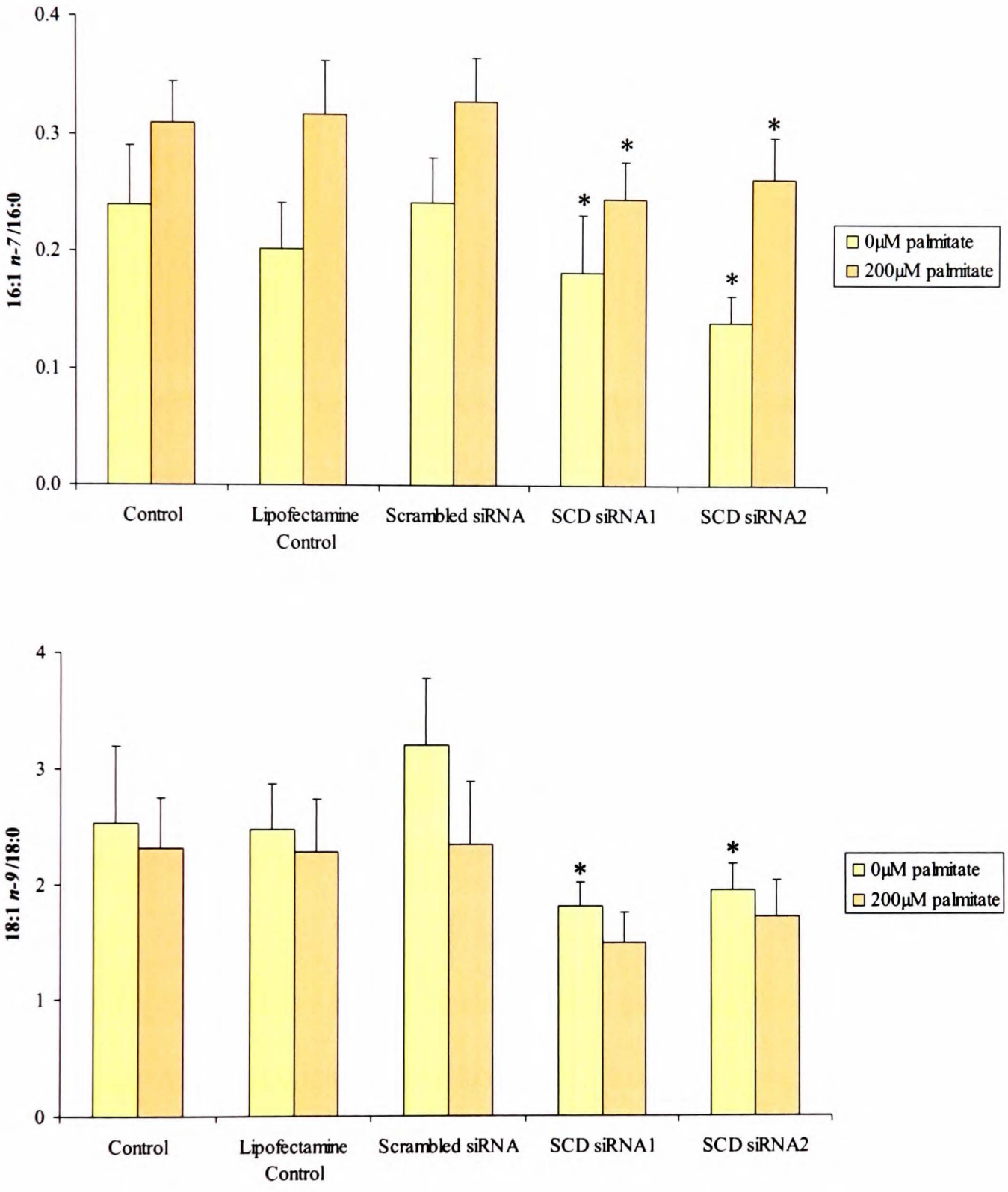


Figure 6-10 Phospholipid 16:1 *n-7*/16:0 and 18:1 *n-9*/18:0 ratios in 0 μM and 200 μM palmitate-treated cells. Data are represented as mean ± SEM (n = 8). *P ≤ 0.042 vs scrambled siRNA

The PL fatty acids showed an increase in palmitic acid elongation in response to SCD knockdown (**Figure 6-11**) although this only reached statistical significance for SCD siRNA2 in the palmitate-free (0 μM) cells (P = 0.009).

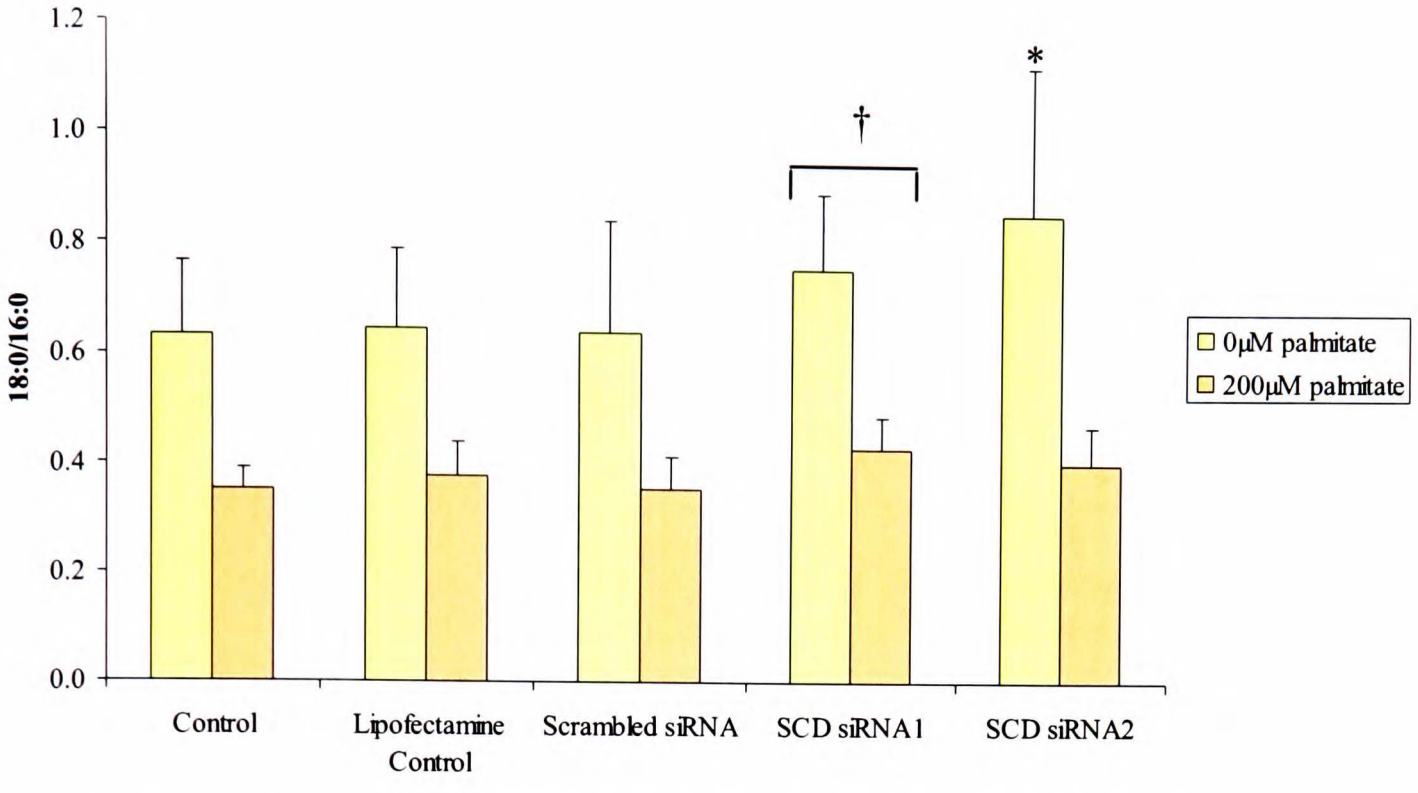
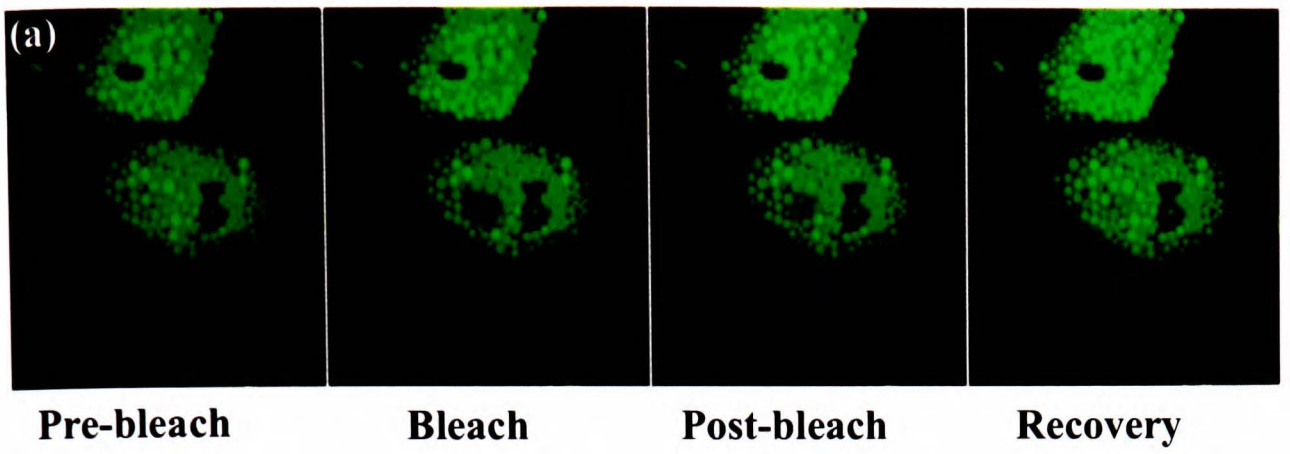


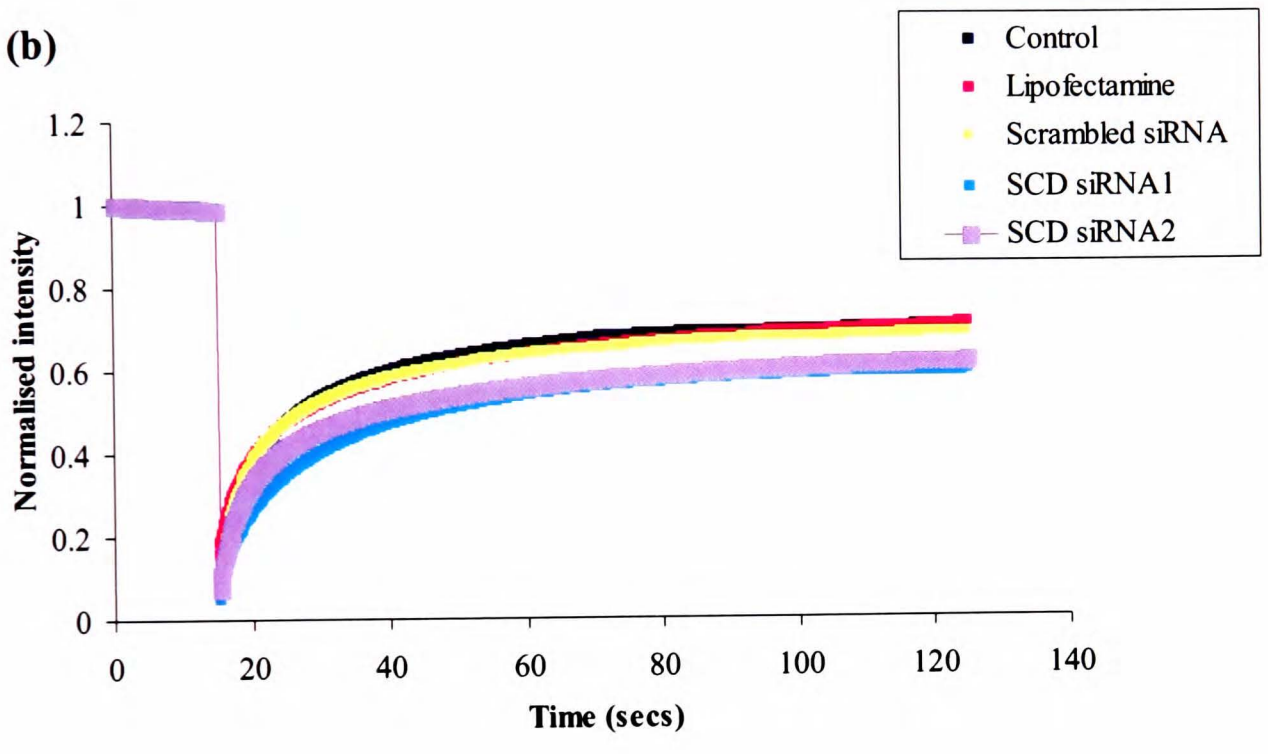
Figure 6-11 Phospholipid 18:0/16:0 ratios in control and palmitate-treated cells.

Data are represented as mean ± SEM (n = 8). * P = 0.009 vs scrambled siRNA, † P = 0.026

6.4.8.2. Fluorescence recovery after photobleaching (FRAP)

Changes in cell membrane fluidity in response to SCD knockdown were also determined using FRAP techniques. Both SCD siRNA1 and 2 reduced cell membrane fluidity, that is, recovery time following photobleaching increased significantly (**Figure 6-12(c)**). SCD siRNA1 reduced cell membrane fluidity, as assessed by FRAP, to a greater extent than SCD siRNA2 (P = 0.004).





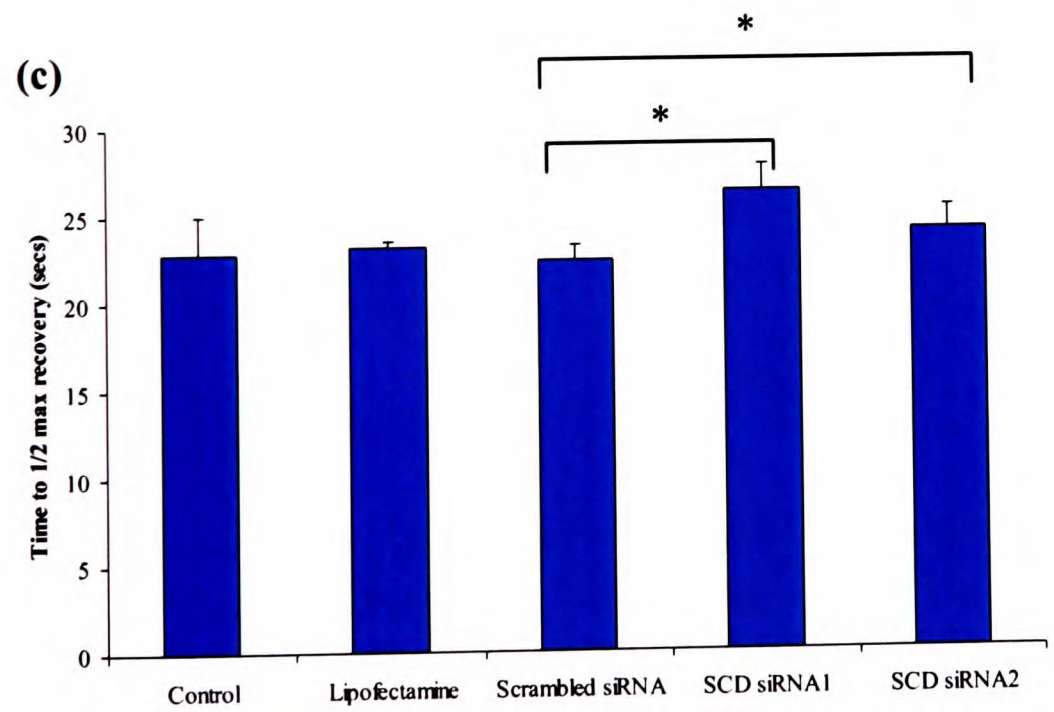


Figure 6-12 Changes in cell membrane fluidity as determined by fluorescence recovery after photobleaching (FRAP) analysis. (a) Fluorescent micrograph images of the main stages of FRAP in the adipocyte (x63 objective), (b) raw data curves of fluorescence intensity (normalised to first frame) and (c) calculated recovery times of adipocytes with SCD silencing. Data are represented as mean ± SEM (n = 4 subjects). *P ≤ 0.052, Student's *t* test

6.4.9. Insulin sensitivity

The effect of SCD knockdown on insulin sensitivity of the adipocyte was determined by radiolabelled 2-deoxyglucose uptake in response to insulin (**Figure 6-13**). A repeated measures ANOVA was used to analyse the effects of SCD knockdown and dose-response to insulin. There were significant main effects for SCD knockdown and insulin concentration (P = 0.009 for both). SCD siRNA-treated cells showed lower uptake of 2-DOG. A Tukey's least significant difference *post hoc* test was used for pairwise comparisons and showed significant differences between scrambled siRNA and SCD siRNA1 and 2 (P = 0.005 and 0.009, respectively) and a significant difference between 0 and 100 nM insulin (P = 0.003).

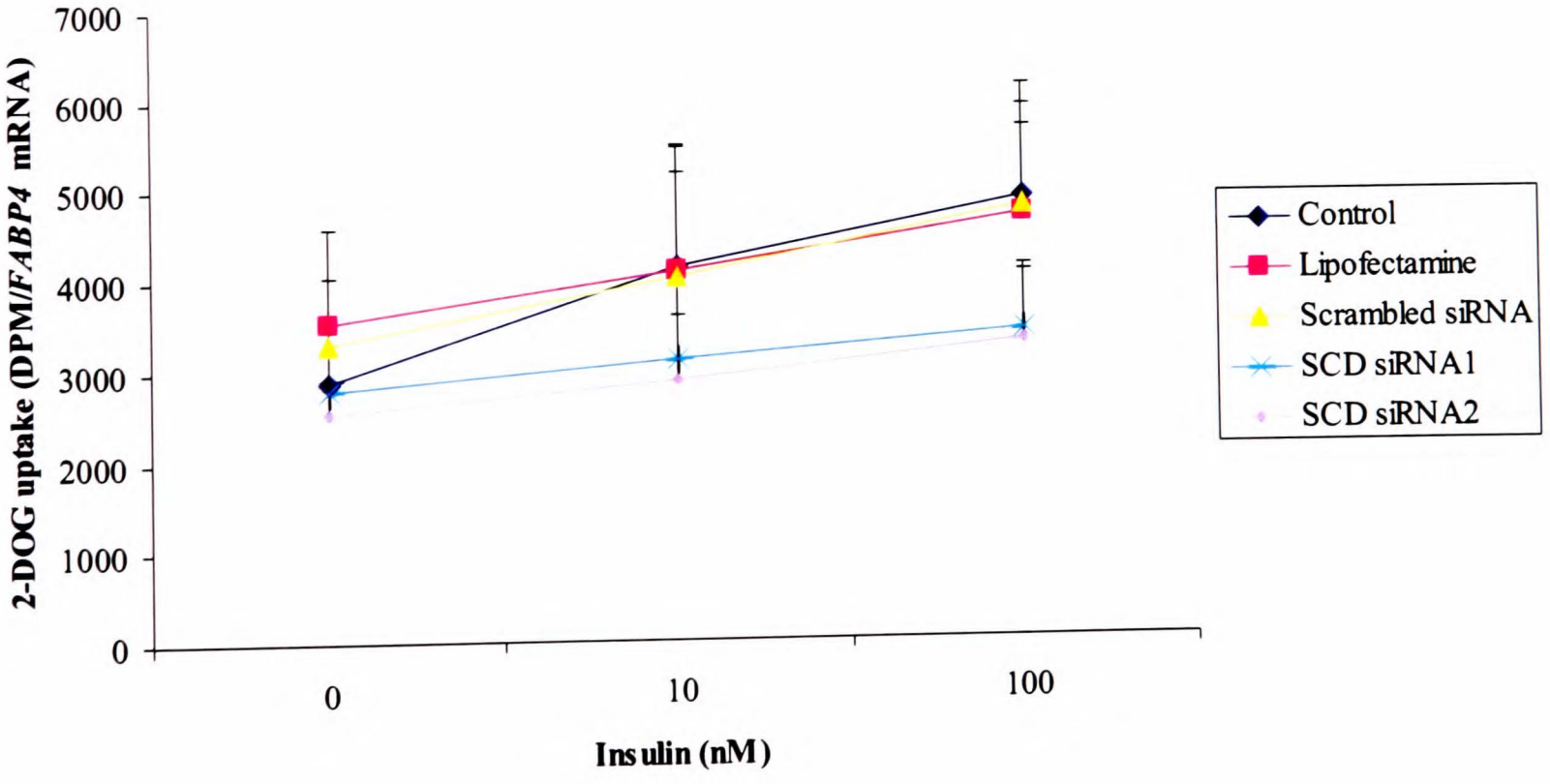


Figure 6-13 Changes in insulin sensitivity of adipocytes in response to SCD knockdown.

Data are represented as mean ± SEM (n = 5).

6.4.10. Effects of SCD knockdown on DNL

SCD and DNL may be tightly and coordinately regulated (Chong *et al.*, 2008); therefore, the effects of SCD on DNL in the human adipocyte were investigated.

6.4.10.1. Changes in DNL gene expression

There was a down-regulation of mRNA expression of the DNL-associated genes *FASN* and *ACACA*, as well as *SREBF*, concomitantly with *SCD* mRNA, in response to SCD knockdown (**Figure 6-14**). The extent of DNL gene down-regulation was not as great as *SCD*, but was, nonetheless, significant ($P \leq 0.028$). SCD siRNA2 had a greater effect on down-regulation of both *SCD* mRNA and DNL gene mRNA (**Table 6-2**).

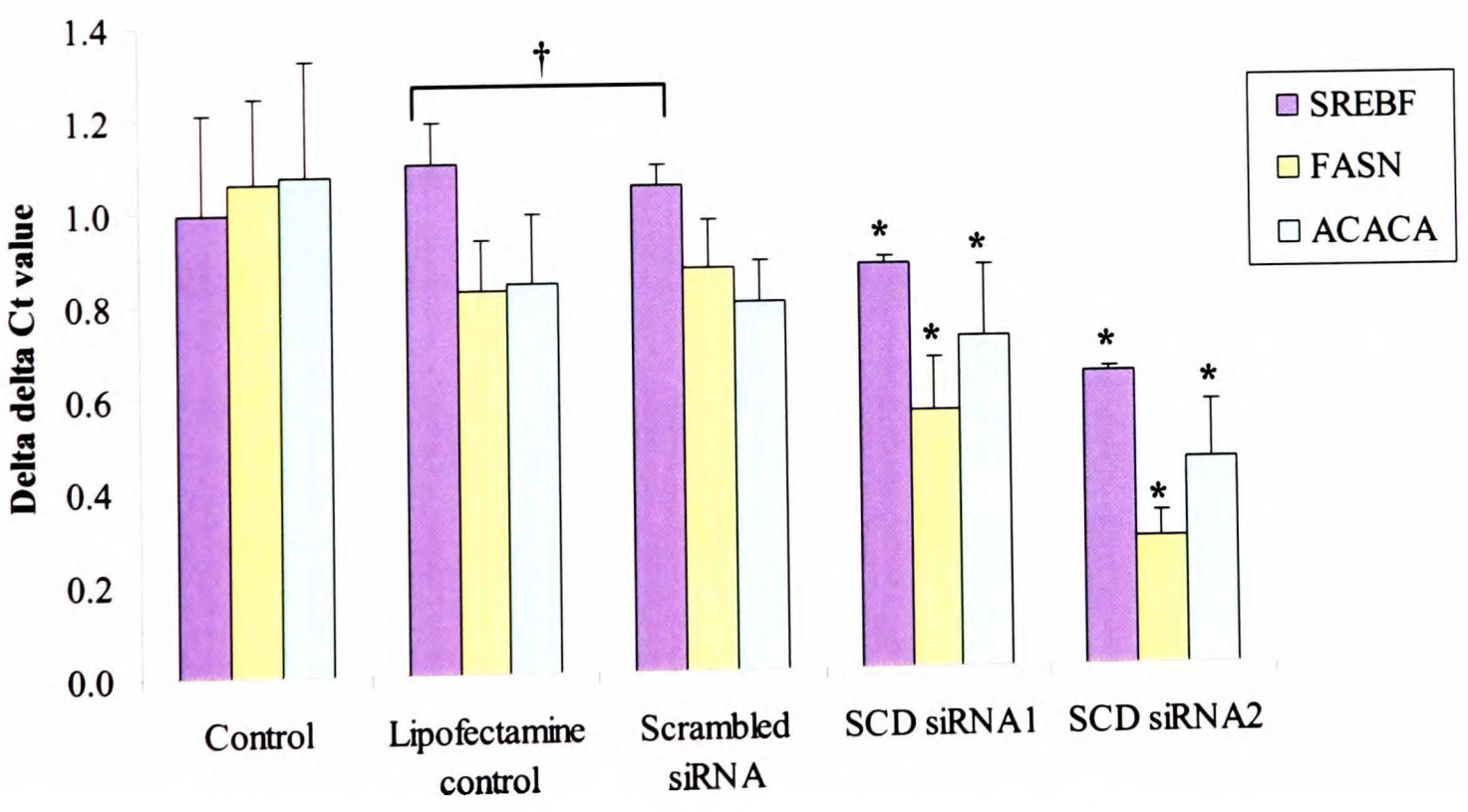


Figure 6-14 Changes in the DNL-associated genes *FASN* and *ACACA* with SCD silencing. Data are represented as mean ± SEM (n = 4).

†P = 0.024 *P ≤ 0.049 vs scrambled siRNA

Gene	SCD siRNA1	SCD siRNA2
SCD	68.3 ± 3.3	87.2 ± 2.7*
FASN	37.9 ± 7.0	69.0 ± 3.1*
ACACA	24.5 ± 6.5	46.3 ± 11.0*

Table 6-2 Knockdown of *SCD*, *FASN* and *ACACA* mRNA with SCD silencing expressed as percent knockdown compared to scrambled siRNA. Values are mean±SEM (n = 4)

***P < 0.02 (difference between siRNA 1 and 2)**

6.4.10.2. Effects on fatty acid synthesis

Despite an apparent coordination of SCD and DNL-associated gene mRNA expression, there was no clear functional effect of *SCD* knockdown on *de novo* fatty acid synthesis either in 0 μM or 200 μM palmitate-treated cells (**Figure 6-15**). However, DNL-derived myristate was slightly reduced in palmitate-free (0 μM) cells with *SCD* knockdown, and DNL-derived palmitate was reduced slightly in both groups. In the palmitate-free (0 μM) cells, this reached borderline significance with SCD siRNA2 (P = 0.055).

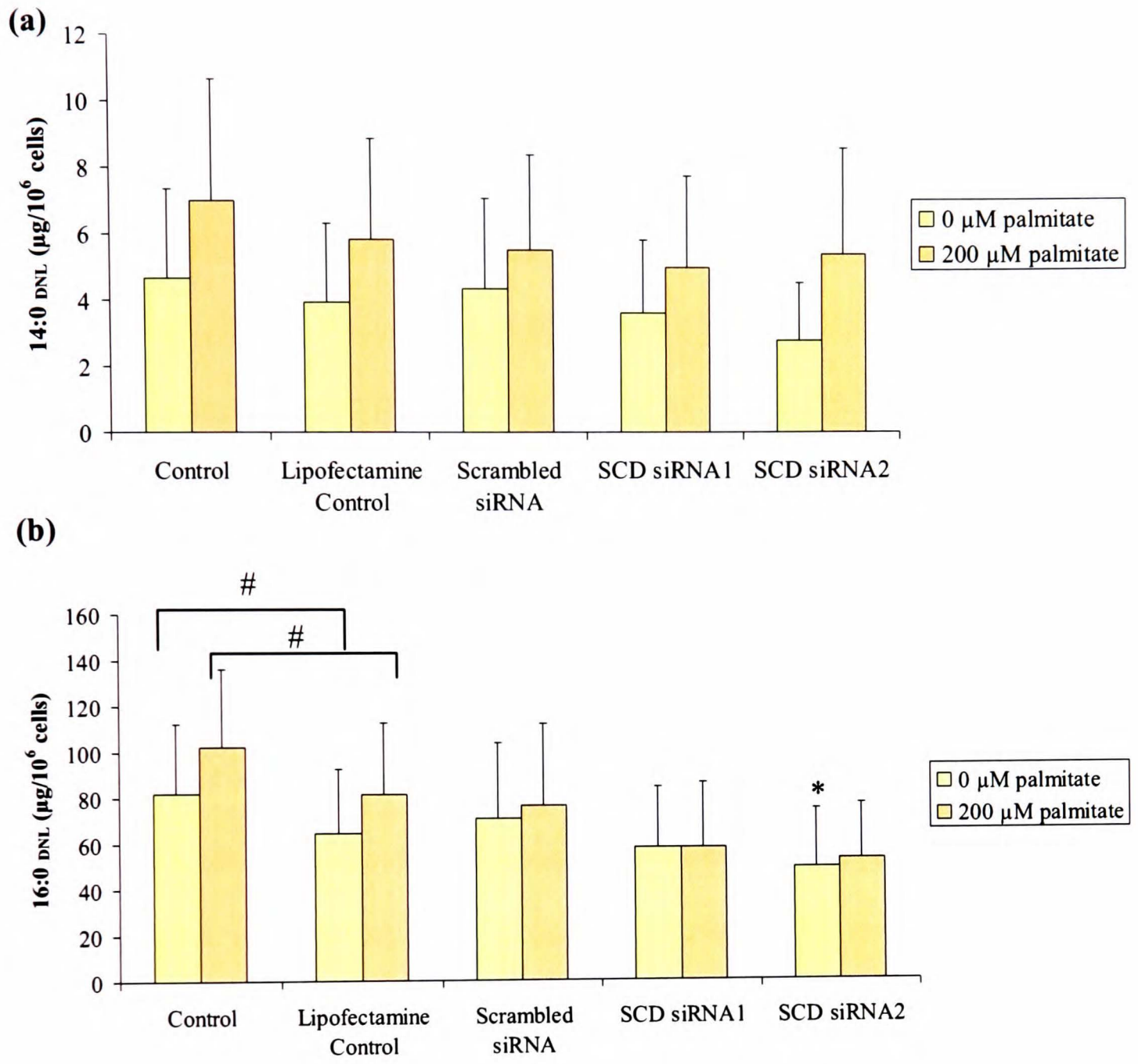


Figure 6-15 Changes in DNL with SCD knockdown as measured by (a) DNL-derived myristate (14:0 $_{DNL}$) and (b) DNL-derived palmitate (16:0 $_{DNL}$).

Data are represented as mean ± SEM (n = 8)

*** P = 0.055 compared with scrambled siRNA, # P ≤ 0.035**

6.5. DISCUSSION

A large proportion of reports on the effects of SCD1 inhibition have focussed on the liver as the major organ of fatty acid metabolism. While a few studies have looked into SCD1 inhibition in adipocytes, this is, to my knowledge, the first to describe the

effects of *SCD1* knockdown in the human adipocyte. The results shown here give an insight into the role of SCD in the differentiated human adipocyte.

There was a subtle decrease in TG accumulation with SCD knockdown in both 0 μM and 200 μM palmitate-treated cells, with statistical significance only with one SCD siRNA in 200 μM pamitate-treated cells. The slight reduction in TG accumulation may have been a consequence of fewer MUFAs within the cell. Endogenously synthesised MUFAs, especially oleate, may be required for TG synthesis (Miyazaki *et al.*, 2001). Acyl-coenzyme A:diacylglycerol acyltransferase 2 (DGAT2) catalyses the addition of the third fatty acyl chain to diacylglycerol, the final step in TG synthesis. SCD and DGAT2 have been shown, in HeLa cells, to be co-localised in a subcellular compartment of the ER known as the mitochondrial-associated membrane, a region of the ER that is close to the outer mitochondrial membrane. The juxtaposition of these enzymes could suggest that SCD, acting upon either DNL-derived or exogenous palmitate or stearate, generates MUFAs in close proximity to the enzyme required for TG synthesis (Man *et al.*, 2006). Interestingly, hepatic *Dgat2* mRNA levels are similar in the *Scd1* knockout and wildtype mice, although the knockout mouse cannot readily make TG, suggesting a role for SCD in the supply of MUFAs for TG synthesis (Ntambi *et al.*, 2002; Dobrzyn *et al.*, 2005b).

An inability to store fatty acids as TG in the adipocyte could have catastrophic knock-on effects. As with lipid storage disorders such as lipodystrophy, an inability to store circulating fatty acids safely in adipose tissue could result in ectopic fat deposition in non-adipose tissues (Garg, 2006), a situation shown to have "lipotoxic" effects on tissues, and linked with metabolic disturbances (Rader, 2007; Rasouli *et al.*, 2007).

Loss of SCD function in differentiated human preadipocytes led to the intracellular accumulation of SAFAs in both TG and PL fractions. SCD knockdown caused an increase in palmitate elongation, increasing stearate levels within the cell. Although the adipocyte is well equipped to store fatty acids as TG, fatty acid composition may be important to the cell. The importance of SCD1 in maintaining lipid homeostasis and cell viability in the liver has recently been reported (Li *et al.*, 2009). Loss of SCD action in hepatocytes increased fatty acid overloading and palmitate-induced apoptosis. In the same study, mice fed a high-fat diet designed to induce hepatic steatosis and features of the metabolic syndrome, had elevated SCD levels, whereas, mice fed a diet designed to induce steatohepatitis showed a decrease in SCD. It was suggested that up-regulation of SCD converts lipotoxic SAFAs to MUFAs that can be more readily stored as TG, whereas the down-regulation of SCD has a more damaging effect as the SAFA overload in the liver causes injury and hepatocyte apoptosis. The saturation state of the intracellular fatty acids had profound effects on the state of the liver. Applying this theory to the adipocyte, the increased SAFAs within the cell may contribute to impairment of normal cellular function.

SCD knockdown also affected cell membrane fluidity. The PL SAFA:MUFA ratio was increased in 0 μM and 200 μM palmitate-treated cells and measurements of cell membrane fluidity showed a reduced fluidity with SCD knockdown. Scaglia *et al.* (2005) showed that up-regulation of SCD activity increased cell membrane fluidity in human neoplastic cells, helping the cells to avoid apoptosis and survive. In addition to the increase in intracellular SAFA accumulation and reduced cell membrane

fluidity, insulin sensitivity of the adipocytes, as measured by insulin-stimulated 2-DOG uptake, was reduced with loss of SCD.

Previously, SAFAs were shown to influence insulin action in differentiated 3T3-L1 preadipocytes (Grunfeld *et al.*, 1981). Differentiation of adipocytes for 10 days with 330 μM palmitate reduced insulin binding by 65 % and showed a 75 % decrease in insulin-stimulated 2-DOG uptake, whereas the same concentration of palmitoleate had little or no effect on insulin binding or action. The same effects were seen with SAFAs and MUFAs of different chain lengths, although there was no correlation between chain length and insulin binding or insulin action. Changes in the plasma membrane fatty acid composition may have downstream effects on insulin binding and insulin action.

In the same cell line, however, inhibition of SCD using sterculic acid, a C18 plant cyclopropenoic fatty acid, had no effect on 2-DOG uptake (Gomez *et al.*, 2003). Differentiation of 3T3-L1 preadipocytes for 10 days with 100 μM sterculic acid directly inhibited SCD activity by 90 %, though *Scd1* mRNA and protein remained unchanged. The 16:1 *n-7*/16:0 and 18:1 *n-9*/18:0 ratios were heavily reduced, but total TG accumulation remained unaltered and cells were larger and had smaller lipid droplets compared to untreated cells.

The first of those two studies supports the results seen here with reduced insulin-stimulated 2-DOG uptake with increased intracellular SAFAs. However, the loss of SCD activity, as achieved with sterculic acid, also caused an increase in intracellular SAFAs. As sterculic acid only accounted for 6.8 % of the total fatty acids in treated

cells, it is unlikely that incorporation of this fatty acid could account for the differences.

These disparities highlight the lack of understanding of the effects of SCD knockdown on insulin action in the adipocyte and the results shown in this chapter contribute towards an insight into this.

DNL was significantly down-regulated at the mRNA level but the TG-fatty acid data were not conclusive enough to state a definite down-regulation of this process. Sampath *et al.* (2007) reported that mice fed a high stearate diet showed up-regulation of *Scd1* prior to other DNL genes such as *Acc*, *Fas* and *Gpat*. If SCD is required for up-regulation of the DNL pathway, then its suppression may result in DNL down-regulation. As discussed in **Chapter 4**, saturated fat may induce *de novo* lipogenesis which may be coordinately regulated with SCD desaturation (Chong *et al.*, 2008). The mechanism of down-regulation of the DNL genes *ACACA* and *FASN* is not known but may have occurred via down-regulation of SREBP1c, as shown in **Figure 6-14**.

The first observation of SCD substrate specificity was that in palmitate-free (0 μM) cells the 18:1 *n-9*/18:0 ratio was around 20 times greater than the 16:1 *n-7*/16:0 ratio and the reduction in 18:1 *n-9*/18:0 was almost 2-fold greater than 16:1 *n-7*/16:0, suggesting stearoyl-CoA is the preferred substrate. SCD showed no substrate-origin preference for palmitate but did preferentially target DNL-derived stearate over exogenous stearate. Substrate specificity was not influenced by SCD knockdown.

Palmitate-free cells had slightly higher elongation ratios than those treated with 200 μM palmitate. SCD knockdown increased the 18:0/16:0 ratio in both control and palmitate-treated cells but not the 18:1 *n-7*/16:1 *n-7* ratio and there was preferential elongation of DNL-derived palmitate. This study has many parallels with a study by Yee *et al.* (2008) who used stable isotopes to study substrate specificity and compartmentalisation of SCD in HepG2 cells. SCD inhibition was achieved using two different chemical SCD inhibitors and *trans*-10,*cis*-12 CLA. Cells incubated with either [U-^{13}C]palmitate or [U-^{13}C]stearate in the presence of an SCD inhibitor had reduced SCD indices. CLA reduced the 18:1 *n-9*/18:0 ratio but failed to reduce the 16:1 *n-7*/16:0 ratio in palmitate-treated cells, which the author suggests may represent compartmentalisation of SCD, making it inaccessible to CLA for inhibition. The study also reported that SCD showed substrate specificity; exogenous palmitate was favoured over palmitate created by chain shortening of stearate, and stearate created by palmitate elongation was favoured over exogenous stearate. Also, the substrate specificity of SCD was not altered by enzyme inhibition. Furthermore, SCD inhibition was associated with chain shortening of stearate and chain elongation of palmitate. The author proposed that there may be different compartments in which saturation, chain shortening and elongation occur within the cell. The substrate specificity for DNL-derived stearate seen in the adipocyte may also support the theory of SCD compartmentalisation as proposed in HepG2 cells. This may, however, be a cell-specific phenomenon as no substrate specificity was noted in a study using SV40-transformed human lung fibroblasts, where there was no preferential desaturation of either DNL-derived or exogenous stearate (Scaglia *et al.*, 2005).

The interest in the development of SCD inhibitors was triggered by reports of the *Scd1* knockout mouse and its resistance to diet-induced obesity, insulin sensitivity and favourable metabolic profile. However, despite initial appearances of SCD being the perfect target for obesity treatment, more recent research concluded that *Scd1* inhibition in a mouse model for hyperlipidaemia and atherosclerosis leads to the development of atherosclerosis, despite the mice showing improved insulin sensitivity, reduced hepatic TGs and resistance to high-fat diet-induced obesity, that is, an apparently anti-atherogenic profile (Brown *et al.* 2008). These findings were later confirmed in another study using LDL receptor null mice (Macdonald *et al.*, 2008). In both cases, an increased inflammatory state within *Scd1*-inhibited models was reported. SCD knockdown using sterculic oil in cholesterol-fed mice resulted in a reduction in overall body weight but did not protect against hypercholesterolaemia (Major *et al.*, 2008). Furthermore, loss of SCD may have other unwanted side-effects; the asebia mouse suffers from alopecia, dry skin and ocular abnormalities (Gates & Karasek, 1965). These findings alert us to the possibility of undesirable side-effects of SCD inhibition.

It is always important to remember that a situation in mice may not translate directly to man (Arner, 2005). Mouse adipose tissue composition and deposition do not directly mirror that in man, the biggest difference being that mice possess brown fat, capable of fatty acid oxidation. Also, whereas mice express four known Scd isoforms, which may have compensatory actions in some tissues with loss of *Scd1*, human *SCD1* is the predominant isoform with one other (*SCD5*) being expressed, primarily in the brain and pancreas.

In conclusion, many studies have investigated SCD knockdown in hepatocytes, cells with a great capacity for fatty acid oxidation, providing a route by which fatty acids may be cleared. The human adipocyte, acting as a fat storage cell, has low numbers of mitochondria and low activity of carnitine palmitoyltransferase 1, thus limiting its ability to oxidise fatty acids (Harper & Saggerson, 1975). The adipocyte stores fatty acids as TG which may later be released into the circulation via lipolysis. From the findings in this chapter, it would appear that lack of SCD, leading to an increase in intracellular SAFAs, impairs adipocyte membrane fluidity and insulin sensitivity. One could speculate this could have adverse knock-on effects to other tissues in the body from the release of stored intracellular SAFAs into the circulation (Wang *et al.*, 2003).

Chapter 7

Final Discussion

The capacity, and requirement, for DNL within the human adipocyte remains a grey area. Compared with rodent adipocytes, DNL in the human adipocyte is low and the enzymes required for this process are not as active. Using small amounts of adipose tissue acquired from adults by needle aspiration, an *in vitro* method was established to study the pathway of DNL within the differentiating human preadipocyte, and its regulation by an exogenous source of its end product, palmitate. In **Chapter 3**, evidence was provided for DNL within the human adipocyte, which was coupled with post-DNL modifications of palmitate, such as desaturation and elongation. This resulted in the production of a variety of SAFAs and MUFAs within the TG fatty acids. Interestingly, as these cells had made all of their fat via DNL, they lacked detectable amounts of essential fatty acids, such as linoleic acid, in their TG stores. These adipocytes expressed the mRNA for the enzymes involved in the DNL pathway, such as *ACACA*, *FASN* and *ACLY*, showing that this process operates within the human adipocyte in an *in vitro* situation.

It would appear that in the glucose- and insulin-rich environment of the cultured adipocytes, glucose acted as the main substrate for fatty acid synthesis, although there was also some contribution from glutamine. As the culture media were also rich in pyruvate, this could also have contributed significantly to fatty acid synthesis, and experiments using differentiation medium containing labelled pyruvate would give an insight into its contribution to DNL. Consistent with previous reports, around 70 % of the glycerol 3-phosphate made for TG synthesis was derived from glucose. Glutamine also contributed to glycerol 3-phosphate production and one could further speculate that pyruvate may also have been involved in this pathway. Under high-

insulin conditions, it is likely that glyceroneogenesis was inhibited, allowing glucose-mediated production of glycerol to prevail.

It would be intuitive to assume that addition of exogenous palmitate to adipocytes would down-regulate DNL. However, 50 to 200 μM [U-^{13}C]palmitate up-regulated DNL, concomitant with an up-regulation of SCD. Many genes involved in fatty acid metabolism and other pathways, such as the insulin signalling pathway, were shown also to be up-regulated with palmitate (maximally by 50 μM). However, the addition of exogenous palmitate increased the ratio of SAFA:MUFA within the PL fatty acids. Although this had no adverse effect on cell membrane fluidity, it did reduce the insulin sensitivity of the adipocytes. These findings were in agreement with other reports of a SAFA-induced reduction in insulin sensitivity in the adipocyte (Grunfeld *et al.*, 1981).

An interesting, and perhaps surprising finding was that differentiation of preadipocytes with a higher palmitate concentration, 400 μM, showed a difference in fatty acid handling in adipocytes originating from different donors. Although adipocytes have been reported to be immune to the so-called lipotoxic effects of saturated fatty acids (Lundgren & Eriksson, 2004), the adipocytes from some donors could not withstand the high palmitate concentration. Storage of fatty acids has been shown to protect against lipotoxicity, as the potentially hazardous fatty acids are packaged away into neutral lipid stores (Listenberger *et al.*, 2003). Listenberger *et al.* (2003) showed that palmitate is poorly incorporated into TG and that co-incubation with a MUFA such as oleate, promoted TG accumulation and protected the cell against palmitate-induced apoptosis. Furthermore, they also showed that TG

accumulation is associated with an increased SCD activity. Features of the palmitate-intolerant adipocytes included a reduced ability to store fatty acids as TG, as well as reduced SCD action. SCD may act to provide the necessary unsaturated fatty acids required for efficient TG storage. This may have been due either directly to reduced SCD activity, or to an indirect effect of a reduced up-regulation of DNL, which may have suppressed SCD activation.

The concept that DNL-derived fatty acids may serve as intracellular regulators is not new and has previously been described in hepatocytes, where PPARα, a key regulator in hepatic fatty acid oxidation, is up-regulated only by "new" fat (Chakravarthy *et al.*, 2005; Gibbons, 2005). Liver-specific fatty acid synthase knockout mice fed a fat-free diet suffered from fatty liver, caused by an inability to activate PPARα-mediated fatty acid oxidation. Chakravarthy *et al.* concluded that only DNL-derived or dietary fat could activate PPARα, whereas fatty acids mobilised from existing stores ("old" fat) could not. Therefore, in the adipocyte, DNL up-regulation, in tandem with an up-regulation of SCD activity may be paramount to cell function and survival: SAFAs are converted into MUFAs, and TG synthesis is promoted. *SCD* silencing in adipocytes down-regulated mRNA expression of DNL-associated genes, but failed to show down-regulation of DNL-derived fatty acids. Therefore, it is unclear whether regulation of fatty acid synthesis and desaturation is mutual, or if DNL acts specifically to up-regulate SCD.

SCD is important to cell function, as an inability to convert SAFAs to MUFAs had adverse effects on the adipocyte. Loss of *SCD* within the adipocyte caused an increase in SAFA:MUFA within the PLs, reduced the cell membrane fluidity and also

led to reduced insulin sensitivity. These findings highlight the fundamental role played by SCD in the maintenance of cell membrane and cell function.

Palmitate-intolerance was also associated with reduced expression of *SFRP1*, an inhibitor of the Wnt signalling pathway, and of *PCK1*, the gene encoding cytosolic PEPCK (PEPCK-c). Whether or not these differences in gene expression contributed significantly to the physiological differences between the cells is unclear, but it could be hypothesised that diminished inhibition of Wnt signalling may result in a reduced availability of adipocytes for fatty acid storage, and that there was a reduction in PEPCK-c that may be required to assist in the esterification of fatty acids. Although microarray analysis provides a useful tool for pathway analysis at the mRNA level, it cannot provide concrete evidence for regulation, and further investigation is required to verify that changes seen at the mRNA level also occur at the protein level.

Another major difference in the handling of exogenous palmitate between palmitate-tolerant and intolerant adipocytes, was the channelling of exogenous palmitate towards PLs. There may be a mechanism by which, when the adipocyte is unable to store a sudden influx of palmitate as TG, the fatty acid is shunted into the membrane PLs. This would act to increase the SAFA:MUFA ratio, making the cells more rigid in structure, and may explain why the adipocytes ruptured.

In the western world, where the typical diet is abundant in fats, dietary fat makes up the majority of adipocyte lipids, and the contribution of DNL to stored fatty acids in the mature adipocyte is low (Hirsch *et al.*, 1960; Diraison *et al.*, 2003). It is unlikely,

therefore, that DNL acts to increase the amount of stored fat within the adipocyte, but it may serve a regulatory function.

Enlarged adipocytes are a feature of obesity and have been linked with a down-regulation of adipose tissue DNL (Kolehmainen *et al.*, 2001; Diraison *et al.*, 2002; Roberts *et al.*, 2009) and with insulin resistance (Smith, 1970; Lundgren *et al.*, 2007; Goossens, 2008). Furthermore, it has even been proposed that there may be a link between adipocyte DNL and whole-body insulin sensitivity (Hoffstedt *et al.*, 2007). In the cultured human adipocytes, uptake of exogenous palmitate led to an increase in TG accumulation, storing TGs rich in SAFAs. Furthermore, *SCD* knockdown also led to an increase in intracellular SAFAs. Therefore, diets high in SAFAs may lead to adipocyte enlargement and SAFA-rich TG stores, and SCD inhibition may also lead to a similar end result. Although exogenous palmitate acted to up-regulate DNL, it is possible that the increase in intracellular SAFA content may contribute to the loss of insulin sensitivity seen in these cells by altering the phospholipid fatty acid composition.

In conclusion, the importance of DNL in the human adipocyte may be as a key regulator of SCD which, in turn, may assist in the maintenance of cell function. A decrease in DNL, as reported in the adipocytes of obese subjects, may act to down-regulate SCD activity. Reduced SCD action may then alter channelling of fatty acids, diverting them away from storage as TGs and shunting them towards incorporation into the plasma membrane phospholipids which may contribute to loss of insulin sensitivity. In extreme cases, this may lead to rupturing of the cell membrane that could, in turn, result in systemic release of fatty acids and ectopic fat deposition.

References

Aarsland A, Chinkes D, Wolfe RR. Hepatic and whole-body fat synthesis in humans during carbohydrate overfeeding. *Am J Clin Nutr* 1997;65:1774-82

Aarsland A, Lundquist M, Borretsen B, Berge RK. On the effect of peroxisomal beta-oxidation and carnitine palmitoyltransferase activity by eicosapentaenoic acid in liver and heart from rats. *Lipids* 1990;25:546-8

Aas V, Kase ET, Solberg R, Jensen J, Rustan AC. Chronic hyperglycaemia promotes lipogenesis and triacylglycerol accumulation in human skeletal muscle cells. *Diabetologia* 2004;47:1452-61

Abumrad N, Coburn C, Ibrahimi A. Membrane proteins implicated in long-chain fatty acid uptake by mammalian cells: CD36, FATP and FABPm. *Biochim Biophys Acta* 1999;1441:4-13

Abumrad N, Harmon C, Ibrahimi A. Membrane transport of long-chain fatty acids: evidence for a facilitated process. *J Lipid Res* 1998;39:2309-18

Abumrad NA, Perkins RC, Park JH, Park CR. Mechanism of long chain fatty acid permeation in the isolated adipocyte. *J Biol Chem* 1981;256:9183-91

Acheson KJ, Flatt JP. Minor importance of de novo lipogenesis on energy expenditure in human. *Br J Nutr* 2002;87:189

Acheson KJ, Schutz Y, Bessard T, Anantharaman K, Flatt JP, Jequier E. Glycogen storage capacity and de novo lipogenesis during massive carbohydrate overfeeding in man. *Am J Clin Nutr* 1988;48:240-7

Allmann DW, Gibson DM. Fatty acid synthesis during early linoleic acid deficiency in the mouse. *J Lipid Res* 1965;6:51-62

Amri EZ, Ailhaud G, Grimaldi PA. Fatty acids as signal transducing molecules: involvement in the differentiation of preadipose to adipose cells. *J Lipid Res* 1994;35:930-7

Amri EZ, Bertrand B, Ailhaud G, Grimaldi P. Regulation of adipose cell differentiation. I. Fatty acids are inducers of the aP2 gene expression. *J Lipid Res* 1991;32:1449-56

Angel A, Bray GA. Synthesis of fatty acids and cholesterol by liver, adipose tissue and intestinal mucosa from obese and control patients. *Eur J Clin Invest* 1979;9:355-62

Arner P. Resistin: yet another adipokine tells us that men are not mice. *Diabetologia* 2005;48:2203-5

Artwohl M, Roden M, Waldhausl W, Freudenthaler A, Baumgartner-Parzer SM. Free fatty acids trigger apoptosis and inhibit cell cycle progression in human vascular endothelial cells. *Faseb J* 2004;18:146-8

Attie AD, Krauss RM, Gray-Keller MP, Brownlie A, Miyazaki M, Kastelein JJ, Lusis AJ, Stalenhoef AF, Stoehr JP, Hayden MR, Ntambi JM. Relationship between

stearoyl-CoA desaturase activity and plasma triglycerides in human and mouse hypertriglyceridemia. *J Lipid Res* 2002;43:1899-907

Avram AS, Avram MM, James WD. Subcutaneous fat in normal and diseased states: 2. Anatomy and physiology of white and brown adipose tissue. *J Am Acad Dermatol* 2005;53:671-83

Azzout-Marniche D, Becard D, Guichard C, Foretz M, Ferré P, Foufelle F. Insulin effects on sterol regulatory-element-binding protein-1c (SREBP-1c) transcriptional activity in rat hepatocytes. *Biochem J* 2000;350 Pt 2:389-93

Bagasra O, Prilliman KR. RNA interference: the molecular immune system. *J Mol Histol* 2004;35:545-53

Ballard FJ, Hanson RW, Leveille GA. Phosphoenolpyruvate carboxykinase and the synthesis of glyceride-glycerol from pyruvate in adipose tissue. *J Biol Chem* 1967;242:2746-50

Banerjee SS, Feinberg MW, Watanabe M, Gray S, Haspel RL, Denkinger DJ, Kawahara R, Hauner H, Jain MK. The Kruppel-like factor KLF2 inhibits peroxisome proliferator-activated receptor-gamma expression and adipogenesis. *J Biol Chem* 2003;278:2581-4

Barak Y, Nelson MC, Ong ES, Jones YZ, Ruiz-Lozano P, Chien KR, Koder A, Evans RM. PPAR gamma is required for placental, cardiac, and adipose tissue development. *Mol Cell* 1999;4:585-95

Barness LA, Opitz JM, Gilbert-Barness E. Obesity: genetic, molecular, and environmental aspects. *Am J Med Genet A* 2007;143:3016-34

Bederman IR, Foy S, Chandramouli V, Alexander JC, Previs SF. Triglyceride synthesis in epididymal adipose tissue: Contribution of glucose and non-glucose carbon sources. *J Biol Chem* 2008;

Bene H, Lasky D, Ntambi JM. Cloning and characterization of the human stearoyl-CoA desaturase gene promoter: transcriptional activation by sterol regulatory element binding protein and repression by polyunsaturated fatty acids and cholesterol. *Biochem Biophys Res Commun* 2001;284:1194-8

Bennett CN, Ross SE, Longo KA, Bajnok L, Hemati N, Johnson KW, Harrison SD, MacDougald OA. Regulation of Wnt signaling during adipogenesis. *J Biol Chem* 2002;277:30998-1004

Beynen AC, Hermus RJ, Hautvast JG. A mathematical relationship between the fatty acid composition of the diet and that of the adipose tissue in man. *Am J Clin Nutr* 1980;33:81-5

Bickerton AS, Roberts R, Fielding BA, Hodson L, Blaak EE, Wagenmakers AJ, Gilbert M, Karpe F, Frayn KN. Preferential uptake of dietary fatty acids in adipose tissue and muscle in the postprandial period. *Diabetes* 2007;56:168-76

Biddinger SB, Miyazaki M, Boucher J, Ntambi JM, Kahn CR. Leptin suppresses stearoyl-CoA desaturase 1 by mechanisms independent of insulin and sterol regulatory element-binding protein-1c. *Diabetes* 2006;55:2032-41

Boden G, Chen X, Ruiz J, White JV, Rossetti L. Mechanisms of fatty acid-induced inhibition of glucose uptake. *J Clin Invest* 1994;93:2438-46

Bolstad BM, Irizarry RA, Astrand M, Speed TP. A comparison of normalization methods for high density oligonucleotide array data based on variance and bias. *Bioinformatics* 2003;19:185-93

Borkman M, Storlien LH, Pan DA, Jenkins AB, Chisholm DJ, Campbell LV. The relation between insulin sensitivity and the fatty-acid composition of skeletal-muscle phospholipids. *N Engl J Med* 1993;328:238-44

Botion LM, Brito MN, Brito NA, Brito SR, Kettelhut IC, Migliorini RH. Glucose contribution to in vivo synthesis of glyceride-glycerol and fatty acids in rats adapted to a high-protein, carbohydrate-free diet. *Metabolism* 1998;47:1217-21

Brasaemle DL, Barber T, Wolins NE, Serrero G, Blanchette-Mackie EJ, Londos C. Adipose differentiation-related protein is an ubiquitously expressed lipid storage droplet-associated protein. *J Lipid Res* 1997;38:2249-63

Brown DA. Lipid droplets: proteins floating on a pool of fat. *Curr Biol* 2001;11:R446-9

Brown JM, McIntosh MK. Conjugated linoleic acid in humans: regulation of adiposity and insulin sensitivity. *J Nutr* 2003;133:3041-6

Bryant NJ, Govers R, James DE. Regulated transport of the glucose transporter GLUT4. *Nat Rev Mol Cell Biol* 2002;3:267-77

Busch AK, Gurisik E, Cordery DV, Sudlow M, Denyer GS, Laybutt DR, Hughes WE, Biden TJ. Increased fatty acid desaturation and enhanced expression of stearoyl coenzyme A desaturase protects pancreatic beta-cells from lipoapoptosis. *Diabetes* 2005;54:2917-24

Caimi G, Lo Presti R, Montana M, Canino B, Ventimiglia G, Romano A, Catania A, Sarno A. Membrane fluidity, membrane lipid pattern, and cytosolic Ca2+ content in platelets from a group of type II diabetic patients with macrovascular complications. *Diabetes Care* 1995;18:60-3

Cao Z, Umek RM, McKnight SL. Regulated expression of three C/EBP isoforms during adipose conversion of 3T3-L1 cells. *Genes Dev* 1991;5:1538-52

Chakravarthy MV, Pan Z, Zhu Y, Tordjman K, Schneider JG, Coleman T, Turk J, Semenkovich CF. "New" hepatic fat activates PPARalpha to maintain glucose, lipid, and cholesterol homeostasis. *Cell Metab* 2005;1:309-22

Chascione C, Elwyn DH, Davila M, Gil KM, Askanazi J, Kinney JM. Effect of carbohydrate intake on de novo lipogenesis in human adipose tissue. *Am J Physiol* 1987;253:E664-9

Chen G, Liang G, Ou J, Goldstein JL, Brown MS. Central role for liver X receptor in insulin-mediated activation of Srebp-1c transcription and stimulation of fatty acid synthesis in liver. *Proc Natl Acad Sci U S A* 2004;101:11245-50

Chen Y, Lagerholm BC, Yang B, Jacobson K. Methods to measure the lateral diffusion of membrane lipids and proteins. *Methods* 2006;39:147-53

Choi CS, Savage DB, Kulkarni A, Yu XX, Liu ZX, Morino K, Kim S, Distefano A, Samuel VT, Neschen S, Zhang D, Wang A, Zhang XM, Kahn M, Cline GW, Pandey SK, Geisler JG, Bhanot S, Monia BP, Shulman GI. Suppression of diacylglycerol acyltransferase-2 (DGAT2), but not DGAT1, with antisense oligonucleotides reverses diet-induced hepatic steatosis and insulin resistance. *J Biol Chem* 2007;282:22678-88

Choi Y, Kim YC, Han YB, Park Y, Pariza MW, Ntambi JM. The trans-10,cis-12 isomer of conjugated linoleic acid downregulates stearoyl-CoA desaturase 1 gene expression in 3T3-L1 adipocytes. *J Nutr* 2000;130:1920-4

Choi Y, Park Y, Storkson JM, Pariza MW, Ntambi JM. Inhibition of stearoyl-CoA desaturase activity by the cis-9,trans-11 isomer and the trans-10,cis-12 isomer of conjugated linoleic acid in MDA-MB-231 and MCF-7 human breast cancer cells. *Biochem Biophys Res Commun* 2002;294:785-90

Chong MF, Fielding BA, Frayn KN. Mechanisms for the acute effect of fructose on postprandial lipemia. *Am J Clin Nutr* 2007;85:1511-20

Chong MF, Hodson L, Bickerton AS, Roberts R, Neville M, Karpe F, Frayn KN, Fielding BA. Parallel activation of de novo lipogenesis and stearoyl-CoA desaturase activity after 3 d of high-carbohydrate feeding. *Am J Clin Nutr* 2008;87:817-23

Chou FS, Wang PS, Kulp S, Pinzone JJ. Effects of thiazolidinediones on differentiation, proliferation, and apoptosis. *Mol Cancer Res* 2007;5:523-30

Chu K, Miyazaki M, Man WC, Ntambi JM. Stearoyl-coenzyme A desaturase 1 deficiency protects against hypertriglyceridemia and increases plasma high-density lipoprotein cholesterol induced by liver X receptor activation. *Mol Cell Biol* 2006;26:6786-98

Claycombe KJ, Jones BH, Standridge MK, Guo Y, Chun JT, Taylor JW, Moustaid-Moussa N. Insulin increases fatty acid synthase gene transcription in human adipocytes. *Am J Physiol* 1998;274:RI253-9

Clifford GM, Londos C, Kraemer FB, Vernon RG, Yeaman SJ. Translocation of hormone-sensitive lipase and perilipin upon lipolytic stimulation of rat adipocytes. *J Biol Chem* 2000;275:5011-5

Cohen P, Miyazaki M, Socci ND, Hagge-Greenberg A, Liedtke W, Soukas AA, Sharma R, Hudgins LC, Ntambi JM, Friedman JM. Role for stearoyl-CoA desaturase-1 in leptin-mediated weight loss. *Science* 2002;297:240-3

Coleman RA, Lee DP. Enzymes of triacylglycerol synthesis and their regulation. *Prog Lipid Res* 2004;43:134-76

Darimont C, Avanti O, Zbinden I, Leone-Vautravers P, Mansourian R, Giusti V, Mace K. Liver X receptor preferentially activates de novo lipogenesis in human preadipocytes. *Biochimie* 2006;88:309-18

Darlington GJ, Ross SE, MacDougald OA. The role of C/EBP genes in adipocyte differentiation. *J Biol Chem* 1998;273:30057-60

Dentin R, Benhamed F, Pegorier JP, Foufelle F, Viollet B, Vaulont S, Girard J, Postic C. Polyunsaturated fatty acids suppress glycolytic and lipogenic genes through the inhibition of ChREBP nuclear protein translocation. *J Clin Invest* 2005;115:2843-54

Dey D, Pal BC, Biswas T, Roy SS, Bandyopadhyay A, Mandal SK, Giri BB, Bhattacharya S. A Lupinoside prevented fatty acid induced inhibition of insulin sensitivity in 3T3 L1 adipocytes. *Mol Cell Biochem* 2007;300:149-57

Diez D, Alvarez R, Dopazo A. Codelink: an R package for analysis of GE healthcare gene expression bioarrays. *Bioinformatics* 2007;23:1168-9

Dimopoulos N, Watson M, Sakamoto K, Hundal HS. Differential effects of palmitate and palmitoleate on insulin action and glucose utilization in rat L6 skeletal muscle cells. *Biochem J* 2006;399:473-81

Diraison F, Dusserre E, Vidal H, Sothier M, Beylot M. Increased hepatic lipogenesis but decreased expression of lipogenic gene in adipose tissue in human obesity. *Am J Physiol Endocrinol Metab* 2002;282:E46-51

Diraison F, Yankah V, Letexier D, Dusserre E, Jones P, Beylot M. Differences in the regulation of adipose tissue and liver lipogenesis by carbohydrates in humans. *J Lipid Res* 2003;44:846-53

Dobrzyn A, Dobrzyn P, Lee SH, Miyazaki M, Cohen P, Asilmaz E, Hardie DG, Friedman JM, Ntambi JM. Stearoyl-CoA desaturase-1 deficiency reduces ceramide synthesis by downregulating serine palmitoyltransferase and increasing beta-oxidation in skeletal muscle. *Am J Physiol Endocrinol Metab* 2005a;288:E599-607

Dobrzyn A, Dobrzyn P, Miyazaki M, Sampath H, Chu K, Ntambi JM. Stearoyl-CoA desaturase 1 deficiency increases CTP:choline cytidylyltransferase translocation into the membrane and enhances phosphatidylcholine synthesis in liver. *J Biol Chem* 2005b;280:23356-62

Dobrzyn A, Ntambi JM. Stearoyl-CoA desaturase as a new drug target for obesity treatment. *Obes Rev* 2005;6:169-74

Dobrzyn P, Dobrzyn A, Miyazaki M, Cohen P, Asilmaz E, Hardie DG, Friedman JM, Ntambi JM. Stearoyl-CoA desaturase 1 deficiency increases fatty acid oxidation by activating AMP-activated protein kinase in liver. *Proc Natl Acad Sci U S A* 2004;101:6409-14

Drolet R, Richard C, Sniderman AD, Mailloux J, Fortier M, Huot C, Rheaume C, Tchernof A. Hypertrophy and hyperplasia of abdominal adipose tissues in women. *Int J Obes (Lond)* 2008;32:283-91

Ducharme NA, Bickel PE. Lipid droplets in lipogenesis and lipolysis. *Endocrinology* 2008;149:942-9

Dulloo AG, Gubler M, Montani JP, Seydoux J, Solinas G. Substrate cycling between de novo lipogenesis and lipid oxidation: a thermogenic mechanism against skeletal muscle lipotoxicity and glucolipotoxicity. *Int J Obes Relat Metab Disord* 2004;28 Suppl 4:S29-37

Eckel RH. Lipoprotein lipase. A multifunctional enzyme relevant to common metabolic diseases. *N Engl J Med* 1989;320:1060-8

Edwards PA, Tabor D, Kast HR, Venkateswaran A. Regulation of gene expression by SREBP and SCAP. *Biochim Biophys Acta* 2000;1529:103-13

Ehehalt R, Fullekrug J, Pohl J, Ring A, Herrmann T, Stremmel W. Translocation of long chain fatty acids across the plasma membrane--lipid rafts and fatty acid transport proteins. *Mol Cell Biochem* 2006;284:135-40

Evans K, Burdge GC, Wootton SA, Collins JM, Clark ML, Tan GD, Karpe F, Frayn KN. Tissue-specific stable isotope measurements of postprandial lipid metabolism in familial combined hyperlipidaemia. *Atherosclerosis* 2008;197:164-70

Farmer SR. Transcriptional control of adipocyte formation. *Cell Metab* 2006;4:263-73

Field CJ, Ryan EA, Thomson AB, Clandinin MT. Dietary fat and the diabetic state alter insulin binding and the fatty acyl composition of the adipocyte plasma membrane. *Biochem J* 1988;253:417-24

Field CJ, Ryan EA, Thomson AB, Clandinin MT. Diet fat composition alters membrane phospholipid composition, insulin binding, and glucose metabolism in adipocytes from control and diabetic animals. *J Biol Chem* 1990;265:11143-50

Fire A. RNA-triggered gene silencing. *Trends Genet* 1999;15:358-63

Fire A, Xu S, Montgomery MK, Kostas SA, Driver SE, Mello CC. Potent and specific genetic interference by double-stranded RNA in Caenorhabditis elegans. *Nature* 1998;391:806-11

Flowers MT, Ntambi JM. Stearoyl-CoA desaturase and its relation to high-carbohydrate diets and obesity. *Biochim Biophys Acta* 2009;1791:85-91

Folch J, Lees M, Sloane Stanley GH. A simple method for the isolation and purification of total lipides from animal tissues. *J Biol Chem* 1957;226:497-509

Forman BM, Tontonoz P, Chen J, Brun RP, Spiegelman BM, Evans RM. 15-Deoxy-delta 12, 14-prostaglandin J2 is a ligand for the adipocyte determination factor PPAR gamma. *Cell* 1995;83:803-12

Franckhauser S, Munoz S, Pujol A, Casellas A, Riu E, Otaegui P, Su B, Bosch F. Increased fatty acid re-esterification by PEPCK overexpression in adipose tissue leads to obesity without insulin resistance. *Diabetes* 2002;51:624-30

Frayn KN. *Studies of human adipose tissue in vivo.* 1992. New York: Raven Press.

Frayn KN. Adipose tissue as a buffer for daily lipid flux. *Diabetologia* 2002;45:1201-10

Fried SK, Bunkin DA, Greenberg AS. Omental and subcutaneous adipose tissues of obese subjects release interleukin-6: depot difference and regulation by glucocorticoid. *J Clin Endocrinol Metab* 1998;83:847-50

Friedman JM, Halaas JL. Leptin and the regulation of body weight in mammals. *Nature* 1998;395:763-70

Galton DJ. Lipogenesis in human adipose tissue. *J Lipid Res* 1968;9:19-26

Garcia-Jimenez C, Hernandez A, Obregon MJ, Santisteban P. Malic enzyme gene expression in differentiating brown adipocytes: regulation by insulin and triiodothyronine. *Endocrinology* 1993;132:1537-43

Garg A. Adipose tissue dysfunction in obesity and lipodystrophy. *Clin Cornerstone* 2006;8 Suppl 4:S7-S13

Garg ML, Snoswell AM, Sabine JR. Influence of dietary cholesterol on desaturase enzymes of rat liver microsomes. *Prog Lipid Res* 1986;25:639-44

Garg ML, Wierzbicki AA, Thomson AB, Clandinin MT. Dietary cholesterol and/or n-3 fatty acid modulate delta 9-desaturase activity in rat liver microsomes. *Biochim Biophys Acta* 1988;962:330-6

Gargiulo CE, Stuhlsatz-Krouper SM, Schaffer JE. Localization of adipocyte long-chain fatty acyl-CoA synthetase at the plasma membrane. *J Lipid Res* 1999;40:881-92

Gates AH, Karasek M. Hereditary absence of sebaceous glands in the mouse. *Science* 1965;148:1471-1473

Gesta S, Lolmede K, Daviaud D, Berlan M, Bouloumie A, Lafontan M, Valet P, Saulnier-Blache JS. Culture of human adipose tissue explants leads to profound alteration of adipocyte gene expression. *Horm Metab Res* 2003;35:158-63

Gibbons G. Old fat, make way for new fat. *Nat Med* 2005;11:722-3

Girard J, Perdereau D, Foufelle F, Prip-Buus C, Ferré P. Regulation of lipogenic enzyme gene expression by nutrients and hormones. *Faseb J* 1994;8:36-42

Gomez FE, Bauman DE, Ntambi JM, Fox BG. Effects of sterculic acid on stearoyl-CoA desaturase in differentiating 3T3-L1 adipocytes. *Biochem Biophys Res Commun* 2003;300:316-26

Gomez FE, Miyazaki M, Kim YC, Marwah P, Lardy HA, Ntambi JM, Fox BG. Molecular differences caused by differentiation of 3T3-L1 preadipocytes in the presence of either dehydroepiandrosterone (DHEA) or 7-oxo-DHEA. *Biochemistry* 2002;41:5473-82

Goossens GH. The role of adipose tissue dysfunction in the pathogenesis of obesity-related insulin resistance. *Physiol Behav* 2008;94:206-18

Gorin E, Tal-Or Z, Shafrir E. Glyceroneogenesis in adipose tissue of fasted, diabetic and triamcinolone treated rats. *Eur J Biochem* 1969;8:370-5

Granneman JG, Moore HP. Location, location: protein trafficking and lipolysis in adipocytes. *Trends Endocrinol Metab* 2008;19:3-9

Green H, Kehinde O. An established preadipose cell line and its differentiation in culture. II. Factors affecting the adipose conversion. *Cell* 1975;5:19-27

Gries FA, Steinke J. Comparative Effects of Insulin on Adipose Tissue Segments and Isolated Fat Cells of Rat and Man. *J Clin Invest* 1967;46:1413-1421

Griffin MJ, Sul HS. Insulin regulation of fatty acid synthase gene transcription: roles of USF and SREBP-1c. *IUBMB Life* 2004;56:595-600

Grohmann M, Stewart C, Welsh G, Hunt L, Tavare J, Holly J, Shield J, Sabin M, Crowne E. Site-specific differences of insulin action in adipose tissue derived from normal prepubertal children. *Exp Cell Res* 2005;308:469-78

Grunfeld C, Baird KL, Kahn CR. Maintenance of 3T3-L1 cells in culture media containing saturated fatty acids decreases insulin binding and insulin action. *Biochem Biophys Res Commun* 1981;103:219-26

Guo W, Wong S, Xie W, Lei T, Luo Z. Palmitate modulates intracellular signaling, induces endoplasmic reticulum stress, and causes apoptosis in mouse 3T3-L1 and rat primary preadipocytes. *Am J Physiol Endocrinol Metab* 2007;293:E576-86

Guo ZK, Cella LK, Baum C, Ravussin E, Schoeller DA. De novo lipogenesis in adipose tissue of lean and obese women: application of deuterated water and isotope ratio mass spectrometry. *Int J Obes Relat Metab Disord* 2000;24:932-7

Gustafson B, Smith U. Cytokines promote Wnt signaling and inflammation and impair the normal differentiation and lipid accumulation in 3T3-L1 preadipocytes. *J Biol Chem* 2006;281:9507-16

Gutierrez-Juarez R, Pocai A, Mulas C, Ono H, Bhanot S, Monia BP, Rossetti L. Critical role of stearoyl-CoA desaturase-1 (SCD1) in the onset of diet-induced hepatic insulin resistance. *J Clin Invest* 2006;116:1686-95

Haemmerle G, Lass A, Zimmermann R, Gorkiewicz G, Meyer C, Rozman J, Heldmaier G, Maier R, Theussl C, Eder S, Kratky D, Wagner EF, Klingenspor M, Hoefler G, Zechner R. Defective lipolysis and altered energy metabolism in mice lacking adipose triglyceride lipase. *Science* 2006;312:734-7

Haemmerle G, Zimmermann R, Hayn M, Theussl C, Waeg G, Wagner E, Sattler W, Magin TM, Wagner EF, Zechner R. Hormone-sensitive lipase deficiency in mice causes diglyceride accumulation in adipose tissue, muscle, and testis. *J Biol Chem* 2002;277:4806-15

Hall AM, Smith AJ, Bernlohr DA. Characterization of the Acyl-CoA synthetase activity of purified murine fatty acid transport protein 1. *J Biol Chem* 2003;278:43008-13

Halperin ML. Studies on the conversion of pyruvate into fatty acids in white adipose tissue. Effects of insulin, alloxan-diabetes and starvation. *Biochem J* 1971;124:615-21

Hamilton JA, Kamp F. How are free fatty acids transported in membranes? Is it by proteins or by free diffusion through the lipids? *Diabetes* 1999;48:2255-69

Hammond LE, Gallagher PA, Wang S, Hiller S, Kluckman KD, Posey-Marcos EL, Maeda N, Coleman RA. Mitochondrial glycerol-3-phosphate acyltransferase-deficient mice have reduced weight and liver triacylglycerol content and altered glycerolipid fatty acid composition. *Mol Cell Biol* 2002;22:8204-14

Han J, Farmer SR, Kirkland JL, Corkey BE, Yoon R, Pirtskhalava T, Ido Y, Guo W. Octanoate attenuates adipogenesis in 3T3-L1 preadipocytes. *J Nutr* 2002;132:904-10

Hansen PA, Han DH, Marshall BA, Nolte LA, Chen MM, Mueckler M, Holloszy JO. A high fat diet impairs stimulation of glucose transport in muscle. Functional evaluation of potential mechanisms. *J Biol Chem* 1998;273:26157-63

Hanson RW, Reshef L. Regulation of phosphoenolpyruvate carboxykinase (GTP) gene expression. *Annu Rev Biochem* 1997;66:581-611

Hanson RW, Reshef L. Glyceroneogenesis revisited. *Biochimie* 2003;85:1199-205

Hargrave KM, Li C, Meyer BJ, Kachman SD, Hartzell DL, Della-Fera MA, Miner JL, Baile CA. Adipose depletion and apoptosis induced by trans-10, cis-12 conjugated linoleic Acid in mice. *Obes Res* 2002;10:1284-90

Harper RD, Saggerson ED. Some aspects of fatty acid oxidation in isolated fat-cell mitochondria from rat. *Biochem J* 1975;152:485-94

Hauner H. The new concept of adipose tissue function. *Physiol Behav* 2004;83:653-8

Hauner H, Entenmann G, Wabitsch M, Gaillard D, Ailhaud G, Negrel R, Pfeiffer EF. Promoting effect of glucocorticoids on the differentiation of human adipocyte precursor cells cultured in a chemically defined medium. *J Clin Invest* 1989;84:1663-70

Hauner H, Rohrig K, Petruschke T. Effects of epidermal growth factor (EGF), platelet-derived growth factor (PDGF) and fibroblast growth factor (FGF) on human adipocyte development and function. *Eur J Clin Invest* 1995;25:90-6

Hauner H, Skurk T, Wabitsch M. Cultures of human adipose precursor cells. *Methods Mol Biol* 2001;155:239-47

Heaton JM. The distribution of brown adipose tissue in the human. *J Anat* 1972;112:35-9

Heffernan AG. Fatty acid composition of adipose tissue in normal and abnormal subjects. *Am J Clin Nutr* 1964;15:5-10

Heinemann FS, Ozols J. Stearoyl-CoA desaturase, a short-lived protein of endoplasmic reticulum with multiple control mechanisms. *Prostaglandins Leukot Essent Fatty Acids* 2003;68:123-33

Hellerstein MK. De novo lipogenesis in humans: metabolic and regulatory aspects. *Eur J Clin Nutr* 1999;53 Suppl 1:S53-65

Hellerstein MK, Kletke C, Kaempfer S, Wu K, Shackleton CH. Use of mass isotopomer distributions in secreted lipids to sample lipogenic acetyl-CoA pool in vivo in humans. *Am J Physiol* 1991;261:E479-86

Hellerstein MK, Neese RA. Mass isotopomer distribution analysis: a technique for measuring biosynthesis and turnover of polymers. *Am J Physiol* 1992;263:E988-1001

Hellerstein MK, Neese RA. Mass isotopomer distribution analysis at eight years: theoretical, analytic, and experimental considerations. *Am J Physiol* 1999;276:E1146-70

Hemmrich K, von Heimburg D, Cierpka K, Haydarlioglu S, Pallua N. Optimization of the differentiation of human preadipocytes in vitro. *Differentiation* 2005;73:28-35

Hillgartner FB, Salati LM, Goodridge AG. Physiological and molecular mechanisms involved in nutritional regulation of fatty acid synthesis. *Physiol Rev* 1995;75:47-76

Hirsch J, Farquhar JW, Ahrens EH, Jr., Peterson ML, Stoffel W. Studies of adipose tissue in man. A microtechnic for sampling and analysis. *Am J Clin Nutr* 1960;8:499-511

Hodson L, Skeaff CM, Fielding BA. Fatty acid composition of adipose tissue and blood in humans and its use as a biomarker of dietary intake. *Prog Lipid Res* 2008;47:348-80

Hoffstedt J, Forster D, Lofgren P. Impaired subcutaneous adipocyte lipogenesis is associated with systemic insulin resistance and increased apolipoprotein B/Al ratio in men and women. *J Intern Med* 2007;262:131-9

Hu CC, Qing K, Chen Y. Diet-induced changes in stearoyl-CoA desaturase 1 expression in obesity-prone and -resistant mice. *Obes Res* 2004;12:1264-70

Hua X, Wu J, Goldstein JL, Brown MS, Hobbs HH. Structure of the human gene encoding sterol regulatory element binding protein-1 (SREBF1) and localization of SREBF1 and SREBF2 to chromosomes 17p11.2 and 22q13. *Genomics* 1995;25:667-73

Hudgins LC, Baday A, Hellerstein MK, Parker TS, Levine DM, Seidman CE, Neese RA, Tremaroli JD, Hirsch J. The effect of dietary carbohydrate on genes for fatty acid synthase and inflammatory cytokines in adipose tissues from lean and obese subjects. *J Nutr Biochem* 2008;19:237-45

Hudgins LC, Hellerstein M, Seidman C, Neese R, Diakun J, Hirsch J. Human fatty acid synthesis is stimulated by a eucaloric low fat, high carbohydrate diet. *J Clin Invest* 1996;97:2081-91

Hulthe J, Hulten LM, Fagerberg B. Low adipocyte-derived plasma protein adiponectin concentrations are associated with the metabolic syndrome and small dense low-density lipoprotein particles: atherosclerosis and insulin resistance study. *Metabolism* 2003;52:1612-4

Hulver MW, Berggren JR, Carper MJ, Miyazaki M, Ntambi JM, Hoffman EP, Thyfault JP, Stevens R, Dohm GL, Houmard JA, Muoio DM. Elevated stearoyl-CoA desaturase-1 expression in skeletal muscle contributes to abnormal fatty acid partitioning in obese humans. *Cell Metab* 2005;2:251-61

Hussain A, Claussen B, Ramachandran A, Williams R. Prevention of type 2 diabetes: a review. *Diabetes Res Clin Pract* 2007;76:317-26

Hwang YH, Kang KJ. Conjugated linoleic acid reduces adipose depots without reduction of stearoyl coenzyme A desaturase I gene expression. *Ann Nutr Metab* 2007;51:126-33

Iizuka K, Bruick RK, Liang G, Horton JD, Uyeda K. Deficiency of carbohydrate response element-binding protein (ChREBP) reduces lipogenesis as well as glycolysis. *Proc Natl Acad Sci U S A* 2004;101:7281-6

Insull W, Jr., Bartsch GE. Fatty acid composition of human adipose tissue related to age, sex, and race. *Am J Clin Nutr* 1967;20:13-23

Jakobsson A, Westerberg R, Jacobsson A. Fatty acid elongases in mammals: their regulation and roles in metabolism. *Prog Lipid Res* 2006;45:237-49

Jiang G, Li Z, Liu F, Ellsworth K, Dallas-Yang Q, Wu M, Ronan J, Esau C, Murphy C, Szalkowski D, Bergeron R, Doebber T, Zhang BB. Prevention of obesity in mice by antisense oligonucleotide inhibitors of stearoyl-CoA desaturase-1. *J Clin Invest* 2005;115:1030-8

Jiang HP, Serrero G. Isolation and characterization of a full-length cDNA coding for an adipose differentiation-related protein. *Proc Natl Acad Sci U S A* 1992;89:7856-60

Jones BH, Standridge MK, Claycombe KJ, Smith PJ, Moustaid-Moussa N. Glucose induces expression of stearoyl-CoA desaturase in 3T3-L1 adipocytes. *Biochem J* 1998;335 (Pt 2):405-8

Jose AA, Gama MA, Lanna DD. Effects of trans-10, cis-12 conjugated linoleic acid on gene expression and lipid metabolism of adipose tissue of growing pigs. *Genet Mol Res* 2008;7:284-94

Joshi VC, Aranda LP. Hormonal regulation of the terminal enzyme of microsomal stearoyl coenzyme A desaturase in cultured avian liver explants. Role of insulin. *J Biol Chem* 1979;254:11779-82

Kaestner KH, Ntambi JM, Kelly TJ, Jr., Lane MD. Differentiation-induced gene expression in 3T3-L1 preadipocytes. A second differentially expressed gene encoding stearoyl-CoA desaturase. *J Biol Chem* 1989;264:14755-61

Kakuma T, Lee Y, Unger RH. Effects of leptin, troglitazone, and dietary fat on stearoyl CoA desaturase. *Biochem Biophys Res Commun* 2002;297:1259-63

Kalhan SC, Mahajan S, Burkett E, Reshef L, Hanson RW. Glyceroneogenesis and the source of glycerol for hepatic triacylglycerol synthesis in humans. *J Biol Chem* 2001;276:12928-31

Kamp F, Guo W, Souto R, Pilch PF, Corkey BE, Hamilton JA. Rapid flip-flop of oleic acid across the plasma membrane of adipocytes. *J Biol Chem* 2003;278:7988-95

Kamp F, Hamilton JA. How fatty acids of different chain length enter and leave cells by free diffusion. *Prostaglandins Leukot Essent Fatty Acids* 2006;75:149-59

Kampf JP, Kleinfeld AM. Fatty acid transport in adipocytes monitored by imaging intracellular free fatty acid levels. *J Biol Chem* 2004;279:35775-80

Kampf JP, Kleinfeld AM. Is membrane transport of FFA mediated by lipid, protein, or both? An unknown protein mediates free fatty acid transport across the adipocyte plasma membrane. *Physiology (Bethesda)* 2007;22:7-14

Kanzaki M, Pessin JE. Insulin-stimulated GLUT4 translocation in adipocytes is dependent upon cortical actin remodeling. *J Biol Chem* 2001;276:42436-44

Kasturi R, Joshi VC. Hormonal regulation of stearoyl coenzyme A desaturase activity and lipogenesis during adipose conversion of 3T3-L1 cells. *J Biol Chem* 1982;257:12224-30

Kern PA, Ranganathan S, Li C, Wood L, Ranganathan G. Adipose tissue tumor necrosis factor and interleukin-6 expression in human obesity and insulin resistance. *Am J Physiol Endocrinol Metab* 2001;280:E745-51

Kern PA, Saghizadeh M, Ong JM, Bosch RJ, Deem R, Simsolo RB. The expression of tumor necrosis factor in human adipose tissue. Regulation by obesity, weight loss, and relationship to lipoprotein lipase. *J Clin Invest* 1995;95:2111-9

Kharroubi I, Ladriere L, Cardozo AK, Dogusan Z, Cnop M, Eizirik DL. Free fatty acids and cytokines induce pancreatic beta-cell apoptosis by different mechanisms: role of nuclear factor-kappaB and endoplasmic reticulum stress. *Endocrinology* 2004;145:5087-96

Kim HJ, Miyazaki M, Ntambi JM. Dietary cholesterol opposes PUFA-mediated repression of the stearoyl-CoA desaturase-1 gene by SREBP-1 independent mechanism. *J Lipid Res* 2002;43:1750-7

Kim HJ, Takahashi M, Ezaki O. Fish oil feeding decreases mature sterol regulatory element-binding protein 1 (SREBP-1) by down-regulation of SREBP-1c mRNA in mouse liver. A possible mechanism for down-regulation of lipogenic enzyme mRNAs. *J Biol Chem* 1999;274:25892-8

Kim JB, Sarraf P, Wright M, Yao KM, Mueller E, Solanes G, Lowell BB, Spiegelman BM. Nutritional and insulin regulation of fatty acid synthetase and leptin gene expression through ADD1/SREBP1. *J Clin Invest* 1998a;101:1-9

Kim JB, Spiegelman BM. ADD1/SREBP1 promotes adipocyte differentiation and gene expression linked to fatty acid metabolism. *Genes Dev* 1996;10:1096-107

Kim JB, Wright HM, Wright M, Spiegelman BM. ADD1/SREBP1 activates PPARgamma through the production of endogenous ligand. *Proc Natl Acad Sci U S A* 1998b;95:4333-7

Kirkland JL, Hollenberg CH, Gillon WS. Age, anatomic site, and the replication and differentiation of adipocyte precursors. *Am J Physiol* 1990;258:C206-10

Kleinfeld AM. Lipid phase fatty acid flip-flop, is it fast enough for cellular transport? *J Membr Biol* 2000;175:79-86

Kletzien RF, Clarke SD, Ulrich RG. Enhancement of adipocyte differentiation by an insulin-sensitizing agent. *Mol Pharmacol* 1992;41:393-8

Kliewer SA, Sundseth SS, Jones SA, Brown PJ, Wisely GB, Koble CS, Devchand P, Wahli W, Willson TM, Lenhard JM, Lehmann JM. Fatty acids and eicosanoids regulate gene expression through direct interactions with peroxisome proliferator-activated receptors alpha and gamma. *Proc Natl Acad Sci U S A* 1997;94:4318-23

Kolehmainen M, Vidal H, Alhava E, Uusitupa MI. Sterol regulatory element binding protein 1c (SREBP-1c) expression in human obesity. *Obes Res* 2001;9:706-12

Kozak LP, Jensen JT. Genetic and developmental control of multiple forms of L-glycerol 3-phosphate dehydrogenase. *J Biol Chem* 1974;249:7775-81

Krey G, Braissant O, L'Horset F, Kalkhoven E, Perroud M, Parker MG, Wahli W. Fatty acids, eicosanoids, and hypolipidemic agents identified as ligands of peroxisome proliferator-activated receptors by coactivator-dependent receptor ligand assay. *Mol Endocrinol* 1997;11:779-91

Kubota N, Terauchi Y, Miki H, Tamemoto H, Yamauchi T, Komeda K, Satoh S, Nakano R, Ishii C, Sugiyama T, Eto K, Tsubamoto Y, Okuno A, Murakami K, Sekihara H, Hasegawa G, Naito M, Toyoshima Y, Tanaka S, Shiota K, Kitamura T, Fujita T, Ezaki O, Aizawa S, Kadowaki T, et al. PPAR gamma mediates high-fat diet-induced adipocyte hypertrophy and insulin resistance. *Mol Cell* 1999;4:597-609

Kurebayashi S, Hirose T, Miyashita Y, Kasayama S, Kishimoto T. Thiazolidinediones downregulate stearoyl-CoA desaturase 1 gene expression in 3T3-L1 adipocytes. *Diabetes* 1997;46:2115-8

Landau JM, Sekowski A, Hamm MW. Dietary cholesterol and the activity of stearoyl CoA desaturase in rats: evidence for an indirect regulatory effect. *Biochim Biophys Acta* 1997;1345:349-57

Lass A, Zimmermann R, Haemmerle G, Riederer M, Schoiswohl G, Schweiger M, Kienesberger P, Strauss JG, Gorkiewicz G, Zechner R. Adipose triglyceride lipase-mediated lipolysis of cellular fat stores is activated by CGI-58 and defective in Chanarin-Dorfman Syndrome. *Cell Metab* 2006;3:309-19

Lee JS, Pinnamaneni SK, Eo SJ, Cho IH, Pyo JH, Kim CK, Sinclair AJ, Febbraio MA, Watt MJ. Saturated, but not n-6 polyunsaturated, fatty acids induce insulin resistance: role of intramuscular accumulation of lipid metabolites. *J Appl Physiol* 2006;100:1467-74

Lee K, Villena JA, Moon YS, Kim KH, Lee S, Kang C, Sul HS. Inhibition of adipogenesis and development of glucose intolerance by soluble preadipocyte factor-1 (Pref-1). *J Clin Invest* 2003;111:453-61

Legrand P, Bensadoun A. Stearyl-CoA desaturase activity in cultured rat hepatocytes. *Biochim Biophys Acta* 1991;1086:89-94

Letexier D, Pinteur C, Large V, Frering V, Beylot M. Comparison of the expression and activity of the lipogenic pathway in human and rat adipose tissue. *J Lipid Res* 2003;44:2127-34

Leung RK, Whittaker PA. RNA interference: from gene silencing to gene-specific therapeutics. *Pharmacol Ther* 2005;107:222-39

Li J, Ding SF, Habib NA, Fermor BF, Wood CB, Gilmour RS. Partial characterization of a cDNA for human stearoyl-CoA desaturase and changes in its mRNA expression in some normal and malignant tissues. *Int J Cancer* 1994;57:348-52

Li JJ, Huang CJ, Xie D. Anti-obesity effects of conjugated linoleic acid, docosahexaenoic acid, and eicosapentaenoic acid. *Mol Nutr Food Res* 2008;52:631-45

Li Z, Berk M, McIntyre TM, Feldstein AE. Hepatic lipid partitioning and liver damage in nonalcoholic fatty liver disease: role of stearoyl-CoA desaturase. *J Biol Chem* 2009;

Lin J, Yang R, Tarr PT, Wu PH, Handschin C, Li S, Yang W, Pei L, Uldry M, Tontonoz P, Newgard CB, Spiegelman BM. Hyperlipidemic effects of dietary saturated fats mediated through PGC-1beta coactivation of SREBP. *Cell* 2005;120:261-73

Listenberger LL, Han X, Lewis SE, Cases S, Farese RV, Jr., Ory DS, Schaffer JE. Triglyceride accumulation protects against fatty acid-induced lipotoxicity. *Proc Natl Acad Sci U S A* 2003;100:3077-82

Listenberger LL, Ory DS, Schaffer JE. Palmitate-induced apoptosis can occur through a ceramide-independent pathway. *J Biol Chem* 2001;276:14890-5

Liu G, Lynch JK, Freeman J, Liu B, Xin Z, Zhao H, Serby MD, Kym PR, Suhar TS, Smith HT, Cao N, Yang R, Janis RS, Krauser JA, Cepa SP, Beno DW, Sham HL, Collins CA, Surowy TK, Camp HS. Discovery of potent, selective, orally bioavailable stearoyl-CoA desaturase 1 inhibitors. *J Med Chem* 2007;50:3086-100

Londos C, Brasaemle DL, Gruia-Gray J, Servetnick DA, Schultz CJ, Levin DM, Kimmel AR. Perilipin: unique proteins associated with intracellular neutral lipid droplets in adipocytes and steroidogenic cells. *Biochem Soc Trans* 1995;23:611-5

Londos C, Brasaemle DL, Schultz CJ, Segrest JP, Kimmel AR. Perilipins, ADRP, and other proteins that associate with intracellular neutral lipid droplets in animal cells. *Semin Cell Dev Biol* 1999;10:51-8

Londos C, Sztalryd C, Tansey JT, Kimmel AR. Role of PAT proteins in lipid metabolism. *Biochimie* 2005;87:45-9

Lu ZH, Mu YM, Wang BA, Li XL, Lu JM, Li JY, Pan CY, Yanase T, Nawata H. Saturated free fatty acids, palmitic acid and stearic acid, induce apoptosis by stimulation of ceramide generation in rat testicular Leydig cell. *Biochem Biophys Res Commun* 2003;303:1002-7

Lundgren M, Eriksson JW. No in vitro effects of fatty acids on glucose uptake, lipolysis or insulin signaling in rat adipocytes. *Horm Metab Res* 2004;36:203-9

Lundgren M, Svensson M, Lindmark S, Renstrom F, Ruge T, Eriksson JW. Fat cell enlargement is an independent marker of insulin resistance and 'hyperleptinaemia'. *Diabetologia* 2007;50:625-33

Maachi M, Pieroni L, Bruckert E, Jardel C, Fellahi S, Hainque B, Capeau J, Bastard JP. Systemic low-grade inflammation is related to both circulating and adipose tissue TNFalpha, leptin and IL-6 levels in obese women. *Int J Obes Relat Metab Disord* 2004;28:993-7

Macdonald ML, van Eck M, Hildebrand RB, Wong BW, Bissada N, Ruddle P, Kontush A, Hussein H, Pouladi MA, Chapman MJ, Fievet C, van Berkel TJ, Staels B, McManus BM, Hayden MR. Despite antiatherogenic metabolic characteristics, Scd1-deficient mice have increased inflammation and atherosclerosis. *Arterioscler Thromb Vasc Biol* 2008;

MacDougald OA, Mandrup S. Adipogenesis: forces that tip the scales. *Trends Endocrinol Metab* 2002;13:5-11

Maedler K, Oberholzer J, Bucher P, Spinas GA, Donath MY. Monounsaturated fatty acids prevent the deleterious effects of palmitate and high glucose on human pancreatic beta-cell turnover and function. *Diabetes* 2003;52:726-33

Maine EM. RNAi As a tool for understanding germline development in Caenorhabditis elegans: uses and cautions. *Dev Biol* 2001;239:177-89

Major CA, Ryan K, Bennett AJ, Lock AL, Bauman DE, Salter AM. Inhibition of stearoyl CoA desaturase activity induces hypercholesterolemia in the cholesterol-fed hamster. *J Lipid Res* 2008;49:1456-65

Man WC, Miyazaki M, Chu K, Ntambi J. Colocalization of SCD1 and DGAT2: implying preference for endogenous monounsaturated fatty acids in triglyceride synthesis. *J Lipid Res* 2006;47:1928-39

Martin BR, Denton RM. The intracellular localization of enzymes in white-adipose-tissue fat-cells and permeability properties of fat-cell mitochondria. Transfer of acetyl units and reducing power between mitochondria and cytoplasm. *Biochem J* 1970;117:861-77

Martinez-Botas J, Anderson JB, Tessier D, Lapillonne A, Chang BH, Quast MJ, Gorenstein D, Chen KH, Chan L. Absence of perilipin results in leanness and reverses obesity in Lepr(db/db) mice. *Nat Genet* 2000;26:474-9

McDevitt RM, Bott SJ, Harding M, Coward WA, Bluck LJ, Prentice AM. De novo lipogenesis during controlled overfeeding with sucrose or glucose in lean and obese women. *Am J Clin Nutr* 2001;74:737-46

Mellati AM, Beck JC, Dupre J, Rubinstein D. Conversion of glucose to lipid by human adipose tissue in vitro. *Metabolism* 1970;19:988-94

Miller CW, Ntambi JM. Peroxisome proliferators induce mouse liver stearoyl-CoA desaturase 1 gene expression. *Proc Natl Acad Sci U S A* 1996;93:9443-8

Minehira K, Bettschart V, Vidal H, Vega N, Di Vetta V, Rey V, Schneiter P, Tappy L. Effect of carbohydrate overfeeding on whole body and adipose tissue metabolism in humans. *Obes Res* 2003;11:1096-103

Minehira K, Vega N, Vidal H, Acheson K, Tappy L. Effect of carbohydrate overfeeding on whole body macronutrient metabolism and expression of lipogenic enzymes in adipose tissue of lean and overweight humans. *Int J Obes Relat Metab Disord* 2004;28:1291-8

Mishra R, Simonson MS. Saturated free fatty acids and apoptosis in microvascular mesangial cells: palmitate activates pro-apoptotic signaling involving caspase 9 and mitochondrial release of endonuclease G. *Cardiovasc Diabetol* 2005;4:2

Miyazaki M, Jacobson MJ, Man WC, Cohen P, Asilmaz E, Friedman JM, Ntambi JM. Identification and characterization of murine SCD4, a novel heart-specific stearoyl-

CoA desaturase isoform regulated by leptin and dietary factors. *J Biol Chem* 2003;278:33904-11

Miyazaki M, Kim YC, Gray-Keller MP, Attie AD, Ntambi JM. The biosynthesis of hepatic cholesterol esters and triglycerides is impaired in mice with a disruption of the gene for stearoyl-CoA desaturase 1. *J Biol Chem* 2000;275:30132-8

Miyazaki M, Kim YC, Ntambi JM. A lipogenic diet in mice with a disruption of the stearoyl-CoA desaturase 1 gene reveals a stringent requirement of endogenous monounsaturated fatty acids for triglyceride synthesis. *J Lipid Res* 2001;42:1018-24

Moffitt JH, Fielding BA, Evershed R, Berstan R, Currie JM, Clark A. Adverse physicochemical properties of tripalmitin in beta cells lead to morphological changes and lipotoxicity in vitro. *Diabetologia* 2005;48:1819-29

Morgan-Lappe SE, Tucker LA, Huang X, Zhang Q, Sarthy AV, Zakula D, Vernetti L, Schurdak M, Wang J, Fesik SW. Identification of Ras-related nuclear protein, targeting protein for xenopus kinesin-like protein 2, and stearoyl-CoA desaturase 1 as promising cancer targets from an RNAi-based screen. *Cancer Res* 2007;67:4390-8

Mounier C, Posner BI. Transcriptional regulation by insulin: from the receptor to the gene. *Can J Physiol Pharmacol* 2006;84:713-24

Mouritsen OG, Zuckermann MJ. What's so special about cholesterol? *Lipids* 2004;39:1101-13

Moustaid N, Jones BH, Taylor JW. Insulin increases lipogenic enzyme activity in human adipocytes in primary culture. *J Nutr* 1996;126:865-70

Napolitano L. The differentiation of white adipose cells. An electron microscope study. *J Cell Biol* 1963;18:663-79

Nechushtan H, Benvenisty N, Brandeis R, Reshef L. Glucocorticoids control phosphoenolpyruvate carboxykinase gene expression in a tissue specific manner. *Nucleic Acids Res* 1987;15:6405-17

Nedergaard J, Bengtsson T, Cannon B. Unexpected evidence for active brown adipose tissue in adult humans. *Am J Physiol Endocrinol Metab* 2007;293:E444-52

Ntambi JM. The regulation of stearoyl-CoA desaturase (SCD). *Prog Lipid Res* 1995;34:139-50

Ntambi JM. Regulation of stearoyl-CoA desaturase by polyunsaturated fatty acids and cholesterol. *J Lipid Res* 1999;40:1549-58

Ntambi JM, Buhrow SA, Kaestner KH, Christy RJ, Sibley E, Kelly TJ, Jr., Lane MD. Differentiation-induced gene expression in 3T3-L1 preadipocytes. Characterization of a differentially expressed gene encoding stearoyl-CoA desaturase. *J Biol Chem* 1988;263:17291-300

Ntambi JM, Miyazaki M, Stoehr JP, Lan H, Kendziorski CM, Yandell BS, Song Y, Cohen P, Friedman JM, Attie AD. Loss of stearoyl-CoA desaturase-1 function protects mice against adiposity. *Proc Natl Acad Sci U S A* 2002;99:11482-6

Olefsky JM. Effect of dexamethasone on insulin binding, glucose transport, and glucose oxidation of isolated rat adipocytes. *J Clin Invest* 1975;56:1499-1508

Olswang Y, Blum B, Cassuto H, Cohen H, Biberman Y, Hanson RW, Reshef L. Glucocorticoids repress transcription of phosphoenolpyruvate carboxykinase (GTP)

gene in adipocytes by inhibiting its C/EBP-mediated activation. *J Biol Chem* 2003;278:12929-36

Olswang Y, Cohen H, Papo O, Cassuto H, Croniger CM, Hakimi P, Tilghman SM, Hanson RW, Reshef L. A mutation in the peroxisome proliferator-activated receptor gamma-binding site in the gene for the cytosolic form of phosphoenolpyruvate carboxykinase reduces adipose tissue size and fat content in mice. *Proc Natl Acad Sci U S A* 2002;99:625-30

Pairault J, Green H. A study of the adipose conversion of suspended 3T3 cells by using glycerophosphate dehydrogenase as differentiation marker. *Proc Natl Acad Sci U S A* 1979;76:5138-42

Pan Z, Agarwal AK, Xu T, Feng Q, Baerson SR, Duke SO, Rimando AM. Identification of molecular pathways affected by pterostilbene, a natural dimethylether analog of resveratrol. *BMC Med Genomics* 2008;1:7

Park KW, Halperin DS, Tontonoz P. Before they were fat: adipocyte progenitors. *Cell Metab* 2008;8:454-7

Park Y, Storkson JM, Ntambi JM, Cook ME, Sih CJ, Pariza MW. Inhibition of hepatic stearoyl-CoA desaturase activity by trans-10, cis-12 conjugated linoleic acid and its derivatives. *Biochim Biophys Acta* 2000;1486:285-92

Parks EJ, Hellerstein MK. Thematic review series: patient-oriented research. Recent advances in liver triacylglycerol and fatty acid metabolism using stable isotope labeling techniques. *J Lipid Res* 2006;47:1651-60

Pasquet P, Brigant L, Froment A, Koppert GA, Bard D, de Garine I, Apfelbaum M. Massive overfeeding and energy balance in men: the Guru Walla model. *Am J Clin Nutr* 1992;56:483-90

Perez-Echarri N, Perez-Matute P, Marcos-Gomez B, Marti A, Martinez JA, Moreno-Aliaga MJ. Down-regulation in muscle and liver lipogenic genes: EPA ethyl ester treatment in lean and overweight (high-fat-fed) rats. *J Nutr Biochem* 2008;

Peter A, Weigert C, Staiger H, Rittig K, Cegan A, Lutz P, Machicao F, Haring HU, Schleicher E. Induction of stearoyl-CoA desaturase protects human arterial endothelial cells against lipotoxicity. *Am J Physiol Endocrinol Metab* 2008;295:E339-49

Petruschke T, Hauner H. Tumor necrosis factor-alpha prevents the differentiation of human adipocyte precursor cells and causes delipidation of newly developed fat cells. *J Clin Endocrinol Metab* 1993;76:742-7

Pinnamaneni SK, Southgate RJ, Febbraio MA, Watt MJ. Stearoyl CoA desaturase 1 is elevated in obesity but protects against fatty acid-induced skeletal muscle insulin resistance in vitro. *Diabetologia* 2006;49:3027-37

Pohl J, Ring A, Korkmaz U, Ehehalt R, Stremmel W. FAT/CD36-mediated long-chain fatty acid uptake in adipocytes requires plasma membrane rafts. *Mol Biol Cell* 2005;16:24-31

Powell DJ, Turban S, Gray A, Hajduch E, Hundal HS. Intracellular ceramide synthesis and protein kinase Czeta activation play an essential role in palmitate-induced insulin resistance in rat L6 skeletal muscle cells. *Biochem J* 2004;382:619-29

Prestwich TC, Macdougald OA. Wnt/beta-catenin signaling in adipogenesis and metabolism. *Curr Opin Cell Biol* 2007;19:612-7

Quinn PG, Yeagley D. Insulin regulation of PEPCK gene expression: a model for rapid and reversible modulation. *Curr Drug Targets Immune Endocr Metabol Disord* 2005;5:423-37

Rader DJ. Effect of insulin resistance, dyslipidemia, and intra-abdominal adiposity on the development of cardiovascular disease and diabetes mellitus. *Am J Med* 2007;120:S12-8

Rasouli N, Molavi B, Elbein SC, Kern PA. Ectopic fat accumulation and metabolic syndrome. *Diabetes Obes Metab* 2007;9:1-10

Rea S, James DE. Moving GLUT4: the biogenesis and trafficking of GLUT4 storage vesicles. *Diabetes* 1997;46:1667-77

Repa JJ, Liang G, Ou J, Bashmakov Y, Lobaccaro JM, Shimomura I, Shan B, Brown MS, Goldstein JL, Mangelsdorf DJ. Regulation of mouse sterol regulatory element-binding protein-1c gene (SREBP-1c) by oxysterol receptors, LXRalpha and LXRbeta. *Genes Dev* 2000;14:2819-30

Reshef L, Hanson RW, Ballard FJ. A possible physiological role for glyceroneogenesis in rat adipose tissue. *J Biol Chem* 1970;245:5979-84

Reshef L, Olswang Y, Cassuto H, Blum B, Croniger CM, Kalhan SC, Tilghman SM, Hanson RW. Glyceroneogenesis and the triglyceride/fatty acid cycle. *J Biol Chem* 2003;278:30413-6

Reynoso R, Salgado LM, Calderon V. High levels of palmitic acid lead to insulin resistance due to changes in the level of phosphorylation of the insulin receptor and insulin receptor substrate-1. *Mol Cell Biochem* 2003;246:155-62

Richards MR, Harp JD, Ory DS, Schaffer JE. Fatty acid transport protein 1 and long-chain acyl coenzyme A synthetase 1 interact in adipocytes. *J Lipid Res* 2006;47:665-72

Richieri GV, Kleinfeld AM. Unbound free fatty acid levels in human serum. *J Lipid Res* 1995;36:229-40

Risérus U. Fatty acids and insulin sensitivity. *Curr Opin Clin Nutr Metab Care* 2008;11:100-5

Risérus U, Sprecher D, Johnson T, Olson E, Hirschberg S, Liu A, Fang Z, Hegde P, Richards D, Sarov-Blat L, Strum JC, Basu S, Cheeseman J, Fielding BA, Humphreys SM, Danoff T, Moore NR, Murgatroyd P, O'Rahilly S, Sutton P, Willson T, Hassall D, Frayn KN, Karpe F. Activation of peroxisome proliferator-activated receptor (PPAR)delta promotes reversal of multiple metabolic abnormalities, reduces oxidative stress, and increases fatty acid oxidation in moderately obese men. *Diabetes* 2008;57:332-9

Risérus U, Tan GD, Fielding BA, Neville MJ, Currie J, Savage DB, Chatterjee VK, Frayn KN, O'Rahilly S, Karpe F. Rosiglitazone increases indexes of stearoyl-CoA desaturase activity in humans: link to insulin sensitization and the role of dominant-negative mutation in peroxisome proliferator-activated receptor-gamma. *Diabetes* 2005;54:1379-84

Robenek H, Hofnagel O, Buers I, Robenek MJ, Troyer D, Severs NJ. Adipophilin-enriched domains in the ER membrane are sites of lipid droplet biogenesis. *J Cell Sci* 2006;119:4215-24

Roberts R, Hodson L, Dennis AL, Neville MJ, Humphreys SM, Harnden KE, Micklem KJ, Frayn KN. Markers of de novo lipogenesis in adipose tissue: associations with small adipocytes and insulin sensitivity in humans. *Diabetologia* 2009;52:882-90

Rodbell M. Metabolism of isolated fat cells. I. Effects of hormones on glucose metabolism and lipolysis. *J Biol Chem* 1964;239:375-80

Ros-Baro A, Lopez-Iglesias C, Peiro S, Bellido D, Palacin M, Zorzano A, Camps M. Lipid rafts are required for GLUT4 internalization in adipose cells. *Proc Natl Acad Sci U S A* 2001;98:12050-5

Rosen ED, MacDougald OA. Adipocyte differentiation from the inside out. *Nat Rev Mol Cell Biol* 2006;7:885-96

Rosen ED, Sarraf P, Troy AE, Bradwin G, Moore K, Milstone DS, Spiegelman BM, Mortensen RM. PPAR gamma is required for the differentiation of adipose tissue in vivo and in vitro. *Mol Cell* 1999;4:611-7

Rosen ED, Spiegelman BM. Molecular regulation of adipogenesis. *Annu Rev Cell Dev Biol* 2000;16:145-71

Rosen ED, Spiegelman BM. PPARgamma : a nuclear regulator of metabolism, differentiation, and cell growth. *J Biol Chem* 2001;276:37731-4

Rosen ED, Walkey CJ, Puigserver P, Spiegelman BM. Transcriptional regulation of adipogenesis. *Genes Dev* 2000;14:1293-307

Ross SE, Hemati N, Longo KA, Bennett CN, Lucas PC, Erickson RL, MacDougald OA. Inhibition of adipogenesis by Wnt signaling. *Science* 2000;289:950-3

Ruddock MW, Stein A, Landaker E, Park J, Cooksey RC, McClain D, Patti ME. Saturated fatty acids inhibit hepatic insulin action by modulating insulin receptor expression and post-receptor signalling. *J Biochem* 2008;144:599-607

Ruderman NB, Saha AK, Vavvas D, Witters LA. Malonyl-CoA, fuel sensing, and insulin resistance. *Am J Physiol* 1999;276:E1-E18

Sabin MA, Holly JM, Shield JP, Turner SJ, Grohmann MJ, Stewart CE, Crowne EC. Mature subcutaneous and visceral adipocyte concentrations of adiponectin are highly correlated in prepubertal children and inversely related to body mass index standard deviation score. *J Clin Endocrinol Metab* 2006;91:332-5

Sabin MA, Stewart CE, Crowne EC, Turner SJ, Hunt LP, Welsh GI, Grohmann MJ, Holly JM, Shield JP. Fatty acid-induced defects in insulin signalling, in myotubes derived from children, are related to ceramide production from palmitate rather than the accumulation of intramyocellular lipid. *J Cell Physiol* 2007;211:244-52

Saggerson D. Malonyl-CoA, a key signaling molecule in mammalian cells. *Annu Rev Nutr* 2008;28:253-72

Saggerson ED. The regulation of glyceride synthesis in isolated white-fat cells. The effects of acetate, pyruvate, lactate, palmitate, electron-acceptors, uncoupling agents and oligomycin. *Biochem J* 1972a;128:1069-78

Saggerson ED. The regulation of glyceride synthesis in isolated white-fat cells. The effects of palmitate and lipolytic agents. *Biochem J* 1972b;128:1057-67

Saggerson ED, Tomassi G. The regulation of glyceride synthesis from pyruvate in isolated fat cells. The effects of palmitate and alteration of dietary status. *Eur J Biochem* 1971;23:109-17

Sampath H, Miyazaki M, Dobrzyn A, Ntambi JM. Stearoyl-CoA desaturase-1 mediates the pro-lipogenic effects of dietary saturated fat. *J Biol Chem* 2007;282:2483-93

Scaglia N, Caviglia JM, Igal RA. High stearoyl-CoA desaturase protein and activity levels in simian virus 40 transformed-human lung fibroblasts. *Biochim Biophys Acta* 2005;1687:141-51

Scaglia N, Igal RA. Inhibition of Stearoyl-CoA Desaturase 1 expression in human lung adenocarcinoma cells impairs tumorigenesis. *Int J Oncol* 2008;33:839-50

Schaffer JE, Lodish HF. Expression cloning and characterization of a novel adipocyte long chain fatty acid transport protein. *Cell* 1994;79:427-36

Scherer PE, Williams S, Fogliano M, Baldini G, Lodish HF. A novel serum protein similar to C1q, produced exclusively in adipocytes. *J Biol Chem* 1995;270:26746-9

Schmidt W, Poll-Jordan G, Loffler G. Adipose conversion of 3T3-L1 cells in a serum-free culture system depends on epidermal growth factor, insulin-like growth factor I, corticosterone, and cyclic AMP. *J Biol Chem* 1990;265:15489-95

Schmitz-Peiffer C, Craig DL, Biden TJ. Ceramide generation is sufficient to account for the inhibition of the insulin-stimulated PKB pathway in C2C12 skeletal muscle cells pretreated with palmitate. *J Biol Chem* 1999;274:24202-10

Schoonjans K, Staels B, Auwerx J. The peroxisome proliferator activated receptors (PPARs) and their effects on lipid metabolism and adipocyte differentiation. *Biochim Biophys Acta* 1996;1302:93-109

Schultz JR, Tu H, Luk A, Repa JJ, Medina JC, Li L, Schwendner S, Wang S, Thoolen M, Mangelsdorf DJ, Lustig KD, Shan B. Role of LXRs in control of lipogenesis. *Genes Dev* 2000;14:2831-8

Schwartz RS, Chiu DT, Lubin B. Plasma membrane phospholipid organization in human erythrocytes. *Curr Top Hematol* 1985;5:63-112

Schwarz JM, Linfoot P, Dare D, Aghajanian K. Hepatic de novo lipogenesis in normoinsulinemic and hyperinsulinemic subjects consuming high-fat, low-carbohydrate and low-fat, high-carbohydrate isoenergetic diets. *Am J Clin Nutr* 2003;77:43-50

Seo JB, Moon HM, Kim WS, Lee YS, Jeong HW, Yoo EJ, Ham J, Kang H, Park MG, Steffensen KR, Stulnig TM, Gustafsson JA, Park SD, Kim JB. Activated liver X receptors stimulate adipocyte differentiation through induction of peroxisome proliferator-activated receptor gamma expression. *Mol Cell Biol* 2004;24:3430-44

Serrero G, Mills D. Physiological role of epidermal growth factor on adipose tissue development in vivo. *Proc Natl Acad Sci U S A* 1991;88:3912-6

Sessler AM, Kaur N, Palta JP, Ntambi JM. Regulation of stearoyl-CoA desaturase 1 mRNA stability by polyunsaturated fatty acids in 3T3-L1 adipocytes. *J Biol Chem* 1996;271:29854-8

Sessler AM, Ntambi JM. Polyunsaturated fatty acid regulation of gene expression. *J Nutr* 1998;128:923-6

Sfeir Z, Ibrahimi A, Amri E, Grimaldi P, Abumrad N. Regulation of FAT/CD36 gene expression: further evidence in support of a role of the protein in fatty acid binding/transport. *Prostaglandins Leukot Essent Fatty Acids* 1997;57:17-21

Shadid S, Koutsari C, Jensen MD. Direct free fatty acid uptake into human adipocytes in vivo: relation to body fat distribution. *Diabetes* 2007;56:1369-75

Shimano H. Sterol regulatory element-binding proteins (SREBPs): transcriptional regulators of lipid synthetic genes. *Prog Lipid Res* 2001;40:439-52

Shimomura I, Shimano H, Korn BS, Bashmakov Y, Horton JD. Nuclear sterol regulatory element-binding proteins activate genes responsible for the entire program of unsaturated fatty acid biosynthesis in transgenic mouse liver. *J Biol Chem* 1998;273:35299-306

Shrago E, Glennon JA, Gordon ES. Comparative aspects of lipogenesis in mammalian tissues. *Metabolism* 1971;20:54-62

Shrago E, Spennetta T, Gordon E. Fatty acid synthesis in human adipose tissue. *J Biol Chem* 1969;244:2761-6

Singh Ahuja H, Liu S, Crombie DL, Boehm M, Leibowitz MD, Heyman RA, Depre C, Nagy L, Tontonoz P, Davies PJ. Differential effects of rexinoids and thiazolidinediones on metabolic gene expression in diabetic rodents. *Mol Pharmacol* 2001;59:765-73

Sjögren P, Sierra-Johnson J, Gertow K, Rosell M, Vessby B, de Faire U, Hamsten A, Hellenius ML, Fisher RM. Fatty acid desaturases in human adipose tissue: relationships between gene expression, desaturation indexes and insulin resistance. *Diabetologia* 2008;51:328-35

Sjöstrom L. Fatty acid synthesis de novo in adipose tissue from obese subjects on a hypercaloric high-carbohydrate diet. *Scand J Clin Lab Invest* 1973;32:339-49

Skurk T, Alberti-Huber C, Herder C, Hauner H. Relationship between adipocyte size and adipokine expression and secretion. *J Clin Endocrinol Metab* 2007;92:1023-33

Smas CM, Chen L, Zhao L, Latasa MJ, Sul HS. Transcriptional repression of pref-1 by glucocorticoids promotes 3T3-L1 adipocyte differentiation. *J Biol Chem* 1999;274:12632-41

Smas CM, Sul HS. Characterization of Pref-1 and its inhibitory role in adipocyte differentiation. *Int J Obes Relat Metab Disord* 1996;20 Suppl 3:S65-72

Smith PJ, Wise LS, Berkowitz R, Wan C, Rubin CS. Insulin-like growth factor-I is an essential regulator of the differentiation of 3T3-L1 adipocytes. *J Biol Chem* 1988;263:9402-8

Smith SJ, Cases S, Jensen DR, Chen HC, Sande E, Tow B, Sanan DA, Raber J, Eckel RH, Farese RV, Jr. Obesity resistance and multiple mechanisms of triglyceride synthesis in mice lacking Dgat. *Nat Genet* 2000;25:87-90

Smith U. Insulin responsiveness and lipid synthesis in human fat cells of different sizes: effect of the incubation medium. *Biochim Biophys Acta* 1970;218:417-23

Spalding KL, Arner E, Westermark PO, Bernard S, Buchholz BA, Bergmann O, Blomqvist L, Hoffstedt J, Naslund E, Britton T, Concha H, Hassan M, Ryden M, Frisen J, Arner P. Dynamics of fat cell turnover in humans. *Nature* 2008;453:783-7

Spector AA. Fatty acid binding to plasma albumin. *J Lipid Res* 1975;16:165-79

Spiegelman BM, Farmer SR. Decreases in tubulin and actin gene expression prior to morphological differentiation of 3T3 adipocytes. *Cell* 1982;29:53-60

Stahl A, Evans JG, Pattel S, Hirsch D, Lodish HF. Insulin causes fatty acid transport protein translocation and enhanced fatty acid uptake in adipocytes. *Dev Cell* 2002;2:477-88

Stefan N, Peter A, Cegan A, Staiger H, Machann J, Schick F, Claussen CD, Fritsche A, Haring HU, Schleicher E. Low hepatic stearoyl-CoA desaturase 1 activity is associated with fatty liver and insulin resistance in obese humans. *Diabetologia* 2008;51:648-56

Strawford A, Antelo F, Christiansen M, Hellerstein MK. Adipose tissue triglyceride turnover, de novo lipogenesis, and cell proliferation in humans measured with ^2H_2O. *Am J Physiol Endocrinol Metab* 2004;286:E577-88

Stremmel W, Pohl L, Ring A, Herrmann T. A new concept of cellular uptake and intracellular trafficking of long-chain fatty acids. *Lipids* 2001;36:981-9

Stubbs CD, Smith AD. The modification of mammalian membrane polyunsaturated fatty acid composition in relation to membrane fluidity and function. *Biochim Biophys Acta* 1984;779:89-137

Stump DD, Fan X, Berk PD. Oleic acid uptake and binding by rat adipocytes define dual pathways for cellular fatty acid uptake. *J Lipid Res* 2001;42:509-20

Stump DD, Zhou SL, Berk PD. Comparison of plasma membrane FABP and mitochondrial isoform of aspartate aminotransferase from rat liver. *Am J Physiol* 1993;265:G894-902

Sul HS, Smas C, Mei B, Zhou L. Function of pref-1 as an inhibitor of adipocyte differentiation. *Int J Obes Relat Metab Disord* 2000;24 Suppl 4:S15-9

Summers LK, Fielding BA, Bradshaw HA, Ilic V, Beysen C, Clark ML, Moore NR, Frayn KN. Substituting dietary saturated fat with polyunsaturated fat changes abdominal fat distribution and improves insulin sensitivity. *Diabetologia* 2002;45:369-77

Swierczynski J, Goyke E, Wach L, Pankiewicz A, Kochan Z, Adamonis W, Sledzinski Z, Aleksandrowicz Z. Comparative study of the lipogenic potential of human and rat adipose tissue. *Metabolism* 2000;49:594-9

Szendroedi J, Roden M. Ectopic lipids and organ function. *Curr Opin Lipidol* 2009;20:50-6

Tabor DE, Kim JB, Spiegelman BM, Edwards PA. Identification of conserved cis-elements and transcription factors required for sterol-regulated transcription of stearoyl-CoA desaturase 1 and 2. *J Biol Chem* 1999;274:20603-10

Tan GD, Debard C, Tiraby C, Humphreys SM, Frayn KN, Langin D, Vidal H, Karpe F. A "futile cycle" induced by thiazolidinediones in human adipose tissue? *Nat Med* 2003;9:811-2

Tan GD, Fielding BA, Currie JM, Humphreys SM, Desage M, Frayn KN, Laville M, Vidal H, Karpe F. The effects of rosiglitazone on fatty acid and triglyceride metabolism in type 2 diabetes. *Diabetologia* 2005;48:83-95

Tan GD, Savage DB, Fielding BA, Collins J, Hodson L, Humphreys SM, O'Rahilly S, Chatterjee K, Frayn KN, Karpe F. Fatty acid metabolism in patients with PPARgamma mutations. *J Clin Endocrinol Metab* 2008;93:4462-70

Tansey JT, Sztalryd C, Gruia-Gray J, Roush DL, Zee JV, Gavrilova O, Reitman ML, Deng CX, Li C, Kimmel AR, Londos C. Perilipin ablation results in a lean mouse with aberrant adipocyte lipolysis, enhanced leptin production, and resistance to diet-induced obesity. *Proc Natl Acad Sci U S A* 2001;98:6494-9

Tanti JF, Cormont M, Gremeaux T, Le Marchand-Brustel Y. Assays of glucose entry, glucose transporter amount, and translocation. *Methods Mol Biol* 2001;155:157-65

Tauchi-Sato K, Ozeki S, Houjou T, Taguchi R, Fujimoto T. The surface of lipid droplets is a phospholipid monolayer with a unique Fatty Acid composition. *J Biol Chem* 2002;277:44507-12

Tayek JA, Katz J. Glucose production, recycling, and gluconeogenesis in normals and diabetics: a mass isotopomer [U-13C]glucose study. *Am J Physiol* 1996;270:E709-17

Tchkonia T, Giorgadze N, Pirtskhalava T, Thomou T, DePonte M, Koo A, Forse RA, Chinnappan D, Martin-Ruiz C, von Zglinicki T, Kirkland JL. Fat depot-specific characteristics are retained in strains derived from single human preadipocytes. *Diabetes* 2006;55:2571-8

Tilghman SM, Hanson RW, Reshef L, Hopgood MF, Ballard FJ. Rapid loss of translatable messenger RNA of phosphoenolpyruvate carboxykinase during glucose repression in liver. *Proc Natl Acad Sci U S A* 1974;71:1304-8

Tobin KA, Ulven SM, Schuster GU, Steineger HH, Andresen SM, Gustafsson JA, Nebb HI. Liver X receptors as insulin-mediating factors in fatty acid and cholesterol biosynthesis. *J Biol Chem* 2002;277:10691-7

Trayhurn P, Wood IS. Adipokines: inflammation and the pleiotropic role of white adipose tissue. *Br J Nutr* 2004;92:347-55

Trigatti BL, Anderson RG, Gerber GE. Identification of caveolin-1 as a fatty acid binding protein. *Biochem Biophys Res Commun* 1999;255:34-9

van Harmelen V, Skurk T, Rohrig K, Lee YM, Halbleib M, Aprath-Husmann I, Hauner H. Effect of BMI and age on adipose tissue cellularity and differentiation capacity in women. *Int J Obes Relat Metab Disord* 2003;27:889-95

van Herpen NA, Schrauwen-Hinderling VB. Lipid accumulation in non-adipose tissue and lipotoxicity. *Physiol Behav* 2008;94:231-41

Vessby B, Gustafsson IB, Tengblad S, Boberg M, Andersson A. Desaturation and elongation of fatty acids and insulin action. *Ann N Y Acad Sci* 2002;967:183-95

Vessby B, Unsitupa M, Hermansen K, Riccardi G, Rivellese AA, Tapsell LC, Nalsen C, Berglund L, Louheranta A, Rasmussen BM, Calvert GD, Maffetone A, Pedersen E, Gustafsson IB, Storlien LH. Substituting dietary saturated for monounsaturated fat impairs insulin sensitivity in healthy men and women: The KANWU Study. *Diabetologia* 2001;44:312-9

Wang H, Iakova P, Wilde M, Welm A, Goode T, Roesler WJ, Timchenko NA. C/EBPalpha arrests cell proliferation through direct inhibition of Cdk2 and Cdk4. *Mol Cell* 2001;8:817-28

Wang J, Yu L, Schmidt RE, Su C, Huang X, Gould K, Cao G. Characterization of HSCD5, a novel human stearoyl-CoA desaturase unique to primates. *Biochem Biophys Res Commun* 2005;332:735-42

Wang L, Folsom AR, Zheng ZJ, Pankow JS, Eckfeldt JH. Plasma fatty acid composition and incidence of diabetes in middle-aged adults: the Atherosclerosis Risk in Communities (ARIC) Study. *Am J Clin Nutr* 2003;78:91-8

Wang Y, Kim KA, Kim JH, Sul HS. Pref-1, a preadipocyte secreted factor that inhibits adipogenesis. *J Nutr* 2006;136:2953-6

Warensjö E, Risérus U, Gustafsson IB, Mohsen R, Cederholm T, Vessby B. Effects of saturated and unsaturated fatty acids on estimated desaturase activities during a controlled dietary intervention. *Nutr Metab Cardiovasc Dis* 2008;18:683-90

Warne JP. Tumour necrosis factor alpha: a key regulator of adipose tissue mass. *J Endocrinol* 2003;177:351-5

Waters KM, Miller CW, Ntambi JM. Localization of a polyunsaturated fatty acid response region in stearoyl-CoA desaturase gene 1. *Biochim Biophys Acta* 1997;1349:33-42

Watkins PA. Very-long-chain acyl-CoA synthetases. *J Biol Chem* 2008;283:1773-7

Watson RT, Pessin JE. Subcellular compartmentalization and trafficking of the insulin-responsive glucose transporter, GLUT4. *Exp Cell Res* 2001;271:75-83

Wei Y, Wang D, Pagliassotti MJ. Saturated fatty acid-mediated endoplasmic reticulum stress and apoptosis are augmented by trans-10, cis-12-conjugated linoleic acid in liver cells. *Mol Cell Biochem* 2007;303:105-13

Wei Y, Wang D, Topczewski F, Pagliassotti MJ. Saturated fatty acids induce endoplasmic reticulum stress and apoptosis independently of ceramide in liver cells. *Am J Physiol Endocrinol Metab* 2006;291:E275-81

Weisberg SP, McCann D, Desai M, Rosenbaum M, Leibel RL, Ferrante AW, Jr. Obesity is associated with macrophage accumulation in adipose tissue. *J Clin Invest* 2003;112:1796-808

Weyer C, Foley JE, Bogardus C, Tataranni PA, Pratley RE. Enlarged subcutaneous abdominal adipocyte size, but not obesity itself, predicts type II diabetes independent of insulin resistance. *Diabetologia* 2000;43:1498-506

Wolfe RR, Herndon DN, Jahoor F, Miyoshi H, Wolfe M. Effect of severe burn injury on substrate cycling by glucose and fatty acids. *N Engl J Med* 1987;317:403-8

Wolins NE, Brasaemle DL, Bickel PE. A proposed model of fat packaging by exchangeable lipid droplet proteins. *FEBS Lett* 2006;580:5484-91

Wolins NE, Quaynor BK, Skinner JR, Schoenfish MJ, Tzekov A, Bickel PE. S3-12, Adipophilin, and TIP47 package lipid in adipocytes. *J Biol Chem* 2005;280:19146-55

Wolins NE, Rubin B, Brasaemle DL. TIP47 associates with lipid droplets. *J Biol Chem* 2001;276:5101-8

Xie W, Hamilton JA, Kirkland JL, Corkey BE, Guo W. Oleate-induced formation of fat cells with impaired insulin sensitivity. *Lipids* 2006;41:267-71

Xu Y, Mirmalek-Sani SH, Lin F, Zhang J, Oreffo RO. Adipocyte differentiation induced using nonspecific siRNA controls in cultured human mesenchymal stem cells. *Rna* 2007;13:1179-83

Xu Y, Mirmalek-Sani SH, Yang X, Zhang J, Oreffo RO. The use of small interfering RNAs to inhibit adipocyte differentiation in human preadipocytes and fetal-femur-derived mesenchymal cells. *Exp Cell Res* 2006;312:1856-64

Yahagi N, Shimano H, Hasty AH, Amemiya-Kudo M, Okazaki H, Tamura Y, Iizuka Y, Shionoiri F, Ohashi K, Osuga J, Harada K, Gotoda T, Nagai R, Ishibashi S, Yamada N. A crucial role of sterol regulatory element-binding protein-1 in the regulation of lipogenic gene expression by polyunsaturated fatty acids. *J Biol Chem* 1999;274:35840-4

Yamashita H, Takenoshita M, Sakurai M, Bruick RK, Henzel WJ, Shillinglaw W, Arnot D, Uyeda K. A glucose-responsive transcription factor that regulates carbohydrate metabolism in the liver. *Proc Natl Acad Sci U S A* 2001;98:9116-21

Yao-Borengasser A, Rassouli N, Varma V, Bodles AM, Rasouli N, Unal R, Phanavanh B, Ranganathan G, McGehee RE, Jr., Kern PA. Stearoyl-coenzyme A desaturase 1 gene expression increases after pioglitazone treatment and is associated with peroxisomal proliferator-activated receptor-gamma responsiveness. *J Clin Endocrinol Metab* 2008;93:4431-9

Yee JK, Mao CS, Hummel HS, Lim S, Sugano S, Rehan VK, Xiao G, Lee WN. Compartmentalization of stearoyl-coenzyme A desaturase 1 activity in HepG2 cells. *J Lipid Res* 2008;49:2124-34

Yoo H, Stephanopoulos G, Kelleher JK. Quantifying carbon sources for de novo lipogenesis in wild-type and IRS-1 knockout brown adipocytes. *J Lipid Res* 2004;45:1324-32

Yu K, Bayona W, Kallen CB, Harding HP, Ravera CP, McMahon G, Brown M, Lazar MA. Differential activation of peroxisome proliferator-activated receptors by eicosanoids. *J Biol Chem* 1995;270:23975-83

Zechner R, Strauss JG, Haemmerle G, Lass A, Zimmermann R. Lipolysis: pathway under construction. *Curr Opin Lipidol* 2005;16:333-40

Zhang L, Ge L, Parimoo S, Stenn K, Prouty SM. Human stearoyl-CoA desaturase: alternative transcripts generated from a single gene by usage of tandem polyadenylation sites. *Biochem J* 1999;340 (Pt 1):255-64

Zhang Y, Proenca R, Maffei M, Barone M, Leopold L, Friedman JM. Positional cloning of the mouse obese gene and its human homologue. *Nature* 1994;372:425-32

Zhao H, Serby MD, Smith HT, Cao N, Suhar TS, Surowy TK, Camp HS, Collins CA, Sham HL, Liu G. Discovery of 1-(4-phenoxypiperidin-1-yl)-2-arylaminoethanone stearoyl-CoA desaturase 1 inhibitors. *Bioorg Med Chem Lett* 2007;17:3388-91

Zheng Y, Eilertsen KJ, Ge L, Zhang L, Sundberg JP, Prouty SM, Stenn KS, Parimoo S. Scd1 is expressed in sebaceous glands and is disrupted in the asebia mouse. *Nat Genet* 1999;23:268-70

Zheng Y, Prouty SM, Harmon A, Sundberg JP, Stenn KS, Parimoo S. Scd3--a novel gene of the stearoyl-CoA desaturase family with restricted expression in skin. *Genomics* 2001;71:182-91

Zhou SL, Stump D, Sorrentino D, Potter BJ, Berk PD. Adipocyte differentiation of 3T3-L1 cells involves augmented expression of a 43-kDa plasma membrane fatty acid-binding protein. *J Biol Chem* 1992;267:14456-61

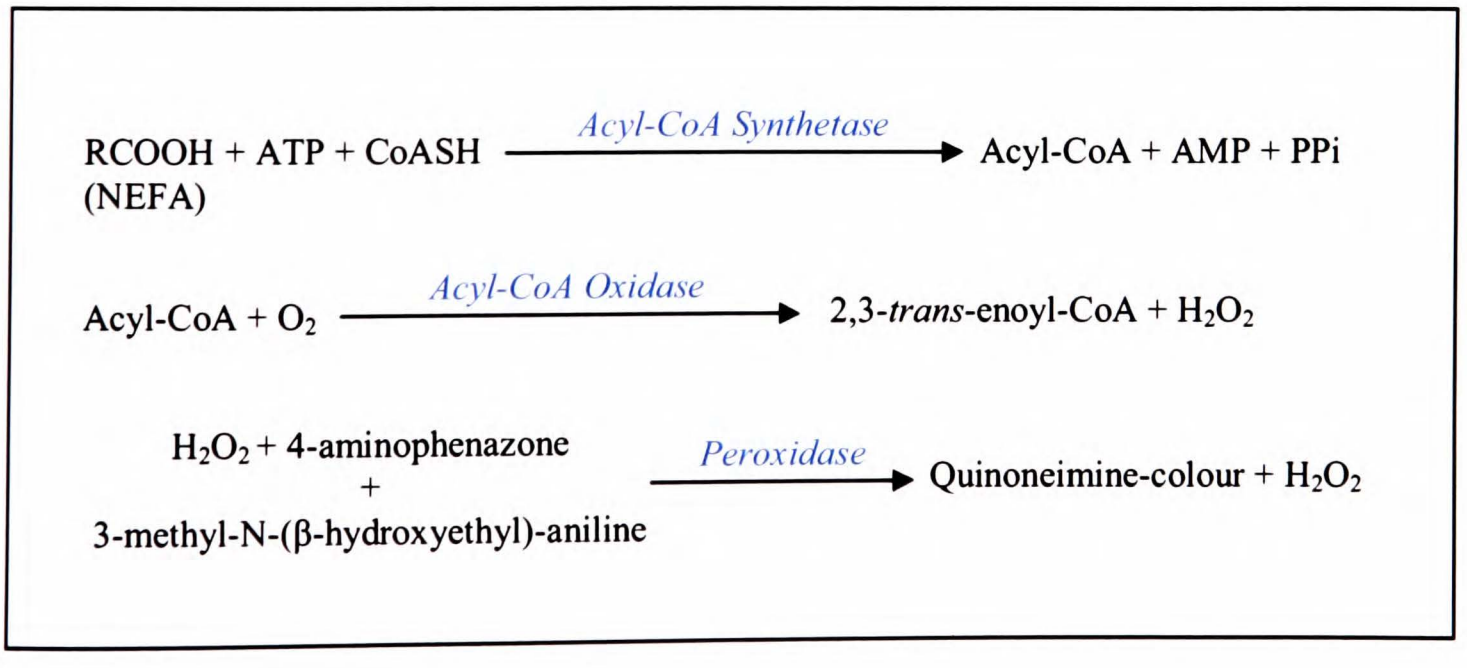
Zimmermann R, Strauss JG, Haemmerle G, Schoiswohl G, Birner-Gruenberger R, Riederer M, Lass A, Neuberger G, Eisenhaber F, Hermetter A, Zechner R. Fat mobilization in adipose tissue is promoted by adipose triglyceride lipase. *Science* 2004;306:1383-6

Appendix 1

Experimental Protocols

A1.1 PREPARATION OF [U-^{13}C]PALMITATE STOCK SOLUTIONS

Stock solutions of approximately 10 mM [U-^{13}C]palmitate were prepared in 10 % fatty acid-free bovine serum albumin (BSA) (Sigma, UK). 10 % BSA solutions were made in Dulbecco's Eagle's Medium Nutrient Mixture (DMEM)/F12 HAM (v/v, 1:1). The uniformly labelled sodium palmitate was added to the 10 % BSA solution and heated to 65 °C (the melting point of palmitate) and then sonicated for 10 seconds, 3 times. The palmitate stock solution was filtered using a 0.2 μm pore sized filter. Due to the insolubility and high melting point of palmitate, this fatty acid does not readily go into solution, therefore, the exact concentration of the fatty acid solution was measured using an enzymatic colourimetric assay. The fatty acid concentration was measured using a commercial non-esterified fatty acid (NEFA) kit (Wako, Alpha Laboratories Ltd, Hampshire, UK) on an ILAB™ 600 Clinical Chemistry Analyser (Instrumentation Laboratories, Warrington, UK). The detection is based on the following principle:



The intensity of the red pigment (quinonimine) is proportional to the concentration of NEFA and is measured at a wavelength of 550 nm.

A1.2 LIPID EXTRACTION FROM ADIPOCYTES

Total lipids were extracted from cells using the method described by Folch *et al.* (Folch *et al.*, 1957). Cells were harvested in 0.5 ml phosphate buffered saline (PBS) and 5 ml of 2:1 (v/v) chloroform/methanol with 100 mg/l butylated hydroxytoluene and 50 µg TG internal standard (tripentadecanoin, 15:0) and 50 µg PL internal standard (phosphatidylcholine, dipentadecanoyl,15:0) were added to the samples. Samples were shaken by hand for 2 minutes then placed on a rotary mixer for a further 15 minutes. Phases were separated by adding 1 ml of 1 M NaCl, samples mixed by vortex then centrifuged for 10 min at 14 °C at 2000 rpm. The upper, aqueous layer was aspirated off and the lower solvent layer was transferred to a fresh tube and evaporated to dryness under nitrogen at 50 °C.

Lipid fractions were separated by solid-phase extraction using aminopropyl columns (Varian Ltd, Oxford, UK) (Burdge *et al.*, 2000). Columns were washed with 2 ml acetone and primed with 2 ml chloroform under vacuum. Dried samples were reconstituted in 1 ml chloroform and added to the columns and allowed to drip through into a clean collection tube. Non-polar lipids (TG and cholesteryl ester) were eluted by adding a further 2 ml chloroform to the column. Collection tubes were replaced with new tubes and the non-acidic phospholipids were eluted using 2 ml 3:2 (v/v) chloroform/methanol. All eluates were evaporated to dryness under nitrogen at 50 °C. The non-polar lipid-containing fraction was further separated using a new set of columns, primed with hexane. The TG fraction was eluted using 2 ml 100:5:5 (v/v/v) hexane: chloroform: ethyl acetate and evaporated to dryness under nitrogen.

Fatty acid methyl esters (FAMEs) were prepared for gas chromatography analysis. Lipid extracts were reconstituted with 400 µl toluene and transferred to a new tube with 800 µl of either 1.5 % (for TG) or 6 % (PL) (v/v) sulphuric acid in methanol. The tubes were mixed by vortex and placed in a water-bath at 80 °C for either 1 h (TG) or 2 h (PL). Samples were then cooled then neutralised with 2 ml neutralising reagent (a solution of 25 g $KHCO_3$ plus 34.g K_2HCO_3, diluted 1 in 5) and 2 ml cyclohexane were added. The tubes were mixed on a rotary mixer for 15 minutes and centrifuged for 10 min at 4 °C at 2000 rpm. The upper solvent phase, containing the FAMEs was transferred into a glass tube and evaporated to dryness under nitrogen. For some samples, the lower aqueous phase, containing glycerol was kept at -20 ° C for derivatisation at a later stage (section **A1.4**). The lipid was reconstituted in 200 µl chloroform, and put into micro GC vials (Hewlett Packard, Wokingham, Berkshire, UK) for analysis.

A1.3 GAS CHROMATOGRAPHY ANALYSIS OF TG AND PL FATTY ACIDS

Gas chromatography was performed using an Agilent 6890N GC (Agilent Technologies, Stockport, UK) fitted with a 25 m x 0.32 mm capillary column (FFAP-CB), with stationary phase composed of polyethylene glycol nitroterephthalic acid ester chemically bonded to a fused silica column. This column was originally designed for the chromatography of free fatty acids, but is also suitable for methyl ester derivatives and has the advantage of stability due to chemically bonded liquid phase. The carrier and make-up gasses were helium and nitrogen respectively with a column flow of 1 ml/min and the samples were run using a splitless injection technique. The GC operated at an initial temperature of 50 °C with a series of

programmed temperature increments to 240 °C, enabling the resolution of fatty acids from 8:0 to 24:0 within 46 min. Individual fatty acid peaks were identified by reference to known FAMEs. The fatty acid concentrations were calculated relative to the internal standard and the results were expressed as μmol/l, or the percentage of a fatty acid was calculated based on the area of the fatty acid peak. **Figure A1-1** shows a typical gas chromatogram of the TG fatty acids present in a sample of adipocytes harvested after 14 days of differentiation without exogenous fatty acids.

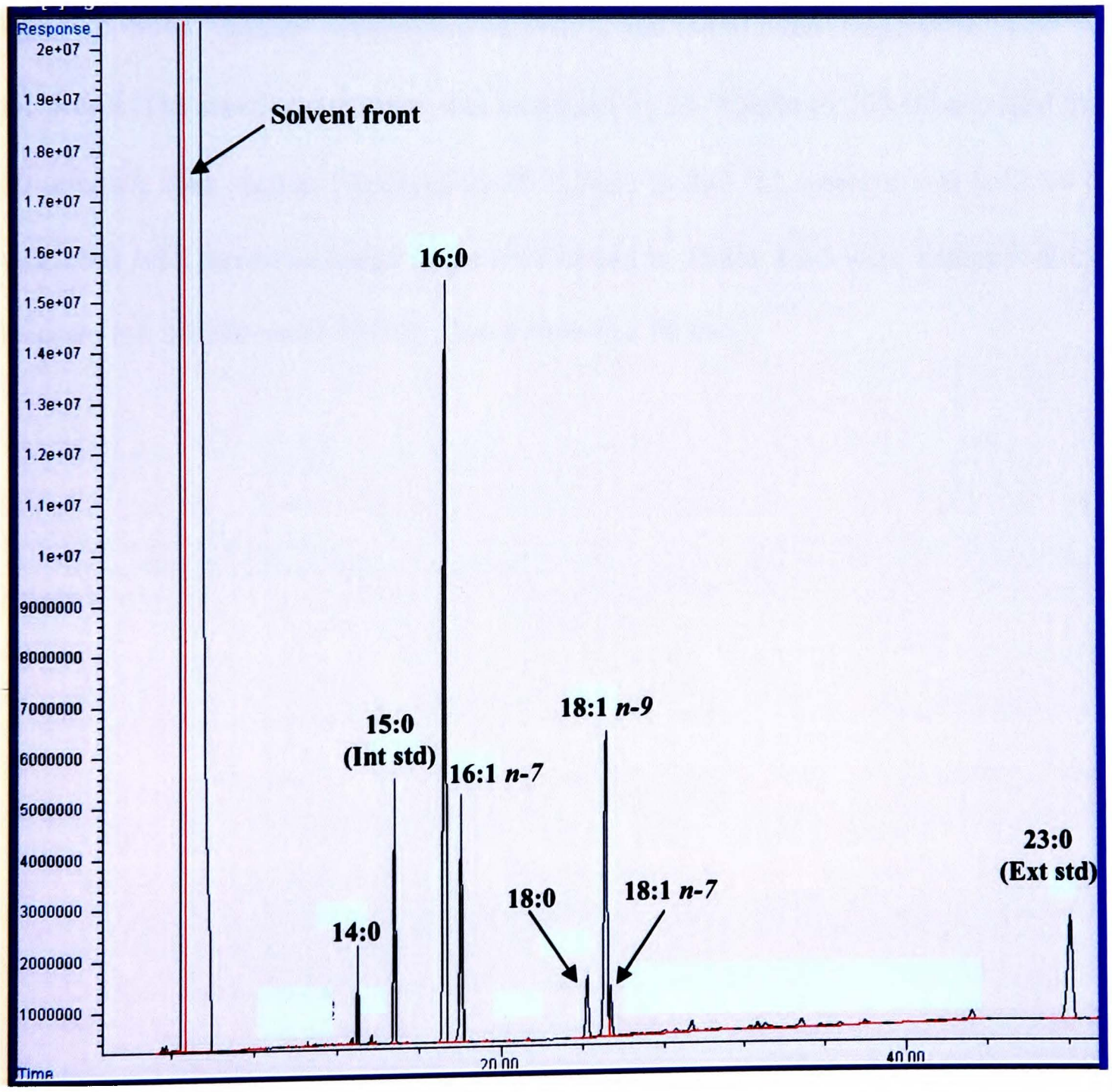


Figure A1-1 Typical gas chromatogram from adipocytes differentiated without exogenous fatty acid. The x-axis shows the retention time of the fatty acid on the GC column and the y-axis shows the response, that is, the abundance of each fatty acid. Int std and ext std = internal standard and external standard, respectively.

A1.4 GAS CHROMATOGRAPHY-MASS SPECTROMETRTY ANALYSIS OF ISOTOPICALLY ENRICHED FATTY ACIDS

Incorporation of ^{13}C into fatty acids was analysed using a 5890 gas chromatograph coupled to a 5973N mass spectrometer (Agilent Technologies, Stockport, UK).

The GC was equipped with a DB-Wax 30 m capillary column (from Agilent, i.d.0.25 mm, film thickness 0.25 μm). The sample (1.0 μl) was introduced using the splitless injection mode, injector temperature of 250 °C and initial oven temperature of 80 °C for 5 min. The oven temperature was increased by 25 °C/min to 200 °C and held for 10 minutes, then further increased by 25 °C/min to 230 °C, where it was held for 2 min. Ions with mass-to-charge ratios (m/z) listed in **Table A1-1** were determined by selected ion measurement (SIM). Dwell time was 50 ms.

Fatty acid	Shorthand name	Isotopomer	m/z
Myristic acid	14:0	M + 0	242.2
		M + 14	256.2
Palmitic acid	16:0	M + 0	270.3
		M + 16	286.3
Palmitoleic acid	16:1 *n-7*	M + 0	268.3
		M + 16	284.3
Stearic acid	18:0	M + 0	298.3
		M + 16	314.3
Oleic acid	18:1 *n-9*	M + 0	296.3
		M + 16	312.3
Vaccenic acid	18:1 *n-7*	M + 0	296.3
		M + 16	312.3

Table A1-1 Mass-to-charge ratios of FAMEs measured using SIM.

As oleic acid and vaccenic acid have the same m/z values, they were distinguished from each other by running individual FAMEs for each of these fatty acids through the GC and overlaying the spectra.

In the experiments in **Chapter 3**, where the carbon contribution from acetate, glucose and glutamine was determined, carbon composition of all DNL-derived fatty acids was calculated from the mass-to-charge ratio determined using SCAN mode. All fatty acids were corrected for natural enrichment using the isotope pattern for each fatty acid methyl ester from control samples (with no labelled exogenous fatty acid

present), which were also compared to isotope patterns obtained from Sheffield ChemPuter (http://winter.group.shef.ac.uk/chemputer/) (**Table A1-2**).

Fatty acid	Formula (FAME)	Mass	% enrichment (calculated from controls)	% enrichment (from ChemPuter)
Myristate	$C_{15}H_{30}O_2$	242	100	100
		243	17.7	16.6
		244	2.1	1.7
		245	0.6	0.1
Palmitate	$C_{17}H_{34}O_2$	270	100	100
		271	21.2	18.8
		272	2.5	2.1
		273	0.2	0.2
Palmitoleate	$C_{17}H_{32}O_2$	268	100	100
		269	21.1	18.8
		270	2.3	2.1
		271	0.7	0.2
Stearate	$C_{19}H_{38}O_2$	298	100	100
		299	21.5	21
		300	2.8	2.5
		301	0.4	0.2
Oleate/Vaccenate	$C_{19}H_{36}O_2$	296	100	100
		297	22.4	21
		298	2.8	2.5
		299	0.3	0.2

Table A1-2 Natural enrichment of fatty acid isotopomers used for corrections in Chapter 3.

A1.4.1 Mass isotopomer distribution analysis (MIDA)

MIDA was developed by Hellerstein and Neese in 1991 to calculate combinatorial probabilities of the polymerisation of repeating monomeric subunits, such as the acetyl-CoA subunits used during fatty acid synthesis, and has since been applied to the analysis of cholesterol and protein synthesis (Hellerstein *et al.*, 1991; Hellerstein & Neese, 1992; Hellerstein & Neese, 1999). By enriching the precursor pool of the polymer to be studied with a stable isotope, end-product polymers are created,

containing the isotopically labelled precursor subunit in different amounts, thus differing in mass. These polymers of different masses are referred to as isotopomers, and their relative abundances can be measured by mass spectrometry analysis. MIDA aims to calculate the frequency distribution of the enriched polymer and can be used to calculate parameters such as the absolute synthesis rate and precursor pool enrichment.

A1.4.2 Purity measurements of isotopically labelled palmitate and glucose

The purity of [U-^{13}C]palmitate was assessed by creating a FAME of the labelled fatty acid and determining its isotopomer composition by GC-MS. The purity was found to be 91.0 %. Importantly, there was no contamination with [U-^{13}C]myristate.

Glucose purity was determined by analysing a derivatised sample of the labelled glucose using GC-MS and measuring the isotopomer composition. The purity of the glucose was found to be 96.0 %.

A1.5 GLYCEROL ANALYSIS

A1.5.1 Glycerol extraction and derivatisation

Glycerol was extracted from the aqueous phase left over after the triglyceride fatty acids was derivatised as follows. Ion exchange columns were prepared by layering 1 cm of a cationic resin (AG 50W-X8, 100-200 mesh, hydrogen form, Bio-Rad Lab, Inc) on top of 1 cm anionic resin (AG-1-X8, 100 - 200 mesh, formate form, Bio-Rad Lab Inc) in polypropylene filter columns (Evergreen Scientific filter column – mesh

300-3366-020). The cationic and anionic resins removed any contaminating amino acids and pyruvate/lactate, respectively. Columns were washed with 3 x 1 ml distilled water. Clean 7 ml screw-topped glass vials were used as collection tubes and the aqueous, glycerol-containing fraction was added to the columns and allowed to drip through. Columns were washed with 3 x 1ml distilled water and the eluate in the same 7 ml collection tubes. Samples were then evaporated to dryness in a centrifugal evaporator for 6 hours at 55 °C.

Lyophilised samples were reconstituted in 100 µl pyridine (Sigma Aldrich P5, 750-6), vortex mixed and 100 µl *N*-Methyl-*N*-[tert-butyldimethyl-silyl]trifluoroacetimide (MTBSTFA) (Perbio Science, UK) added, vials capped and vortex mixed. Samples were heated in a heating block at 70 °C for 4 hours then left at room temperature overnight. Samples were evaporated to dryness in a centrifugal evaporator for 100 minutes at 5 °C before being reconstituted in 200 µl of pyridine and transferred to a gas chromatography vial.

Glycerol was extracted using ion exchange chromatography and tert.-butyldimethylsilyl glycerol derivatives created and analysed by GC-MS.

A1.5.2 Measurement of glycerol by GC-MS

Glycerol was measured using a GC equipped with a DB-Wax 30 m capillary column (from Agilent, i.d.0.25 mm, film thickness 0.25 µm). The sample (1 µl) was injected onto the column at an initial oven temperature of 110 °C. The oven temperature was ramped at 10 °C/min to 210 °C and then at 20 °C/min to 310 °C and was held at this temperature for 3 min for a total of 18 min. Injector and interface were 320 °C and gas

flow 1.1 ml/min. The sample was injected at split ratio 50:1. The major peak corresponds to a fragmentation where a butyl group is removed and results in a molecule with a mass to charge ratio (*m/z*) of 377.3, thus, the peaks of *m/z* 377.3 and *m/z* 382.3 were measured using SIM.

Glycerol was corrected for natural enrichment using the isotope pattern obtained from Sheffield ChemPuter (http://winter.group.shef.ac.uk/chemputer/) (**Table A1-3**).

Mass	% enrichment
377	100
378	34.2
379	15.9
380	3.7

Table A1-3 Natural enrichment of glycerol

A1.6 GENE EXPRESSION ANALYSES

A1.6.1 Total RNA extraction

Cells were harvested in 0.5 ml Tri Reagent (Ambion, Texas, USA) and transferred to a 2 ml PhaseLock gel Eppendorf tube (catalogue number. 955154045, Eppendorf, UK). 100 µL of chloroform was added, shaken by hand for 15 seconds and incubated at room temperature for 2-3 minutes before centrifugation at 12,000g for 15 minutes at 4 °C. The upper, RNA-containing aqueous phase was transferred to a clean tube and an equal volume of isopropanol added. Samples were precipitated at -80 °C overnight. RNA was then collected by centrifugation at 12,000g for 20 minutes at 4 °C, isopropanol aspirated off then the pellets washed with 0.5 ml 70 % ethanol. The pellets were once again collected by centrifugation at 7,500g for 5 minutes at 4 °C, ethanol aspirated off and the pellets were then air dried at room temperature. Once

dry, RNA was resuspended in 10 µL RNA storage solution (Ambion, Texas, USA). Any contaminating genomic DNA was digested using 1 µl of DNase buffer and 0.5 µl of DNase I (DNA-*free*™, Ambion, Texas, USA).

A1.6.2 cDNA synthesis and real-time PCR

cDNA was synthesized by reverse transcription from 500 ng RNA using SuperScript III First-Strand Synthesis System (Invitrogen, Paisley, UK). A cDNA standard was created from a pool of each sample and diluted 1/50, 1/100, 1/500 and 1/1000 in 10 mM Tris, pH 8.0. All samples were diluted 1/100 and mRNA expression analysed in triplicate by real-time polymerase chain reaction (PCR) using the Applied Biosystems (Warrington, UK) Assays-on Demand TaqMan® gene expression assays listed in **Table A1-4** with TaqMan® Universal PCR Master Mix (Applied Biosystems, Warrington, UK) and run on either a Rotorgene real-time PCR machine (Corbett Research, Sydney, Australia) or an Applied Biosystems 7900HT real-time PCR machine (Applied Biosystems, Warrington, UK) in a final volume of 8 µl. All target genes were normalised to the geometric mean of three housekeeping genes: *PPIA*, *PGK1*, and *S18* (listed in red in **Table A1-4**).

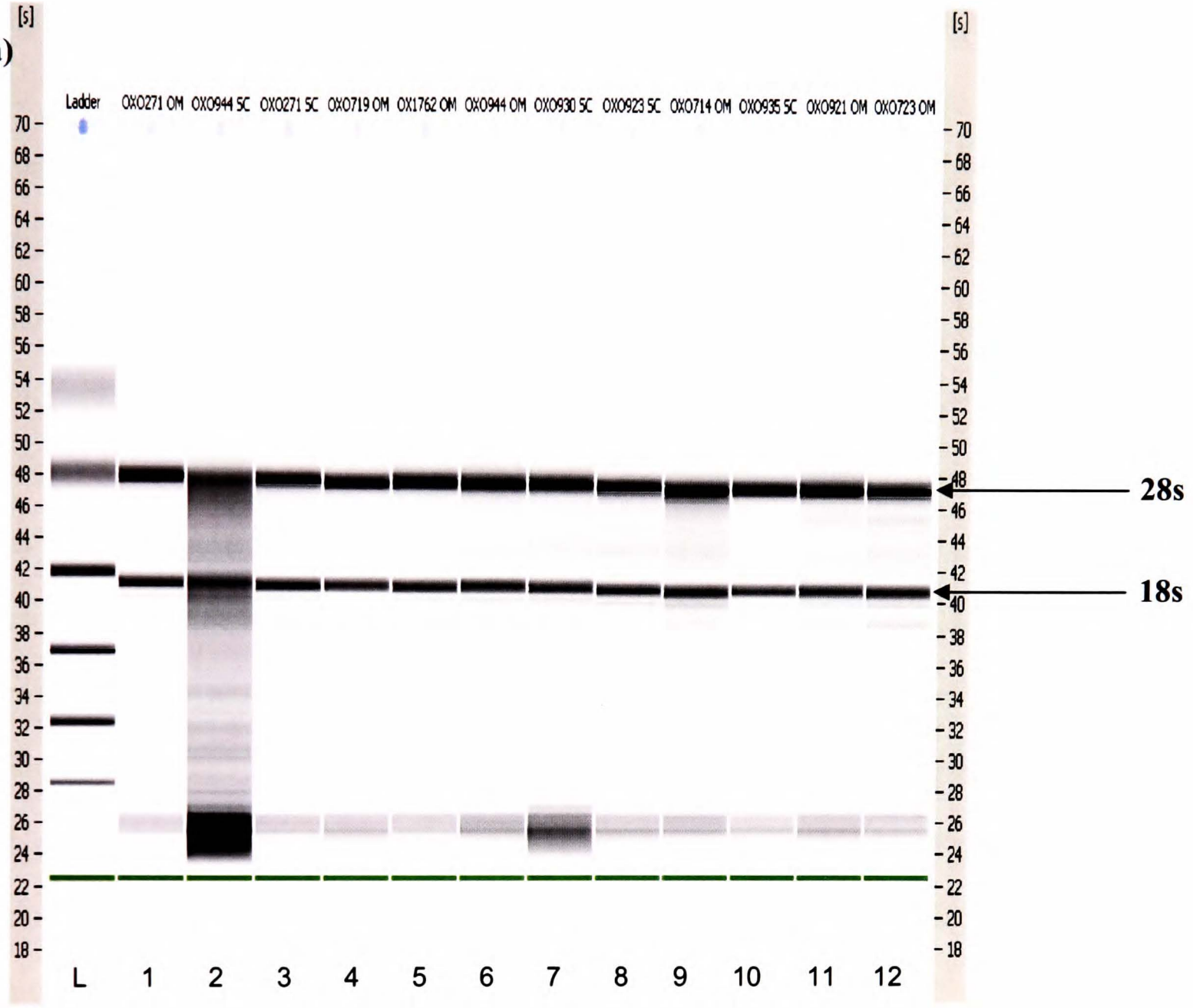
Gene symbol	Gene name	ABI assay ID
ACACA	Acetyl-CoA carboxylase	Hs00167385_m1
ACLY	ATP-citrate lyase	Hs00153764_m1
ADIPOQ	Adiponectin, C1Q and collagen domain containing	Hs00605917_m1
AIFM2	Apoptosis-inducing factor, mitochondrion-associated, 2	Hs00262251_m1
CD36	CD36 molecule (thrombospondin receptor)	Hs00169627_m1
COL11A1	Collagen, type XI, alpha 1	Hs00266273_m1
DDIT4L	DNA-damage-inducible transcript 4-like	Hs00293956_m1
DGAT2	diacylglycerol O-acyltransferase homolog 2	Hs00261438_m1
ELOVL6	ELOVL family member 6, elongation of long chain fatty acids	Hs00225412_m1
FABP4	Fatty acid binding protein 4	Hs00609791_m1
FABP5	fatty acid binding protein 5 (psoriasis-associated)	Hs02339439_g1
FASN	Fatty acid synthase	Hs00188012_m1
FSTL1	Follistatin-like 1	Hs00200053_m1
G6PD	Glucose-6 phosphate dehydrogenase	Hs00166169_m1
INMT1	Indolethylamine N-methyltransferase	Hs00198941_m1
LEP	Leptin	Hs00174877_m1
LPL	Lipoprotein lipase	Hs00173425_m1
PPARG	Peroxisome proliferator-activated receptor gamma	Hs00234592_m1
PLIN	Perilipin	Hs00160173_m1
PTPRF	Protein tyrosine phosphatase, receptor type, F	Hs00160858_m1
SC4MDL	Sterol-C4-methyl oxidase-like	Hs00198833_m1
SCD	Stearoyl-CoA desaturase	Hs00748952_s1
SFRP1	Secreted frizzled-related protein 1	Hs00610060_m1
SREBF1	Sterol regulatory element binding protein 1c	Hs00231674_m1
TNC	Tenascin C (hexabrachion)	Hs00233648_m1
PGK1	Phosphoglycerate kinase 1	Hs99999906_m1
PPIA	Cyclophilin	Hs99999904_m1
S18	Eukaryotic 18S rRNA	Hs99999901_s1

Table A1-4 Applied Biosystems Assays-on-Demand TaqMan® gene expression assays

A1.7 MICROARRAY ANALYSIS

Microarrays were used to assess global changes in gene expression in response to palmitate. Isolated RNA from cultured adipocytes was used to generate labelled cRNA which was then fragmented and hybridised to microarray slides. RNA concentration was determined using a NanoDrop ND-1000 spectrophotometer (Thermo Fisher Scientific, Basingstoke, UK) and each sample was diluted to a concentration of 250 ng/μl. Prior to cRNA synthesis, RNA quality was assessed using an Agilent 2100 Bioanalyzer and an Agilent RNA 6000 Nano kit (Agilent Technologies Inc, Waldbronn, Germany) (**Figure A1-2**). Quality was determined from the ratio of 28s/18s, an ideal ratio being 2.

(a)



(b)

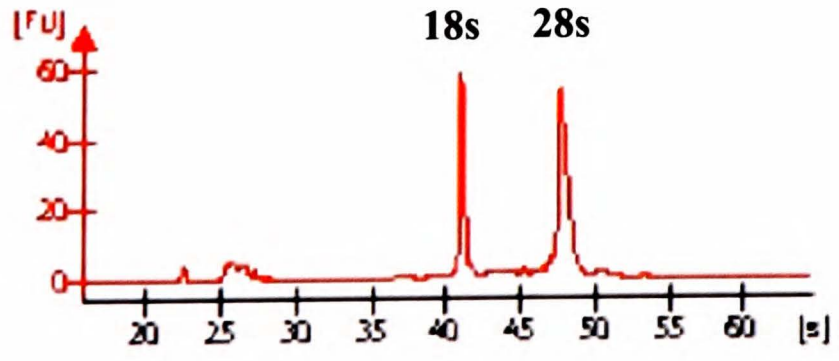


Figure A1-2 Quality assessment of RNA showing (a) a simulated gel image (x-axis is labelled L for ladder and samples 1 to 12) and (b) an electropherogram for one of the samples

A1.7.1 cRNA synthesis

Biotin-labelled cRNA was synthesised using the Codelink™ iExpress assay reagent kit (Applied Microarrays, Warrington, UK). Synthesis of first-strand cDNA was prepared as follows. For each RNA sample, 2 µl RNA (500 ng), 1 µl T7 Oligo(dT) Primer was added to a microcentrifuge tube. Each sample was spiked with 2.5 µl of a stock solution of 50.2 pg/µl bacterial mRNA (ranging in concentration from 1:1,000 to 1:1,024,000), acting as a positive control. The final volume was made up to 12 µl with 7.5 µl nuclease-free water. Each sample was incubated for 10 minutes at 70 °C, to denature the RNA, then immediately placed on ice for 3 minutes to cool. The samples were centrifuged for 5 seconds at full speed to collect the sample at the bottom of the tubes, and placed back on ice. To each sample the following was added: 2 µl 10x First Strand Buffer, 4 µl 5 mM dNTP mix, 1 µl RNase Inhibitor and 1 µl ArrayScript (giving a final volume of 20 µl per sample). Samples were centrifuged at full speed for 5 seconds and incubated for 2 hours at 42 °C in an air incubator. After 2 hours, samples were centrifuged at full speed for 5 seconds and placed on ice.

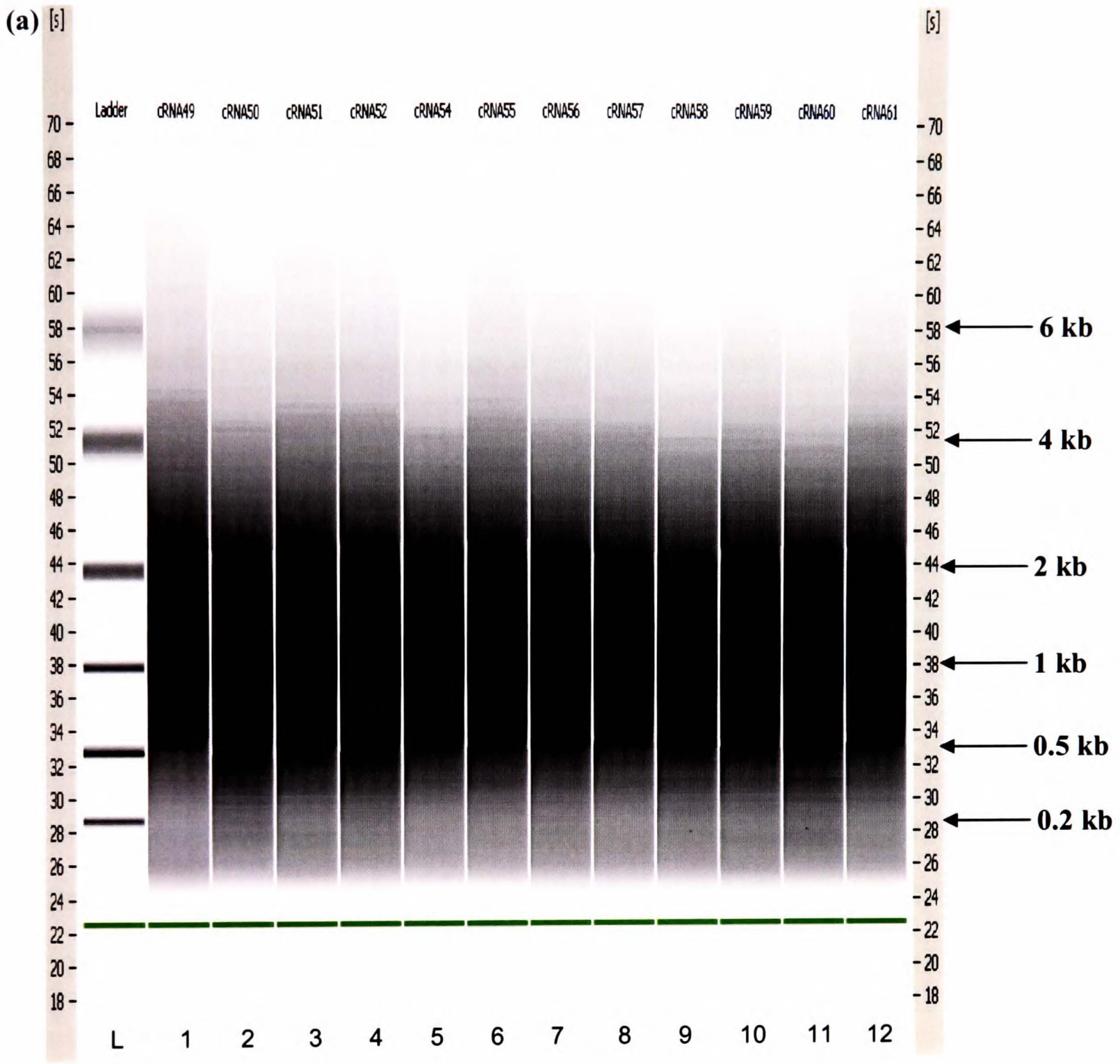
Second-strand cDNA synthesis buffer containing 63 µl nuclease-free water, 10 µl Second Strand Buffer, 4 µl 5 mM dNTP Mix, 2 µl DNA Polymerase and 1 µl RNase H (80 µl final volume) was prepared for each sample. This was added to the 20 µl first-strand cDNA sample, centrifuged at full speed for 5 seconds and incubated for 2 hours at 16 °C in a pre-chilled refrigerated incubator. The samples were then placed on ice.

The double-stranded cDNA was next purified. 250 µl cDNA Binding Buffer was added to the double-stranded cDNA sample and mixed by gently pipetting up and down. The samples were then carefully transferred to the centre of a cDNA filter cartridge (seated in a collection centrifuge tube). The lid of the collection tube was closed over the cartridge and the samples were centrifuged at 10,000 x g for 1 minute. The eluate was discarded from the collection tube, the cartridge was placed back into the tube and the lid was closed before centrifuging the sample for 1 minute at 10,000 x g for 1 minute to dry the column. The cartridge was then transferred to a clean collection tube. The cDNA was eluted using 12 µl nuclease-free water, preheated to 50 to 55 °C, which was added to the centre of the filter of the cartridge. The collection tube was closed and allowed to stand for 2 minutes at room temperature before being centrifuged at 10,000 x g for 1.5 minutes. This step was repeated once more to generate a final volume of 20 µl purified cDNA.

The next step was to synthesise biotin-labelled cRNA. An *in vitro* transcription (IVT) mix was prepared for each sample consisting of 12 µl Biotin-NTP Mix, 4 µl 10x T7 Reaction Buffer and 4 µl 10x T7 Enzyme Mix (final volume of 20 µl). The mix was centrifuged at full speed for 5 seconds and placed on ice. 20 µl IVT mix was then transferred to each purified cDNA sample and gently pipetted up and down, and gently flicked, to mix. The contents of the tube were then collected at the bottom of the tube by centrifugation at full speed for 5 seconds. The samples were incubated for 14 hours overnight in an air incubator at 36 °C. After 14 hours, the total volume of each sample was adjusted to 100 µl by adding 60 µl of nuclease-free water (at room temperature). Samples were briefly vortexed and centrifuged for 5 seconds at full speed. To each sample, 350 µl cRNA Binding Buffer was added, then 250 µl of

100 % ethanol. Samples were mixed by gentle pipetting up and down. Each sample was carefully transferred to a cRNA filter cartridge, seated in a collection centrifuge tube. The lids were sealed and samples were centrifuged for 1 minute at 10,000 x g. The eluate was discarded and the cartridge was replaced in the tube. 650 µl of Wash Buffer was added to each cartridge and samples were centrifuged at 10,000 x g for 1 minute. The eluate was again discarded and the cartridge was place back into the collection tube. The collection tubes were sealed and were centrifuged once more at 10,000 x g for 1 minute to dry each cRNA filter cartridge. The cRNA filter cartridge was placed into a clean collection tube and 100 µl of nuclease-free water (pre-heated to 50 to 60 °C) was pipetted directly onto the cRNA filter cartridge membrane. The lids of the collection tubes were closed and the tubes were left to sit at room temperature for 2 minutes. The cRNA was eluted by centrifugation at 10,000 x g for 1.5 minutes. The columns were then removed, leaving the purified labelled cRNA in the tube.

The quantity of the labelled cRNA was measured using a NanoDrop ND-1000 spectrophotometer. cRNA quality was assessed using an Agilent 2100 Bioanalyzer and an Agilent RNA 6000 Nano kit (Agilent Technologies Inc, Waldbronn, Germany) (**Figure A1-3**). A good cRNA reaction was represented by a smear of products falling between 0.5 and 3 kilobases (kb) long, with a peak between 1 and 2 kb.



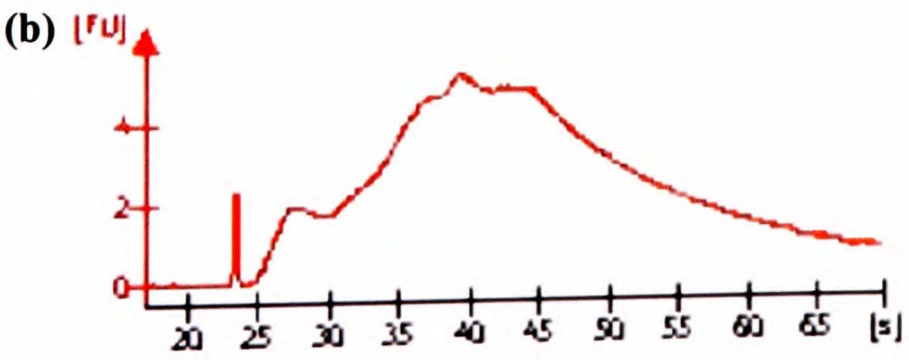


Figure A1-3 Quality assessment of labelled cRNA showing (a) a simulated gel image (x-axis is labelled L for ladder and samples 1 to 12) and (b) an electropherogram for one of the samples.

A1.7.2 Microarray hybridisation and detection

Hybridisation and detection of biotin-labelled cRNA was achieved using the Codelink gene expression system: Single-assay bioarray hybridisation and detection kit (GE Healthcare).

cRNA was first fragmented by adding 10 µg of cRNA (made up to a final volume of 20 µl using nuclease-free water) to 5 µl of fragmentation buffer and incubated at 94 °C for 20 minutes. Hybridisation reaction mixture was prepared using the 10 µg sample of fragmented cRNA, 78 µl of hybridisation buffer component A and 130 µl of hybridisation buffer component B to a final volume of 260 µl. This was incubated for 5 minutes at 90 °C then immediately chilled on ice of 5 to 30 minutes. 250 µl of the hybridisation reaction mixture was slowly and carefully loaded onto the microarray slide through an input port in the corner of the slide, and the ports sealed. The slides were then placed in a shaking incubator set to 300 rpm for 24 hours at 37 °C for hybridisation to occur. The slides were then unsealed, the protective covers removed, and washed in a reservoir containing 0.75 x TNT[5] solution, then transferred to another reservoir containing 0.75 x TNT preheated to 46 °C and incubated at 46 °C for exactly 1 hour.

Microarray slides were then incubated for 30 minutes at room temperature in a 1:500 solution of Cy5-Streptavidin (diluted in TNB solution comprising 0.1 M Tris-HCl, pH 7.6, 0.15 M NaCl and 0.5 % NEN blocking reagent). Microarray slides were next washed 3 times with 1 x TNT solution, for 5 minutes each wash, then rinsed in 0.1 x SSC/0.05 % Tween (comprising 994.5 ml deionised water, 0.5 ml Tween and 5 ml of

[5] 1 x TNT buffer consisted of 0.10 M Tris-HCl, pH 7.6, 0.15 M NaCl and 0.05% Tween 20. A 0.75 solution was made by diluting the 1 x TNT solution with distilled water.

20 x SSC buffer (Ambion)). Slides were then immediately centrifuged at 2, 000rpm for 3 minutes to dry and stored in the dark.

A1.8 STAINING OF CELLULAR PROTEINS AND LIPIDS

A1.8.1 Oil red O staining of neutral lipids

Differentiated preadipocytes, cultured on 8-well Permanox chambered slides (Nunc, New York, USA) were washed with phosphate buffered saline (PBS) and fixed in 2.5 % paraformaldehyde prior to staining. 0.5 % oil red O (ORO) in propan-2-ol (w/v) was diluted 3:2 with distilled water and filtered. Slides were stained with filtered ORO for 30 minutes at 37 °C, destained briefly with 60 % isopropanol and washed with water. Cells were then counterstained with haematoxylin for 1-2 minutes, washed with water, the chambers were removed and the slides mounted in PBS/glycerol.

A1.8.2 Pref-1 staining

Preadipocytes and adipocytes grown on 8-well Permanox slides (Nunc, New York, USA) were washed with PBS and fixed in 2.5 % paraformaldehyde for at least 20 minutes. The paraformaldehyde was aspirated off and cells were washed 3 times for 5 minutes in Tris buffered saline (TBS) (0.2M TrisHCl, pH7.4 diluted 1/10 with 0.9 % NaCl). One of these washes contained 0.001 % Triton X to permeablise the cell membrane. Endogenous peroxidase activity was blocked by incubating the cells in 0.3 % in 0.3% H_2O_2 in methanol for 20 minutes at room temperature, then washed 3

times for 5 minutes with TBS. Slides were then incubated in normal swine serum, diluted 1/20 with Tris buffer (TB) (0.2M TrisHCl, pH7.4), for 30 minutes, to block any non-specific antibody binding. The swine serum was removed and cells were next incubated with 2 μg/ml Pref-1 rabbit polyclonal antibody (AbCam, Cambridge, UK) overnight at 4 °C.

The next day, cells were washed 3 times for 5 minutes in TBS the incubated with anti-rabbit biotin (Dako, Denmark), diluted 1/100 for 30 minutes. Cells were washed again 3 times for 5 minutes in TBS then incubated with horseradish peroxidise-avidin (Vector Laboratories, California, USA), diluted 1 in 1000, for 30 minutes at room temperature. Cells were finally incubated in diaminobenzidine hydrochloride (DAB)/hydrogen peroxide for a maximum of 5 minutes, washed twice with TBS and mounted in PBS/glycerol.

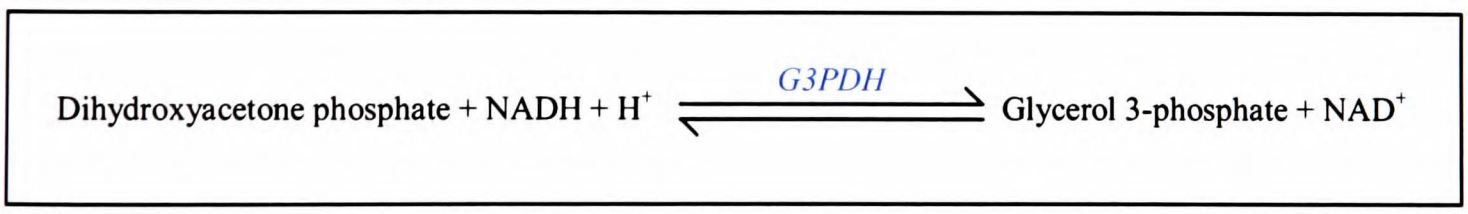
A1.8.3 SCD staining

Adipocytes grown on 8-well Permanox slides (Nunc, New York, USA) were washed with PBS and fixed in 2.5 % paraformaldehyde for 20 minutes. The paraformaldehyde was aspirated off and cells were washed 3 times in Tris buffered saline (TBS). One of these washes contained 0.001 % Triton X to permeablise the cell membrane. Cells were then incubated in swine serum, diluted 1/20 with Tris buffer (TB), for 30 minutes. The swine serum was removed and cells were next incubated with 4 μg/ml SCD goat polyclonal antibody (SantaCruz Biotechnology, Heidelberg, Germany) overnight at 4 °C.

The next day, the primary antibody was removed and the cells were washed 3 times in TBS. Cells were then incubated with a secondary antibody (anti-goat IgG)conjugated to tetramethylrhodamine isothiocyanate (TRITC) conjugate, diluted 1/100, in the dark for 30 minutes at room temperature. The secondary antibody was aspirated off and cells were washed 3 times with TBS on a shaker in the dark. Cells were mounted in Vectashield® mounting medium for fluorescence with DAPI stain to visualise the nuclei.

A1.9 MEASUREMENT OF GLYCEROL 3-PHOSPHATE DEHYDROGENASE ACTIVITY

Glycerol-3-phosphate dehydrogenase (G3PDH) is a key enzyme in the production of TG, catalyzing the production of glycerol 3-phosphate, and is can be used as a marker of adipocyte differentiation (Pairault & Green, 1979). It catalyses the following reaction:



Measurements were made using a modified method of Kozak and Jensen (Kozak & Jensen, 1974) and measured on an ILAB™ 600 Clinical Chemistry Analyser (Instrumentation Laboratories, Warrington, UK). The assay measured the decrease in absorbance of NADH at a wavelength of 340nm to determine the rate of extinction of dihydroxyacetone phosphate due to G3PDH activity.

Adipocytes were harvested in 100 µl of cell lysis solution[6] and collected in a microcentrifuge tube using a cell scraper and pipette. Samples were placed immediately on ice and sonicated three times for 10 seconds (placing on ice in-between) to break up the cells.

For G3PDH enzyme activity measurements, a final reaction volume of 290µl was used. This comprised 20µl of cell lysate, 125µl assay reagent[7], 125µl distilled water and 20µl of 20 mM dihydroxyacetone phosphate (DHAP) (Sigma, UK). The DHAP was added to start the reaction and absorbance was read every 18 seconds for 3 minutes at 340nm.

Using the same cell lysate sample, cellular protein was determined using the Bradford assay. The Bradford dye stock was prepared as follows: 100mg of Coomassie Blue G (Sigma, UK) was dissolved in 50ml of methanol and filtered. The solution was added to 100ml of 85 % H_3PO_4 and diluted to 200 ml with distilled water (pH 0.01). The Bradford assay reagent was prepared by diluting 1 volume of Bradford dye stock with 4 volumes of distilled water (pH 1.1). Protein standards were prepared using 2 mg/ml bovine serum albumin (BSA) (Sigma, UK). For the standard curve, 0.5 to 15 µl (1 to 30 µg) of BSA was added to plastic cuvettes (Sarstedt, Leicester, UK), and in separate cuvettes, 20 µl of cell lysate was added. Next, 1ml of Bradford assay reagent was added to each cuvette and he samples were mixed. The absorbance read at a wavelength of 575 nm using a spectrophotometer. Total protein per flask was calculated by multiplying the measured protein concentration by 5.

---

[6] Cell lysis solution consisted of 0.05 M Tris HCl, 1 mM EDTA and 1 mM β-mercaptoethanol

[7] Assay reagent was made up of 10 ml of 100 mM triethanolamine-HCl, 12.5 mM EDTA, pH 7.5, 200 µl 0.2 M ascorbic acid and 100 µL of 0.5 % NADH.

Enzyme activity was calculated as the change in absorbance per minute per μg of protein (Δ Abs / min / μg protein).

REFERENCES

Folch J, Lees M, Sloane Stanley GH. A simple method for the isolation and purification of total lipides from animal tissues. *J Biol Chem* 1957;226:497-509

Hellerstein MK, Kletke C, Kaempfer S, Wu K, Shackleton CH. Use of mass isotopomer distributions in secreted lipids to sample lipogenic acetyl-CoA pool in vivo in humans. *Am J Physiol* 1991;261:E479-86

Hellerstein MK, Neese RA. Mass isotopomer distribution analysis: a technique for measuring biosynthesis and turnover of polymers. *Am J Physiol* 1992;263:E988-1001

Hellerstein MK, Neese RA. Mass isotopomer distribution analysis at eight years: theoretical, analytic, and experimental considerations. *Am J Physiol* 1999;276:E1146-70

Kozak LP, Jensen JT. Genetic and developmental control of multiple forms of L-glycerol 3-phosphate dehydrogenase. *J Biol Chem* 1974;249:7775-81

Pairault J, Green H. A study of the adipose conversion of suspended 3T3 cells by using glycerophosphate dehydrogenase as differentiation marker. *Proc Natl Acad Sci U S A* 1979;76:5138-42

Appendix 2

Microarray Data

A2.1 GENES CHANGING IN RESPONSE TO PALMITATE, TOLERANCE AND INTERACTION AS DETERMINED BY 2-WAY ANOVA

Gene Title	Gene ID	Ontology	P value
Reticulon 4 receptor-like 1	*RTN4RL1*	Axon regeneration	0.004
Tenascin C (hexabrachion)	*TNC*	Cell adhesion	0.004
G protein-coupled receptor 124	*GPR124*	Signal transduction	0.005
Prolactin regulatory element binding	*PREB*	Transcription	0.005
KIAA1217	*KIAA1217*	Multicellular organismal development	0.005
Forkhead box O3	*FOXO3*	Transcription	0.010
Myosin, heavy chain 8, skeletal muscle, perinatal	*MYH8*	Striated muscle contraction	0.010
Transcribed locus	-		0.010
Apoptosis-inducing factor, mitochondrion-associated, 2	*AIFM2*	Apoptosis	0.012
Follistatin-like 1	*FSTL1*	Bmp signalling pathway	0.012
Palmdelphin	*PALMD*	Regulation of cell shape	0.016
Dual specificity phosphatase 4	*DUSP4*	MAPKKK cascade	0.016
Tripartite motif-containing 16-like	*TRIM16L*	Cytoplasm	0.016
N-acetyltransferase 8-like	*NAT8L*	Metabolic process	0.016
Kinesin-associated protein 3	*KIFAP3*	Protein complex assembly	0.016
Ring finger protein 20	*RNF20*	Ubiquitin-dependent protein catabolic process	0.016
RAD21 homolog (S. pombe)	*RAD21*	Double-strand break repair	0.016
Transmembrane protein 119	*TMEM119*	Membrane	0.016
Fibrillin 1	*FBN1*	Skeletal development	0.016
Transcribed locus, strongly similar to NP_997234.3 proline-rich transmembrane protein 3 [Homo sapiens]	-		0.018

Dermatan sulfate epimerase	*DSE*	Dermatan sulfate biosynthetic process	0.018
Sorting nexin 10	*SNX10*	Cell communication	0.019
Histone cluster 1, H4h	*HIST1H4H*		0.019
ATPase, H+ transporting V0 subunit e2	*ATP6V0E2*	Ion transport	0.019
Stathmin-like 2	*STMN2*	Intracellular signalling cascade	0.019
Zinc finger family member 673	*ZNF673*	Regulation of transcription, DNA-dependent	0.019
Aldehyde dehydrogenase 3 family, member B1	*ALDH3B1*	Cellular alcohol metabolic process	0.019
Transcribed locus	-		0.019
CDNA FLJ12405 fis, clone MAMMA1002838	-		0.019
Leucine zipper-EF-hand containing transmembrane protein 1	*LETM1*	Signal transduction	0.019
Transmembrane protein 45A	*TMEM45A*	Membrane	0.019
Transcribed locus	-		0.019
Microfibrillar-associated protein 4	*MFAP4*	Cell adhesion	0.019
Indolethylamine N-methyltransferase	*INMT*	Methyltransferase activity	0.019
Glypican 1	*GPC1*	Extracellular region	0.020
Follistatin	*FST*	Negative regulation of transcription from RNA polymerase II promoter	0.020
G protein-coupled bile acid receptor 1	*GPBAR1*	Signal transduction	0.021
Mevalonate kinase	*MVK*	Cholesterol biosynthetic process	0.021
GE608612	-		0.021
Splicing factor, arginine/serine-rich 11	*SFRS11*	Nuclear mRNA splicing, via spliceosome	0.021
GE86790	-		0.021
GE86703	-		0.022
SEC11 homolog C (S. cerevisiae)	*SEC11C*	Signal peptide processing	0.022

C-type lectin domain family 2, member D	*CLEC2D*	Cell surface receptor linked signal transduction	0.023
Transcribed locus	-		0.024
Transcribed locus	-		0.024
Mitochondrial carrier homolog 1 (C. elegans)	*MTCH1*	Transport	0.024
Chromosome 17 open reading frame 65	*C17orf65*		0.024
Transcribed locus	-		0.024
Microfibrillar associated protein 5	*MFAP5*	Extracellular matrix structural constituent	0.024
Limb bud and heart development homolog (mouse)	*LBH*	Transcription	0.024
Snail homolog 2 (Drosophila)	*SNAI2*	Negative regulation of transcription from RNA polymerase II promoter	0.024
Bardet-Biedl syndrome 10	*BBS10*	Retina homeostasis	0.024
Tumor necrosis factor, alpha-induced protein 6	*TNFAIP6*	Inflammatory response	0.024
Nuclear factor of activated T-cells, cytoplasmic, calcineurin-dependent 4	*NFATC4*	Regulation of transcription, DNA-dependent	0.025
GE83406	-	Protein binding	0.026
Electron-transferring-flavoprotein dehydrogenase	*ETFDH*	Transport	0.026
Lumican	*LUM*	Visual perception	0.026
FK506 binding protein 9, 63 kDa	*FKBP9*	Protein folding	0.026
MRNA; cDNA DKFZp564H0616 (from clone DKFZp564H0616)	-		0.026
Abhydrolase domain containing 2	*ABHD2*	Biological_process	0.026
Kringle containing transmembrane protein 1	*KREMEN1*	Cell communication	0.026
Osteomodulin	*OMD*	Cell adhesion	0.026
Acyl-CoA synthetase long-chain family member 3	*ACSL3*	Lipid metabolic process	0.026
Laminin, beta 1	*LAMB1*	Cell adhesion	0.026
Transcribed locus	-		0.026
Transcribed locus	-		0.026

Alcohol dehydrogenase 5 (class III), chi polypeptide	*ADH5*	Retinoid metabolic process	0.027
Indolethylamine N-methyltransferase	*INMT*	Methyltransferase activity	0.029
Lysophosphatidic acid receptor 1	*LPAR1*	Signal transduction	0.029
Mesoderm induction early response 1, family member 3	*MIER3*	Transcription	0.029
Interleukin 32	*IL32*	Defense response	0.030
Collagen, type XII, alpha 1	*COL12A1*	Skeletal development	0.031
2',5'-oligoadenylate synthetase 1, 40/46kDa	*OAS1*	Nucleobase, nucleoside, nucleotide and nucleic acid metabolic process	0.031
Myosin X	*MYO10*	Signal transduction	0.031
Transcribed locus	-		0.032
RAB GTPase activating protein 1	*RABGAP1*	Cell cycle	0.032
Transcribed locus	-		0.032
Argininosuccinate synthetase 1	*ASS1*	Urea cycle	0.032
G protein-coupled receptor 109B	*GPR109B*	Signal transduction	0.032
Nuclear factor of kappa light polypeptide gene enhancer in B-cells inhibitor, zeta	*NFKBIZ*	Transcription	0.032
Coenzyme Q6 homolog, monooxygenase (S. cerevisiae)	*COQ6*	Cellular aromatic compound metabolic process	0.033
Transforming, acidic coiled-coil containing protein 1	*TACC1*	Cell cycle	0.033
Hypothetical protein MGC12972	*FKSG24*	Membrane	0.034
Zinc finger homeobox 4	*ZFHX4*	Regulation of transcription, DNA-dependent	0.034
VAMP (vesicle-associated membrane protein)-associated protein A, 33kDa	*VAPA*	Membrane fusion	0.034
Phosphodiesterase 4D interacting protein (myomegalin)	*PDE4DIP*	Cytoskeleton organization	0.034

Serine/threonine kinase 24 (STE20 homolog, yeast)	*STK24*	Protein amino acid phosphorylation	0.034
GE86023	-	Translation	0.035
Enhancer of zeste homolog 1 (Drosophila)	*EZH1*	DNA repair	0.036
Histone cluster 2, H2aa3	*HIST2H2AA3*	Nucleosome assembly	0.036
CDNA clone IMAGE:5500261	-		0.036
Chromosome 1 open reading frame 38	*C1orf38*	Cell adhesion	0.036
MAP kinase interacting serine/threonine kinase 2	*MKNK2*	Regulation of translation	0.036
Pyridoxal (pyridoxine, vitamin B6) kinase	*PDXK*	Cell proliferation	0.036
Forkhead box N3	*FOXN3*	DNA damage checkpoint	0.036
CDNA FLJ38449 fis, clone FEBRA2019389	-		0.036
Fibroblast growth factor receptor substrate 3	*FRS3*	Signal transduction	0.036
Hypothetical protein LOC90110	*LOC90110*		0.036
Zinc finger protein 770	*ZNF770*	Transcription	0.036
Sushi, von Willebrand factor type A, EGF and pentraxin domain containing 1	*SVEP1*	Cell adhesion	0.036
CTD (carboxy-terminal domain, RNA polymerase II, polypeptide A) small phosphatase-like	*CTDSPL*	Biological_process	0.036
RAB12, member RAS oncogene family	*RAB12*	Small GTPase mediated signal transduction	0.036
ATP-binding cassette, sub-family A (ABC1), member 10	*ABCA10*	Transport	0.036
Solute carrier family 5 (sodium-dependent vitamin transporter), member 6	*SLC5A6*	Ion transport	0.036
Chromosome 1 open reading frame 21	*C1orf21*		0.036
Indolethylamine N-methyltransferase	*INMT*	Methyltransferase activity	0.036
CD34 molecule	*CD34*	Cell adhesion	0.036
C1q and tumor necrosis factor related protein 1	*C1QTNF1*	Extracellular region	0.037

CDNA FLJ26671 fis, clone MPG03325	-		0.037
Nidogen 1	*NID1*	Cell adhesion	0.037
CDNA: FLJ22522 fis, clone HRC12491	-		0.038
GE549025	-	Cell adhesion	0.038
Dual specificity phosphatase 6	*DUSP6*	Inactivation of MAPK activity	0.040
Claudin 23	*CLDN23*	Calcium-independent cell-cell adhesion	0.040
Low density lipoprotein receptor (familial hypercholesterolemia)	*LDLR*	Protein amino acid O-linked glycosylation	0.040
Transcribed locus, strongly similar to XP_001717612.1 PREDICTED: similar to hCG15011 [Homo sapiens]	-		0.040
REV3-like, catalytic subunit of DNA polymerase zeta (yeast)	*REV3L*	Nucleobase, nucleoside, nucleotide and nucleic acid metabolic process	0.040
Acylphosphatase 2, muscle type	*ACYP2*	Phosphate metabolic process	0.040
CDNA FLJ10247 fis, clone HEMBB1000705	-		0.040
Sp4 transcription factor	*SP4*	Transcription	0.040
Transcription elongation factor A (SII)-like 3	*TCEAL3*	Transcription	0.040
Olfactomedin-like 3	*OLFML3*	Extracellular region	0.040
Transcribed locus	-		0.040
Acetyl-Coenzyme A acyltransferase 2	*MYO5B*	Nucleotide binding	0.040
Histone cluster 1, H2bd	*HIST1H2BD*	Nucleosome assembly	0.042
Transcribed locus	-		0.043
KIAA0922	*KIAA0922*	Membrane	0.043
Protein tyrosine phosphatase-like A domain containing 2	*PTPLAD2*	Membrane	0.043
RUN and FYVE domain containing 3	*RUFY3*	Multicellular organismal development	0.044
Forkhead box O3	*FOXO3*	Transcription	0.045
Propionyl Coenzyme A carboxylase, beta polypeptide	*PCCB*	Propionyl-Coa carboxylase activity	0.046

Transcribed locus	-		0.047
Solute carrier family 16, member 5 (monocarboxylic acid transporter 6)	*SLC16A5*	Transport	0.047
CDNA FLJ27020 fis, clone SLV06144	-		0.048
PQ loop repeat containing 3	*PQLC3*	Membrane	0.049

Table A2-1 Genes changing signigicantly in reponse to palmitate (2-way ANOVA, P < 0.05).

Gene Title	Gene ID	Ontology	P values
Dual specificity phosphatase 6	*DUSP6*	Inactivation of MAPK activity	0.035
Apoptosis-inducing factor, mitochondrion-associated, 2	*AIFM2*	Apoptosis	0.035
MAP kinase interacting serine/threonine kinase 2	*MKNK2*	Regulation of translation	0.016
Hypothetical LOC554202	*LOC554202*		0.035
Hypothetical protein LOC100132181	*LOC100132181*		0.008
Chordin-like 1	*CHRDL1*	Ossification	0.006
Glutathione S-transferase M3 (brain)	*GSTM3*	Establishment of blood-nerve barrier	0.029
GE86023	-	Translation	0.006
Visinin-like 1	*VSNL1*	Calcium ion binding	0.016
Kinesin-associated protein 3	*KIFAP3*	Protein complex assembly	0.050
Capping protein (actin filament), gelsolin-like	*CAPG*	Protein complex assembly	0.028
REV3-like, catalytic subunit of DNA polymerase zeta (yeast)	*REV3L*	Nucleobase, nucleoside, nucleotide and nucleic acid metabolic process	0.030
GE86790	-		0.006
TNF receptor-associated protein 1	*TRAP1*	Protein folding	0.029
Alcohol dehydrogenase 5 (class III), chi polypeptide	*ADH5*	Retinoid metabolic process	0.016
Ras interacting protein 1	*RASIP1*	Signal transduction	0.035
GE87779	-		0.031
GE731878	-		0.035
Proprotein convertase subtilisin/kexin type 9	*PCSK9*	Kidney development	0.050
Sphingomyelin phosphodiesterase, acid-like 3A	*SMPDL3A*	Sphingomyelin catabolic process	0.017

Aryl hydrocarbon receptor nuclear translocator	*ARNT*	Response to hypoxia	0.042
Hairless homolog (mouse)	*HR*	Regulation of transcription, DNA-dependent	0.048
Aldehyde dehydrogenase 3 family, member B1	*ALDH3B1*	Cellular alcohol metabolic process	0.008
Transcribed locus	-		0.035
Progestin and adipoQ receptor family member VI	*PAQR6*	Receptor activity	0.034
GE719646	-		0.010
CDNA FLJ12405 fis, clone MAMMA1002838	-		0.035
Papilin, proteoglycan-like sulfated glycoprotein	*PAPLN*	Metalloendopeptidase activity	0.035
Hypothetical protein LOC285084	*LOC285084*		0.042
Microfibrillar associated protein 5	*MFAP5*	Extracellular matrix structural constituent	0.042
Sushi, von Willebrand factor type A, EGF and pentraxin domain containing 1	*SVEP1*	Cell adhesion	0.035
G protein-coupled receptor 124	*GPR124*	Signal transduction	0.003
Leiomodin 1 (smooth muscle)	*LMOD1*	Tropomyosin binding	0.011
VAMP (vesicle-associated membrane protein)-associated protein A, 33kDa	*VAPA*	Membrane fusion	0.022
Transmembrane protein 119	*TMEM119*	Membrane	0.035
Protein tyrosine phosphatase-like A domain containing 2	*PTPLAD2*	Membrane	0.035
GE726669	-		0.049
Follistatin-like 1	*FSTL1*	BMP signalling pathway	0.042
CDNA FLJ10247 fis, clone HEMBB1000705	-		0.035
Protein tyrosine phosphatase-like A domain containing 2	*PTPLAD2*	Membrane	0.035
GE54881	-	Membrane	0.035
Transcribed locus	-		0.049
Complement component 5	*C5*	Activation of MAPK activity	0.035

CDNA clone IMAGE:4827685	-		0.034
Secreted frizzled-related protein 2	*SFRP2*	Somitogenesis	0.003
Limb bud and heart development homolog (mouse)	*LBH*	Transcription	0.038
Paired immunoglobin-like type 2 receptor alpha	*PILRA*	Signal transduction	0.034
Stathmin-like 2	*STMN2*	Intracellular signalling cascade	0.008
Chromosome 5 open reading frame 23	*C5orf23*	Protein complex	0.004
Myosin X	*MYO10*	Signal transduction	0.035
Nuclear factor of activated T-cells, cytoplasmic, calcineurin-dependent 4	*NFATC4*	Regulation of transcription, DNA-dependent	0.036
Transcribed locus	-		0.016
GE88736	-		0.029
Microfibrillar-associated protein 4	*MFAP4*	Cell adhesion	0.035
Leptin	*LEP*	Glucose metabolic process	0.039
Immunoglobulin superfamily, member 10	*IGSF10*	Ossification	0.038
Follistatin	*FST*	Negative regulation of transcription from rna polymerase II promoter	0.028
Transcribed locus	-		0.006
Tenascin C (hexabrachion)	*TNC*	Cell adhesion	0.003
Myosin, heavy chain 8, skeletal muscle, perinatal	*MYH8*	Striated muscle contraction	0.003

Table A2-2 Genes changing significantly in response to tolerance (2-way ANOVA, P < 0.05)

Gene Title	Gene ID	Ontology	P value
Serum deprivation response (phosphatidylserine binding protein)	*SDPR*	Phosphatidylserine binding	0.043
Reticulon 4 receptor-like 1	*RTN4RL1*	Axon regeneration	0.011
Histone cluster 1, H4h	*HIST1H4H*		0.025
Hypothetical protein LOC100129436	*LOC100129436*		0.033

Inscuteable homolog (Drosophila)	*INSC*	Multicellular organismal development	0.014
CDNA clone IMAGE:4826441	-		0.031
Single-minded homolog 2 (Drosophila)	*SIM2*	Negative regulation of transcription from RNA polymerase II promoter	0.034
Transcribed locus	-		0.021
Major histocompatibility complex, class II, DM beta	*HLA-DMB*	Antigen processing and presentation of peptide or polysaccharide antigen via MHC class II	0.019
Hypothetical gene supported by BC052596	*LOC388564*		0.007
GE754120	-		0.032
CDNA FLJ41071 fis, clone 3NB692003538	-		0.034
GE714686	-		0.036
GE732790	-		0.026
Kinesin family member 1A	*KIF1A*	Microtubule-based movement	0.046
Transcribed locus	-		0.040
WD repeat domain 61	*WDR61*		0.019
Transcribed locus	-		0.045
CDNA clone IMAGE:4825100	-		0.015
Transcribed locus	-		0.018
Transcribed locus	-		0.024
GE84344	-		0.041
EF-hand calcium binding domain 6	*EFCAB6*	Transcription	0.044
Transcribed locus	-		0.024
Transcribed locus	-		0.024
Synaptopodin	*SYNPO*	Positive regulation of actin filament bundle formation	0.040
GE754125	-		0.039
Transcribed locus	-		0.023
Chloride channel 5 (nephrolithiasis 2, X-linked, Dent disease)	*CLCN5*	Ion transport	0.030
Glutamate receptor interacting protein 2	*GRIP2*	Protein binding	0.035
PHD finger protein 12	*PHF12*	Transcription	0.048
GE729841	-		0.034

GE781171	-		0.024
Transcribed locus	-		0.048
Sterol-C4-methyl oxidase-like	*SC4MOL*	Fatty acid biosynthetic process	0.038
Transcribed locus, strongly similar to NP_997234.3 proline-rich transmembrane protein 3 [Homo sapiens]	-		0.014
Palmdelphin	*PALMD*	Regulation of cell shape	0.022
Transcribed locus	-		0.030
Dual specificity phosphatase 4	*DUSP4*	MAPKKK cascade	0.041
Clone NBB7 Cri-du-chat critical region mRNA	-		0.050
RAD21 homolog (S. pombe)	*RAD21*	Double-strand break repair	0.002
RAB8B, member RAS oncogene family	*RAB8B*	Small gtpase mediated signal transduction	0.031
EPH receptor A4	*EPHA4*	Protein amino acid phosphorylation	0.042
Microfibrillar associated protein 5	*MFAP5*	Extracellular matrix structural constituent	0.031
V-fos FBJ murine osteosarcoma viral oncogene homolog	*FOS*	DNA methylation	0.011
YTH domain containing 1	*YTHDC1*	mRNA processing	0.046
Dermatan sulfate epimerase	*DSE*	Dermatan sulfate biosynthetic process	0.015
SH3 and PX domains 2B	*SH3PXD2B*	Cell communication	0.026
Platelet-derived growth factor receptor, alpha polypeptide	*PDGFRA*	Cell activation	0.046
Laminin, gamma 1 (formerly LAMB2)	*LAMC1*	Protein complex assembly	0.043
Transmembrane protein 119	*TMEM119*	Membrane	0.048
Platelet-derived growth factor receptor, beta polypeptide	*PDGFRB*	Signal transduction	0.040
Follistatin-like 1	*FSTL1*	BMP signalling pathway	0.009
Forkhead box O3	*FOXO3*	Transcription	0.003
Sphingosine-1-phosphate receptor 3	*S1PR3*	Cytokine production	0.020
Bardet-Biedl syndrome 10	*BBS10*	Retina homeostasis	0.027
Laminin, beta 1	*LAMB1*	Cell adhesion	0.036

Tenascin C (hexabrachion)	*TNC*	Cell adhesion	0.005

Table A2-3 Genes changing due to "interaction" (that is, effects of palmitate and tolerance together).

A2.2 PAIRED *T* TEST ANALYSES OF GENES CHANGING IN RESPONSE TO PALMITATE

Gene name	Direction	P value
Myosin, heavy chain 8, skeletal muscle, perinatal	Down	0.009
Matrix metallopeptidase 3 (stromelysin 1, progelatinase)	Down	0.009
Interleukin 33	Down	0.009
Naked cuticle homolog 2 (Drosophila)	Up	0.009
CD34 molecule	Down	0.009
Stathmin-like 2	Down	0.009
Transcribed locus	Down	0.009
Transcribed locus	Down	0.009
Insulin induced gene 1	Up	0.009
Protein phosphatase 1, regulatory (inhibitor) subunit 14A	Down	0.009
Synapsin II	Up	0.009
Calcium channel, voltage-dependent, beta 2 subunit	Down	0.009
Olfactomedin-like 2B	Down	0.009
Limb bud and heart development homolog (mouse)	Down	0.009
Transcribed locus	Down	0.009
Apoptosis-inducing factor, mitochondrion-associated, 2	Up	0.009
Heart and neural crest derivatives expressed 2	Down	0.009
MAP kinase interacting serine/threonine kinase 2	Up	0.009
KIAA1217	Down	0.009
Transforming, acidic coiled-coil containing protein 1	Down	0.009
Follistatin	Down	0.009
Neurocalcin delta	Down	0.009
Secreted frizzled-related protein 1	Down	0.009
DNA-damage-inducible transcript 4-like	Up	0.009
Chromosome 1 open reading frame 21	Down	0.009
Angiopoietin 1	Down	0.009
GE559890	Down	0.009
Transcribed locus	Down	0.009
GE530117	Up	0.009
Hypothetical protein LOC120376	Down	0.009
CDNA FLJ13937 fis, clone Y79AA1000805	Down	0.009
Actin binding LIM protein family, member 2	Up	0.009
Indolethylamine N-methyltransferase	Down	0.010
Indolethylamine N-methyltransferase	Down	0.010
Hypothetical LOC441027	Down	0.010
Calponin 1, basic, smooth muscle	Down	0.010
Chromosome 1 open reading frame 21	Down	0.010
Sparc/osteonectin, cwcv and kazal-like domains proteoglycan (testican) 1	Down	0.010
Pyridoxal (pyridoxine, vitamin B6) kinase	Up	0.010
Transcribed locus	Down	0.010
Transcribed locus	Down	0.010
Dual specificity phosphatase 6	Up	0.010
GE84428	Up	0.011

Integral membrane protein 2A	Down	0.011
Synapsin II	Up	0.011
Malic enzyme 1, NADP(+)-dependent, cytosolic	Up	0.011
Myosin X	Down	0.012
Scavenger receptor class A, member 5 (putative)	Down	0.012
Indolethylamine N-methyltransferase	Down	0.012
Xg pseudogene, Y-linked 2	Down	0.013
Activated leukocyte cell adhesion molecule	Down	0.013
Fatty acid desaturase 1	Up	0.013
TYRO3 protein tyrosine kinase	Up	0.013
Transcribed locus	Down	0.013
WNT1 inducible signalling pathway protein 2	Down	0.013
Transcribed locus	Down	0.013
Rho GTPase activating protein 28	Down	0.013
Immunoglobulin superfamily, member 10	Down	0.013
Phospholipase A2, group V	Down	0.014
Microfibrillar-associated protein 4	Down	0.014
Transcribed locus	Up	0.014
Angiopoietin-like 1	Down	0.014
MAM domain containing 2	Down	0.014
Insulin-like growth factor 2 (somatomedin A)	Down	0.015
G0/G1switch 2	Up	0.015
Wingless-type MMTV integration site family, member 11	Down	0.015
Cysteine-rich secretory protein LCCL domain containing 2	Down	0.015
Reticulon 4 receptor-like 1	Up	0.016
Dermatopontin	Down	0.016
GE646842	Up	0.016
Potassium voltage-gated channel, Shal-related subfamily, member 1	Down	0.016
Solute carrier family 10 (sodium/bile acid cotransporter family), member 1	Up	0.016
Family with sequence similarity 107, member A	Down	0.017
Doublecortin-like kinase 1	Down	0.017
CDNA clone IMAGE:4610527	Down	0.017
Transcribed locus	Down	0.017
ATPase, H+ transporting V0 subunit e2	Up	0.017
Nuclear factor of activated T-cells, cytoplasmic, calcineurin-dependent 4	Down	0.018
Sorbin and SH3 domain containing 2	Down	0.019
Dual specificity phosphatase 4	Up	0.019
Collagen, type XI, alpha 1	Down	0.019
Cartilage oligomeric matrix protein	Down	0.019
Transcribed locus	Down	0.019
Lactotransferrin	Up	0.019
N-acetyltransferase 8-like	Up	0.019
Transcribed locus	Down	0.019
Nudix (nucleoside diphosphate linked moiety X)-type motif 8	Up	0.019
GE549025	Down	0.019
CD9 molecule	Up	0.019
Eomesodermin homolog (Xenopus laevis)	Up	0.019

Protein phosphatase 1, regulatory (inhibitor) subunit 16A	Up	0.019
GE83406	Up	0.019
Fumarylacetoacetate hydrolase (fumarylacetoacetase)	Up	0.019
Scrapie responsive protein 1	Down	0.019
Acyl-CoA synthetase short-chain family member 2	Up	0.019
GE902881	Up	0.019
Transcribed locus	Up	0.019
GE615286	Down	0.019
Aminoacylase 1	Up	0.019
Similar to metallo-beta-lactamase superfamily protein	Up	0.019
Synaptopodin 2	Down	0.019
Leucine-rich repeats and immunoglobulin-like domains 1	Up	0.019
Nidogen 1	Down	0.019
Receptor (G protein-coupled) activity modifying protein 2	Down	0.019
Vitrin	Down	0.020
Transcribed locus	Down	0.020
Lipopolysaccharide binding protein	Up	0.020
SET binding protein 1	Down	0.020
Rho GTPase activating protein 6	Down	0.020
Nebulette	Down	0.020
Transcribed locus	Up	0.020
Transmembrane protein 45A	Down	0.020
SPOC domain containing 1	Up	0.020
Cartilage intermediate layer protein, nucleotide pyrophosphohydrolase	Down	0.020
Transcribed locus	Up	0.020
Glycosyltransferase 8 domain containing 2	Down	0.021
Transcription elongation factor A (SII)-like 3	Down	0.021
G protein-coupled bile acid receptor 1	Up	0.021
Protein tyrosine phosphatase, receptor type, F	Up	0.021
Synaptogyrin 2	Up	0.021
Acyl-CoA synthetase short-chain family member 2	Up	0.021
CDNA clone IMAGE:4838390	Up	0.021
Macrophage receptor with collagenous structure	Up	0.021
Tenascin C (hexabrachion)	Down	0.021
Histone cluster 1, H4h	Up	0.021
Solute carrier family 2 (facilitated glucose/fructose transporter), member 5	Up	0.021
Palmdelphin	Up	0.021
G protein-coupled receptor 109B	Up	0.021
Islet cell autoantigen 1, 69kDa	Up	0.021
Transcribed locus	Up	0.021
Claudin 23	Up	0.021
Hypothetical LOC389033	Down	0.021
Potassium channel, subfamily K, member 3	Up	0.022
Secretory carrier membrane protein 1	Up	0.022
Fatty acid binding protein 5 (psoriasis-associated)	Up	0.022
Collagen, type XII, alpha 1	Down	0.022
GE82839	Up	0.022
Transcribed locus	Up	0.023

Heme oxygenase (decycling) 1	Up	0.023
Chromosome 1 open reading frame 38	Up	0.023
V-maf musculoaponeurotic fibrosarcoma oncogene homolog (avian)	Down	0.023
Transmembrane 7 superfamily member 2	Up	0.023
Low density lipoprotein-related protein 1B (deleted in tumors)	Down	0.023
Transcribed locus	Up	0.023
Alpha-2-glycoprotein 1, zinc-binding	Up	0.023
Integrin, alpha 6	Up	0.024
Glycerol-3-phosphate acyltransferase, mitochondrial	Up	0.024
Solute carrier family 29 (nucleoside transporters), member 4	Up	0.024
Histone cluster 2, H2aa3	Up	0.026
Laminin, beta 1	Down	0.026
Transmembrane protein 59-like	Down	0.027
Lipase, hormone-sensitive	Up	0.027
Nuclear receptor subfamily 1, group H, member 3	Up	0.029
Calcium channel, voltage-dependent, beta 2 subunit	Down	0.029
Hypothetical protein LOC729085	Down	0.029
Fucosyltransferase 1 (galactoside 2-alpha-L-fucosyltransferase, H blood group)	Up	0.030
Creatine kinase, mitochondrial 2 (sarcomeric)	Up	0.030
Hepatocellular carcinoma-associated gene TD26	Up	0.032
Follistatin-like 1	Down	0.032
Transmembrane protein 37	Up	0.032
Acyl-CoA synthetase family member 2	Up	0.032
Glycerol-3-phosphate dehydrogenase 1 (soluble)	Up	0.033
Transmembrane 4 L six family member 1	Up	0.033
Amine oxidase, copper containing 2 (retina-specific)	Up	0.033
Receptor tyrosine kinase-like orphan receptor 2	Down	0.033
Phosphodiesterase 3B, cGMP-inhibited	Up	0.033
Paired immunoglobin-like type 2 receptor alpha	Down	0.033
Retinol saturase (all-trans-retinol 13,14-reductase)	Up	0.033
Phosphoenolpyruvate carboxykinase 1 (soluble)	Up	0.033
Cyclin-dependent kinase inhibitor 2C (p18, inhibits CDK4)	Up	0.033
Guanine nucleotide binding protein (G protein), gamma 2	Up	0.033
Serum amyloid A2	Up	0.034
Vascular endothelial growth factor C	Down	0.034
Leukocyte-associated immunoglobulin-like receptor 1	Up	0.034
Transcribed locus	Down	0.034
Fatty acid binding protein 4, adipocyte	Up	0.034
Transmembrane protein 176B	Down	0.034
Transcribed locus	Up	0.035
Histone cluster 1, H2bd	Up	0.035
Transcribed locus	Down	0.035
Microtubule-associated protein tau	Up	0.035
Peroxisomal trans-2-enoyl-CoA reductase	Up	0.036
Calbindin 2	Up	0.037
MRNA; cDNA DKFZp564F172 (from clone DKFZp564F172)	Up	0.037
Aquaporin 7	Up	0.037
Hypothetical gene supported by AK095441	Up	0.038

Leptin	Down	0.038
Lectin, galactoside-binding, soluble, 12 (galectin 12)	Up	0.038
Perilipin	Up	0.038
Histone cluster 2, H2be	Up	0.038
Protein phosphatase 1, regulatory (inhibitor) subunit 1A	Up	0.040
Thyroid hormone responsive (SPOT14 homolog, rat)	Up	0.040
Tumor necrosis factor, alpha-induced protein 6	Down	0.040
Stearoyl-CoA desaturase (delta-9-desaturase)	Up	0.040
Klotho beta	Up	0.040
Solute carrier family 25 (mitochondrial carrier; dicarboxylate transporter), member 10	Up	0.041
Chromosome 5 open reading frame 4	Down	0.043
Neurogenin 1	Up	0.043
ELOVL family member 5, elongation of long chain fatty acids (FEN1/Elo2, SUR4/Elo3-like, yeast)	Up	0.043
ADAM metallopeptidase domain 33	Down	0.043
Prostaglandin I2 (prostacyclin) synthase	Down	0.045
Flavin containing monooxygenase 1	Up	0.047
Adiponectin, C1Q and collagen domain containing	Up	0.049
CD36 molecule (thrombospondin receptor)	Up	0.049

Figure A2-4 List of genes changing significantly from 0 to 50 μM palmitate (paired *t* test, P < 0.05)

Gene Name	Direction	P value
Lactotransferrin	Up	0.001
CD34 molecule	Down	0.013
Matrix metallopeptidase 3 (stromelysin 1, progelatinase)	Down	0.021
CDNA FLJ20833 fis, clone ADKA02957	Up	0.021
Histone cluster 2, H2aa3	Up	0.021
Scavenger receptor class A, member 5 (putative)	Down	0.021
CD34 molecule	Down	0.021
Cartilage intermediate layer protein, nucleotide pyrophosphohydrolase	Down	0.021
Proprotein convertase subtilisin/kexin type 9	Up	0.021
Serum amyloid A2	Up	0.024
Histone cluster 1, H2bd	Up	0.030
Chromosome 10 open reading frame 116	Up	0.036
Collagen, type VIII, alpha 1	Up	0.036
Protein phosphatase 1, regulatory (inhibitor) subunit 1A	Up	0.036
Hepatocellular carcinoma-associated gene TD26	Up	0.036
Adiponectin, C1Q and collagen domain containing	Up	0.036
Thymidine kinase 1, soluble	Up	0.036
GE84428	Up	0.036
Metallothionein 1G	Up	0.038
Aurora kinase B	Up	0.038

Figure A2-5 List of genes changing significantly from 0 to 200 μM palmitate (paired *t* test, P < 0.05)

Gene Name	Direction	P value
Macrophage receptor with collagenous structure	Down	0.000
Stathmin-like 2	Up	0.001
Secreted frizzled-related protein 1	Up	0.001
GE559890	Up	0.001
SPOC domain containing 1	Down	0.002
Tenascin C (hexabrachion)	Up	0.003
Retinol dehydrogenase 10 (all-trans)	Up	0.003
Tumor necrosis factor, alpha-induced protein 6	Up	0.003
Osteomodulin	Up	0.004
Transcribed locus	Down	0.004
Follistatin	Up	0.004
Transcribed locus	Up	0.004
Interleukin 33	Up	0.004
Protein tyrosine phosphatase-like A domain containing 2	Up	0.004
DEP domain containing 6	Up	0.004
Transcribed locus	Up	0.005
Protein phosphatase 1, regulatory (inhibitor) subunit 14A	Up	0.005
Naked cuticle homolog 2 (Drosophila)	Down	0.005
Immunoglobulin superfamily, member 10	Up	0.005
Myosin, heavy chain 8, skeletal muscle, perinatal	Up	0.005
Complement factor B	Up	0.005
Indolethylamine N-methyltransferase	Up	0.005
Limb bud and heart development homolog (mouse)	Up	0.005
Transcribed locus	Up	0.005
Cathepsin H	Up	0.005
Transcribed locus	Up	0.005
Low density lipoprotein-related protein 1B (deleted in tumors)	Up	0.005
Limbic system-associated membrane protein	Up	0.005
Collagen, type XI, alpha 1	Up	0.005
Calponin 1, basic, smooth muscle	Up	0.005
Reticulon 4 receptor-like 1	Down	0.006
Indolethylamine N-methyltransferase	Up	0.006
G protein-coupled bile acid receptor 1	Down	0.006
Leptin	Up	0.006
Creatine kinase, mitochondrial 1B	Down	0.007
DNA-damage-inducible transcript 4-like	Down	0.007
Family with sequence similarity 107, member A	Up	0.007
Ovary-specific acidic protein	Up	0.007
Corin, serine peptidase	Up	0.008
Hypothetical LOC441027	Up	0.008
Protease, serine, 23	Up	0.008
Retinoic acid receptor responder (tazarotene induced) 2	Up	0.008
MRNA full length insert cDNA clone EUROIMAGE 1913076	Up	0.009
Transmembrane protein 176B	Up	0.012
Nuclear receptor subfamily 1, group H, member 3	Down	0.012
Ets variant gene 1	Down	0.012
Nidogen 1	Up	0.012
Interferon, alpha-inducible protein 27	Up	0.012
Collagen, type VIII, alpha 1	Up	0.013

Interleukin 32	Up	0.013
RAS-like, estrogen-regulated, growth inhibitor	Up	0.013
Histone cluster 1, H3d	Down	0.013
CDNA FLJ26671 fis, clone MPG03325	Up	0.014
Transcribed locus, strongly similar to XP_001143167.1 PREDICTED: hypothetical protein [Pan troglodytes]	Up	0.014
Follistatin-like 1	Up	0.015
Microfibrillar-associated protein 4	Up	0.015
LIM and cysteine-rich domains 1	Up	0.017
Transcribed locus, weakly similar to XP_001147891.1 PREDICTED: similar to peptidylprolyl isomerase isoform 2 [Pan troglodytes	Up	0.018
Indolethylamine N-methyltransferase	Up	0.018
Chemokine (C-X-C motif) ligand 14	Down	0.018
Interferon, alpha-inducible protein 27	Up	0.020
Cartilage oligomeric matrix protein	Up	0.021
Interferon-induced protein 44-like	Up	0.021
Hyaluronan and proteoglycan link protein 1	Up	0.023
Periostin, osteoblast specific factor	Up	0.024
Solute carrier family 38, member 2	Up	0.047

Figure A2-6 List of genes changing significantly from 50 to 200 μM palmitate (paired *t* test, P < 0.05)